Development of a liver-pancreas in vitro model using microfluidic organ-on-chip technologies

Amal Essaouiba

Par **Amal ESSAOUIBA**

Development of a liver-pancreas in vitro model using microfluidic organ-on-chip technologies

Thèse présentée
pour l'obtention du grade
de Docteur de l'UTC

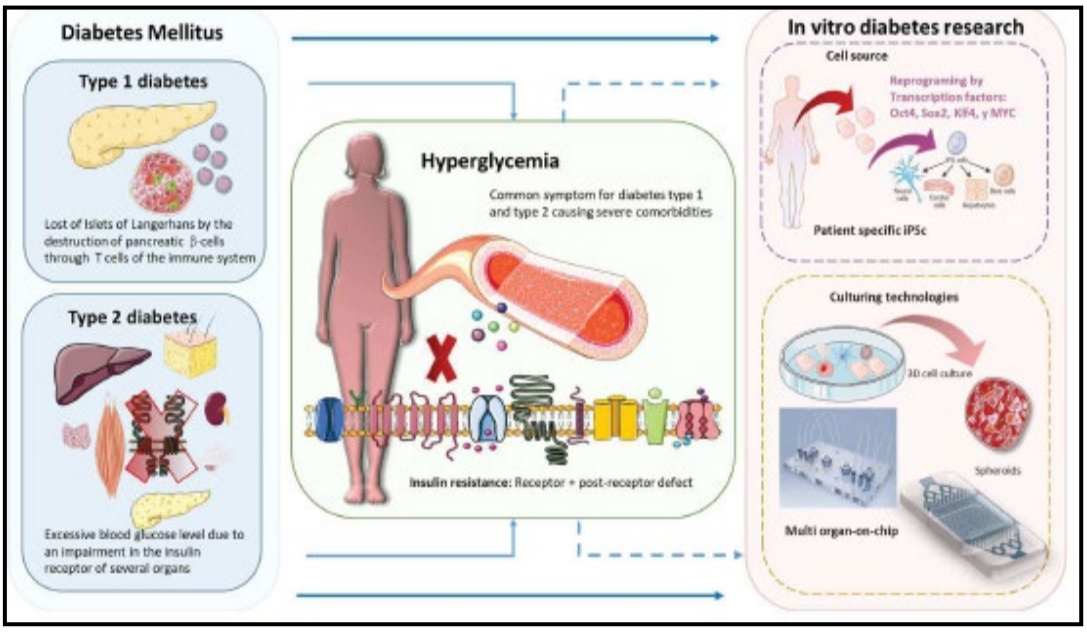

Soutenue le 11 décembre 2020
Spécialité : Biomécanique et Bio-ingénierie : Unité de Recherche Biomécanique et Bio-ingénierie (UMR-7338)
D2573

Thèse présentée pour l' obtention du grade de Docteur de
l' Université de Technologie de Compiègne
Ecole doctorale n° 71 : Sciences pour l' ingénieur
Spécialité : Biomécanique et Bio-ingénierie
BMBI CNRS UMR 7338

Development of a liver-pancreas *in vitro* model using microfluidic organ-on-chip technologies

Amal Essaouiba

11 décembre 2020

Membres du jury:

Pr. RAMÓN-AZCÓN J., ICREA, BIST, IBEC - Barcelona – Spain	Rapporteur
Pr. ABDERRAHMANI A., CNRS UMR 8520 - Lille – France	Rapporteur
Dr. FOUFELLE F., DR INSERM U1138 - Paris – France	Examinatrice
Dr. DUBART-KUPPERSCHMITT A., DR INSERM U1193 - Villejuif – France	Examinatrice
Pr. VAYSSADE M., Université de Technologie de Compiègne – France	Examinatrice
Dr. LEGALLAIS C., DR CNRS UMR 7338 - Compiègne – France	Directrice de thèse
Dr. LECLERC E., DR CNRS UMR 7338 - Compiègne – France	Directeur de thèse
Pr. SAKAI Y., School of Engineering, University of Tokyo – Tokyo – Japan	Encadrant de thèse

Résumé

Le diabète mellitus, également désigné comme la maladie du siècle, est une pathologie mortelle qui affecte le système endocrinien. Les mécanismes liés à la rupture de la boucle de rétroaction, qui régule le métabolisme et induit le diabète, ne sont pas entièrement connus. La compréhension des mécanismes d'action de l'insuline est donc essentielle pour le développement de stratégies thérapeutiques efficaces afin du lutter contre cette maladie. Par conséquent, il est impératif de trouver un modèle robuste et fiable, capable de surmonter les limites de la culture cellulaire traditionnelle en 2D et de l'expérimentation animale, pour la recherche sur le diabète. L'objectif de cette thèse est de développer un nouveau modèle de co-culture foie-pancréas en utilisant des systèmes microphysiologiques avancés (MPs) afin d'aborder plus efficacement le mécanisme impliqué dans la régulation endocrinienne hépatique et pancréatique. Ce travail met en évidence la capacité des systèmes multi-organes sur puce qui combinent la compartimentation avancée des cellules en 3D, la microfluidique et la technologie des cellules souches pluripotentes induites (iPSC), pour atteindre une complexité biologique élevée et des fonctions rarement reproduites par une seule de ces technologies d'ingénierie tissulaire.

Abstract

Diabetes mellitus (DM) or the so called disease of the century is a life threatening dysfunction that affects the endocrine system. The mechanisms underlying the break in the feedback loop that regulates the metabolism and the consequent diabetes induction are not fully known. Understanding the mechanisms of insulin action is therefore crucial for the further development of effective therapeutic strategies to combat DM. Accordingly, it is imperative to find a robust and reliable model for diabetes research able to overcome the limitations of traditional 2D *in vitro* cell culture and animal experimentation. The aim of this thesis is to develop a new liver-pancreas co-culture model using advanced microphysiological systems (MPs) to tackle more effectively the mechanism involving the hepatic and pancreatic endocrine regulation. This work highlights the power of multi organ-on-chip systems that combines the advanced 3D-cell compartmentalization, microfluidics and induced pluripotent stem cells (iPSC) technology to achieve a high biological complexity and functions that are rarely reproduced by only one of these tissue engineering technologies.

TABLE OF CONTENTS

General introduction

Diabetes mellitus (DM) is the most important dysfunction of the endocrine system of the pancreas that triggers a break in the feedback closed loop that regulates the metabolism. In the human body, that feedback loop is based on endocrine signaling between pancreas, liver, and glucose-consuming tissues. The physiopathology underlying pancreatic β- cell failure in type 1 diabetes mellitus and type 2 diabetes mellitus are still poorly defined.

Two dimensional cell culture and animal models have been used for decades in preclinical studies of human diseases and drug screening. However, the disparities between the human physiology and those models drastically reduce their cost-effectiveness. Therefore, advanced *in vitro* models of human organs emerged from the urgent need to propose alternatives. Organ-on-chip technology, represents a powerful bioengineering tool to investigate physiological *in vitro* response in drug screening development and in disease advanced models. Understanding the mechanisms of insulin action is therefore crucial for the further development of effective therapeutic strategies to combat diabetes.

The aim of my PhD thesis is to develop a novel approach of co-culture which, by fulfilling the limitations of previous multi-organ-on-chip systems, could tackle more effectively the metabolic regulation mechanism involving the hepatic and pancreatic endocrine regulation. To approach this research work, we took inspiration from the technological advances in stem cell-based organoids and new configurations of Microphysiological systems (MPs). Accordingly, the co-culture model was established using MPs, which are miniaturised culture devices that combine 3D-cell compartmentalization with fluid physics. The aim is to bridge the gap between *in vitro* and *in vivo* animal models.

With our multi-organ-on-chip, we aimed to create a microscale physiologically relevant biological testing system suitable for academic research and drug development. Its accomplishment required several steps which are the subject of the following chapters. In brief, these consisted in:

- First, we adapted the microstructure of our well-established microfluidic device to host spheroids and 3D-cell structure without compromising the continuous perfusion flow and the shear stress. The biochip design allowed the aggregates trapping efficiently with the flexibility to host a wide range of amount of tissue (necessary to keep the proportionality of tissue while emulating the *in vivo* conditions).
- Our strategy is to tackle the establishment of a co-culture model without contact and study the crosstalk between the pancreas and the liver. In this context, we used as a cell source the primary rat hepatocytes and islets of Langerhans. The *in vitro* model of the multi-organ MPs was used as a proof of concept to validate the new microstructure design of 3D culture in a microfluidic environment (**chapter 3**) for the pancreas-on-chip compartment. As liver-on-chip compartment was already established and fully assessed through a previous PhD thesis, the following step, was the adjustment of the co-culture parameters, including the culture media and the global experimental setup.
- After the establishment of the optimal co-culture conditions, we proceeded with the characterization of the resulting model in terms of endocrine regulation, effectiveness and

functional assessment (**chapter 4**). Moreover, metabolomic analysis were performed in order to understand the signalling pathways activated in the pancreatic and hepatic compartment during the co-culture.

- Regarding the human model, we choose human induced pluripotent stem cells derived to beta cells (hiPS β-cells) spheroids for the human pancreas-on-chip model. For that purpose, we used Cellartis hiPS β-cells and the honeycomb microwell plates technology developed at the University of Tokyo (**chapter 5**).
- In recent years, my team of research has been working in collaboration with the Sakai-Nishikawa Laboratory from the University of Tokyo on the differentiation of hiPS cells to hepatocytes in a microfluidic environment. So, the strategy for the co-culture model without contact aimed to achieve a beneficial effect in maturation and functionality of both tissues following the embryonic developmental process (**chapter 6**).

In summary, the core of this thesis is to highlight the power of multi-organoids systems that combines the advanced 3D culture, microfluidic biochips, human iPS cell and multi-organ MP systems to achieve a high biological complexity and functions that are rarely reproduced by only one of these tissue engineering technologies.

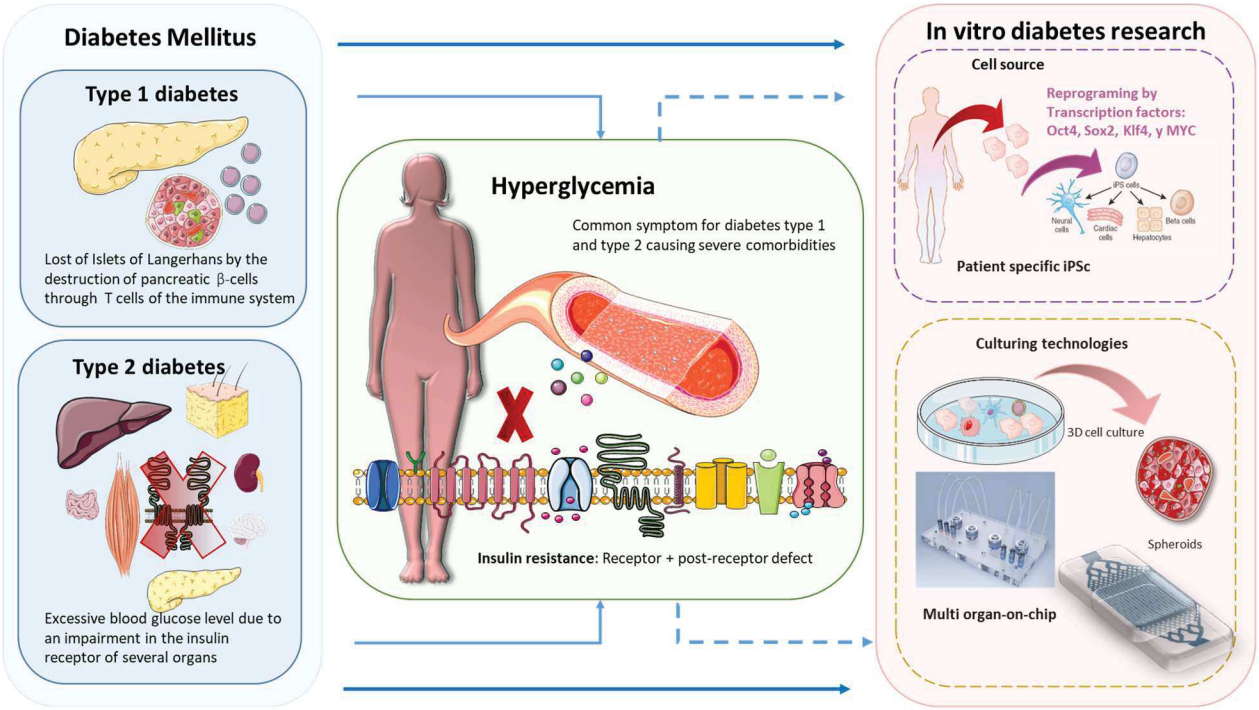

Figure: Graphical abstract

Chapter I: General context

This chapter provide an overview of the state of art of MicroPhysiological Systems technology applied to liver and pancreas *in vitro* modeling and the different applications for those organs. Some sections of this chapter are literally extracted from our chapter: "Membrane bioreactors for bio-artificial pancreas" of a book that assembles reports on membrane applications in the field of biomedical engineering, ranging from artificial organs, to tissue engineering:

Jellali R, **Essaouiba A**, Leclerc E, Legallais C, Chapter 4: Membrane bioreactors for bio-artificial pancreas in Current Trends and Future Developments on (Bio-) Membranes, 1st Edition, Membrane Applications in Artificial Organs and Tissue Engineering, 11th October 2019, **Editors:** Angelo Basile Maria Annesini Vincenzo Piemonte Catherine Charcosset. https://doi.org/10.1016/B978-0-12-814225-7.00004-8

The book chapter is provided as an annex of the thesis. The thesis bibliography has been extended by the integrations of specific sections on liver physiology, liver pancreas interactions, *in vitro* screening tools, multi-organ-on-chip models and therapeutic issues to overcame.

Chapter I: General context

1.1. Mechanisms of glycemic regulation

1.1.1. Liver: anatomy & physiology

The liver is a vital organ with a complex microarchitecture and a wide variety of vital functions: metabolic, blood filtration, synthesis activities, immune response and drug metabolism. Anatomically, the liver is organized into functional units called lobules that are constituted by different types of cells, with different functions depending on their size and location along the portal triad (Figure 1.1). Parenchymal hepatocytes represent the 70-85% of the liver volume[1]. Their main functions are: gluconeogenesis, amino acid decomposition, urea synthesis, nutrients storage, removal of toxins, drugs and xenobiotic metabolism, secretion of bile and not less important, the synthesis of proteins that are essential for life such like albumin, transferrin, fibrinogen and clotting factors [2,3].

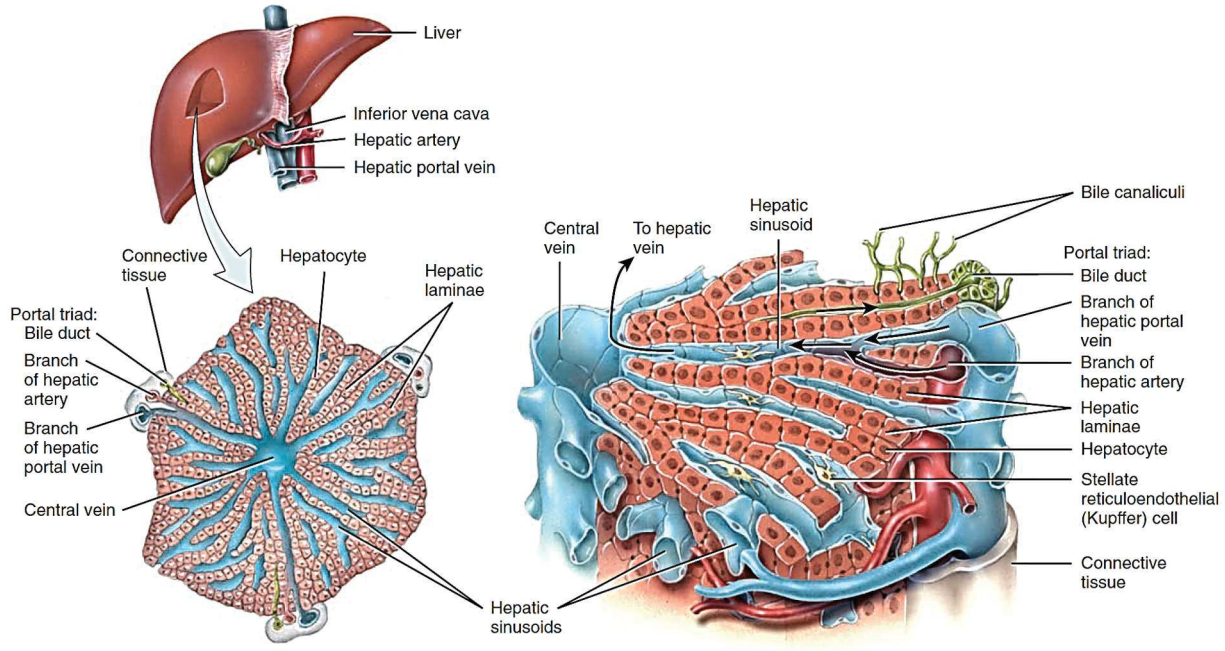

Figure 1.1: Overview of histological components of the liver (reproduced with permission from the book of "Principles of Anatomy and Physiology[2])

During the xenobiotic metabolism process, the cytochrome P450 (CYP) is the main enzyme responsible of the phase I of metabolism that includes oxidation, reduction and hydroxylation processes[4,5]. Meanwhile, transferases in phase II carry out the conjugation of the molecules processed in phase I with charged compounds such as glycine, sulfate, glucoronate, or

glutathione. The final purpose of the detoxification process is to obtain and transfer harmless compounds to the stream blood[3,4].

1.1.2. Pancreas: anatomy & physiology

The pancreas is an organ with a glandular structure located in the curve of duodenum just behind the stomach (Figure 1.2). It is divided into three regions[6]: (i) the head, connected to the duodenum, is the widest and most medial region of the organ; (ii) the body is located behind the stomach; and (iii) the tapered tail region is located in the left side of the abdomen near the spleen. The vascularization of the pancreas is ensured by the anterior pancreaticoduodenal artery (head of the pancreas) and multiple branches of the splenic artery (body and tail of the pancreas). Pancreatic vein joins the splenic vein to form the hepatic portal vein together with the inferior and superior mesenteric veins.

The pancreas is a heterocrine gland involved in both exocrine and endocrine regulation. The exocrine cells of the pancreas represent more than 90% of the pancreatic tissue and are grouped in structures called acini (Figure 1.2), whose function is the synthesis and secretion of enzymes implicated in the digestion process (pancreatic lipase and amylase, phospholipase, nucleases)[7]. Digestive enzymes are drained by the pancreatic ductal tree into the intestine where they aid in nutrient metabolism. The functional units of the endocrine system represent approximately 2% of the pancreas (2 million cells in human adults) and are made up of pancreatic islets or islets of Langerhans. They are clusters of cells whose size varies from 20 to 500 µm, with five different cell types: α-, β-, δ-, ε-, and γ- (PP) cells[7,8]. The most abundant cells include the glucagon-producing α-cells and insulin-producing β-cells. The small proportion of δ-, ε-, and γ-cells secrete somatostatin, ghrelin and pancreatic polypeptides, respectively. Despite comprising only 2% of the total mass of the pancreas, the islets receive around 15% of the pancreatic blood supply, allowing their secreted hormones ready access to the circulation[9]. At the islet level, the oxygen partial pressure (PO2) is about 40 mmHg. The hormones released to the bloodstream is

also controlled by the nervous system thanks to the sensory neurons that enervate the islets of Langerhans[10,11].

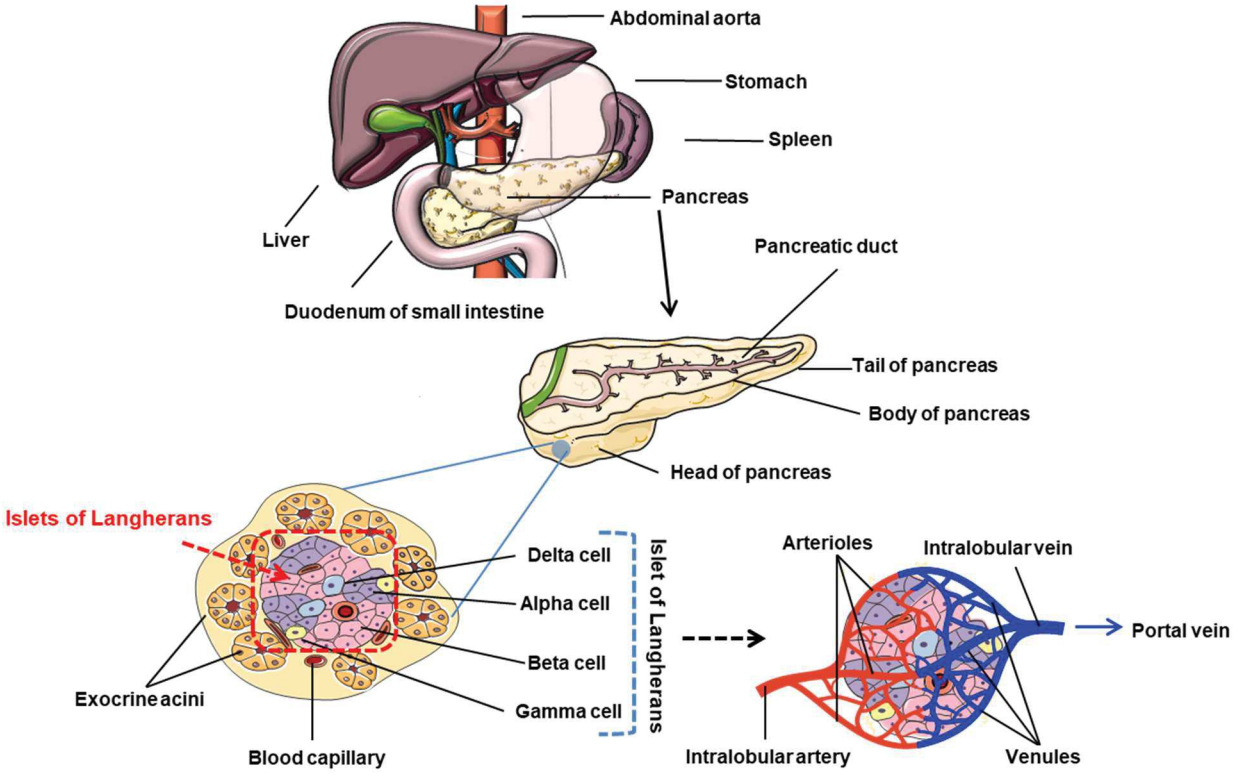

Figure 1.2: Overview of location, blood supply, histology of the pancreas and composition of islets of Langerhans (reproduced with permission from Jellali et al. 2020[12])

During the embryonic development, the cells from the gut endoderm portion differentiate to a variety of cells that constitute the endocrine and exocrine phenotypes of the pancreas thanks to a precise orchestration of the gene expression and cell signaling[13]; the acini and the islets of Langerhans differentiate from the same progenitor. Studies have shown the implication of fibroblast growth factor (FGF) and forming growth factor β (TGF- β) in the signaling pathway in the first stages during the organ development. Vascular epithelial growth factor (VEGF) is involved in endocrine cell differentiation[14,15].

1.1.3. Glucose homeostasis maintenance

The control of glucose levels in the blood is carried out by the interaction of two antagonistic hormones secreted by pancreatic α and β cells. Glucagon (alpha cells) increases glucose levels in the fasting period activating the glycogenolysis and gluconeogenesis in the liver in coordination with cortisol (hormone secreted by the adrenal gland). While insulin activates the uptake and storage of glucose in the muscle, fatty tissue and most importantly the liver through glycogenesis thereby decreasing blood sugar levels in postprandial[3] (Figure 1.3).

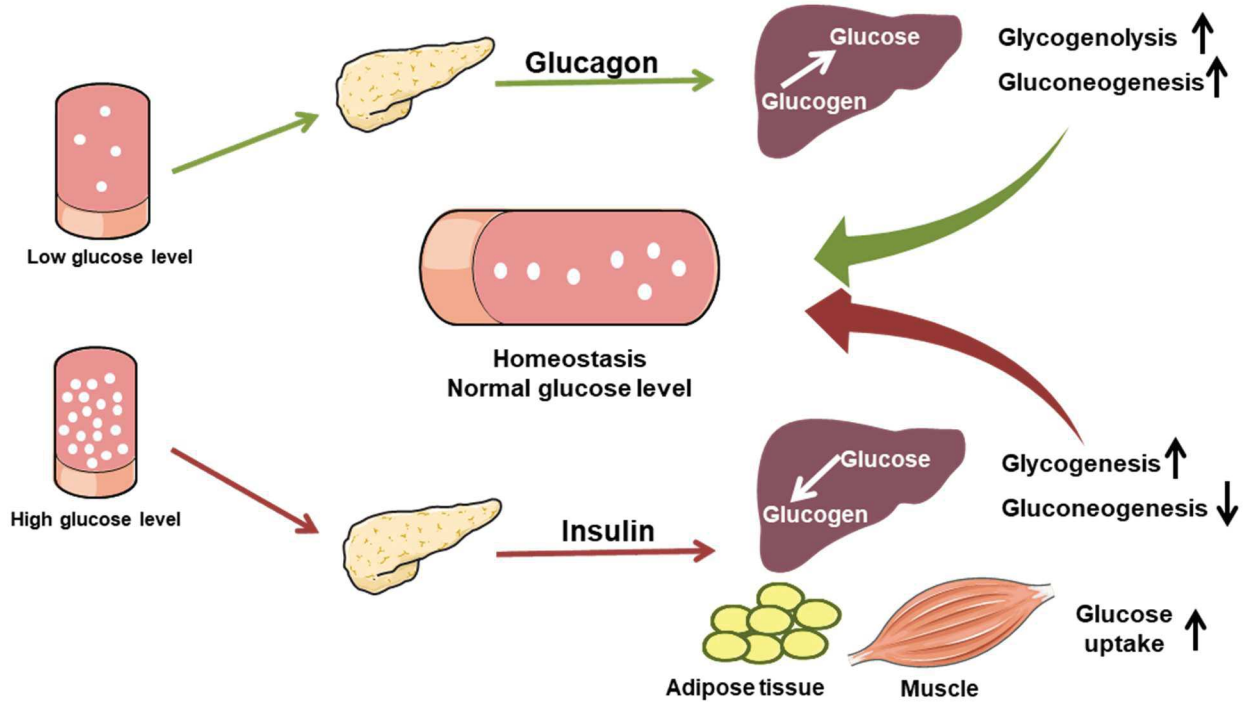

Figure 1.3: Negative feedback regulation of the glucagon secretion (green arrows) and insulin secretion (red arrows). Reproduced with permission from Jellali et al. 2020

The mechanism of regulation of blood glucose begins with the stimulation of insulin secretion that intensifies when blood glucose levels increase. The beta cells of the pancreas respond in a biphasic manner to this stimulus. First there is a rapid and brief rise (in the form of a peak) of insulin release, followed by a slower but constant release of the hormone (in the form of a plateau) over time[16].

The feedback loop that involves carbohydrates as an input signal and the synchronization of the insulin and glucagon release as an output allows the control of blood glucose and insulinemia to occur accurately and precisely[17].

The secretion of the two antagonist hormones is carried out in a pulsatile manner so that a simultaneous peak of insulin and glucagon would never occur. The synchronization of

hormones is of great importance for the regulation of blood glucose by the liver. This synergy between hormones is crucial considering that the liver is the main organ target to achieve glucose homeostasis in a reasonable time, since the organ uses about 70% of the hormones released from the pancreas during the first passage[18]. In the liver insulin activates glycogenesis, glycolysis and lipids synthesis, but unlike the mechanism in skeletal muscle and fatty tissues it does not stimulate glucose transport. The glycogen synthesis from glucose that occurs in the hepatocytes depends on the extracellular glucose concentration and on the presence of insulin, which triggers the glycogenesis pathway over a wide range of glucose concentrations. On the other hand, the glucagon activates the glucose release from the liver to the blood stream through the glycogenolysis pathway either from stored glycogen or by the gluconeogenesis mechanism from other precursors like lactate, glycerol and alanine[19].

1.2. Diabetes mellitus: physiology, pathology & treatment

1.2.1 Prevalence and healthcare impact

Diabetes mellitus (DM) is the most important dysfunction of the endocrine system of the pancreas that triggers a break in feedback closed loop that regulates the metabolism. DM have become the disease of the century due to the high morbidity and mortality with a prevalence of 463 million of diagnosed adults worldwide according to the International Diabetes Federation[20,21] (IDF and WHO official web sites, 2020). It can reach up to 20% of group population in 65 old people according to the IDF reports[23] (Figure 1.4). In fact, by 2045, it is estimated that people living with DM will reach 700 million. This is a group of metabolic disorders related with the endocrine pancreas.

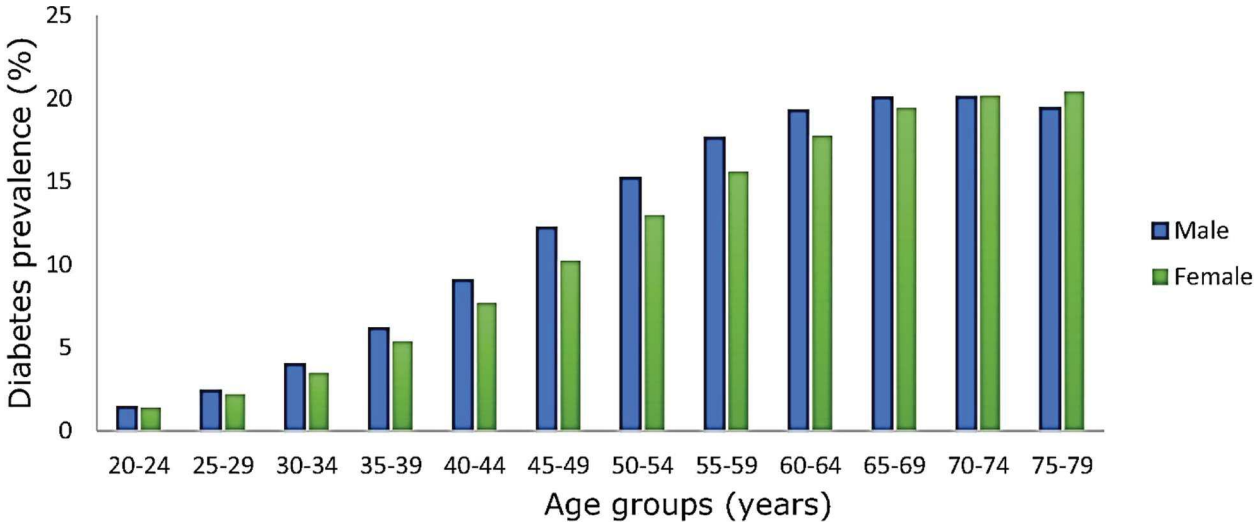

Figure 1.4: Diabetes prevalence worldwide in 2019 ranged by age and sex (reproduced with permission from Saeedi et al. 2020)

1.2.2. Physiopathology and treatment

Type I diabetes mellitus (T1DM) affects about 5%–10% of diabetes patients, mostly the young population. It is a chronic pathology occurring due to the autoimmune destruction of pancreatic beta cells. As a result, there is a disorder in blood glucose levels caused by hyperglycemia and the inability to store glucose due to the absence of insulin. It is a pathology with a complex clinical picture. The breakdown of the control mechanism of blood glucose severely affects other organs and systems on long term basis, causing blindness, kidney failure, cardiac arrest, stroke, limb amputation due to thrombosis, and even death[22,24]. The genetic predisposition to this form of diabetes is associated with mutations on chromosome 6 while the environmental predisposition causes that trigger the T-cells attack are even less known[25,26]. The early detection of antibodies in the blood can help to determine the state and differentiate the individuals with T1DM from other types of DM.

The function to be replaced in the case of insulin dependent diabetes is thus primarily the secretion of insulin by the pancreatic islet β cells, which has four characteristics: (a) it is continuous, even in the postabsorptive state, with rapid and transient peaks during meals; (b) it undergoes automatic regulation by blood glucose levels; (c) insulin is delivered into the portal blood system; (d) the endocrine pancreas is (of course) an internal organ placed within the body.

The most widespread treatment of T1DM is the daily and scheduled administration of insulin based on previous monitoring with a glucometer[27,28]. In the best cases, insulin injections, glucose levels monitoring, and a restrictive diet could successfully keep the patient safe from the risks of the extreme hyperglycemia. However, the variety of the clinical profile of the patients and the age reveals the limitations of insulin injections as a treatment. On the one hand, the production of insulin usually decreases progressively as the disease progresses, so the patient continues to produce their own insulin in small quantities. This makes it difficult to estimate the amount of exogenous insulin to be administered at each moment. On the other hand, due to the nature of the pathology, it usually manifests at an early age. This makes it difficult to control certain variables such as intake and physical exercise especially in neonates and children. In addition, to correctly apply the treatment, continuous education of the patient is required to maintain glucose in the appropriate ranges[29].

Another treatment based on the same principle as insulin injections, but with some improvements is the insulin pump or also called “continuous subcutaneous therapy”[30]. This approach is based on the subcutaneous delivery of insulin through a catheter connected to a peristaltic pump[31]. This allows the control of the glycemia 24 h maintaining the basal level of glucose in the blood. The control carried out by the insulin pump mimics quite well the pattern of glucose concentration given by a healthy pancreas. However, possible infections and fibrosis

at the site of catheter insertion are limiting factors of the use of the insulin pump as therapy. Despite the great advances that have been made in recent years for the development of this device[32], the response time is another limiting factor in terms of abrupt changes in glucose concentration[33].

Depending on the patient clinical profile of the T1DM, transplantation of the pancreas is sometimes chosen as a strategy to control glycemia. Since 1966, the success rates of transplantation of the pancreas have been increasing thanks to technical improvements in extraction, preservation and implantation. Up to now, more than 1500 pancreas transplants have been carried out according to the Collaborative Islet Transplant Registry (CITR)[34]. However, it remains an invasive intervention that is usually carried out when kidney transplantation is also required. And most importantly, it involves the submission of the patient to immunosuppressants for the rest of his life.

The transplantation of islets of Langerhans is another approach that is applied to the treatment of diabetes[35–38] Since the 1960s, the purification of pancreatic islets and their transplantation into different animal models have been the objects of many groups of research. Pancreatic islet transplantation is a promising therapy for patients with T1DM difficult to control[39]. It is a technique that provides an efficient and robust control of the homeostasis of glucose against the administration of insulin. However, islet transplantation remains controversial because it requires continuous immunosuppression that is harmful to both the graft and the patient[40].

Recent studies suggest that instead of focusing in beta cell mass replacement as a therapy for some types of DM, the development of new approaches to protect and restore beta-cells might be more efficient for the treatment and prevention of DM[41].

Type II diabetes mellitus (T2DM) is a heterogeneous set of pathologies that represents the 90 % of patients in the world. It is a disease with a complex clinical picture where the hyperglycemia results from a deficient insulin secretion combined with an insulin resistance. Beta cells dysfunction is not related to an autoimmune attack in this case, but is more related to the glucolipotoxicity[42–44]. Experts have named T2DM the disease of the century because of is increasing its prevalence exponentially in the last decades. T2DM induces the so called metabolic syndrome than includes several cardiovascular pathologies, hypertension and obesity. Environmental and genetic factors are involved in the development of T2DM[45,46]. However, the heterogeneity in the phenotype of the disease complicates its diagnosis and treatment. To this day, no definitive cure of neither T2DM or T1DM is available due the complexity of the disease and the lake of information about early detection, prevention and cure. The actual methods of study are based on extrapolating data of the mechanisms of organogenesis, function and

pathogenesis from animal to human preclinical studies. But again, this lacks accuracy due to the differences in the evolution of the species.

One of the key features of T2DM is the subsequent insulin-resistance state characterized by a drop-down of glucose uptake by the skeletal muscle, fatty tissue and liver. The insulin-resistance triggers the feedback loop break producing relative insulin insufficiency (Figure 1.5). From the pointview of predictive analytics, there is a direct correlation between obesity and T2DM. Studies have shown that both genetic and environmental factors are involved in the disparity of insulin secretion and action. Also, the deregulation of the chain reactions in the liver lead to glycogen depletion and glucose release to the bloodstream stimulating the chronic hyperglycemic state. From the endocrine pancreas side, the state of hyperglycemia and hyperinsulinemia triggers the increase if insulin production and beta cell proliferation as a compensatory effect of insulin resistance state[47–49].

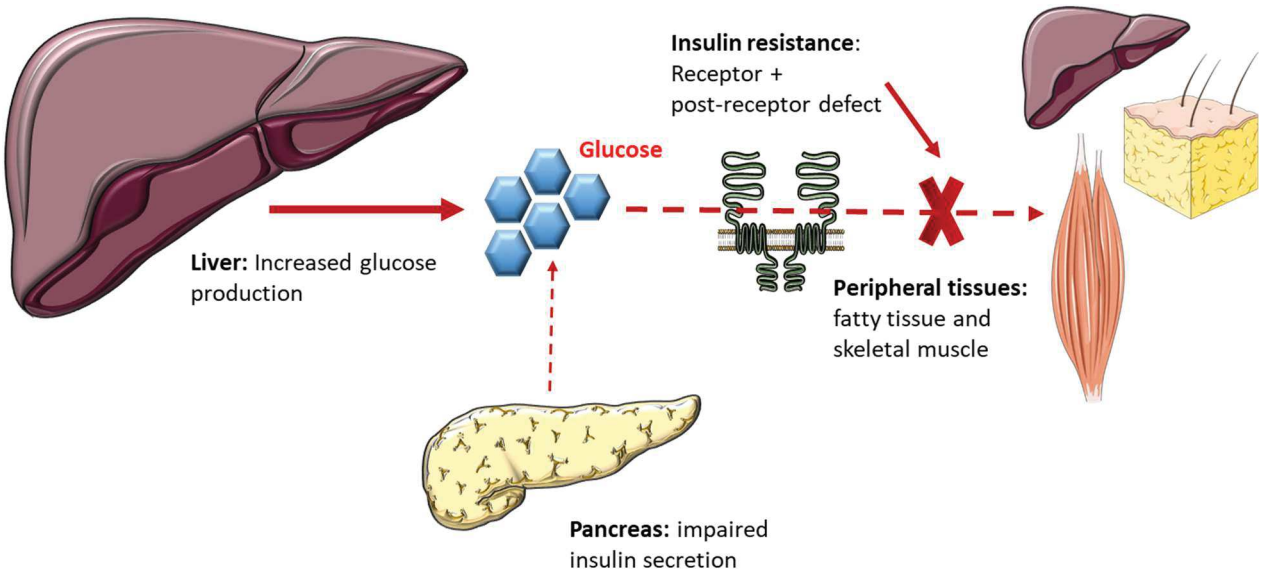

Figure 1.5: Metabolic abnormalities in type 2 diabetes mellitus that contribute to hyperglycemia (adapted from Jameson et al. 2015)

The current paradigm of care in T2DM patients includes a lifestyle intervention at one or several levels that can be combined or not with medication. The purpose of giving the patient a comprehensive diabetes education is to improve the outcomes of diabetes management since they are responsible for almost every diabetes related behavior and decision. Studies have shown that diabetes self-management education can be cost-effective and might induce the success of the treatment plan[50,51]. Sensitization about the importance of a continuous self-monitoring of blood glucose, the combination of exercise with an adequate nutrition by individualized dietary advice makes a substantial difference in T2DM progress and control. Moreover, the pharmacotherapy for the management of type 2 diabetes has been subject of extensive reviews

and guidelines from specialist groups and they can be classified according to the targeted tissue, speed of action, insulin analogues, insulin secretagogues or insulin sensitizers among others[52,53]. The future directions of T2DM therapy focus in new combinations of agents and existing drugs like insulin with GLP-1RA, an incretin-based drug (See next section) is a very promising approach that can allow patients to dispense with daily injections[54,55].

1.2.3. Insulin signalling mechanism and T2DM

As we previously mentioned, glucose metabolism is regulated by two antagonist hormones produced respectably by β and α cells of the pancreatic islets: insulin and glucagon. After a food intake, insulin is released to the bloodstream in response to high blood glucose levels and regulates glucose metabolism through its actions on skeletal muscle, liver, and adipose tissue. The binding of insulin to its receptor activates multiple proteins including Phosphatidylinositol 3-Kinase (PI3K) at the cell membrane. PI3K activity controls pathways regulating glucose transporter 4 (Glut4) translocation to the membrane, lipolysis, and glycogen synthesis. The activation of PI3K results in the uptake of glucose into the liver, skeletal and adipose tissues and storage of excess glucose as glycogen (liver and muscle). Insulin resistance in skeletal muscle is associated with impaired signaling through the insulin receptor/PI3K signaling axis with subsequent defects in Glut4 (the insulin-dependent glucose transporter) translocation and glycogen synthesis. In adipose tissue, insulin resistance is associated with a lowering fat storage and increased fatty acid mobilization. Insulin affects two major processes within hepatocytes, gluconeogenesis and triglyceride synthesis. Upon insulin receptor signaling, the transcription factor FoxO1 becomes phosphorylated and is excluded from the nucleus. FoxO1 controls the transcription of factors involved in gluconeogenesis, and inactivation of this protein normally results in a down-regulation of gluconeogenic activities. Insulin also activates the transcription factor SREBP-1c, which controls triglyceride synthesis. Under normal conditions, insulin signaling results in decreased hepatocyte glucose production and increased triglyceride synthesis (Figure 1.6). Individuals with insulin resistance present with hyperglycemia and hypertriglyceridemia even in the presence of high plasma insulin levels (hyperinsulinemia). This strongly suggests that within the liver, insulin resistance is partial. Insulin fails to suppress gluconeogenesis while the triglyceride synthesis pathway remains sensitive to insulin. This results in hyperglycemia and hypertriglyceridemia[2,3,56].

The insulin released inhibits hepatic glucose output while enhancing glucose uptake into muscle and adipose cells. Glucose is secreted through the glucose transporter GLUT2 in the liver, whereas the insulin-sensitive GLUT4 mediates glucose uptake in hepatocytes and adipocytes. The most important insulin signaling cascade required for this maintenance of blood glucose levels activates a key protein kinase Akt. This Akt protein kinase is required for insulin regulation of the pathways that control systemic glucose homeostasis, including glucose transport (GLUTs) in

adipocytes and muscle, inhibition of hepatic gluconeogenesis and cell-autonomous activation of hepatic lipogenesis[57]. Glucose transporter isoform 2 (GLUT2) is the most abundant member of the GLUT family and is highly expressed in the liver, pancreatic beta cells, and on the basolateral surface of kidney and small intestine epithelia. The GLUT2 (SLC2A2) can efficiently transport sugars due to its high V_{max} and K_m for glucose, and is well suited to managing large bi-directional fluxes of glucose in and out of cells. It plays a crucial role in glucose-sensing cells (beta cells and hepatocytes), which is sampling a wide range of blood glucose concentrations. In pancreatic beta cells, GLUT2 is required for the control of glucose-stimulated insulin secretion (GSIS)[58]. Moreover, it also transports other types of sugar such as galactose, mannose and fructose. The expression levels of glucose transporters is not exclusively regulated by glucose and insulin levels but also by cytokines including interleukin-6, which is highly expressed in diabetes and can amplify insulin resistance via effects on GLUT4[59,60].

Insulin exerts all of its known physiological effects by binding to the insulin receptor (INSR) on the plasma membrane of target cells. There are two INSR isoforms, A and B, but the most specific one for insulin is the B type; it is mainly expressed in differentiated liver, muscle, and white adipose tissue. Consequently, INSR is responsible of most metabolic effects of insulin. In all cell types, INSR binding activates the cascade of the metabolic signaling by first recruiting phosphotyrosine-binding scaffold proteins, which in turn activate downstream effectors[60]. The

recruitment of diverse phosphotyrosine-binding proteins to INSR allows an early ramification of insulin signaling in order to activate various functional modules[60,61].

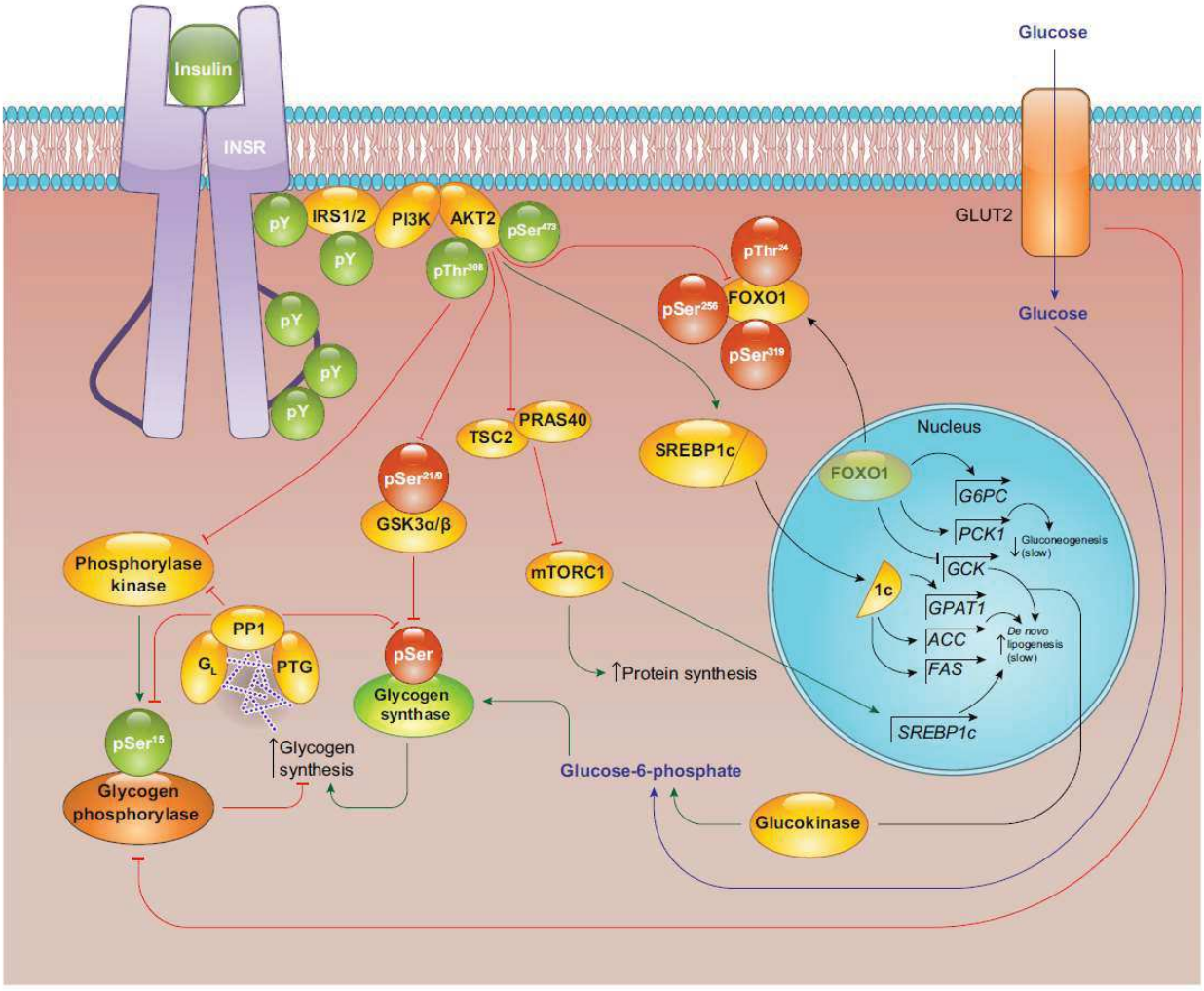

Figure 1.6: Hepatic insulin signaling (reproduced with permission from Petersen et al. 2018)

The liver plays a key role in the glucose homeostasis mechanism. Previous studies have shown that the beta cells regeneration and proliferation is regulated by a signaling pathway controlled by the liver and mediated by the nervous system and endocrine factors [62,63]. Araujo et al. reported the relevance of hepatocyte grow factor (HGF) as a mediator in the compensatory response during the insulin-resistance state [64–66]. However, the cellular mechanism that triggers the signaling pathway to produce this hepatic humoral response remains unknown.

Liver insulin resistance is the most relevant characteristic of T2DM pathophysiology. Hepatic insulin resistance has been characterized by a reduction of insulin-stimulated signal transduction pathways for hepatic glucose production, including INSRs and downstream mediators[58,60]. Chronic hyperglycemia and excessive glucose intake by the liver associated with the accumulation of hepatotoxic lipids as well. This “glucotoxicity” also includes the activation of

lipogenic enzymes and induction of endoplasmic reticulum stress, eventually leading to steatosis and apoptosis[60].

Glucagon (GCG), which is released from pancreatic alpha cells in response to low blood glucose levels, acts on hepatocytes to promote glycogen breakdown (glycogenolysis) and to promote glucose synthesis via gluconeogenesis. While, glucagon-like peptide 1 and glucagon-like peptide 2 (GLP-1 and GLP-2) are secreted by intestinal endocrine L- cells. They also considered a key regulator of glucose homeostasis and intestinal epithelial function. The 3 peptides carry out their action via interaction with specific receptors that exhibits distinct patterns of tissue specific expression[55]. The net effect of glucagon signaling is an increase in blood glucose levels (Figure 1.7). The secretion and inhibition of glucagon is regulated by neuropeptides, hormones, metabolites and the autonomic nervous system. For reasons that are not entirely clear, patients with type 2 diabetes often present with hyperglucagonaemia which results in continued glucose output by hepatic cells. This suggests that targeting glucagon signaling in hepatocytes may be a viable treatment option for type 2 diabetes[67]. Therefore, glucagon-like-peptide were developed as candidate therapy. Among them GLP-1 analogues improve hyperglycemia in T2DM patients[68–72].

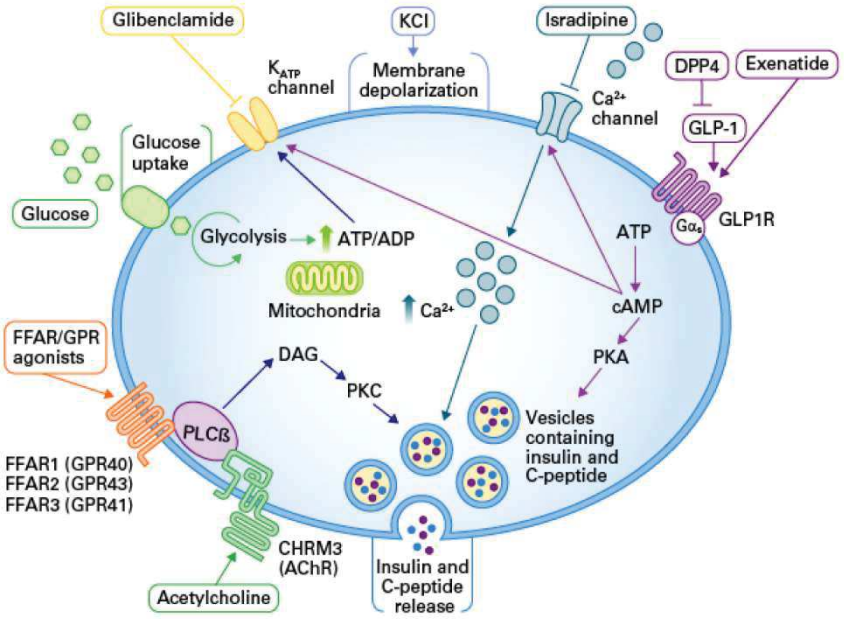

Figure 1.7: Interaction mechanism of drugs like GLP-1 with pancreatic beta cells (reproduced with permission from TAKARA Bio catalogue)

1.3. In vitro models for diabetes research

In order to establish therapies and new treatments of DM, it is necessary to understand the human endocrine system, its function and the consequences of its failure. Studies have shown that both genetic and environmental factors are involved in the disparity of insulin secretion and action.

The vast majority of the available information on β-cell mass and function in DM comes from experiments on rodent models (mostly mouse)[73]. However, many studies have shown how rodent Islets of Langerhans differ from human ones at all levels, especially regarding β-cell mass regulation[41,67]. Primates and pigs are the closest large animal to the human physiology, in particular when it comes to the development and the study of the disease progression of DM[74,75]

The main challenge for researchers focused on studying diabetes and other metabolic disorders is the disease progression modelling in an accurate and reproducible way. Currently, the gold standard in diabetes research and drug screening is the use of models based on some insulin-producing beta cell lines or primary pancreatic islets of Langerhans. However, despite the huge progress done in the field of *in vitro* models, and besides the conventional drawbacks related to the cost, the low reproducibility due to different genetic backgrounds and the lake of donors, the variability introduced by cell type and assays lead to bias in the interpretation. Therefore, it is essential to propose advanced *in vitro* model as alternative to animal trials.

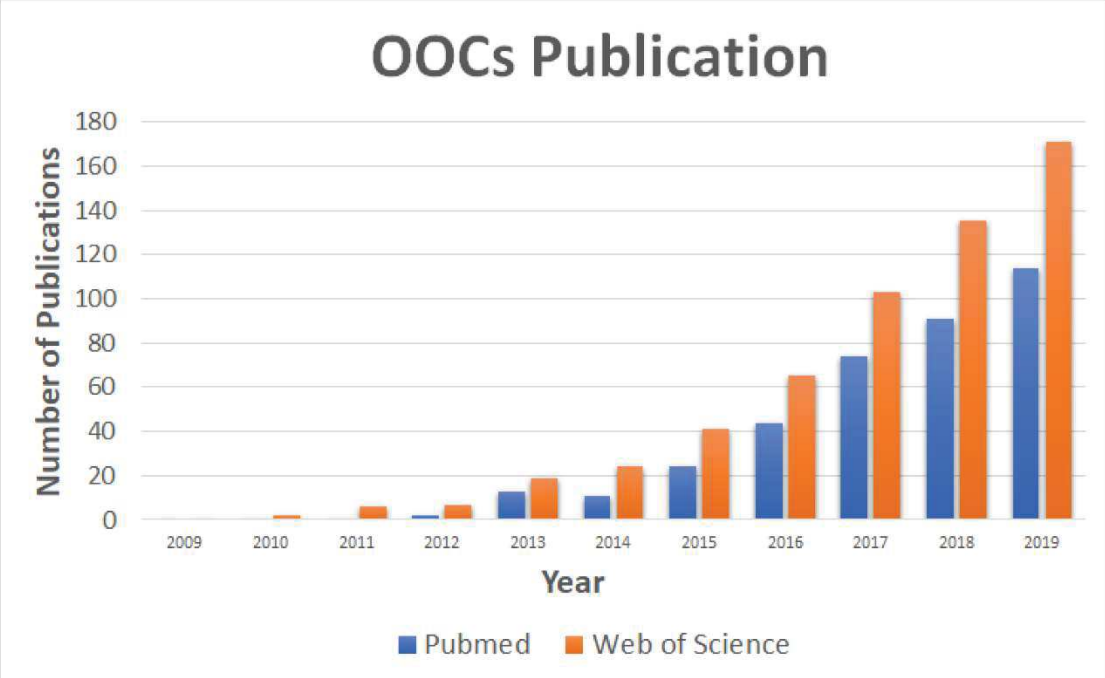

Figure 1.8: The publication history of organs-on-chips (OOCs) over the past decade according to Web of Science and Pubmed (reproduced with permission from Puryear III et al. 2020)

In addition, cohort studies have found a direct relationship between liver related diseases and diabetes mellitus. Notably, there is a high susceptibility of diabetes development in the post-operatory of liver transplantation. While Diabetes Mellitus is considered a high risk factor of hepatocarcinoma and chronic liver diseases[76–81]. The crossed mechanisms of induction between these pathologies remains unclear[82]. Therefore, several studies aimed to explore the interaction between the liver and the pancreas in a healthy and pathological model as well[83,84]. Based on our previous consideration of important liver pancreas interaction, we will focus on advanced *in vitro* models related to organ-on-chip technology and co-culture modalities. Briefly organ-on-chip consists of miniaturized bioreactors that can mimic and reproduce several physiological features of specific cell types or tissues at a microscale level. The power of organs-on-chips (OOCs) to reproduce a physiologically relevant microenvironment for drug testing and disease modelling is behind the tremendous growth and fast evolution of this technology over the last decades[85] (Figure 1.8). Before describing the advanced in vitro tools, we propose herafter first a focus on data analysis, that should then be performed with the different models.

1.3.1. Current analytical tools for model assessment and analysis

The development of high throughput technology in the last decades has powered the discovery-based approach by providing access to larger quantitative datasets. Omics technologies provide a global picture of the molecules involved in the reaction chains and dynamic networks that make up the central dogma of molecular biology. Significant progress has been made in disease research thanks to the disciplines that study the different biological layers: genomics, epigenomics, transcriptomics, proteomics, metabolomics and microbiomics[86]. The integration of multi-omics layers provides a unique opportunity to understand and assess the interactions of a set of molecules behind the biological phenomena[87] (Figure 1.9).

A variety of analytical platforms are available to characterize the behaviour and the activity of cells as they should react to physical or chemical challenges. These platforms provide a high sample throughput and the generation of big data sets. Omics are part of these analytical platforms. Among those techniques, there are genomics that provide the individual genetic blueprint and how is dynamically regulated in different states of health, disease, toxicity and aging. Transcriptomic methods are designed to provide a complete analysis of the mRNA level of gene expression transcribed in a specific moment. Proteomics, the study of the proteome, includes all the proteins that make up a cell compartment, a cell, a tissue or an entire living organism. The metabolomics, or the study of the metabolome, consists of analysing the compounds produced during chemical reactions taking place in cells or body. It allows the assessment of the cell status and detect small variations during *in vitro* culture. In our context, the metabolomics can provide useful details to establish pancreatic disorder signatures and to search early biomarkers[82,88–91].

The objective of all these omics techniques is to understand how tissue behaves at various levels. This particularly requires an understanding of the relationships between the factors that alter omic responses and the effects of these responses on the organism. The biomarkers are then identified by applying meta-statistical analysis on the corresponding datasets. Appropriate

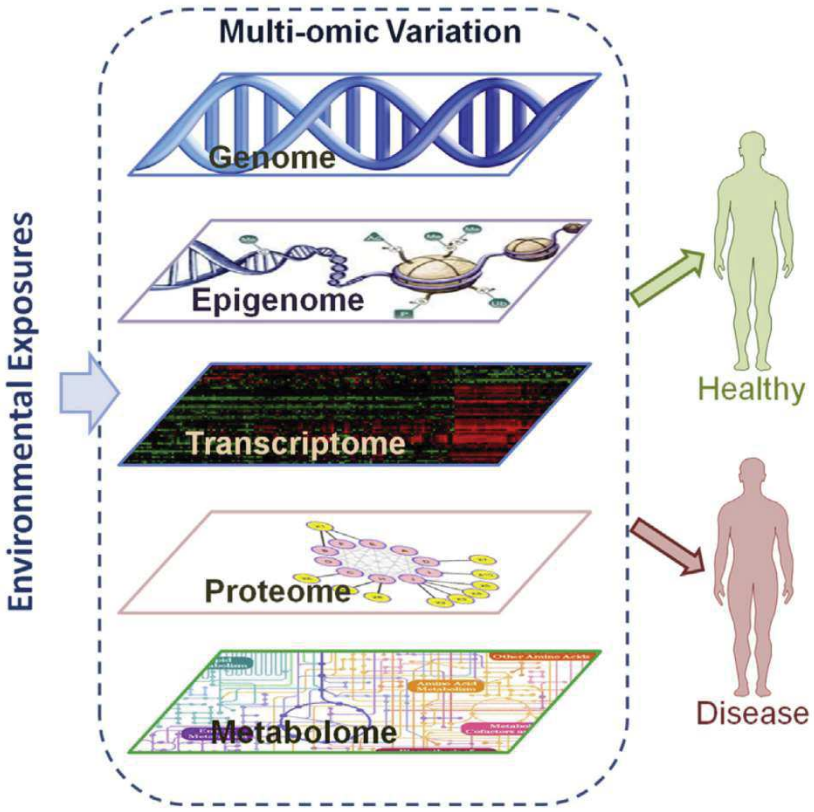

Figure 1.9: Conceptual model of multi-omics and human disease (reproduced with permission from Sun et al. 2016)

statistic methods, including adequate sample size, proper adjustments, and correction for multiple testing are required[92]. Data-driven approaches (data reduction via clustering, classification using for instance neural network, visualization using principal component analysis and then network analysis) make use of now-prevalent high throughput datasets that facilitate the elucidation of underlying structure. Knowledge-based approach relies on the increase use of systems biology to integrate heterogeneous data into existing knowledge-databases (Metabolite Set Enrichment Analysis MSEA, pathway network-KEGG, customized system biology model, etc…). Knowledge-based approach aims to facilitate the understanding of disease and biological process mechanisms (mechanistic analysis) at the systemic level[87].

Additionally, to the omics profiling, in order to understand the flow information and the crosstalk between multiple molecular layers involved in a biological phenomenon, the integrative analysis of multi-omics data will address the gap in our current knowledge of molecular mediation mechanisms[87,93,94]. The bottleneck for life science studies has shifted from generating

the data to interpreting results so as to derive insights into biological mechanisms. Thus, the development of refined *in vitro* strategies and of pertinent *in vivo* models to reproduce human physiology, human disease and thus to the identification of robust biomarkers requires careful attention[95].

1.3.2. Potential cell source for liver and pancreas modelling

Modelling endocrine pancreatic cells physiology and dysfunction *in vitro* is essential to understand the pathomechanisms underlying DM[96]. The cell sources used for those culture models can be classified in 3 groups: human or animal cell lines (EndoC-βH1–3[97,98], MIN6[99], INS-1[100],RIN5-F[101] αTC1.9[99]), primary islets of Langerhans (from human, rodents or pig) and human stem cells (embryonic pluripotent stem cells (EPSC)[102,103] or induced pluripotent stem cells (iPSC)[104,105]). Meanwhile, liver modelling has been extensively used for drug testing and hepatic disease research and the cell source is currently chosen according to the application of the liver *in vitro* model[106]. The available hepatic cell sources for *in vitro* culture are also classified in 3 groups: primary hepatocytes or non-parenchymal cells, stem cells (hESCs or hiPSCs) and immortalized cell lines (hepatoma cell lines[107], HepG2 cell lines[108,109] and HepaRG cell lines[110]).

Cells source	Advantages	Drawbacks
Stem cells **hESCs and hiPSCs**	▪ Availability ▪ Feasibility of healthy and pathological profiles ▪ Reproducibility ▪ Unlimited growth ▪ Patient-specific derivation	▪ Limited functions ▪ Lake of full maturity ▪ Ethical preoccupation (hESCs) ▪ Epigenetic memory (iPCSs) ▪ Risk of mutagenesis due to vectors used for reprogramming ▪ High cost
Immortalized cell lines	▪ Unlimited sources (easily proliferate) ▪ Low cost ▪ Easy to maintain ▪ Suitable for long-term ▪ Well characterized	▪ Low functionality ▪ Differs from primary cells ▪ Limited genetic modification
Primary cells & ex vivo tissues	▪ High functionality ▪ Reflect in vivo physiology ▪ Well characterized	▪ Rapid de-differentiation *in vitro* ▪ No proliferation *in vitro*

		▪ Limited availability (donors) ▪ Inter-donor variability

According to the features reported in the literature, primary cells still being the most suitable to investigate complex drug effects or disease and the lack of long-term viability and function can be solved with the use of bioreactors, microfluidic chips and co-culture with other cell types (see table). However, the shortage of donors and the imminent de-differentiation of the ex vivo cells lead to consider iPSC as an alternative since they allow the establishment of cell models with the desired disease-associated genetic background[96] (Figure 1.10). Meanwhile,

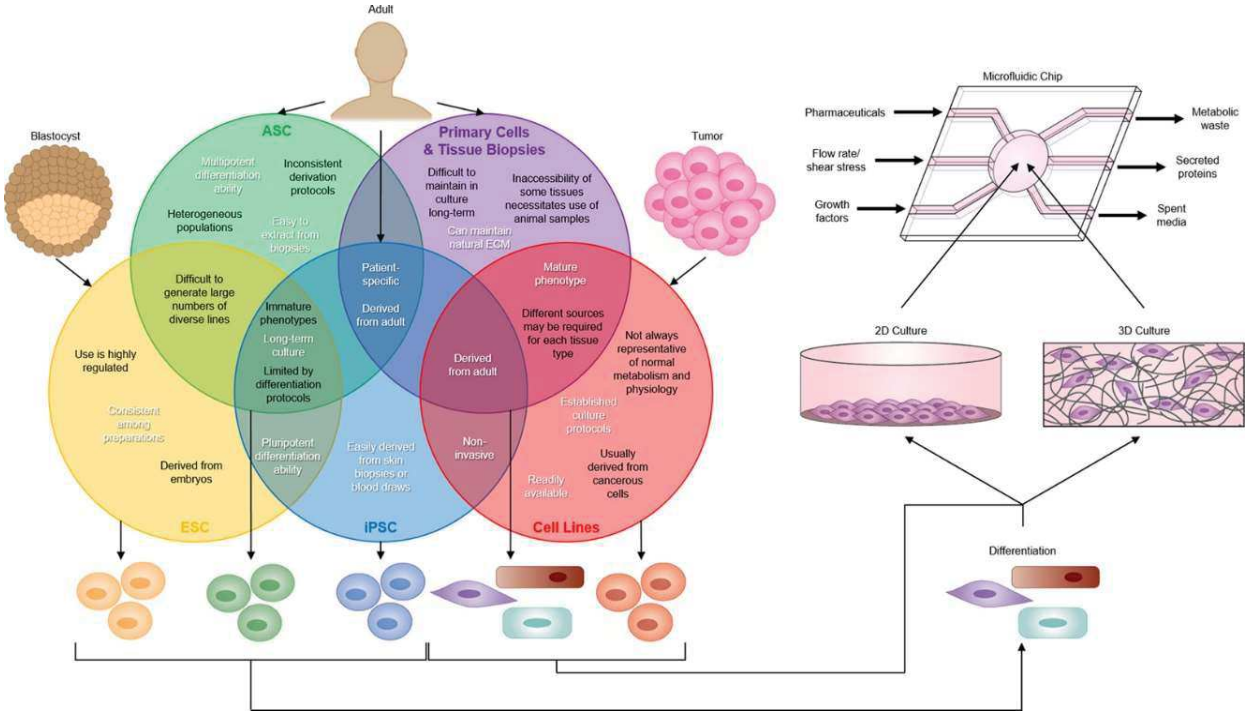

Figure 1.10: Tissue sources for organ-on-chip modeling (reproduced with permission from Wnorowski et al.2019)

hepatic and pancreatic cell lines have been extensively used within *in vitro* models due to the easy access and maintenance. But in the case of liver, they do not express most of the Phases I and II metabolic enzymes, and those that are expressed are not physiologically relevant[5]. In parallel, the available cell lines for endocrine pancreas modeling do not have the same insulin secretion profile and glucose responsiveness comparable to the primary cells[15].

1.3.3. Benefit of co-cultures

In order to improve and preserve hepatocytes and endocrine pancreatic cells function and performance for long-term, several culture configurations have been developed[4]. It is well known that non-parenchymal liver cells play a crucial role in modulating liver homeostasis,

organogenesis and injuries repairing through growth factors, inflammatory mediators and reactive intermediates[111,112]. LSECs, Kupffer cells and stellar cells not only support and contribute to compounds metabolism but also enhance hepatocytes performance and function *in vitro* studies[113–115]. On this basis, several groups of research tempted the co-culture of hepatocytes not only with non-parenchymal cells but also other tissues.

On the one hand, with the aim of enhancing hepatocytes *in vitro* culture, Kaufmman et al. used pancreatic islets of Langerhans for the continuous hepatotrophic stimulation (insulin, glucagon, somatostatin and hepatocytes growth factor and epidermal growth factor) witch was proved to be necessary for transplantable bio-artificial liver (BAL) systems[116]. Similar study was carried out by Kuo et al. were they investigated the effect on viability and function of pancreatic islets over hepatocytes from different species of mice and their possible application for the BAL[117]. Considering that the main source of hepatotrophic factors necessary of the BAL is the endocrine pancreas through the portal venous blood, Lee et al. aimed to make a new type of spheroids and evaluate the effect of pancreatic islets on hepatocytes. The aggregates were formed without dissociating the rat islets of Langerhans. Hepatocytes and islets were cultured as a suspension in spinner flasks, and spheroids were formed by hepatocytes aggregation around the pancreatic islets without considering the ratio of cell types. The purpose of this study was to reflect *in vitro* the clinical conditions of hepatotrophic stimulation in a future hepatocytes transplantation or in a BAL system[118].

Pancreatic islets have proven to be an excellent in vivo hepatic functional supporting system[119]. On basis of the previous reports, Gao et al. aimed to confirm the feasibility of xenotransplantation of microencapsulated of islets of Langerhans and hepatocytes as a BAL system. The alginate microcapsules with different ratios of hepatocytes to pancreatic islets were injected in the abdominal cavity. The hybridization between pancreatic cells and hepatocytes has shown a high performance compared to encapsulated hepatocytes xenotransplantation[120].

On the other hand, considering that the most common engraftment site of pancreatic islets transplantation (T1DM therapy) is the portal vein of the pancreas, there was an imminent need to explore the effect of hepatocytes over pancreatic islets and study their interaction in order to prevent bioartificial pancreas intrahepatic transplantation failure[121]. Accordingly, Kim et al. studied *in vitro* the behaviour of spheroids made by a mixture of hepatocellular carcinoma cell line (Hep-G2) and the rat insulin-secreting cell line (RIN-5F). They reported synergistic effects between the hepatocyte cell line and insulin-secreting cells. Especially, a beneficial effect of hepatocytes as a support of insulin-secreting cells for the generation of artificial islets[101]. They extended their *in vitro* study performing the co-culture under hypoxic conditions of incubation in order to mimic the ischemic conditions of pancreatic islets after transplantation[122].

To enhance beta-cells survival, insulin secretion, proliferation and gluco-cytotoxicity resistance, Green et al. co-cultured clonal β-cells with GLP-1 and glucagon-secreting cell line. They suggest the consideration of therapeutic approaches using antagonists' hormones (insulin and glucagon) to address effectively diabetes treatment. Glucagon and GLP-1 are minted to directly enhance β-cell function and indirectly promote insulin sensitivity and reducing blood glucose levels[99].

Other research groups chose to address diabetes modeling by the creation of an insulin resistance model, one of the main characteristics of T2DM, choosing other organs or tissues different than the pancreas and the liver [123]. Park et al. developed a 3D co-culture model with the aim of increasing the selectivity of anti-diabetic and anti-obesity drugs –metabolic syndrome- for humans. For that purpose, they cultured and differentiated alginate-encapsulated Human Adipose-derived mesenchymal stem cells (ADMSC) and human RAW264.7 macrophages in a 3D environment. They claimed a successful performance of the in vitro model to mimic insulin resistance and realistic response to anti-diabetic and anti-obesity drugs like: Acarbose, metformin, exendin-4, KR-1, KR-2, and KR-3 [124].

1.3.4 Organoids/spheroids

The 3D cell culture models, also called multicellular spheroids or organoids (mixture of different cell types) are commonly formed by self-assembly of single cells. The aim of this culture modality is to bridge the gap between animal models and conventional 2D cultures in monolayer[125]. Spheroids vary in size and in shape depending on their heterogeneity, cell type composition, developmental stage or maturity and the organ or tissue aimed to reproduce. The current standardized methods of spheroids formation with a defined diameter and spheroidal shape are: suspension culture technologies[126,127], hanging drop[128], and non-adhesive surfaces[125,129]. Several studies have reported the development of microfluidic biochips with clever design for the automation of spheroid formation, manipulation, high-throughput screening and long-term culture[130].

A key feature to enhance cell viability in large aggregates with a high cell density is the oxygen supply for long-term cultures. Accordingly, Shinohara et al. proposed a PDMS based plate that combines a non-adhesive honeycomb microwell structure that enhances spheroids formation in a short-time with the high permeability to oxygen provided by the PDMS support

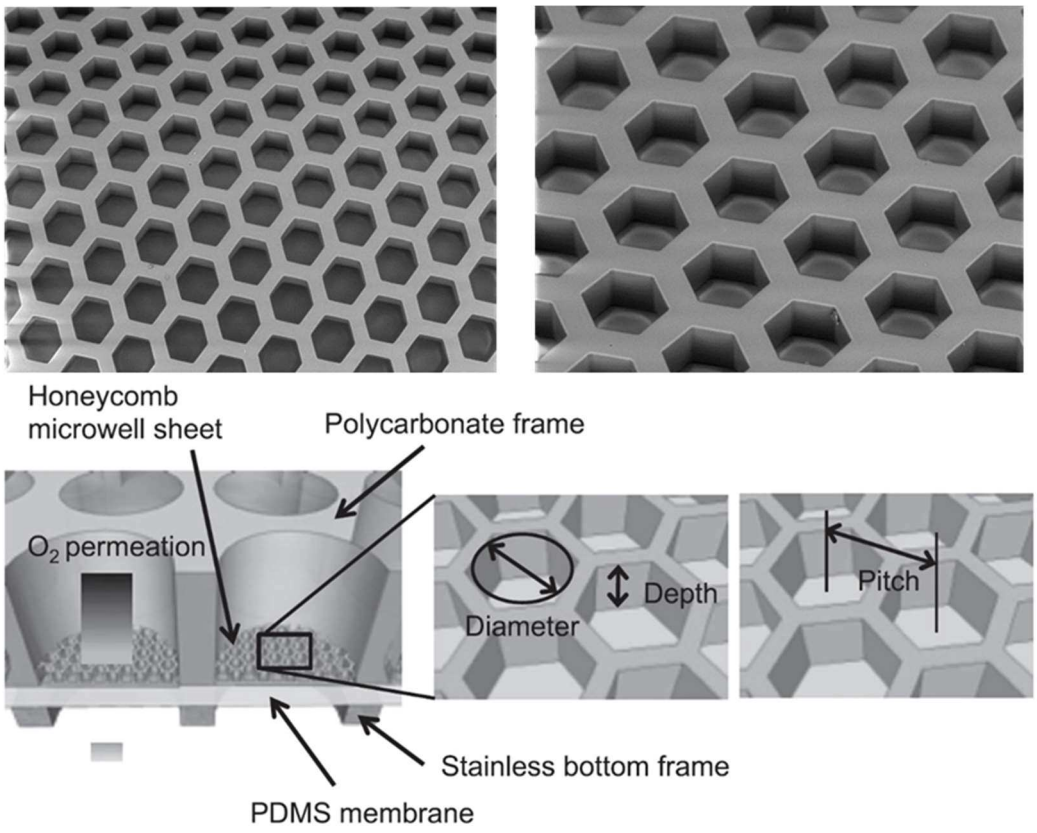

Figure 1.11: Schematic illustration of the oxygen permeable PDMS-based Honeycomb microwells plate (adapted with permission from Shinohara et al. 2017)

material[131,132] (Figure 1.11). They reported an efficient formation of MIN6 aggregates (insulinoma cell line) using the honeycomb microwell culture system with different sizes[131]. Thanks to controlled size and density, spheroids are ideally suitable for integration on microfluidic chip platforms[133,134]. Another unique approach for organoids generation from single cells was reported by Fu et al. where they used a U-shape obstacles in a microfluidic device perfused vertically they succeeded to make functional organoids[130]. Cell trapping and aggregation was achieved by applying gravity against perfusion flow and the sizes of MCS was tuned according to the magnitudes of the U microstructure. The U-shape PEG hydrogel microstructures protected cells from shear force damage without depriving them from diffusion of nutrients and wastes. The spheroids generated from a mixture of Balb/c 3T3 fibroblasts and HepG2 (hepatocarcinoma cell line) had a homogeneous size and high viability. Additionally, the sequence of cell loading to the biochip and the speed of cell inoculation conditioned the cell distribution in the resulting aggregates[130].

In order to improve the understanding of cell-to-cell or organ-to-organ interaction between hepatocytes and islets of Langerhans in vivo, a spheroidal 3D co-culture model of rat hepatocytes and dissociated islets of Langerhans was developed by Jun et al. The hybrid spheroids were encapsulated with an alginate-based hollow fibre using a microfluidic device in order to prevent immune rejection of xenotransplantation. The resulting aggregates were assessed in vitro and they harvested them before encapsulation by a PDMS-based device. Then they transplanted the graft into intraperitoneal cavity of diabetic mice. Both in vitro and ex vivo analysis have shown a long-term stability and functionality of beta-cells functions (Figure 1.12). Moreover, the in vivo tests suggest that co-culture with hepatocytes could solve partially the shortage of donors for pancreatic islets transplantation[84,135].

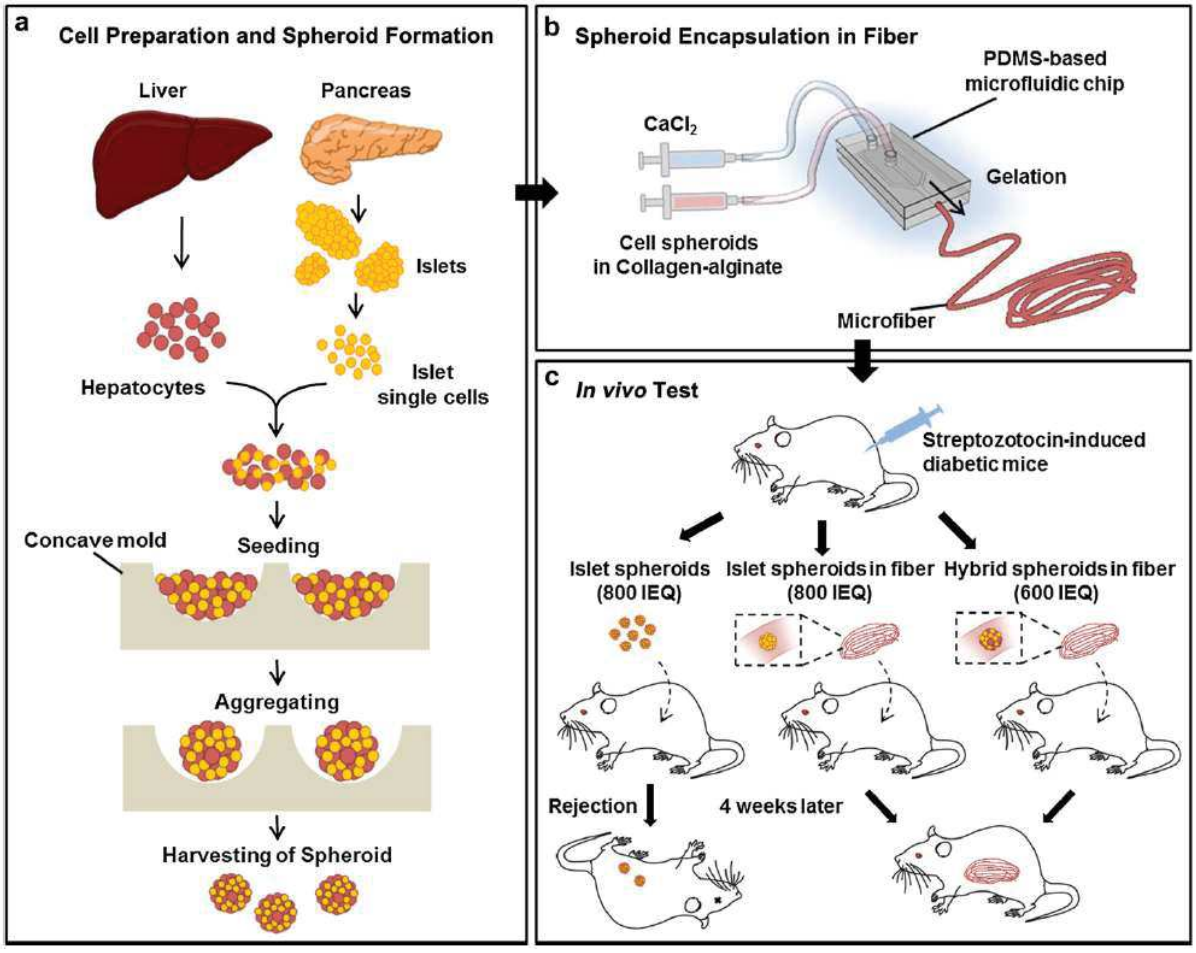

Figure 1.12: Schematic representation of the hybrid spheroids fabrication, encapsulation and transplantation in the intraperitoneal cavity of diabetic mice (reproduced with permission from Jun et al. 2013)

1.3.5. 3D bioprinting

Some simple culture designs lack the capacity to emulate the complex 3D multicellular architecture effectively for some specific function or disease mechanism that involve the cell-to-cell interaction and a particular ECM composition. For that purpose, emerging bioengineering techniques like 3D bioprinting have displayed a high performance controlling the creation of geometries and structures approaching the complexity of native organs/tissues[136]. 3D bioprinting is defined as is an additive manufacturing technique capable of producing scaffolds with defined architecture for multiple bioengineering applications. It is an advanced fabrication process where cell-charged bioinks are used to create native 3D tissue-like cell organization[137]. It offers a precise control over the special placement of biomaterials, cells and biologically active molecules to guide the morphogenesis of the tissue[138–140]. Matai et al. reviewed the different bioprinting modalities and their applications in the field of cancer research, bioartificial organs, high-throughput screening and organ-on-a-chip models[141]. The emergence of synergistic approaches that combines bioprinted tissues has the potential to revolutionize *in vitro* testing platforms and reach a more relevant microenvironment overcoming once for all the mass transfer limitations[137].

One of the main issues for liver *in vitro* modeling is the lack of longevity and tissue-level complexity (hepatic functions). With the aim of solving those problems, Grix et al. reported the development of a bioprinted liver organoids HepaRG-based using a stereolithographic printing approach. They demonstrated the perfusability of the organoids' intrinsic channel system for a future organ-on-chip application[110]. Proof of concept experiments were presented by different groups for a bioprinted liver-on-chip system combining different parenchymal and non-parenchymal liver cells, for the assessment of drug-induced liver toxicity[108,109] or to reproduce the *in vivo* microenvironment by integrating the biliary system[142]. While for the 3D bioprinting implementation with pancreas-on-chip models, is still in development[140]. In this case, the requirements are challenging since the density of native pancreatic islets is very high witch implies the conception of a highly vascularized system within the scaffold. Few studies have achieved bioprinting islets of Langerhans within a biomaterial and characterize the printed tissue *in vitro* and *in vivo*[143,144].

Ultimately, the combination 3D bioprinting, microfluidics, organoids and stem cell technology is the future of in vitro modeling of human surrogates to effectively create more in-vivo like 3D microenvironments[145]. Compared to conventional organ-on-chip models, bioprinted micro-tissues inside microphysiological systems will provide much more shear stress through the perfusion flows due to their spatial architecture. The fusion will allow the creation of customized scaffolds structure and optimized coating for better cell adherence in order to preserve the structural integrity over the long-term[137,146].

1.4. Microfluidic systems and cell culture

1.4.1. Microphysiological model of human liver tissue

Organ-on-chip technology is a powerful bioengineering tool to investigate physiological *in vitro* response in drug screening development and in disease advanced models. It allows mimicking the native microarchitecture, it enables the construction of well-controlled microenvironment bridging the gap between *in vitro* and *in vivo* animal model. in order to overcome the limitations of the conventional liver model and get a reliable high-throughput results in a cost-effective way, many liver-on-a-chip and micro platform-based bioreactors have been developed in recent decades[147].

In this frame, our laboratory has been developing over the past two decades a liver-on-chip system with a simple design proving the power of microfluidic-based models for the discovery of new insight in liver metabolism[148–150], biomarkers identification[151–154] and predictive toxicology coupling *in silico* models[155]. Therefore, those models were able to predict well the human hepatoxicity by identifying biomarkers and metabolic signatures in response to drugs (such as paracetamol, which provides potential new ways to evaluate risk factors by clinicians); Those data were correlated with GSH depletion kinetics using mathematical system biology models to propose in vivo extrapolation (and thus replying to industrial demand to understand GSH biomarker kinetics[155]. They also explored possible alternatives to PDMS as standard for biochip support material such like the perfluoropolyether dimethacrylate in order to improve oxygen permeability[156]. Meanwhile, they built several prototypes with real-time monitoring of the metabolic activity using a liver on chip coupled with mass spectrometry to reply to industrial practical implementation of biomarker identification but also to follow complex biomarker kinetics for clinical diagnosis[157]. In parallel, for automation and multi-organ integration they proposed an Integrated Dynamical Cell Culture in Microsystems (IDCCM) box[153,158–160].

Illustrating the increasing interest of liver disease application, few groups studied the none alcoholic liver disorders using a human liver on chip approach. In parallel, other studies focused on toxicological effects of pesticides using liver human primary tissue demonstrated also steatosis formation in organ-on-chip technology[161,162]. However, those studies did not consider (i) the human variability; (ii) the liver complexity of the disease involving hepatocytes, endothelial and cholangyocytes cells, (iii) the liver-multi organ system complexity of diseases such like the metabolic syndrome; (iv) the integration of *in vivo* cohorts for further validation[163].

1.4.2. Microphysiological model of endocrine pancreas

Pancreas-on-chip application can be classified in 4 groups with different state of progress in each one of the possible application (Figure 1.13). So far, the most largely explored application group is the trapping and interrogating the ex vivo islets of Langerhans before transplantation [164–167].

1.4.2.1. Specific cell tissue differentiation

Hirano et al. reported the use of a PDMS-based biochip with an open channel and a microstructure design with 382 microwells for human iPSC differentiation to pancreatic islets-like. They successfully differentiated hiPSCs to pancreatic islets-like from single cells with a homogeneous size of spheroids. The viability of the aggregates was over 95% and they expressed typical endocrine hormones such like insulin, glucagon and somatostatin. Similar approach was reported by Tao et al. with a successful differentiation of hiPSC to islets organoids. The novelty of their device is the integrated analytical tool allowing a real-time imaging of the spheroids during the differentiation process[168]. Those studies highlight the power of organ-on-chip device to optimize the culture and differentiation of hiPSC to functional pancreatic islets.

1.4.2.2. Islets evaluation and drug screening

Microfluidic biochips have been extensively explored for functionality assessment of the pancreatic islets before transplantation in order to reduce the bioartificial pancreas failure. They mostly focus in the short-term culture of islets of Langerhans and the optimization or automation of the sampling process[169–172]. With the same goal, different approaches of microphysiological platforms have been reported for evaluating the islets responsiveness to glucose stimulation[173,174]. Lin et al. have used a cell line based pancreas-on chip model to study the effect of adiponectin as an antiapoptotic therapy strategy[175].

It should be noted that progress has to be made in order to produce a cost-effective analytical platform for *ex vivo* islets assessment prior to transplantation in patients with T1DM[40]. The ultimate goal of the organ-on-chip technology in this scope is to became a pre-treatment platform for islets to enhance the intracellular flow and reduce the necrotic core[176].

1.4.2.3. Study and diagnosis of pancreatic cancer (PCa)

Pancreatic adenocarcinoma is a lethal disease that affects more than 484486 worldwide and is causing more than 456280 deaths by the end of 2020 according to the International Agency for Research on Cancer[177,178]. The poor treatment outcome of the PCa is due to the rapid and often symptoms-free progression compromising the survival rate of patients. Over a 90% of PCa

are diagnosed in the metastatic stage[179]. Several studies including the meta-analysis carried out by Stevens et al. have concluded that diabetes mellitus is a definitive risk factor for pancreatic cancer[180]. However, recent studies provided evidence of the bidirectional causality between PCa and DM[181].

The early diagnosis and detection of carcinogenesis biomarkers is the key to improve the survival rate of patients with PCa. In this context, biosensors and microfluidic device platforms have been developed for the capture and analysis of circulating biomarkers including: proteins, glycoproteins, nucleic acids, exosomes and cancer cells in the blood sample or biopsies[182–187]. Thege et al. reported the use of a microfluidic chip that captures circulating tumor cells from blood or cell suspension with cancer-specific antibodies inmunocapture (MUC1 and EpCAM)[183,188,189].

1.4.2.4. Study of islets physiology

Microphysiological systems dedicated to *ex vivo* culture of pancreatic islets in a controlled microenvironment with integrated analytical tools offer a new and robust engineering approach[190]. In order to maintain the islets functionality for long-term cultures, it is necessary to understand the intracellular mechanisms of pathogenesis[176,191]. Lee et al. reported a new microphysiological analysis platform (MAP) that allows the generation of 3D beta-cell spheroids and create a glucolipotoxicity-induced diabetes model[192].

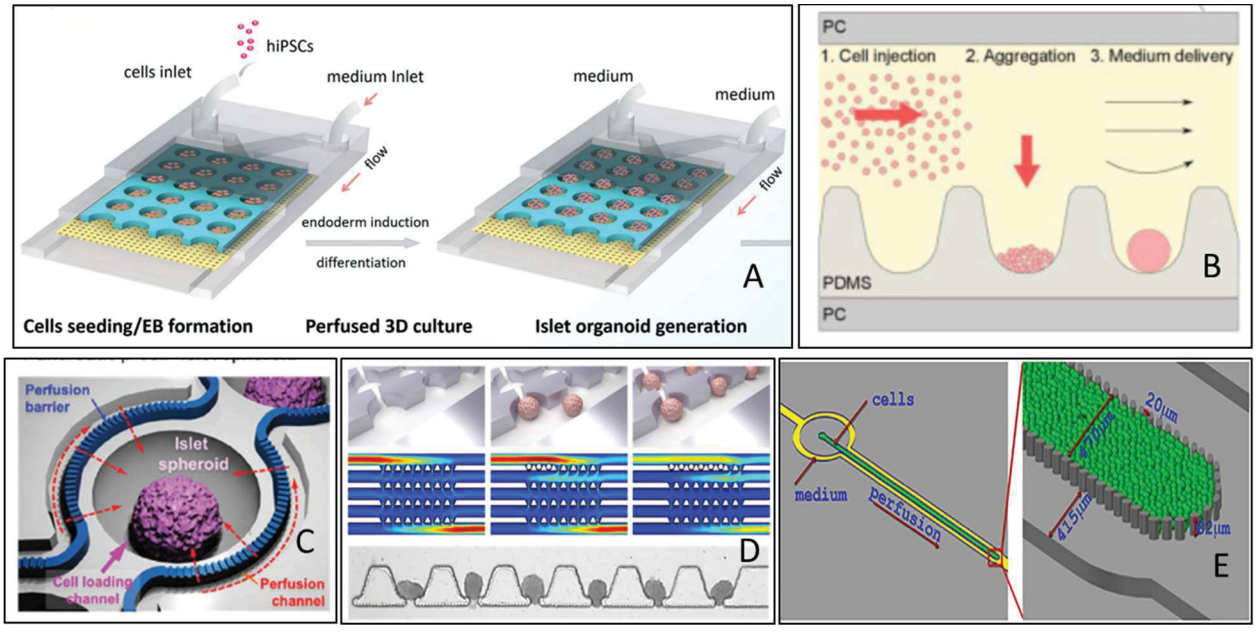

Figure 1.13: Geometric solutions reported by different groups of research that enables 3D cell culture within a microfluidic environment. (reproduced with permission from A. Tao et al. 2010; B. Hirano et al. 2017; C. Lee et al. 2018; D. Zbinden et al. 2018; E.Nguyen et al. 2017)

1.4.3. Multi-organ-on-chip: towards human on chip

There is an urgent need for the development of reliable "human surrogates" that recapitulate the complex biological physiology of the human species for preclinical drug testing and diseases modeling[193,194]. Microfluidics-based platforms have successfully shown their ability to reproduce a tissue/organ functions and they have overstepped the limitations conventional 2D classic culture capturing the tissue architecture[195].

Several multi-organ microphysiological systems have been proposed to interconnect multiple organs with a closed loop perfusion system in order to mimic the organ-to-organ interactions through an artificial microvasculature. These devices are particularly versatile since they allow the culture and characterization in a wide range from organoids or multicellular tissues down to individual cells[196]. The integration of various organs/tissues in the in vitro model is providing some much relevant outcomes for endocrine signaling and toxicity studies[197–200]. In that context Nahivandi et al. reviewed the current application of microfluidic biochips in cell signaling research. Cell signaling is a complex biological process that involves transfer of information to generate an adequate response in order to coordinate the physiological functions of the body[201]. intracellular signaling mechanisms can be classified in 5 types of communication: endocrine, paracrine, autocrine, juxtacrine, synaptic and gap junctions signaling. Fundamental processes in living organisms relay on stimulus-response mechanisms and cell sensing including cell regeneration, growth, differentiation and apoptosis, immune response, organogenesis, tissue repair and homeostasis control[202,203]. In particular, the endocrine signaling involves the communication between organs through hormones secreted into the circulatory system to act in a long distant target site. In that sense the authors highlighted the potential of MPs as a tool to advance intracellular signaling research overcoming the drawbacks of conventional methods[201]. The most important limitation for investigation of cell signaling mechanisms is the lack of precision over spatial and temporal cells 'control response and interactions. Such a control of variables can be achieved with microfluidic technology thanks to a highly controlled microenvironment and precise capture of response to induced stimulations (mechanical, chemical or physical stimulation). Furthermore, the ease of integration of analytical tools and the handling of small volumes allow the capture of rapid changes in the kinetics and the detection of signaling molecules difficult to achieve in conventional models. Moreover, the organ-on-chip models can recreate accurately a 3D microarchitecture recapitulating effectively the in vivo functions, particularly, for the real-time analysis of endocrine signaling in its appropriate context[204].

Nguyen et al. proposed endocrine system on chip that involves intestine cells and pancreatic cells for a diabetes treatment model. For that purpose, they used, an open loop perfusion system with two microfluidic biochips connected serially with a vascular network

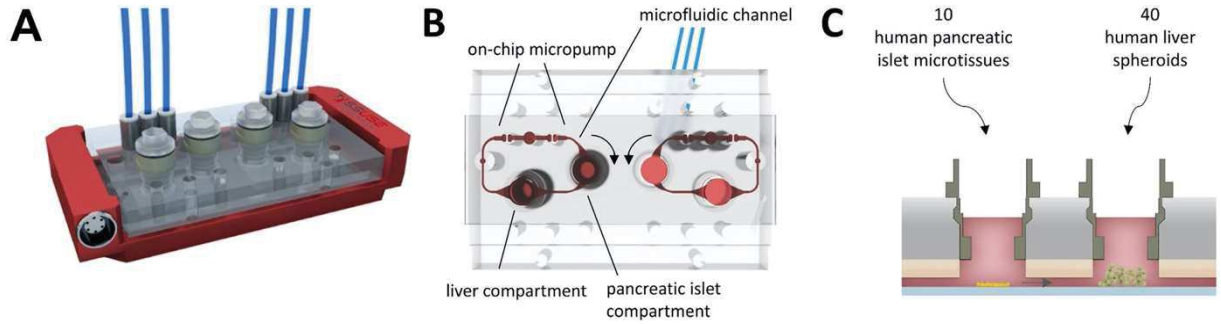

Figure 1.14: The microphysiological two-organ-chip (2-OC) device commercialized by TissUse GmbH, Berlin, Germany. (A) A 3D view of the assembled device including temperature support (red). (B) Illustration of the view from underneath with media circuits, respective culture compartments and micropump valves highlighted in red. (C) Standard tissue loading scheme of organ equivalents for 2-OC co-culture. (reproduced with permission from Bauer et al. 2017)

(Figure 1.13.E). They have shown the potential of co-culture model to screen drugs effectively integrating analytical tools for real time analysis[100]. In the same line, Bauer et al. used a different approach to address the in vitro modeling of T2DM. Therefore, they combined organoids culture with a microfluidic platform suitable for 3D cell culture. They co-cultured ex vivo human islets of Langerhans with human liver aggregates generated from HepaRG cell line in a device with two microchambers connected serially and perfused in a closed-loop by an integrated micropump[83].

A more interesting approach was recently proposed by Lee et al. to recapitulate the glucose metabolism regulation and homeostasis. They co-cultured a pancreatic cell line (INS-1) with a myoblasts cell line in a microphysiological system without contact in order to track the glucose uptake and insulin secretion. They validated the model mathematically with *in silico* simulation with an upgrade by including the liver as an important player in the metabolism regulation[205].

A new discovery involving the metabolic syndrome, insulin resistance and consequently T2DM induction was reported by Tanataweethum et al. using an organ-on-chip model. they developed a microfluidic platform to study the crosstalk between the adipose tissue (white and brown) and the liver since they are highly implicated in glucose metabolism and regulation in the body[206]. The co-culture without contact of hepatocytes and adipocytes was carried out with two interconnected microfluidic devices under continuous perfusion. They reported potential new therapeutic targets for T2DM. specifically, to address the hepatic insulin sensitivity[206].

1.5. Objectives and Approach of the Thesis

Following those multi-organ models approaches, the aim of this thesis is the study of inter-organs crosstalk such as pancreatic islets and hepatic cells similarly to the strategy reported by Bauer et al.,[83](Figure 1.14). The multi-organ interactions can be assembled by connecting both organ biochips, liver and pancreas, to each other through a microfluidic system allowing recirculation of

the media and endocrine communication. Each organ will thus be exposed to metabolites and hormones secreted by cells of the other biochip. In this configuration, we can investigate whether the organ-organ co-culture enables further differentiation and obtaining higher level of maturation of hepatic and pancreatic tissue. We will focus on the pancreas-liver communication via the glycaemia homeostasis.

We specifically developed a new pancreas organ-on-chip (chapter III). We characterized the pancreatic rat islets. We also confirmed the islet functionality by checking glucose stimulated insulin production (GSIS) and GLP1 stimulations. Then we use the advanced liver-on-chip technology developed in our laboratory to build a liver pancreas co-culture model. The technology was applied with rat cells as a first demonstrator. We investigated both effect of liver on pancreas and effect of pancreas on liver in chapter IV.

Researchers involved in DM studies and other metabolic disorders are facing big challenges when modeling disease progression in an accurate and reproducible manner. At present, the gold standard in diabetes modeling and drug screening involves the use of islets of Langerhans. Aside from the complexity of the isolation process and the high cost, primary islets come from donors with different genetic backgrounds, confounding results by adding variability to cellular models and assays. As an alternative to islets, a rapidly renewable source of human induced pluripotent stem (hiPS) cell-derived beta cells from a single donor could be used as a powerful screening tool for drug discovery and as a physiologically relevant model of insulin production and release. For that purpose, we collaborated with the University of Tokyo as they hold one of the pioneers' approaches for iPSC differentiation to hepatocytes. We investigated iPSC beta cells organ on chip in 2D and 3D configuration, checked mRNA levels and differentiation process in biochips, and confirmed the beta cells responsiveness to GSIS, GLP-1 in chapter V.

Although we generated liver-pancreas human iPSCs co-culture model, we will not present all those work in this manuscript because of the lack of time in the analysis and due to patent issue considerations on the liver iPSC protocol involving other teams. However, we will provide few preliminary results in chapter VI.

Finally, we discussed and concluded our work.

1.6. References

1. Almazroo OA, Miah MK, Venkataramanan R. Drug Metabolism in the Liver. *Clin Liver Dis*. 2017;21(1):1-20. doi:10.1016/j.cld.2016.08.001

2. Tortora GJ, Derrickson B. *Principles of Anatomy and Physiology*. 14th edition.; 2013. https://www.wiley.com/en-us/Principles+of+Anatomy+and+Physiology%2C+14th+Edition-p-9781118345009. Accessed September 3, 2018.

3. Kim E. Barrett, Susan M. Barman, Scott Boitano HLB. *Ganong's Review of Medical Physiology*. 25th ed. (Professional MH, ed.).; 2015. https://books.google.fr/books?id=IUPNCgAAQBAJ&q=ganong+physiology&dq=ganong+physiology&hl=es&sa=X&ved=0ahUKEwjOjdHHm9TWAhWREVAKHX4-D1QQ6AEIJzAA. Accessed October 3,

2017.

4. Usta OB, McCarty WJ, Bale S, et al. Microengineered cell and tissue systems for drug screening and toxicology applications: Evolution of in-vitro liver technologies . *TECHNOLOGY*. 2015;03(01):1-26. doi:10.1142/s2339547815300012

5. Moradi E, Jalili-Firoozinezhad S, Solati-Hashjin M. Microfluidic Organ-on-a-Chip Models of Human Liver Tissue. *Acta Biomater*. September 2020. doi:10.1016/j.actbio.2020.08.041

6. Mahadevan V. Anatomy of the pancreas and spleen. *Surg*. 2016;34(6):261-265. doi:10.1016/j.mpsur.2016.03.014

7. Jouvet N, Estall JL. The pancreas: Bandmaster of glucose homeostasis. *Exp Cell Res*. 2017;360(1):19-23. doi:10.1016/j.yexcr.2017.03.050

8. Kumar M, Melton D. Pancreas specification: a budding question. *Curr Opin Genet Dev*. 2003;13(4):401-407. http://www.ncbi.nlm.nih.gov/pubmed/12888014. Accessed June 25, 2018.

9. Jansson L, Barbu A, Bodin B, et al. Pancreatic islet blood flow and its measurement. *Ups J Med Sci*. 2016;121(2):81-95. doi:10.3109/03009734.2016.1164769

10. Thorens B. Neural regulation of pancreatic islet cell mass and function. *Diabetes, Obes Metab*. 2014;16:87-95. doi:10.1111/dom.12346

11. Rodriguez-Diaz R, Caicedo A. Neural control of the endocrine pancreas. *Best Pract Res Clin Endocrinol Metab*. 2014;28(5):745-756. doi:10.1016/j.beem.2014.05.002

12. Jellali R, Essaouiba A, Leclerc E, Legallais C. Membrane bioreactors for bio-artificial pancreas. In: *Current Trends and Future Developments on (Bio-) Membranes*. Elsevier; 2020:77-108. doi:10.1016/b978-0-12-814225-7.00004-8

13. Madsen OD, Serup P. Towards cell therapy for diabetes. *Nat Biotechnol*. 2006;24(12):1481-1483. doi:10.1038/nbt1206-1481

14. Zaret KS, Grompe M. Generation and regeneration of cells of the liver and pancreas. *Science (80-)*. 2008;322(5907):1490-1494. doi:10.1126/science.1161431

15. Bakhti M, Böttcher A, Lickert H. Modelling the endocrine pancreas in health and disease. *Nat Rev Endocrinol*. 2019;15(3):155-171. doi:10.1038/s41574-018-0132-z

16. Tortora GJ, Derrickson B. *Principales of Anatomy and Physiology*.

17. Miller RE. Pancreatic neuroendocrinology: Peripheral neural mechanisms in the regulation of the islets of langerhans. *Endocr Rev*. 1981;2(4):471-494. doi:10.1210/edrv-2-4-471

18. Korsgren O. Islet Encapsulation: Physiological Possibilities and Limitations. *Diabetes*. 2017;66:1748-1754. doi:10.2337/db17-0065

19. Adeva-Andany MM, Pérez-Felpete N, Fernández-Fernández C, Donapetry-García C, Pazos-García C. Liver glucose metabolism in humans. *Biosci Rep*. 2016;36(6):416. doi:10.1042/BSR20160385

20. International Diabetes Federation - Home. https://www.idf.org/. Accessed August 30, 2018.

21. OMS | Diabetes. *WHO*. 2016.

22. World Health Oorganization (WHO) Official Web Site. WHO. http://www.who.int/diabetes/en/. Published 2018. Accessed August 30, 2018.

23. Saeedi P, Petersohn I, Salpea P, et al. Global and regional diabetes prevalence estimates for 2019 and projections for 2030 and 2045: Results from the International Diabetes Federation Diabetes Atlas, 9th edition. *Diabetes Res Clin Pract*. 2019;157. doi:10.1016/j.diabres.2019.107843

24. Amer LD, Mahoney MJ, Bryant SJ. Tissue engineering approaches to cell-based type 1 diabetes therapy. *Tissue Eng Part B Rev*. 2014;20(5):455-467. doi:10.1089/ten.TEB.2013.0462

25. Åkerblom HK, Vaarala O, Hyöty H, Ilonen J, Knip M. Environmental factors in the etiology of type 1 diabetes. *Am J Med Genet - Semin Med Genet*. 2002;115(1):18-29. doi:10.1002/ajmg.10340

26. Lindley S, Dayan CM, Bishop A, Roep BO, Peatman M, Tree TIM. Defective suppressor function in CD4+CD25+ T-cells from patients with type 1 diabetes. *Diabetes*. 2005;54(1):92-99. doi:10.2337/diabetes.54.1.92

27. Klonoff DC, Ahn D, Drincic A. Continuous glucose monitoring: A review of the technology and clinical use. *Diabetes Res Clin Pract*. 2017;133:178-192. doi:10.1016/j.diabres.2017.08.005

28. Stephens E. Insulin Therapy in Type 1 Diabetes. *Med Clin North Am*. 2015;99(1):145-156. doi:10.1016/j.mcna.2014.08.016

29. Malik FS, Taplin CE. Insulin Therapy in Children and Adolescents with Type 1 Diabetes. *Pediatr Drugs*. 2014;16(2):141-150. doi:10.1007/s40272-014-0064-6

30. Bruttomesso D, Costa S, Baritussio A. Continuous subcutaneous insulin infusion (CSII) 30 years later: still the best option for insulin therapy. *Diabetes Metab Res Rev*. 2009;25(2):99-111. doi:10.1002/dmrr.931

31. Galderisi A, Schlissel E, Cengiz E. Keeping Up with the Diabetes Technology: 2016 Endocrine Society Guidelines of Insulin Pump Therapy and Continuous Glucose Monitor Management of Diabetes. *Curr Diab Rep*. 2017;17(11):111. doi:10.1007/s11892-017-0944-6

32. El-Khatib FH, Balliro C, Hillard MA, et al. Home use of a bihormonal bionic pancreas versus insulin pump therapy in adults with type 1 diabetes: a multicentre randomised crossover trial. *Lancet (London, England)*. 2017;389(10067):369-380. doi:10.1016/S0140-6736(16)32567-3

33. Tauschmann M, Hovorka R. Insulin pump therapy in youth with type 1 diabetes: toward closed-loop systems. *Expert Opin Drug Deliv*. 2014;11(6):943-955. doi:10.1517/17425247.2014.910192

34. Shapiro AMJ, Pokrywczynska M, Ricordi C. Clinical pancreatic islet transplantation. *Nat Rev Endocrinol*. 2016;13(5):268-277. doi:10.1038/nrendo.2016.178

35. Chang CA, Lawrence MC, Naziruddin B. Current issues in allogeneic islet transplantation. *Curr Opin Organ Transplant*. 2017;22(5):437-443. doi:10.1097/MOT.0000000000000448

36. Ludwig B, Reichel A, Steffen A, et al. Transplantation of human islets without immunosuppression. *Proc Natl Acad Sci*. 2013;110(47):19054-19058. doi:10.1073/pnas.1317561110

37. Ludwig B, Rotem A, Schmid J, et al. Improvement of islet function in a bioartificial pancreas by enhanced oxygen supply and growth hormone releasing hormone agonist. *Proc Natl Acad Sci U S A*. 2012;109(13):5022-5027. doi:10.1073/pnas.1201868109

38. Ludwig B, Ludwig S. Transplantable bioartificial pancreas devices: Current status and future prospects. *Langenbeck's Arch Surg*. 2015;400(5):531-540. doi:10.1007/s00423-015-1314-y

39. Bertuzzi F, De Carlis L, Marazzi M, et al. Long-term Effect of Islet Transplantation on Glycemic Variability. *Cell Transplant*. 2018;27(5):840-846. doi:10.1177/0963689718763751

40. Nourmohammadzadeh M, Lo JF, Bochenek M, et al. Microfluidic Array with Integrated Oxygenation Control for Real-Time Live-Cell Imaging: Effect of Hypoxia on Physiology of Microencapsulated Pancreatic Islets. *Anal Chem*. 2013;85(23):11240-11249. doi:10.1021/ac401297v

41. Chen C, Cohrs CM, Stertmann J, Bozsak R, Speier S. Human beta cell mass and function in diabetes: Recent advances in knowledge and technologies to understand disease pathogenesis. *Mol Metab*. 2017;6(9):943-957. doi:10.1016/j.molmet.2017.06.019

42. Shimabukuro M, Zhou YT, Levi M, Unger RH. Fatty acid-induced β cell apoptosis: A link between obesity and diabetes. *Proc Natl Acad Sci U S A*. 1998;95(5):2498-2502. doi:10.1073/pnas.95.5.2498

43. Poitout V, Robertson RP. Minireview: Secondary β-Cell Failure in Type 2 Diabetes—A Convergence of Glucotoxicity and Lipotoxicity. *Endocrinology*. 2002;143(2):339-342. doi:10.1210/endo.143.2.8623

44. Robertson RP, Harmon J, Tran POT, Poitout V. β-Cell Glucose Toxicity, Lipotoxicity, and Chronic Oxidative Stress in Type 2 Diabetes. In: *Diabetes*. Vol 53. American Diabetes Association Inc.; 2004:S119-S124. doi:10.2337/diabetes.53.2007.s119

45. Hupfeld CJ, Courtney CH. TYPE 2 DIABETES MELLITUS: Etiology, Pathogenesis, and Natural History. 2010.

46. Care D. *Diagnosis and Classification of Diabetes Mellitus*.; 2005.

47. Biddinger SB, Hernandez-Ono A, Rask-Madsen C, et al. Hepatic Insulin Resistance Is Sufficient to Produce Dyslipidemia and Susceptibility to Atherosclerosis. *Cell Metab*. 2008;7(2):125-134. doi:10.1016/j.cmet.2007.11.013

48. D'Alessio D. The role of dysregulated glucagon secretion in type 2 diabetes. *Diabetes, Obes Metab*. 2011;13:126-132. doi:10.1111/j.1463-1326.2011.01449.x

49. Michael MD, Kulkarni RN, Postic C, et al. Loss of insulin signaling in hepatocytes leads to severe insulin resistance and progressive hepatic dysfunction. *Mol Cell*. 2000;6(1):87-97. doi:10.1016/S1097-2765(05)00015-8

50. Herman WH, Hoerger TJ, Brandle M, et al. The cost-effectiveness of lifestyle modification or metformin in preventing type 2 diabetes in adults with impaired glucose tolerance. *Ann Intern Med*. 2005;142(5):323-332. doi:10.7326/0003-4819-142-5-200503010-00007

51. Li R, Zhang P, Barker LE, Chowdhury FM, Zhang X. Cost-effectiveness of interventions to prevent and control diabetes mellitus: A systematic review. *Diabetes Care*. 2010;33(8):1872-1894. doi:10.2337/dc10-0843

52. Garber AJ, Handelsman Y, Grunberger G, et al. Consensus statement by the American Association of clinical Endocrinologists and American College of Endocrinology on the comprehensive type 2

diabetes management algorithm - 2020 executive summary. *Endocr Pract*. 2020;26(1):107-139. doi:10.4158/CS-2019-0472

53. Inzucchi SE, Bergenstal RM, Buse JB, et al. Management of hyperglycemia in type 2 diabetes: A patient-centered approach. *Diabetes Care*. 2012;35(6):1364-1379. doi:10.2337/dc12-0413

54. Moreira RO, Cobas R, Coelho RCLA. Combination of basal insulin and GLP-1 receptor agonist: Is this the end of basal insulin alone in the treatment of type 2 diabetes? *Diabetol Metab Syndr*. 2018;10(1):26. doi:10.1186/s13098-018-0327-4

55. Endocrinology: Adult and Pediatric, 2-Volume Set - 9780323189071 | US Elsevier Health Bookshop. https://www.us.elsevierhealth.com/endocrinology-adult-and-pediatric-2-volume-set-9780323189071.html. Accessed June 2, 2020.

56. J. Larry Jameson LJDG. Endocrinology: Adult and Pediatric - J. Larry Jameson, Leslie J. De Groot - Google Books. https://books.google.fr/books?id=W4dZ-URK8ZoC&pg=PR20&lpg=PR20&dq=The+Mechanisms+of+Insulin+Action+Morris+F.+White+and+Kyle+D.+Copps&source=bl&ots=T9pEFo8B_d&sig=ACfU3U1K6S8MqYLZpox_TLkEErGMDUP6xA&hl=es&sa=X&ved=2ahUKEwiB5Kn1pq7qAhVSTBoKHfpLBRUQ6AEwBXoECA. Accessed July 2, 2020.

57. Czech MP. Insulin action and resistance in obesity and type 2 diabetes. *Nat Med*. 2017;23(7):804-814. doi:10.1038/nm.4350

58. Chadt A, Al-Hasani H. Glucose transporters in adipose tissue, liver, and skeletal muscle in metabolic health and disease. *Pflugers Arch Eur J Physiol*. 2020;472(9):1273-1298. doi:10.1007/s00424-020-02417-x

59. Karim S, Adams DH, Lalor PF. Hepatic expression and cellular distribution of the glucose transporter family. *World J Gastroenterol*. 2012;18(46):6771-6781. doi:10.3748/wjg.v18.i46.6771

60. Petersen MC, Shulman GI. Mechanisms of insulin action and insulin resistance. *Physiol Rev*. 2018;98(4):2133-2223. doi:10.1152/physrev.00063.2017

61. J. Larry Jameson LJDG. Endocrinology - E-Book: Adult and Pediatric - J. Larry Jameson, Leslie J. De Groot - Google Libros. https://books.google.fr/books?id=W4dZ-URK8ZoC&pg=PR20&lpg=PR20&dq=The+Mechanisms+of+Insulin+Action+Morris+F.+White+and+Kyle+D.+Copps&source=bl&ots=T9pEFo8B_d&sig=ACfU3U1K6S8MqYLZpox_TLkEErGMDUP6xA&hl=es&sa=X&ved=2ahUKEwiB5Kn1pq7qAhVSTBoKHfpLBRUQ6AEwBXoECA. Accessed July 2, 2020.

62. Imai J. Regulation of compensatory β-cell proliferation by inter-organ networks from the liver to pancreatic β-cells. *Endocr J*. 2018;65(7):677-684. doi:10.1507/endocrj.EJ18-0241

63. Odom DT, Zizlsperger H, Gordon DB, et al. Control of Pancreas and Liver Gene Expression by HNF Transcription Factors. *Science (80-)*. 2004;303(5662):1378-1381. doi:10.1126/science.1089769

64. Moreau F, Seyfritz E, Toti F, et al. Early effects of liver regeneration on endocrine pancreas: In vivo change in islet morphology and in vitro assessment of systemic effects on β-Cell function and viability in the rat model of two-thirds hepatectomy. *Horm Metab Res*. 2014;276(6):921-926. doi:10.1055/s-0034-1389995

65. Yamamoto J, Imai J, Izumi T, et al. Neuronal signals regulate obesity induced β-cell proliferation by FoxM1 dependent mechanism. *Nat Commun*. 2017;8(1):1-10. doi:10.1038/s41467-017-01869-7

66. Araújo TG, Oliveira AG, Carvalho BM, et al. Hepatocyte growth factor plays a key role in insulin resistance-associated compensatory mechanisms. *Endocrinology*. 2012;153(12):5760-5769. doi:10.1210/en.2012-1496

67. Da Silva Xavier G. The Cells of the Islets of Langerhans. *J Clin Med*. 2018;7(3):54. doi:10.3390/jcm7030054

68. Drucker DJ. Glucagon-Like Peptide-1 and the Islet β-Cell: Augmentation of Cell Proliferation and Inhibition of Apoptosis. *Endocrinology*. 2003;144(12):5145-5148. doi:10.1210/en.2003-1147

69. Müller TD, Finan B, Bloom SR, et al. Glucagon-like peptide 1 (GLP-1). 2019. doi:10.1016/j.molmet.2019.09.010

70. Drucker DJ, Nauck MA. The incretin system: glucagon-like peptide-1 receptor agonists and dipeptidyl peptidase-4 inhibitors in type 2 diabetes. *Lancet*. 2006;368(9548):1696-1705. doi:10.1016/S0140-6736(06)69705-5

71. DeFronzo RA, Ratner RE, Han J, Kim DD, Fineman MS, Baron AD. Effects of exenatide (exendin-4) on glycemic control and weight over 30 weeks in metformin-treated patients with type 2. *Diabetes Care*. 2005;28(5):1092-1100. doi:10.2337/diacare.28.5.1092

72. Vilsbøll T. Liraglutide: A once-daily GLP-1 analogue for the treatment of Type 2 diabetes mellitus. *Expert Opin Investig Drugs*. 2007;16(2):231-237. doi:10.1517/13543784.16.2.231

73. Gittes GK. Developmental biology of the pancreas: A comprehensive review. *Dev Biol*. 2009;326(1):4-35. doi:10.1016/j.ydbio.2008.10.024

74. Tyrberg B, Andersson A, Borg LAH. Species differences in susceptibility of transplanted and cultured pancreatic islets to the β-cell toxin alloxan. *Gen Comp Endocrinol*. 2001;122(3):238-251. doi:10.1006/gcen.2001.7638

75. Heller RS. The comparative anatomy of islets. *Adv Exp Med Biol*. 2010;654:21-37. doi:10.1007/978-90-481-3271-3_2

76. HJALGRIM H, FRISCH M, EKBOM A, KYVIK KO, MELBYE M, GREEN A. Cancer and diabetes - a follow-up study of two populationbased cohorts of diabetic patients. *J Intern Med*. 2007;241(6):471-475. doi:10.1111/j.1365-2796.1997.tb00004.x

77. Koh WP, Wang R, Jin A, Yu MC, Yuan JM. Diabetes mellitus and risk of hepatocellular carcinoma: Findings from the Singapore Chinese Health Study. *Br J Cancer*. 2013;108(5):1182-1188. doi:10.1038/bjc.2013.25

78. Zendehdel K, Nyren O, ÖStenson CG, Adami HO, Ekbom A, Ye W. Cancer incidence in patients with type 1 diabetes mellitus: A population-based cohort study in Sweden. *J Natl Cancer Inst*. 2003;95(23):1797-1800. doi:10.1093/jnci/djg105

79. Pazhanivel M. J V. Diabetes mellitus and cirrhosis liver. - *Minerva Gastroenterol e Dietol ;56(1)7-11 - Minerva Medica - Journals*. 2010. https://www.minervamedica.it/en/journals/gastroenterologica-dietologica/article.php?cod=R08Y2010N01A0007. Accessed September 17, 2020.

80. Ramachandran TM, Rajneesh AHR, Zacharia GS, Adarsh RP. Cirrhosis of liver and diabetes mellitus: The diabolic duo? *J Clin Diagnostic Res*. 2017;11(9):OC01-OC05.

doi:10.7860/JCDR/2017/30705.10529

81. Kawaguchi T, Taniguchi E, Itou M, Sakata M, Sumie S, Sata M. Insulin resistance and chronic liver disease. *World J Hepatol*. 2011;3(5):99-107. doi:10.4254/wjh.v3.i5.99

82. Suh S, Kim K-W. Diabetes and Cancer: Cancer Should Be Screened in Routine Diabetes Assessment. 2019. doi:10.4093/dmj.2019.0177

83. Bauer S, Wennberg Huldt C, Kanebratt KP, et al. Functional coupling of human pancreatic islets and liver spheroids on-a-chip: Towards a novel human ex vivo type 2 diabetes model. *Sci Rep*. 2017;7(1):1-11. doi:10.1038/s41598-017-14815-w

84. Jun Y, Kang AR, Lee JS, et al. 3D co-culturing model of primary pancreatic islets and hepatocytes in hybrid spheroid to overcome pancreatic cell shortage. *Biomaterials*. 2013;34(15):3784-3794. doi:10.1016/j.biomaterials.2013.02.010

85. Puryear JR, Yoon JK, Kim YT. Advanced fabrication techniques of microengineered physiological systems. *Micromachines*. 2020;11(8):730. doi:10.3390/MI11080730

86. Hasin Y, Seldin M, Lusis A. Multi-omics approaches to disease. *Genome Biol*. 2017;18(1):1-15. doi:10.1186/s13059-017-1215-1

87. Sun Y V., Hu YJ. Integrative Analysis of Multi-omics Data for Discovery and Functional Studies of Complex Human Diseases. *Adv Genet*. 2016;93:147-190. doi:10.1016/bs.adgen.2015.11.004

88. Gooding JR, Jensen M V., Newgard CB. Metabolomics applied to the pancreatic islet. *Arch Biochem Biophys*. 2016;589:120-130. doi:10.1016/j.abb.2015.06.013

89. Bain JR, Stevens RD, Wenner BR, Ilkayeva O, Muoio DM, Newgard CB. Metabolomics applied to diabetes research: Moving from information to knowledge. *Diabetes*. 2009;58(11):2429-2443. doi:10.2337/db09-0580

90. Mehta KY, Wu H-J, Menon SS, et al. Metabolomic biomarkers of pancreatic cancer: a meta-analysis study. *Oncotarget*. 2017;8(40):68899-68915. doi:10.18632/oncotarget.20324

91. Wallace M, Whelan H, Brennan L. Metabolomic analysis of pancreatic beta cells following exposure to high glucose. *Biochim Biophys Acta - Gen Subj*. 2013;1830(3):2583-2590. doi:10.1016/j.bbagen.2012.10.025

92. Mischak H, Allmaier G, Apweiler R, et al. Recommendations for biomarker identification and qualification in clinical proteomics. *Sci Transl Med*. 2010;2(46). doi:10.1126/scitranslmed.3001249

93. Yan J, Risacher SL, Shen L, Saykin AJ. Network approaches to systems biology analysis of complex disease: Integrative methods for multi-omics data. *Brief Bioinform*. 2017;19(6):1370-1381. doi:10.1093/bib/bbx066

94. Merrick BA, London RE, Bushel PR, Grissom SF, Paules RS. Platforms for biomarker analysis using high-throughput approaches in genomics, transcriptomics, proteomics, metabolomics, and bioinformatics. *IARC Sci Publ*. 2011;(163):121-142. https://europepmc.org/article/med/22997859. Accessed September 15, 2020.

95. Alyass A, Turcotte M, Meyre D. From big data analysis to personalized medicine for all: Challenges and opportunities. *BMC Med Genomics*. 2015;8(1). doi:10.1186/s12920-015-0108-y

96. Balboa D, Saarimäki-Vire J, Otonkoski T. Concise Review: Human Pluripotent Stem Cells for the Modeling of Pancreatic β-Cell Pathology. *Stem Cells*. 2019;37(1):33-41. doi:10.1002/stem.2913

97. Tsonkova VG, Sand FW, Wolf XA, et al. The EndoC-βH1 cell line is a valid model of human beta cells and applicable for screenings to identify novel drug target candidates. *Mol Metab*. 2018;8:144-157. doi:10.1016/j.molmet.2017.12.007

98. Spelios MG, Afinowicz LA, Tipon RC, Akirav EM. Human EndoC-βH1 β-cells form pseudoislets with improved glucose sensitivity and enhanced GLP-1 signaling in the presence of islet-derived endothelial cells. *Am J Physiol Endocrinol Metab*. 2018;314(5):E512-E521. doi:10.1152/ajpendo.00272.2017

99. Green AD, Vasu S, Moffett RC, Flatt PR. Co-culture of clonal beta cells with GLP-1 and glucagon-secreting cell line impacts on beta cell insulin secretion, proliferation and susceptibility to cytotoxins. *Biochimie*. 2016;125:119-125. doi:10.1016/j.biochi.2016.03.007

100. Nguyen DTT, Noort D van, Jeong I-K, Park S. Endocrine system on chip for a diabetes treatment model. *Biofabrication*. 2017;9:015021. doi:10.1088/1758-5090/aa5cc9

101. Kim JY, Kim HW, Bae SJ, et al. Hybrid cellular spheroids from hepatocellular carcinoma and insulin-secreting cell lines. *Transplant Proc*. 2012;44(4):1095-1098. doi:10.1016/j.transproceed.2012.02.016

102. Van Hoof D, Mendelsohn AD, Seerke R, Desai TA, German MS. Differentiation of human embryonic stem cells into pancreatic endoderm in patterned size-controlled clusters. *Stem Cell Res*. 2011;6(3):276-285. doi:10.1016/j.scr.2011.02.004

103. Petersen MBK, Azad A, Ingvorsen C, et al. Single-Cell Gene Expression Analysis of a Human ESC Model of Pancreatic Endocrine Development Reveals Different Paths to β-Cell Differentiation. *Stem Cell Reports*. 2017;9(4):1246-1261. doi:10.1016/j.stemcr.2017.08.009

104. Yabe SG, Fukuda S, Takeda F, Nashiro K, Shimoda M, Okochi H. Efficient generation of functional pancreatic β-cells from human induced pluripotent stem cells. *J Diabetes*. 2017;9(2):168-179. doi:10.1111/1753-0407.12400

105. Yabe SG, Fukuda S, Nishida J, Takeda F, Nashiro K, Okochi H. Induction of functional islet-like cells from human iPS cells by suspension culture. *Regen Ther*. 2019;10:69-76. doi:10.1016/j.reth.2018.11.003

106. Zeilinger K, Freyer N, Damm G, Seehofer D, Knöspel F. Cell sources for *in vitro* human liver cell culture models. *Exp Biol Med*. 2016;241(15):1684-1698. doi:10.1177/1535370216657448

107. Lv H, Zhang Z, Wu X, et al. Preclinical Evaluation of Liposomal C8 Ceramide as a Potent anti-Hepatocellular Carcinoma Agent. Calvisi D, ed. *PLoS One*. 2016;11(1):e0145195. doi:10.1371/journal.pone.0145195

108. Bhise NS, Manoharan V, Massa S, et al. A liver-on-a-chip platform with bioprinted hepatic spheroids. *Biofabrication*. 2016;8(1):014101. doi:10.1088/1758-5090/8/1/014101

109. Mi S, Yi X, Du Z, Xu Y, Sun W. Construction of a liver sinusoid based on the laminar flow on chip and self-assembly of endothelial cells. *Biofabrication*. 2018;10(2):025010. doi:10.1088/1758-5090/aaa97e

110. Grix T, Ruppelt A, Thomas A, et al. Bioprinting Perfusion-Enabled Liver Equivalents for Advanced Organ-on-a-Chip Applications. *Genes (Basel)*. 2018;9(4):176. doi:10.3390/genes9040176

111. Peters SJAC, Vanhaecke T, Papeleu P, Rogiers V, Haagsman HP, Van Norren K. Co-culture of primary rat hepatocytes with rat liver epithelial cells enhances interleukin-6-induced acute-phase protein response. *Cell Tissue Res*. 2010;340(3):451-457. doi:10.1007/s00441-010-0955-y

112. Gebhardt R. Co-cultivation of liver epithelial cells with hepatocytes. *Methods Mol Biol*. 2002;188:337-346. doi:10.1385/1-59259-185-x:337

113. Bilzer M, Roggel F, Gerbes AL. Role of Kupffer cells in host defense and liver disease. *Liver Int*. 2006;26(10):1175-1186. doi:10.1111/j.1478-3231.2006.01342.x

114. Thomas RJ, Bhandari R, Barrett DA, et al. The Effect of Three-Dimensional Co-Culture of Hepatocytes and Hepatic Stellate Cells on Key Hepatocyte Functions in vitro. *Cells Tissues Organs*. 2005;181(2):67-79. doi:10.1159/000091096

115. Lee DH, Yoon HH, Lee JH, et al. Enhanced liver-specific functions of endothelial cell-covered hepatocyte hetero-spheroids. *Biochem Eng J*. 2004;20(2-3):181-187. doi:10.1016/j.bej.2003.07.005

116. Kaufmann PM, Fiegel HC, Kneser U, Pollok JM, Kluth D, Rogiers X. Influence of pancreatic islets on growth and differentiation of hepatocytes in Co-culture. *Tissue Eng*. 1999;5(6):583-596. doi:10.1089/ten.1999.5.583

117. Kuo CH, Juang JH, Peng HL. Coculture of hepatocytes with islets. *Transplant Proc*. 2011;43(9):3167-3170. doi:10.1016/j.transproceed.2011.09.013

118. Lee KW, Lee SK, Joh JW, et al. Influence of pancreatic islets on spheroid formation and functions of hepatocytes in hepatocyte-pancreatic islet spheroid culture. *Tissue Eng*. 2004;10(7-8):965-977. doi:10.1089/ten.2004.10.965

119. Ricordi C, Lacy PE, Callery MP, Park PW, Flye MW. Trophic factors from pancreatic islets in combined hepatocyte-islet allografts enhance hepatocellular survival. *Surgery*. 1989;105(2 I):218-223. https://europepmc.org/article/med/2492681. Accessed September 16, 2020.

120. Gao Y, Xu J, Sun B, Jiang HC. Microencapsulated hepatocytes and islets as in vivo bioartificial liver support system. *World J Gastroenterol*. 2004;10(14):2067-2071. doi:10.3748/wjg.v10.i14.2067

121. Moberg L, Johansson H, Lukinius A, et al. Production of tissue factor by pancreatic islet cells as a trigger of detrimental thrombotic reactions in clinical islet transplantation. *Lancet*. 2002;360(9350):2039-2045. doi:10.1016/S0140-6736(02)12020-4

122. Joo DJ, Kim JY, Lee JI, et al. Impact of coculture with ischemic preconditioned hepatocellular carcinoma cell line (Hep-G2) cells on insulin secreting function of rat insulin-secreting cell line (RIN-5F) cells. In: *Transplantation Proceedings*. Vol 44. Elsevier; 2012:1099-1103. doi:10.1016/j.transproceed.2012.02.024

123. Park SB, Lee SY, Jung WH, et al. Development of in vitro three-dimensional co-culture system for metabolic syndrome therapeutic agents. *Diabetes, Obes Metab*. 2019;21(5):1146-1157. doi:10.1111/dom.13628

124. Park SB, Koh B, Jung WH, et al. Development of a three-dimensional *in vitro* co-culture model to

increase drug selectivity for humans. *Diabetes, Obes Metab*. 2020;22(8):1302-1315. doi:10.1111/dom.14033

125. Silva Santisteban T, Rabajania O, Kalinina I, Robinson S, Meier M. Rapid spheroid clearing on a microfluidic chip. *Lab Chip*. 2018;18(1):153-161. doi:10.1039/c7lc01114h

126. Tanaka H, Tanaka S, Sekine K, et al. The generation of pancreatic β-cell spheroids in a simulated microgravity culture system. *Biomaterials*. 2013;34(23):5785-5791. doi:10.1016/j.biomaterials.2013.04.003

127. Lock LT, Laychock SG, Tzanakakis ES. Pseudoislets in stirred-suspension culture exhibit enhanced cell survival, propagation and insulin secretion. *J Biotechnol*. 2011;151(3):278-286. doi:10.1016/j.jbiotec.2010.12.015

128. Kim HJ, Alam Z, Hwang JW, et al. Optimal formation of genetically modified and functional pancreatic islet spheroids by using hanging-drop strategy. *Transplant Proc*. 2013;45(2):605-610. doi:10.1016/j.transproceed.2012.11.014

129. Costa EC, de Melo-Diogo D, Moreira AF, Carvalho MP, Correia IJ. Spheroids Formation on Non-Adhesive Surfaces by Liquid Overlay Technique: Considerations and Practical Approaches. *Biotechnol J*. 2018;13(1):1700417. doi:10.1002/biot.201700417

130. Fu CY, Tseng SY, Yang SM, Hsu L, Liu CH, Chang HY. A microfluidic chip with a U-shaped microstructure array for multicellular spheroid formation, culturing and analysis. *Biofabrication*. 2014;6(1):015009. doi:10.1088/1758-5082/6/1/015009

131. Shinohara M, Kimura H, Montagne K, Komori K, Fujii T, Sakai Y. Combination of microwell structures and direct oxygenation enables efficient and size-regulated aggregate formation of an insulin-secreting pancreatic β-cell line. *Biotechnol Prog*. 2014;30(1):178-187. doi:10.1002/btpr.1837

132. Rizki-Safitri A, Shinohara M, Miura Y, et al. Efficient functional cyst formation of biliary epithelial cells using microwells for potential bile duct organisation in vitro. *Sci Rep*. 2018;8(1):1-11. doi:10.1038/s41598-018-29464-w

133. Frey O, Misun PM, Fluri DA, Hengstler JG, Hierlemann A. Reconfigurable microfluidic hanging drop network for multi-tissue interaction and analysis. *Nat Commun*. 2014;5(1):1-11. doi:10.1038/ncomms5250

134. Shinohara M, Komori K, Fujii T, Sakai Y. Enhanced self-organization of size-controlled hepatocyte aggregates on oxygen permeable honeycomb microwell sheets. *Biomed Phys Eng Express*. 2017;3(4):045016. doi:10.1088/2057-1976/aa7c3d

135. Jun Y, Kang AR, Lee JS, et al. Microchip-based engineering of super-pancreatic islets supported by adipose-derived stem cells. *Biomaterials*. 2014;35(17):4815-4826. doi:10.1016/j.biomaterials.2014.02.045

136. Duin S, Schütz K, Ahlfeld T, et al. 3D Bioprinting of Functional Islets of Langerhans in an Alginate/Methylcellulose Hydrogel Blend. *Adv Healthc Mater*. 2019;8(7):1801631. doi:10.1002/adhm.201801631

137. Fetah K, Tebon P, Goudie MJ, et al. The emergence of 3D bioprinting in organ-on-chip systems. *Prog Biomed Eng*. 2019;1(1):012001. doi:10.1088/2516-1091/ab23df

138. Nie M, Takeuchi S. Bottom-up biofabrication using microfluidic techniques. *Biofabrication*. 2018;10(4). doi:10.1088/1758-5090/aadef9

139. Vijayavenkataraman S, Yan WC, Lu WF, Wang CH, Fuh JYH. 3D bioprinting of tissues and organs for regenerative medicine. *Adv Drug Deliv Rev*. 2018;132:296-332. doi:10.1016/j.addr.2018.07.004

140. Ravnic DJ, Leberfinger AN, Ozbolat IT. Bioprinting and Cellular Therapies for Type 1 Diabetes. *Trends Biotechnol*. 2017;35(11):1025-1034. doi:10.1016/j.tibtech.2017.07.006

141. Matai I, Kaur G, Seyedsalehi A, McClinton A, Laurencin CT. Progress in 3D bioprinting technology for tissue/organ regenerative engineering. *Biomaterials*. 2020;226:119536. doi:10.1016/j.biomaterials.2019.119536

142. Lee H, Chae S, Kim JY, et al. Cell-printed 3D liver-on-a-chip possessing a liver microenvironment and biliary system. *Biofabrication*. 2019;11(2):025001. doi:10.1088/1758-5090/aaf9fa

143. Duin S, Schütz K, Ahlfeld T, et al. 3D Bioprinting of Functional Islets of Langerhans in an Alginate/Methylcellulose Hydrogel Blend. *Adv Healthc Mater*. 2019;8(7):1801631. doi:10.1002/adhm.201801631

144. Liu X, Carter SD, Renes MJ, et al. Development of a Coaxial 3D Printing Platform for Biofabrication of Implantable Islet-Containing Constructs. *Adv Healthc Mater*. 2019;8(7):1801181. doi:10.1002/adhm.201801181

145. Ozbolat IT, Yu Y. Bioprinting toward organ fabrication: Challenges and future trends. *IEEE Trans Biomed Eng*. 2013;60(3):691-699. doi:10.1109/TBME.2013.2243912

146. Miri AK, Mostafavi E, Khorsandi D, Hu SK, Malpica M, Khademhosseini A. Bioprinters for organs-on-chips. *Biofabrication*. 2019;11(4):42002. doi:10.1088/1758-5090/ab2798

147. Deng J, Wei W, Chen Z, et al. Engineered liver-on-a-chip platform to mimic liver functions and its biomedical applications: A review. *Micromachines*. 2019;10(10). doi:10.3390/mi10100676

148. Jellali R, Gilard F, Pandolfi V, et al. Metabolomics-on-a-chip approach to study hepatotoxicity of DDT, permethrin and their mixtures. *J Appl Toxicol*. 2018;38(8):1121-1134. doi:10.1002/jat.3624

149. Jellali R, Zeller P, Gilard F, et al. Effects of DDT and permethrin on rat hepatocytes cultivated in microfluidic biochips: Metabolomics and gene expression study. *Environ Toxicol Pharmacol*. 2018;59:1-12. doi:10.1016/j.etap.2018.02.004

150. Jellali R, Bricks T, Jacques S, et al. Long-term human primary hepatocyte cultures in a microfluidic liver biochip show maintenance of mRNA levels and higher drug metabolism compared with Petri cultures. *Biopharm Drug Dispos*. 2016;37(5):264-275. doi:10.1002/bdd.2010

151. Prot JM, Videau O, Brochot C, Legallais C, Bénech H, Leclerc E. A cocktail of metabolic probes demonstrates the relevance of primary human hepatocyte cultures in a microfluidic biochip for pharmaceutical drug screening. *Int J Pharm*. 2011;408(1-2):67-75. doi:10.1016/j.ijpharm.2011.01.054

152. Prot JM, Aninat C, Griscom L, et al. Improvement of HepG2/C3a cell functions in a microfluidic biochip. *Biotechnol Bioeng*. 2011;108(7):1704-1715. doi:10.1002/bit.23104

153. Baudoin R, Prot JM, Nicolas G, et al. Evaluation of seven drug metabolisms and clearances by

cryopreserved human primary hepatocytes cultivated in microfluidic biochips. *Xenobiotica*. 2013;43(2):140-152. doi:10.3109/00498254.2012.706725

154. Baudoin R, Griscom L, Prot JM, Legallais C, Leclerc E. Behavior of HepG2/C3A cell cultures in a microfluidic bioreactor. *Biochem Eng J*. 2011;53(2):172-181. doi:10.1016/j.bej.2010.10.007

155. Leclerc E, Hamon J, Legendre A, Bois FY. Integration of pharmacokinetic and NRF2 system biology models to describe reactive oxygen species production and subsequent glutathione depletion in liver microfluidic biochips after flutamide exposure. *Toxicol Vitr*. 2014;28(7):1230-1241. doi:10.1016/j.tiv.2014.05.003

156. Jellali R, Duval JL, Leclerc E. Analysis of the biocompatibility of perfluoropolyether dimethacrylate network using an organotypic method. *Mater Sci Eng C*. 2016;65:295-302. doi:10.1016/j.msec.2016.04.057

157. Merlier F, Jellali R, Leclerc E. Online monitoring of hepatic rat metabolism by coupling a liver biochip and a mass spectrometer. *Analyst*. 2017;142(19):3747-3757. doi:10.1039/c7an00973a

158. Baudoin R, Alberto G, Paullier P, Legallais C, Leclerc E. Parallelized microfluidic biochips in multi well plate applied to liver tissue engineering. *Sensors Actuators, B Chem*. 2012;173:919-926. doi:10.1016/j.snb.2012.06.050

159. Jellali R, Paullier P, Fleury MJ, Leclerc E. Liver and kidney cells cultures in a new perfluoropolyether biochip. *Sensors Actuators, B Chem*. 2016;229:396-407. doi:10.1016/j.snb.2016.01.141

160. Baudoin R, Alberto G, Legendre A, et al. Investigation of expression and activity levels of primary rat hepatocyte detoxication genes under various flow rates and cell densities in microfluidic biochips. *Biotechnol Prog*. 2014;30(2):401-410. doi:10.1002/btpr.1857

161. Gori M, Simonelli MC, Giannitelli SM, Businaro L, Trombetta M, Rainer A. Investigating nonalcoholic fatty liver disease in a liver-on-a-chip microfluidic device. *PLoS One*. 2016;11(7). doi:10.1371/journal.pone.0159729

162. Kostrzewski T, Cornforth T, … SS-W journal of, 2017 undefined. Three-dimensional perfused human in vitro model of non-alcoholic fatty liver disease. *ncbi.nlm.nih.gov*. https://www.ncbi.nlm.nih.gov/pmc/articles/PMC5236500/. Accessed October 5, 2020.

163. Hassan S, Sebastian S, Maharjan S, et al. Liver-on-a-Chip Models of Fatty Liver Disease. *Hepatology*. 2020;71(2):733-740. doi:10.1002/hep.31106

164. Perestrelo AR, Águas ACP, Rainer A, Forte G. Microfluidic organ/body-on-a-chip devices at the convergence of biology and microengineering. *Sensors (Switzerland)*. 2015;15(12):31142-31170. doi:10.3390/s151229848

165. Wang Y, Lo JF, Mendoza-Elias JE, et al. Application of microfluidic technology to pancreatic islet research: First decade of endeavor. *Bioanalysis*. 2010;2(10):1729-1744. doi:10.4155/bio.10.131

166. Rogal J, Zbinden A, Schenke-Layland K, Loskill P. Stem-cell based organ-on-a-chip models for diabetes research. *Adv Drug Deliv Rev*. 2019;140:101-128. doi:10.1016/j.addr.2018.10.010

167. Sokolowska P, Janikiewicz J, Jastrzebska E, Brzozka Z, Dobrzyn A. Combinations of regenerative medicine and Lab-on-a-chip systems: New hope to restoring the proper function of pancreatic

islets in diabetes. *Biosens Bioelectron*. 2020;167:112451. doi:10.1016/j.bios.2020.112451

168. Tao T, Wang Y, Chen W, et al. Engineering human islet organoids from iPSCs using an organ-on-chip platform. *Lab Chip*. 2019;19(6):948-958. doi:10.1039/C8LC01298A

169. Mohammed J, Wang Y, Harvat T, Chip JO-L on a, 2009 undefined. Microfluidic device for multimodal characterization of pancreatic islets. *pubs.rsc.org*. https://pubs.rsc.org/en/content/articlehtml/2009/lc/b809590f. Accessed September 10, 2020.

170. Brooks J, Ford K, Holder D, Holtan M, Analyst CE-, 2016 undefined. Macro-to-micro interfacing to microfluidic channels using 3D-printed templates: application to time-resolved secretion sampling of endocrine tissue. *pubs.rsc.org*. https://pubs.rsc.org/en/content/articlehtml/2016/an/c6an01055e?casa_token=qrwu8XzzEG8AAAAA:Cq8hAZ1gTtUcyZpugW0zMf9olfO9IskAsD8K5i4TC1zEYxE34RGXK5Jg3PlmbaAqGr_wyQQiCVoRRNg. Accessed September 10, 2020.

171. Li X, Brooks JC, Hu J, Ford KI, Easley CJ. 3D-templated, fully automated microfluidic input/output multiplexer for endocrine tissue culture and secretion sampling. *Lab Chip*. 2017;17(2):341-349. doi:10.1039/c6lc01201a

172. Schulze T, Mattern K, Früh E, Hecht L, Rustenbeck I, Dietzel A. A 3D microfluidic perfusion system made from glass for multiparametric analysis of stimulus-secretion coupling in pancreatic islets. doi:10.1007/s10544-017-0186-z

173. Li X, Brooks JC, Hu J, Ford KI, Easley CJ. 3D-templated, fully automated microfluidic input/output multiplexer for endocrine tissue culture and secretion sampling Graphical Abstract HHS Public Access An automated 16-channel microfluidic multiplexer (μMUX) was developed for dynamic stimulation and interrogation of islets and adipose tissue. 2017;17(2):341-349. doi:10.1039/x0xx00000x

174. Lenguito G, Chaimov D, Weitz JR, et al. Resealable, optically accessible, PDMS-free fluidic platform for ex vivo interrogation of pancreatic islets. *Lab Chip*. 2017;17(5):772-781. doi:10.1039/c6lc01504b

175. Lin P, Chen L, Li D, et al. Adiponectin reduces glucotoxicity-induced apoptosis of INS-1 rat insulin-secreting cells on a microfluidic chip. *Tohoku J Exp Med*. 2009;217(1):59-65. doi:10.1620/tjem.217.59

176. Silva PN, Green BJ, Altamentova SM, Rocheleau J V. A microfluidic device designed to induce media flow throughout pancreatic islets while limiting shear-induced damage. *Lab Chip*. 2013;13(22):4374-4384. doi:10.1039/c3lc50680k

177. Global Cancer Observatory. https://gco.iarc.fr/. Accessed September 9, 2020.

178. Cancer Tomorrow. https://gco.iarc.fr/tomorrow/graphic-isotype?type=1&type_sex=0&mode=population&sex=0&populations=900&cancers=13&age_group=value&apc_male=0&apc_female=0&single_unit=100000&print=0. Accessed September 9, 2020.

179. Mcguigan A, Kelly P, Turkington RC, Jones C, Coleman HG, Mccain S. Pancreatic cancer: A review of clinical diagnosis, epidemiology, treatment and outcomes. doi:10.3748/wjg.v24.i43.4846

180. Stevens RJ, Roddam AW, Beral V. Pancreatic cancer in type 1 and young-onset diabetes:

Systematic review and meta-analysis. *Br J Cancer*. 2007;96(3):507-509. doi:10.1038/sj.bjc.6603571

181. Mizuno S, Nakai Y, Ishigaki K, et al. diagnostics Screening Strategy of Pancreatic Cancer in Patients with Diabetes Mellitus. doi:10.3390/diagnostics10080572

182. Qian L, Li Q, Baryeh K, et al. Biosensors for early diagnosis of pancreatic cancer: a review. *Transl Res*. 2019;213:67-89. doi:10.1016/j.trsl.2019.08.002

183. Thege FI, Lannin TB, Saha TN, et al. Microfluidic immunocapture of circulating pancreatic cells using parallel EpCAM and MUC1 capture: characterization, optimization and downstream analysis. *Lab Chip*. 2014;14(10):1775-1784. doi:10.1039/c4lc00041b

184. Rhim AD, Thege FI, Santana SM, et al. Detection of circulating pancreas epithelial cells in patients with pancreatic cystic lesions. *Gastroenterology*. 2014;146(3):647-651. doi:10.1053/j.gastro.2013.12.007

185. Fernandes TG, Kwon SJ, Lee MY, Clark DS, Cabral JMS, Dordick JS. On-chip, cell-based microarray immunofluorescence assay for high-throughput analysis of target proteins. *Anal Chem*. 2008;80(17):6633-6639. doi:10.1021/ac800848j

186. Sheng W, Ogunwobi OO, Chen T, et al. Capture, release and culture of circulating tumor cells from pancreatic cancer patients using an enhanced mixing chip. *Lab Chip*. 2014;14(1):89-98. doi:10.1039/c3lc51017d

187. Das R, Murphy RG, Seibel EJ. Beyond isolated cells: microfluidic transport of large tissue for pancreatic cancer diagnosis. *Proc SPIE--the Int Soc Opt Eng*. 2015;9320:1-29. doi:10.1117/12.2076833

188. Thege FI, Gruber CN, Cardle II, Cong SH, Lannin TB, Kirby BJ. anti-EGFR capture mitigates EMT- and chemoresistance-associated heterogeneity in a resistance-profiling CTC platform. *Anal Biochem*. 2019;577:26-33. doi:10.1016/j.ab.2019.02.003

189. Huang C, Smith JP, Saha TN, Rhim AD, Kirby BJ. Characterization of microfluidic shear-dependent epithelial cell adhesion molecule immunocapture and enrichment of pancreatic cancer cells from blood cells with dielectrophoresis. *Biomicrofluidics*. 2014;8(4):044107. doi:10.1063/1.4890466

190. Castiello FR, Heileman K, Tabrizian M. Microfluidic perfusion systems for secretion fingerprint analysis of pancreatic islets: Applications, challenges and opportunities. *Lab Chip*. 2016;16(3):409-431. doi:10.1039/c5lc01046b

191. Dhumpa R, Truong TM, Wang X, Roper MG. Measurement of the entrainment window of islets of Langerhans by microfluidic delivery of a chirped glucose waveform. *Integr Biol (United Kingdom)*. 2015;7(9):1061-1067. doi:10.1039/c5ib00156k

192. Lee SH, Hong S, Song J, et al. Microphysiological Analysis Platform of Pancreatic Islet β-Cell Spheroids. *Adv Healthc Mater*. 2018;7(2):1701111. doi:10.1002/adhm.201701111

193. Skardal A, Shupe T, Atala A. Organoid-on-a-chip and body-on-a-chip systems for drug screening and disease modeling. *Drug Discov Today*. 2016;21(9):1399-1411. doi:10.1016/j.drudis.2016.07.003

194. Sung JH, Koo J, Shuler ML. Mimicking the Human Physiology with Microphysiological Systems

(MPS). *Biochip J*. 2019;13(2):115-126. doi:10.1007/s13206-019-3201-z

195. Lee SH, Sung JH. Organ-on-a-Chip Technology for Reproducing Multiorgan Physiology. *Adv Healthc Mater*. 2018;7(2):1700419. doi:10.1002/adhm.201700419

196. Oleaga C, Lavado A, Riu A, et al. Long-Term Electrical and Mechanical Function Monitoring of a Human-on-a-Chip System. *Adv Funct Mater*. 2018;29(8):1805792. doi:10.1002/adfm.201805792

197. Wagner I, Materne EM, Brincker S, et al. A dynamic multi-organ-chip for long-term cultivation and substance testing proven by 3D human liver and skin tissue co-culture. *Lab Chip*. 2013;13(18):3538-3547. doi:10.1039/c3lc50234a

198. Maschmeyer I, Hasenberg T, Jaenicke A, et al. Chip-based human liver-intestine and liver-skin co-cultures - A first step toward systemic repeated dose substance testing in vitro. *Eur J Pharm Biopharm*. 2015;95:77-87. doi:10.1016/j.ejpb.2015.03.002

199. Materne E-M, Ramme AP, Terrasso AP, et al. A multi-organ chip co-culture of neurospheres and liver equivalents for long-term substance testing. *J Biotechnol*. 2015;205:36-46. doi:10.1016/j.jbiotec.2015.02.002

200. Chen WLK, Edington C, Suter E, et al. Integrated gut/liver microphysiological systems elucidates inflammatory inter-tissue crosstalk. *Biotechnol Bioeng*. 2017;114(11):2648-2659. doi:10.1002/bit.26370

201. Nahavandi S, Tang S-Y, Baratchi S, et al. Microfluidic Platforms for the Investigation of Intercellular Signalling Mechanisms. *Small*. 2014;10(23):4810-4826. doi:10.1002/smll.201401444

202. John T. Hancock. *Cell Signalling*. Fourth Edi. (Oxford University Press, ed.). New York; 2010.

203. Alberts, B., Johnson, A., Lewis, J., Raff, M., Roberts, K. and Walter P. *Molecular Biology of the Cell*. Vol 91. 4th editio. Oxford University Press (OUP); 2003. doi:10.1093/aob/mcg023

204. Zbinden A, Marzi J, Schlünder K, et al. Non-invasive marker-independent high content analysis of a microphysiological human pancreas-on-a-chip model. *Matrix Biol*. 2020;85-86:205-220. doi:10.1016/j.matbio.2019.06.008

205. Lee DW, Lee SH, Choi N, Sung JH. Construction of pancreas–muscle–liver microphysiological system (MPS) for reproducing glucose metabolism. *Biotechnol Bioeng*. 2019;116(12):3433-3445. doi:10.1002/bit.27151

206. TANATAWEETHUM N, TRANG A, ANNEPUREDDY L, MEHTA J, COHEN RN, BHUSHAN A. 1752-P: Discovery of Targets for Insulin Resistance by Microfluidic Organ-on-Chip Models. *Diabetes*. 2020;69(Supplement 1):1752-P. doi:10.2337/db20-1752-p

Chapter II: Materials and methods

In this chapter we will present all the materials and methods used in the thesis. They are the extension with a more precise description of the ones presented in our papers:

Essaouiba A, Okitsu T, Jellali R, Shinohara M, Danoy M, Tauran Y, Legallais C, Sakai Y, Leclerc E, Microwell-based pancreas-on-chip model enhances genes expression and functionality of rat islets of Langerhans, Molecular and Cellular Endocrinology, Volume 514, 20 August 2020, https://doi.org/10.1016/j.mce.2020.110892

Essaouiba A, Okitsu T, Kinoshita R, Jellali R, Shinohara M, Danoy M, Legallais C, Sakai Y, Leclerc E, Development of a pancreas-liver coculture model for organ-to-organ interaction studies, Biochemical Engineering Journal, Volume 164, 15 December 2020, https://doi.org/10.1016/j.bej.2020.107783

Amal Essaouiba, Rachid Jellali, Marie Shinohara, Benedikt Scheidecker, Cécile Legallais, Yasuyuki Sakai, Eric Leclerc, Analysis of the behavior of 2D monolayers and 3D spheroid human pancreatic beta cells derived from induced pluripotent stem cells in a microfluidic environment, SUBMITTED. (in 2nd review)

Chapter II: Materials & Methods

2.1. Biochip design and fabrication

Both of the different designs of the microfluidic biochip microstructures have been conditioned by: 1) the culture mode (2D monolayer or 3D islets and spheroids); 2) the size of the spheroids and 3) the cell type source (organ).

The PDMS biochips were manufactured using a replica molding process. First, photolithography was performed to create the mold masters of the bottom and top layer of the biochips using SU-8 photosensitive resin. Then, PDMS prepolymer (mixture of 10:1 base polymer/curing agent; Sylgard 184, Dow Corning) was poured onto the SU-8 master and cured for 2 h at 75°C. The surfaces of the PDMS layers obtained were activated with reactive air plasma (1 min; Harrick Scientific) and brought together immediately to form an irreversible seal.

Concerning the liver-on-chip model for both human or animal cell sources, we used a micro-structured bottom layer composed of microchannels and microchambers network in a cell culture chamber measuring 1.2 cm in length, 1 cm in width and 100 µm in height (Fig.2.1A). The second PDMS layer, with a reservoir (depth of 100 µm, Fig.2.1A), was sealed on top of the first layer. As described above, a microchannels network was also present in the inlet and outlet to

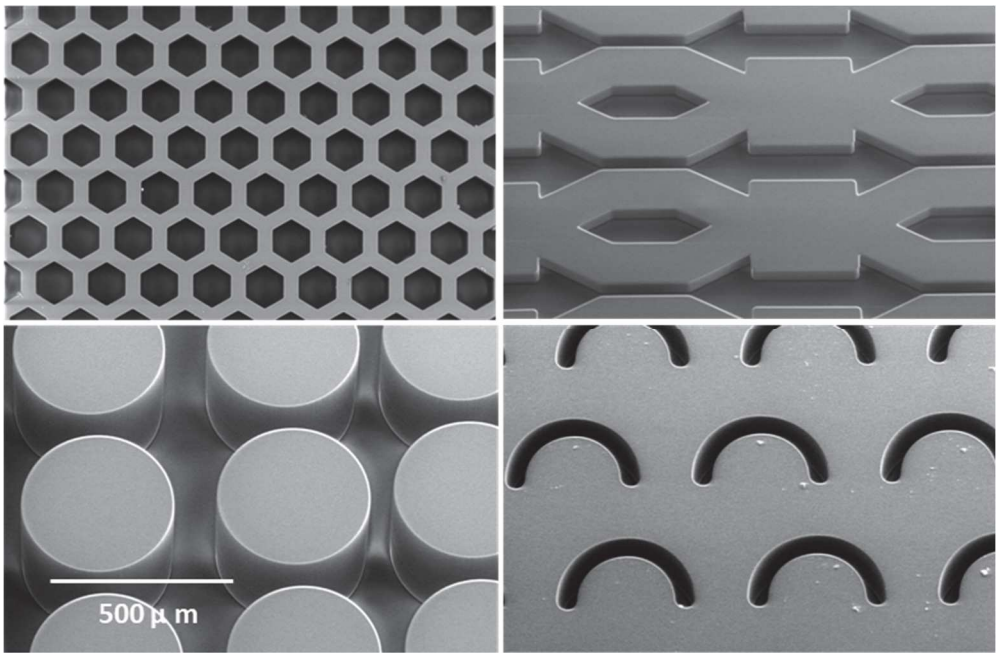

Figure 2.1: SEM images of the fabricated microstructures. Positive master mold used for PDMS replica molding process

ensure homogenous culture medium distribution. The design and dimensions of the biochip were described in our previous work[1–3].

In the pancreas-on-chip model, the micro-structured bottom layer, used to trap islets, was composed of 600 microwells measuring 400 µm in diameter (depth of 300 µm), and spaced by 50 µm (Figure 2). The second PDMS layer, with a reservoir with a depth of 100 µm (Figure 2), was placed on top of the first layer and included an inlet and outlet for culture medium perfusion. A microchannels network placed at the inlet and outlet of each layer made it possible to distribute the culture medium homogenously in the biochip (Figure 2). The detailed of each biochip will be given in the next sections.

The microfluidic co-culture consists of two different biochips (one for the liver, one for the pancreas) that were connected serially. Each biochip was manufactured with two polydimethylsiloxane (PDMS) layers.

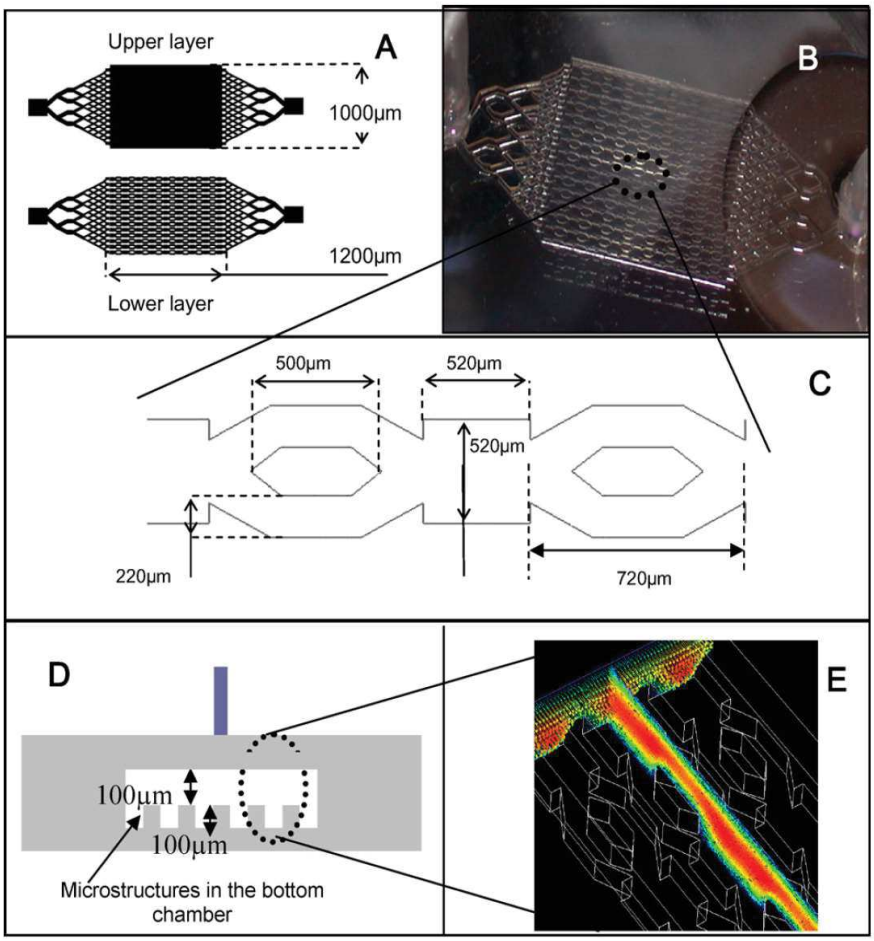

Figure 2.2: Microstructure design of the liver-on-chip device. A: upper and lower geometry; B: PDMS assembled device; C: detailed of the microchannels & microchambers networks; D: transversal view; E: fluid flow simulation illustrating the velocity field in the device (reproduced with permission from Baudoin et al.)

2.2. Cell sources and culture assessment

Pancreatic islets and hepatocytes were isolated from male Wistar rats aged 8-9 and 6 weeks old, respectively (CLEA Japan, Inc, Tokyo, Japan). The rats were housed at the University of Tokyo with a 12-h light/dark cycle at 22°C with food and water *ad libitum*. All animal experimentation procedures were carried out according to the guidelines of the University of Tokyo and the Japanese Ministry of Education.

2.2.1. Isolation of islets

Islets of Langerhans were isolated from male Wistar rats (8–9 weeks old, 200–300 g) (CLEA Japan, Inc, Tokyo, Japan) following a slight modification to the protocol described by Yonekawa et al. (2006)[4] and Kiba et al. (2013)[5]. All animal experimentation procedures were carried out in accordance with the guidelines of the University of Tokyo and the Japanese Ministry of Education.

The rats were anesthetized with isoflurane inhalation solution (Pfizer). The abdomen was disinfected with 70% Ethanol and acidic hypochlorous acid solution. Then the laparotomy was performed midline incision. The distal end of the common bile duct (CBD) at the duodenum using a microvascular clamp. The catheter is inserted on the CBD after a small incision in its proximal portion to the portal triad and knocked to it as Shown in figure. 2.3. After clamping of all irrigation blood vessels, the animal was blooded by transitioning the infrarenal aorta. the enzymatic solution (Liberase™ TL by Roche) was injected through the bile duct, previously identified and clamped. After the pancreatectomy, there was selective chemical digestion of the organ at 37°C for 30 min with Liberase TL/ ET-K solution (ET-Kyoto solution, Otsuka Pharmaceutical). The digestion was followed by washing and purification steps using a discontinuous OptiPrep® (Sigma-Aldrich) density gradient. The islets of Langerhans were then identified and selected by removing the two layers (borders of 1.08/1.10, 1.10/1.125) of the density gradient solution after centrifuge at low temperature (figure. 2.4). The islets were individually hand-picked with a Pasteur pipette under a stereomicroscope (Leica S9 D), and transferred to a cold preservation solution made of UW solution (University of Wisconsin, Kneteman et al., 1990)[6] complemented with Miraclid (Mochika pharmacy, Japan) and heparin (Mochika pharmacy, Japan). After assessing and counting the islets, the tissue was stored at 4 °C until starting the culture in order to maintain full functional properties as shown in Kimura et al. (2013)[7].

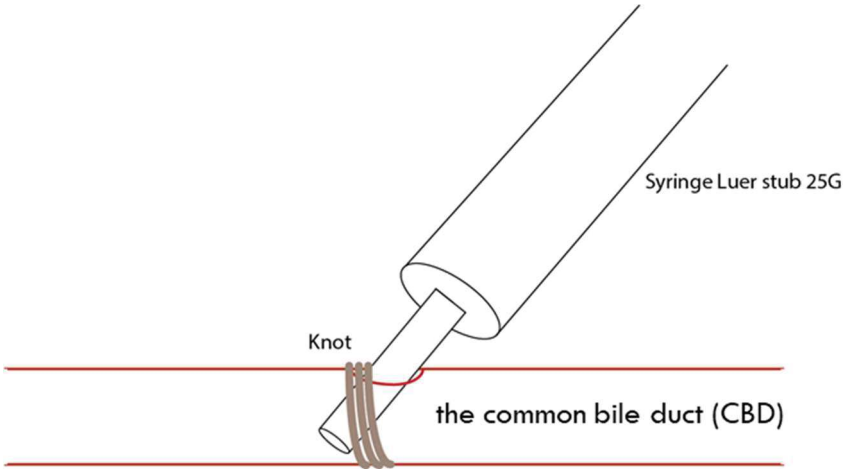

Figure 2.3: Detailed drawing of the catheter insertion site

2.2.2. Isolation of hepatocytes

Primary hepatocytes were isolated using the two-step collagenase protocol based on the protocol of Seglen[8]. Briefly, after animal anesthesia by isoflurane inhalation solution (Pfizer), the liver was perfused with buffer solution in order to washout the blood. Then, the buffer was switched with the collagenase IV solution (Wako Pure Chemical Industries) to start the tissue's chemical digestion. Subsequently, the liver was extracted, deposited in Dulbecco's Modified Eagle Medium (DMEM, Gibco™ – Life Technologies) and the tissue was gently disrupted. The digested tissues were filtered through 100 µm filters (cell strainer 100 µm nylon; Falcon®) and the liver cell suspensions were centrifuged three times. The resulting pellets were mixed and suspended in Percoll (Sigma-Aldrich) and HBSS (Sigma-Aldrich) separating solution. Percoll isogradient centrifugation was performed to isolate both dead cells and a significant portion of the nonparenchymal cells in a floating top layer that was discarded. Finally, the cells obtained were suspended in seeding medium (William's E medium (Gibco™) supplemented with 10% fetal

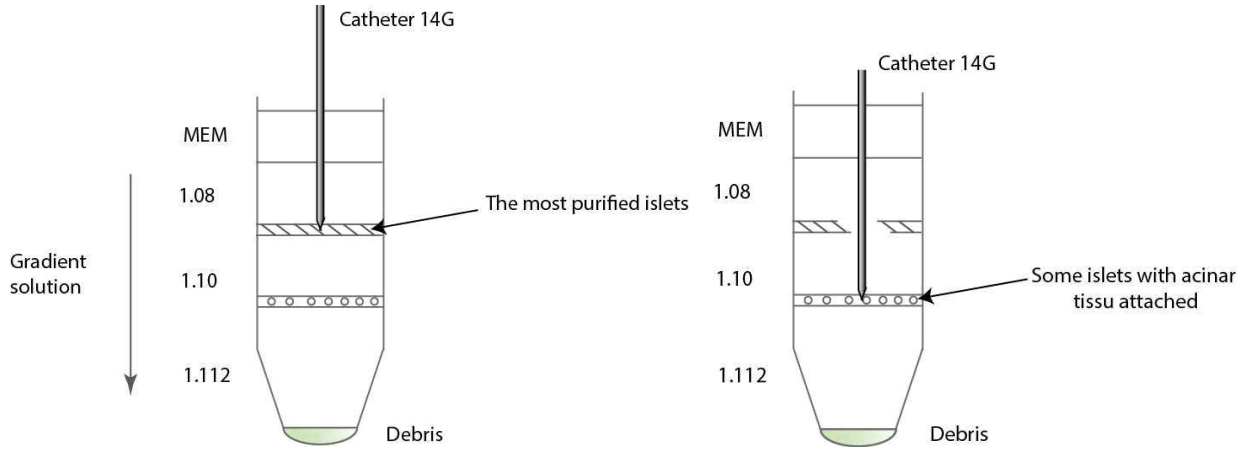

Figure 2.4: Step-by-step extraction by suction of the pancreatic islets trapped between 2 layers of the gradient density solution

bovine serum (FBS, Gibco™), 100 units/mL of penicillin and 100 mg/mL of streptomycin (Gibco™). Cell viability was assessed by Trypan blue dye exclusion and hepatocytes cultures with a viability of more than 85% were used. The purity obtained was over 98%.

2.2.3. Cellartis human iPSC derived β-cells maturation

Then as a second source of pancreatic cells, we investigate the potential of induced pluripotent stem cells. The cells used in this work (Cellartis hiPS derived β-cells) were provided from Takara Bio (Japan). Cellartis hiPS beta cells have been differentiated from ChiPSC12 lines. The hiPS derived β-cells were differentiated into insulin-producing cells using hiPS beta cell media kit (cat. N° Y10108, Takara Bio, Japan), according to the manufacturer's instructions in 2D Petri monolayers. The specific modifications of the protocol are detailed in the next section describing the 3D cultures and the organ on chip processes.

2.3 Organ-on-chip cultures

2.3.1 Experimental setup for the rat pancreas model

The biochips and perfusion circuits (silicone/Teflon tubing and bubble trap) were sterilized by autoclaving and dried in an oven. The biochips were then assembled with the perfusion system and filled with culture medium in order to remove air bubbles and moisturize the circuits. The bubble trap was used as a reservoir interconnected to the biochips by the silicone/Teflon tubing of 0.65 mm in diameter. The preconditioning process was carried out for one hour at 37° C in the incubator. The entire setup is presented in Fig.2.5 and Fig 2.6.

The pancreatic islets in the preservation solution were washed with cold culture medium and gently diluted in the appropriate amounts in order to ensure fair and even distribution of the tissue in the biochips and Petri culture. The estimated number of islets per biochip or well is ≈40. In order to minimize damage to the islets, wide orifice pipette tips with low binding were used throughout the handling process. Once the islets were loaded in the biochips from the inlet port or seeded in the 24-well plate, the counting step took place under the microscope in order to keep a record of the islets per biochip and/or well. The cultures were continuously maintained at 37 °C in a 5% CO_2 supplied incubator.

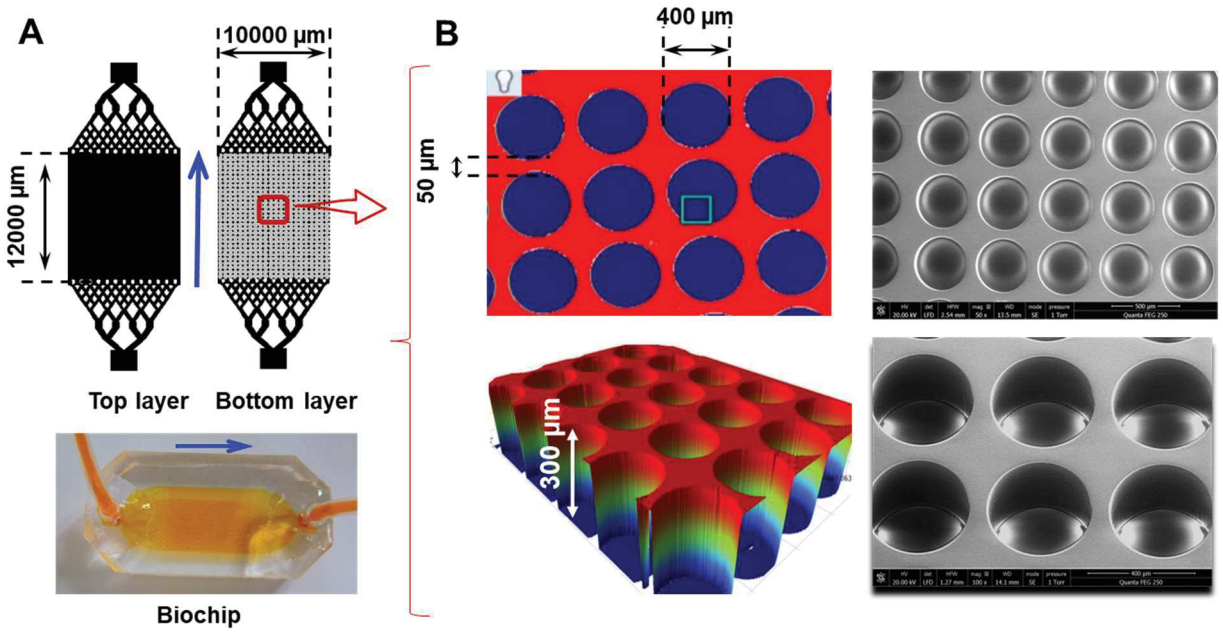

Figure 2.5: Biochip design: (A) top and bottom layers used in the biochip manufacturing (the blue arrowa indicate the flow direction) and (B) structures of microwells in culture chamber (bottom layer)

Two groups of study (biochip and Petri) and 4 conditions were established: Petri control; Petri with GLP-1 drug (drug rational is provide in the assay section); biochip control and biochip with GLP-1. The basal culture medium used in our study were the classic RPMI 1640 Medium (Gibco, 2.5 mM of glucose) supplemented with 10% FBS (Gibco), 100 units/mL of penicillin, 100 mg/mL streptomycin (Gibco) and GlutaMAX™ (Gibco™) at 10 mM. The medium was renewed every 2 days. In static conditions, the islets were seeded in 1 mL of medium/well and the culture medium was exchanged every day.

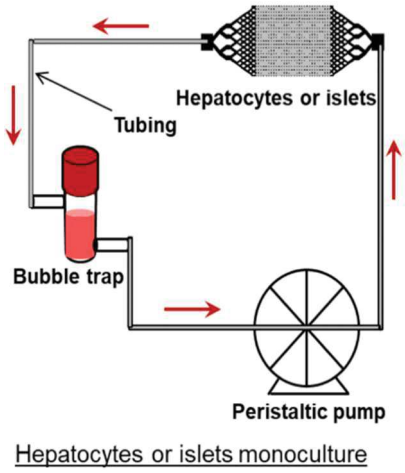

Figure 2.6: Setup used for dynamic culture in biochip

2.3.2 Experimental setup for the rat liver-pancreas model

2.3.2.1 Co-culture concept

The concept of the co-culture is shown in Fig 2.7. The experimental setup used for culture in the biochip was composed of a perfusion loop, including the culture medium tank (bubble trap), the peristaltic pump, and one or two biochips. They were interconnected using 0.65 mm interior diameter silicone/Teflon tubing (Fig.2.8). The bubble trap contained 2 mL of culture

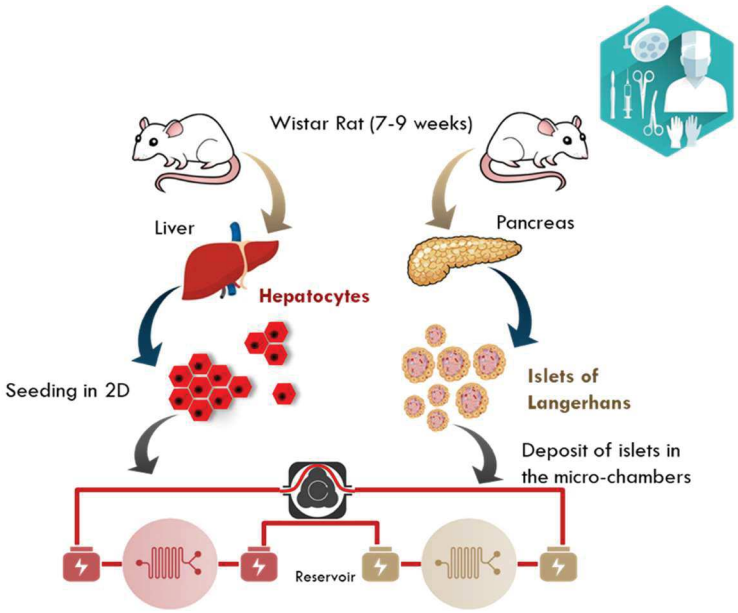

Figure 2.7: Schematic overview of the co-culture model

medium and the flow rate was set at 20 µL/min. Before each experiment, the circuit (biochip, tubing and bubble trap) was sterilized by autoclaving and dried in an oven.

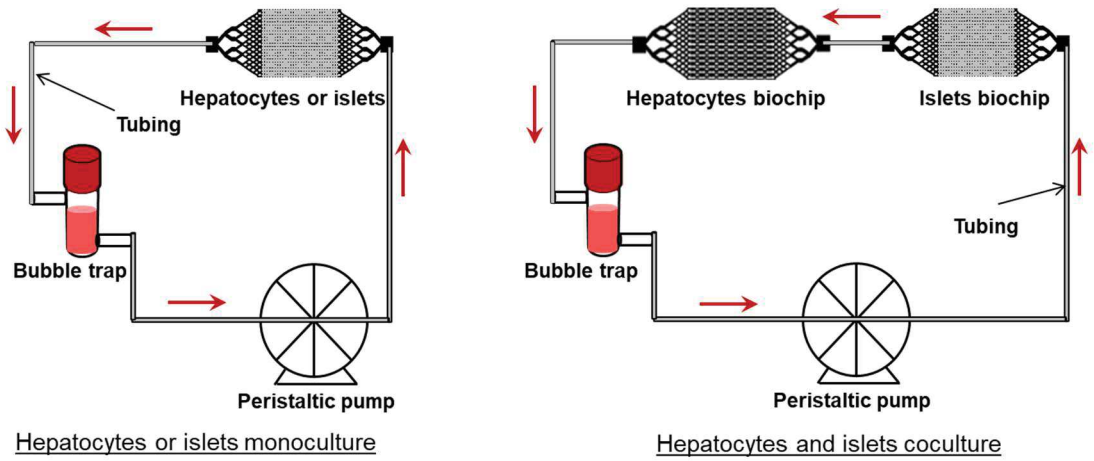

Figure 2.8: Perfusion set up used for dynamic culture in biochip

2.3.2.2. Pancreatic islet culture in the biochip (pancreas-on-chip)

The pancreatic control is similar to the previous section description. Briefly, the biochips were previously filled with culture media in order to remove the air bubbles and moisturize the circuits. The preconditioning process was carried out for one hour at 37° C in the incubator. The pancreatic islets in the preservation solution were washed with cold culture media and gently diluted in the appropriate amount. In order to minimize islets damage, wide orifice pipette tips with low binding were used throughout the handling process. After loading in the biochips, the islets were counted under microscope in order to keep a record of the islets number per biochip (≈40 islets/biochip). The circuit was then connected to the peristaltic pump and the perfusion started. The entire setup was continuously incubated at 37 °C in a 5% CO_2 supplied incubator. The basal culture medium used for the pancreatic islets culture was a classic RPMI 1640 medium (Gibco™) supplemented with 10% FBS (Gibco™), 100 units/mL of penicillin, 100 mg/mL of streptomycin (Gibco™) and GlutaMAX™ (Gibco™) at 10 mM.

2.3.2.3 Hepatocytes biochip culture (liver-on-chip)

After sterilization, the biochips were coated with rat tail type 1 collagen (Corning®, 300 µg/mL in phosphate-buffered saline: PBS Gibco™) and incubated at 37°C in an atmosphere supplied with 5% CO_2. After 1h, the collagen solution was washed using the seeding medium and the freshly isolated hepatocytes (5x10^5 cells/biochip) loaded into the microfluidic device via

biochip inlet ports using a micropipette tip. To keep the seeding medium inside the culture chamber, the biochip inlet ports were closed using two syringes (containing 500 µL of seeding medium), and the biochips were placed in an incubator at 37°C and 5% CO_2. After 24 h of static conditions to promote cell adhesion, the seeding medium was replaced by the culture medium, and the biochip integrated into the perfusion experimental setup to launch the dynamic culture.

The primary hepatocytes culture medium was composed of William's E medium (Gibco™) supplemented with 100 units/mL of penicillin / 100 mg/mL of streptomycin (Gibco™), GlutaMAX™ (Gibco™) at 10 mM, 1% non-essential amino acids (Invitrogen), 3% Bovine Serum Albumin (BSA, Sigma), 1% Insulin-Transferrin-Selenium ITS-100X (PanBiotech), 0.1 µM Dexamethasone (Wako Pure Chemical Industries), 10 ng/ml mouse Epidermal Growth Factor (Takara Bio), 0.5 mM ascorbic acid 2-phosphate (from magnesium salt n-hydrate; Wako Pure Chemical Industries) and 20 mM HEPES (Gibco™). For the hepatocytes monoculture without insulin (monoculture ITS -), we used the same medium composition excluding ITS.

2.3.2.4 Hepatocytes/islets co-culture (pancreas/liver-on-chip)

The liver and pancreas biochips were prepared separately. First, the hepatocytes were inoculated into the liver biochip (as in section above). After 24h of adhesion, the hepatocytes were cultivated inside the liver biochips for 24h in perfusion (this resulted in 48h of culture in the liver biochip including 24h for adhesion in static conditions and 24h of perfusion). The pancreatic islet biochips were prepared after those 48h. The islets were inoculated into the biochips as described in previous section. After 1h at rest and islets sedimentation, the liver perfusions were stopped and one pancreas biochip and one liver biochip were serially connected to each other to create a pancreas-liver co-culture model (Fig. 2.8). The culture medium for the co-culture condition was a 1:1 mixture of pancreatic islets (RPMI 1640) and hepatocytes (William's E) media, excluding ITS from the last one. The overall experimental design in summarized in Figure 2.9.

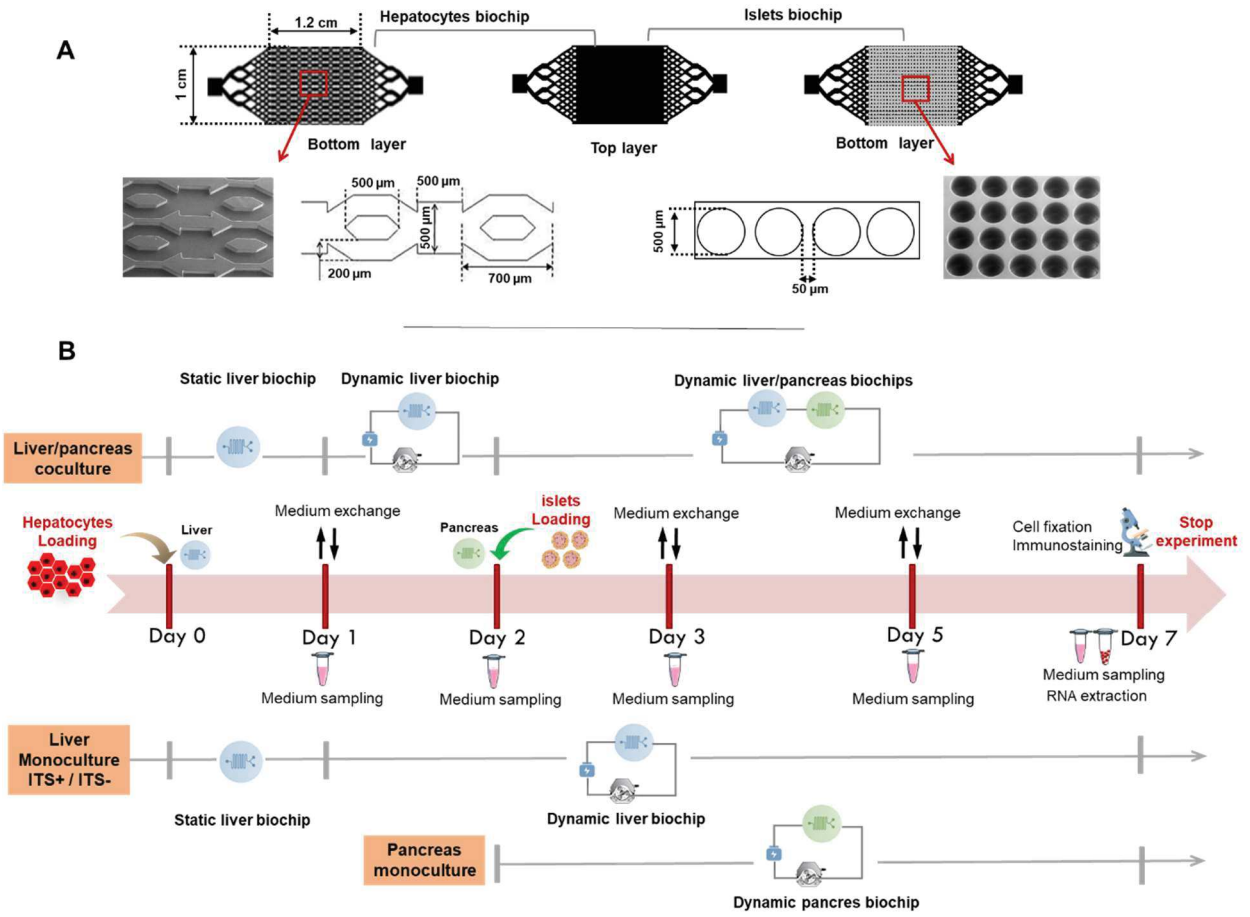

Figure 2.9: (A) design of biochips used for hepatocytes and islets cultures; (B) experimental procedures

Finally, four groups of biochips were investigated and compared: (i) hepatocytes biochip monoculture with insulin (hepatocytes monoculture ITS +); (ii) hepatocytes biochip monoculture without insulin (hepatocytes monoculture ITS -); (iii) pancreatic islets biochip monoculture (islet monoculture) and (iv) hepatocytes/islets biochips co-culture without insulin (hepatocytes/islets co-culture).

2.3.3 Experimental setup for the human pancreas model

We extend our development by investigation the possibility to develop human model.

2.3.3.1 2D Petri pancreatic β-cell culture protocol

Culture dishes (24-well plate) were coated with Cellartis beta cell coating (cat. N° Y10103) and incubated at 37°C. After 1h, coating solution was removed and 500 µL of maintenance culture medium (Cellartis beta cell basal medium Y10104, supplemented with beta cell supplement Y10102) containing cells were added in each well. The cells were inoculated at a

density of $2x10^5$ cells/cm^2 and the plate incubated at 37°C in an atmosphere supplied with 5% CO_2. The maintenance culture medium was used for 12 days and changed every day. Then, the assay medium (Cellartis cell medium 2 Y10105, supplemented with cell supplement Y10102) was used from day 12 to day 15 (Fig. 2.10).

2.3.3.2. 3D spheroid culture using honeycomb technology

To create the spheroids, we used the honeycomb technology previously developed by Shinohara et al.[9,10],. Briefly, the honeycomb polygons are made of PDMS and with the geometric characteristics of 126 µm width and 129 µm depth (Fig. 2.11). The PDMS honeycomb sheet is seed on a bottomless 24 well plate. Each well of the 24-well plate contained 8000 honeycombs. The plates were sterilized with ethanol for one hour, coated with pluronic-PBS solution overnight (Pluronic® F-127 Sigma) and rinsed three time with phosphate-buffered saline (PBS, Gibco) and one time with maintenance culture medium. After thawing, the β-cells were dropped in the honeycomb in 500 µL of maintenance medium and incubated at 37°C in an atmosphere supplied with 5% CO_2. Two densities were tested $2x10^5$ cells per dish (low density, LD) and $6x10^5$ cells per dish per well (high density, HD). The culture medium change sequence was exactly the same as the 2D Petri monolayer cultures. Nevertheless, after 24h, the medium was adjusted to 1mL. Then, we removed 600µL at each culture medium change that were replaced by 600µL fresh medium (leading thus to always keep 400 µL in the honeycombs to avoid spheroids sucking).

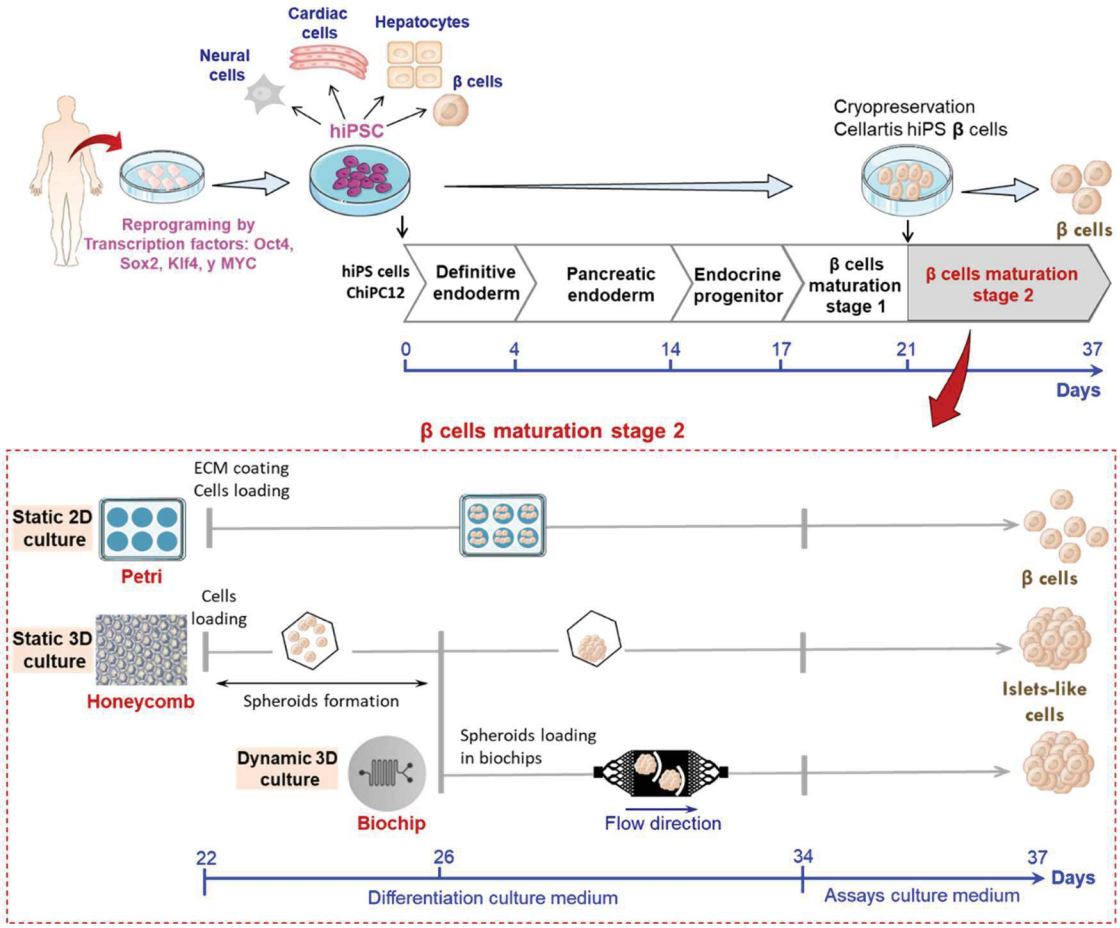

Figure 2.10: Schematic representation of the differentiation procedure of Cellartis ®hiPSC beta-cells. The cells are generated with a four-step protocol of differentiating stem cells to mature beta-cells First, the undifferentiated hiPSC is assembled in spheres for suspension culture. The spheres are then subsequently differentiated to Definitive Endoderm (DE), Pancreatic Endoderm (PE), Endocrine Progenitor (EP) and, finally, ending up in a beta-cell maturation step generating functional beta-cells. The differentiation process takes approximately 5 weeks. The spheroid are dissociated and cryopreserved as single cell suspension, thus facilitating handling procedures and transportation. Our experimental setup starts after thawing this cells with plating in the coated TCPS multiwells and the honeycombs microwells PDMS-based plate

2.3.3.3 Dynamic culture in biochip

We have tested two strategies of biochip cultures. The first one is a “2D monolayer”, where cells adhere to the surface culture inside the biochip. The second strategy consisted of the dynamic culture of the 3D β-cells spheroids.

Before cell experiments, the biochips and the perfusion circuits (silicone tubing and bubble trap) were sterilized by autoclaving and dried in oven. Then, the biochips were assembled with the perfusion system and filled with culture media in order to remove the air bubbles and moisturize the circuits. The bubble trap was used as a reservoir interconnected to the biochips

by the silicone/Teflon tubing with 0.65 mm in diameter. The assembled experimental setup (biochip, tubing, reservoir and peristaltic pump) is the represented in Fig. 2.6.

The protocol for 2D culture in biochip was similar to the protocol used in 2D Petri culture (section 2.2.3). For that purpose, the biochips were coated using the extracellular matrix solution provided in the β-cells kit (Cellartis beta cell coating, cat. N° Y10103) and incubated at 37°C. Then several parameters were tested to established the best attachment protocol as shown in table 2.1. It included the modulation of the inoculation cell density, the incubator oxygen concentration, the composition of the culture medium, the time of adhesion before perfusion.

Table 2.1: Matrix of tested conditions to plate the β-cell in biochips after thawing. Data results from 3 cryotubes of cellartis ChiPSC12 kit, n is the number of biochips per conditions, k is the cryotube number. K1 and K2 cryotubes were used to generate biochips and Petri 2D cultures, K3 was used only for biochip experiments due to larger inoculation density

2D Biochip tests	Modification compared to Petri
Condition-1, n=5, k1	None
Condition-2, n=3, k2	ECM-4h coating
Condition-3, n=3, k2	ECM-24h coating
Condition-4, n=3, k2	ECM-4h+high cell density
Condition-5, n=4, k3	ECM-24h+high cell density
Condition-6, n=4, k3	ECM-24h+high cell density+rock inhibitor
Condition-7, n=2, k3	ECM-24h+high cell density+rock inhibitor+low oxygen incubator
Condition-8, n=4, k3	Conditions 5 and 6 with aggregates + 10µL/min

In 3D biochip culture, the β cells spheroids were formed using the honeycomb technology as described in the above section. After 4 days of culture in the honeycombs, the formed spheroids were collected and seeded in biochips. In order to minimize the spheroid damage, wide orifice pipette tips with low binding were used during all the handling process. After spheroids seeding, the biochips were incubated at 37 °C in a 5% CO_2 supplied incubator for 1h to allow spheroid trapping by the crests as obstacles in the surface of the macrochamber. Then, the biochips were connected to the perfusion circuits and peristaltic pump, and the perfusion started at 20 µL/min. The entire setup was continuously incubated at 37 °C in a 5% CO_2 supplied incubator. The culture medium change sequence was the same as the 2D Petri monolayer cultures and 3D static cultures.

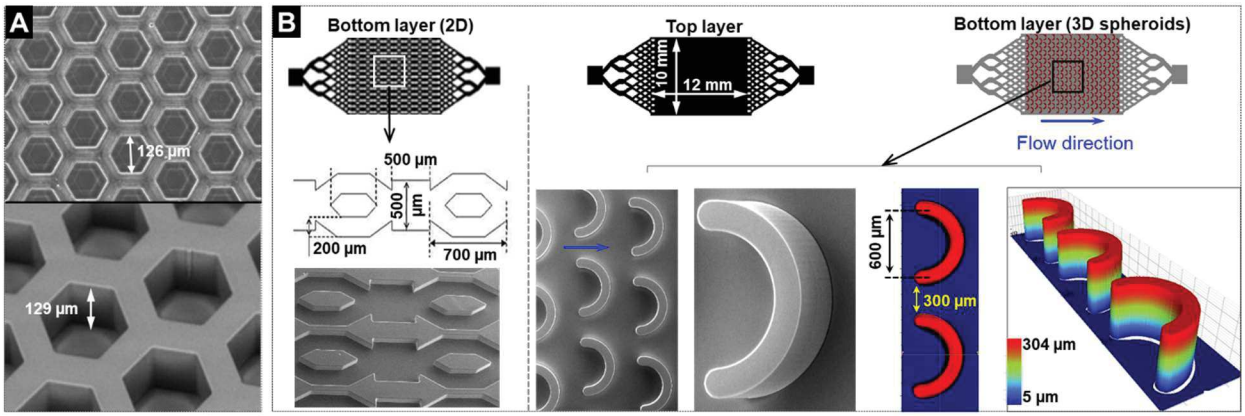

Figure 2.11: (A) SEM image of the honeycombs microwells plate structure used for Spheroids generation. (B) biochip microstructure design for spheroids perfusion system

2.4. Biological assays

2.4.1 Primary hepatocytes and pancreatic islets viability

2.4.1.1 Islets viability

At the end of the experiment, the islets were incubated in a solution of propidium iodide (PI) at 4.5 µmol/L and calcein-AM at 2 µmol/L (Cellstain kit, Dojingo) in RPMI 1640 medium for 30 min in the dark. Then, the samples were washed with RPMI 1640 medium and observed under an epifluorescence microscope (Olympus, Japan). The size of necrotic core was quantified by ImageJ software (NIH, Bethesda, Maryland) using the collected images. The area of the cells stained with PI was measured and normalized by the islet area.

2.4.1.2 Hepatocytes viability in the biochips

Since the static culture in the classic TCPS petri dish failed after 2 days of culture we decided to compare static (2 changes per day) biochips with the dynamic ones connected to a peristaltic pump. The hepatocytes monolayer in the biochips were incubated in a solution of propidium iodide (PI) at 4.5 µmol/L and calcein-AM at 2 µmol/L (Cellstain kit, Dojingo) in William's E without phenol red medium for 30 min in the dark. Then, the samples were washed with William's E medium and observed under an epifluorescence microscope (Olympus, Japan).

2.4.2 Glucagon-like peptide-1 (GLP1) stimulations

For the rat model, GLP1 was used in order to assess the pancreatic islets' β-cells responsiveness to the drug (Fig 2.12). For the hormone-stimulated media, GLP-1 (Peprotech,

USA) was added for a final concentration of 100 nM. The biochips were perfused in a circuit loop containing ≈2 ml of culture medium with a peristaltic pump (flow rate of 20 µL/min).

In order to test the response of the iPSC-derived to β-cells to drug stimulations for the human model, we exposed the culture to GLP1. For that purpose, we added 100nM of GLP1 in the culture medium for the last 24h of culture, at day 13, until day 14. It resulted to 24h exposure to the drug.

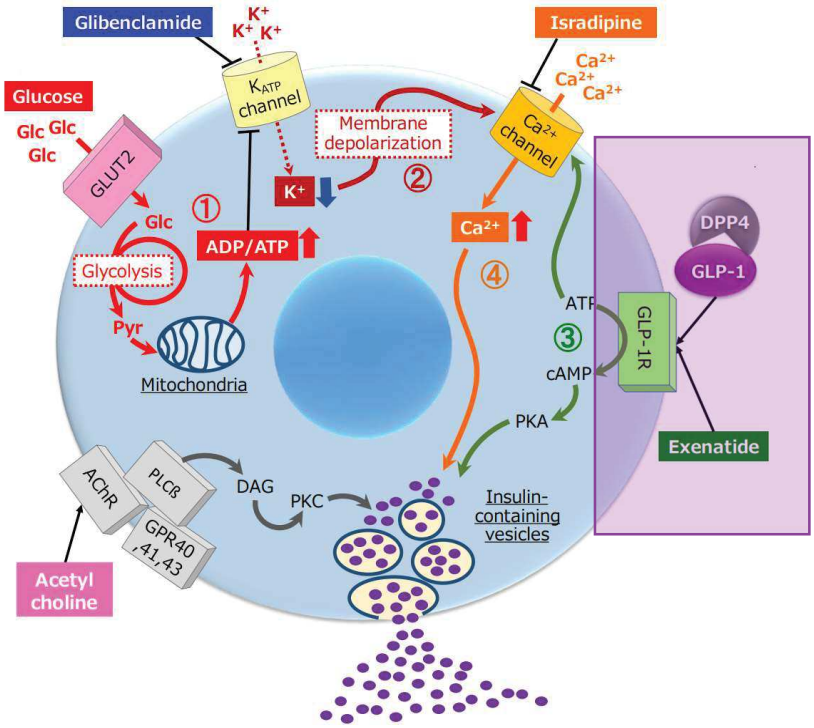

Figure 2.12: GLP-1 Stimulation of insulin secretion mechanism and Isradipine inhibition mechanism

2.4.3. RTqPCR assays

Total RNAs were extracted and purified from samples using a hybrid protocol that combines Trizol™ Reagent (Life Technologies) and RNeasy Mini Kit (QIAGEN 74104) following the manufacturer's instructions. Concentrations and qualities of extracted RNAs were assessed using a BioSpec-nano (Shimadzu Scientific Instruments). Reverse-transcription into cDNA was performed from 0.5 (primary hepatocytes or hiPSC derived heaptocytes) and 0.1 µg (rat islets of Langerhans or human islets-like) of total RNA using the ReverTra Ace qPCR RT Master Mix with gDNA Remover (TOYOBO). Real-time quantitative reverse transcription polymerase chain reaction (RTqPCR) was then performed with the THUNDERBIRD SYBR qPCR Mix (TOYOBO) according to the manufacturer's protocol and a StepOnePlus Real-Time PCR system (Applied Biosystems). The primer sequences of the genes are shown in Table 2.2 and 2.3 (Rattus norvegicus taxid:10116) and table 2.4 (Homo Sapiens taxid:9606). β-Actin was used as the

reference gene. Fresh primary cells (days 0) were used as the reference sample for the normalization of gene expression data in the rat models.

Table 2.2: Primers used in RTqPCR analysis of rat islets genes

Gene	Sequences
Ins1	f_TCCCGTCGTGAAGTGGAG r_CAGTTGGTAGAGGGAGCAGAT
Ins2	f_ GGCCCTGTGGATCCGCT r_ GCCTAGTTGCAGTAGTTCTCCA
Sst	f_ GTTTCTGCAGAAGTCTCTGGC r_ AGTTCTTGCAGCCAGCTTTG
Gcg	f_ ATCATTCCCAGCTTCCCAGAC r_ CGGTTCCTCTTGGTGTTCATC
App	f_ GTCCTCCCACCAACCAATGT r_ AGCACAGGCACGTTGTTGTA
Glp1r	f_ GCATCGTGATAGCCAAGCTGA r_ GCAGTACAAGACAGCCACCA
Pdx1	f_ACATCTCCCCATACGAAGTGC r_AGTTGAGCATCACTGCCAGC
Reg3a	f_ACGCTGCTCTACTACCTGTTCA r_TTGTTGTTCACTCTGCCTGTCA
Neurod	f_GGAGTAGGGATGCACCGG r_CTTGGCCAAGAACTATATCTGGG
Neurog3	f_TGGCGCCTCATCCCTTG r_CAGTCACCTGCTTCTGCTTC
Gapdh	f_GCATCGTGGAAGGGCTCATG r_GCCAGTGAGCTTCCCGTTC
Glut2	f_ CTCTGGTCTCTGTCTGTGTCC r_ TGGAACCAGTCCTGAAATTAGCC
Insr	f_TGGCGCTGTGTAAACTTCAG

	r_TAGGACAGGGTCCCAGACAC
Gcgr	f_ AGAAAGGGCCTCACAAGACA
	r_ CATGGAACATGGCAACACTC
B_actine	f_GTCGTACCACTGGCATTGTG
	r_TCTCAGCTGTGGTGGTGAAG

Table 2.3: Primers used in RTqPCR analysis of rat hepatic genes

Gene	**Sequences**
Hnf4α	f_ CTCTCTCCTGCTGTCCCAAC
	r_ CAAGAATCGTCGTGATGTGG
Igfbp1	f_ GATCACTGACCTCAAGAAATGGAAG
	r_ GCGGCAGCTAATCTCTCTAACA
Ugt1a	f_ TGCTCTGCTGACAGACCCT
	r_ ACCCGCTGCAGGAAGTTC
G6pc	f_ GACCTCAGGAACGCCTTCTAT
	r_ ATTGATGCCCACAGTCTCTTGA
Alb	f_ CTGGCACAATGAAGTGGGTAAC
	r_ GGGCGATCTCACTCTTGTGT
Cyp1a2	f_ TAGTGAAGCAGGGGGATGAC
	r_ ATGTGGGGTCTGAGGCTATG
Cyp2d4	f_ GTGTCCACCTTCCGTCACTT
	r_ GACGCGATCACGTTACACAC
Cyp3a2	f_ GCATAAGCACCGAGTGGATT
	r_ CGATCTCCTCCTGCAGTTTC
Mrp2	f_CGGTCATCACTATCGCACAC
	r_GCTAGAGCTCCGTGTGGTTC
Pck1	f_ATGACATTGCCTGGATGAAGTTTG
	r_CCGTTTTCTGGGTTGATGGC
Gapdh	f_GCATCGTGGAAGGGCTCATG
	r_GCCAGTGAGCTTCCCGTTC

Glut2	f_ CTCTGGTCTCTGTCTGTGTCC r_ TGGAACCAGTCCTGAAATTAGCC
Insr	f_TGGCGCTGTGTAAACTTCAG r_TAGGACAGGGTCCCAGACAC
Gcgr	f_ AGAAAGGGCCTCACAAGACA r_ CATGGAACATGGCAACACTC
B_actine	f_GTCGTACCACTGGCATTGTG r_TCTCAGCTGTGGTGGTGAAG

Table 2.4: Primers used in RTqPCR analysis of human cells

Gene	Sequences
Gapdh	f_ TGCACCACCAACTGCTTAG r_ GGCATGGACTGTGGTCATG
Insr	f_ GACAACGAGGAGTGTGGAGA r_ TACAGATGGTCGGGCAAACT
G6pd	f_ ACAGAGTGAGCCCTTCTTCAA r_ GGAGGCTGCATCATCGTACT
Ptf1a	f_ ATAGAAAACGAACCACCATTTGAGT r_ CAGGACGTTTTCTGGCCAGA
Ucn3	f_ GGCCTCCCCCACAAGTTCT r_ TCTCTTTGCCCTCCTCCTCC
Pcsk1	f_ TGATCCCACAAACGAGAACAAAC r_ TGTGATTATTTGCTTGCATGGCA
Pdx1	f_ CTTGGAAACCAACAACTATTCAC r_ ATTAAGCATTTCCCACAAACA
Mafa	f_ GTCAGCAAGGAGGAGGTGATC r_ TCACCAACTTCTCGTATTTCTCCT

Neurod	f_ ATGACCAAATCGTACAGCGAG r_ GTTCATGGCTTCGAGGTCGT
Ngn3	f_ TTGCGCCGGTAGAAAGGATGAC r_ TCAGTGCCAACTCGCTCTTAGG
Slc30a8	f_ GAGCGCCTGCTGTATCCTG r_ TGCACAAAAGCAGCTCTGAC
Glut2	f_ TGGGCTGAGGAAGAGACTGT r_ CCCATCAAGAGAGCTCCAACT
Ins	f_ CATCAGAAGAGGCCATCAAG r_ TCTTGGGTGTGTAGAAGAAGC
Gcg	f_ CAGAAGAGGTCGCCATTGTT r_ TGGCTAGCAGGTGATGTTGT
Sst	f_ CCCAGACTCCGTCAGTTTCTG r_ TCATTCTCCGTCTGGTTGGGT
Gck	f_ CACTGCTGAGATGCTCTTCGAC r_ CCACGACATTGTTCCCTTCTG
Oaz1	f_ CGACAAGACGAGGATTCTC r_ AAGACTCTCTCTCGAACGTGTAGG
NKX2.2	f_ ATGTAAACGTTCTGACAACT r_ TTCCATATTTGAGAAATGTTTGC
NKX6.1	f_ TCAACAGCTGCGTGATTTTC r_ CCAAGAAGAAGCAGGACTCG
B_actine	f_ CCTCATGAAGATCCTCACCGA r_ TTGCCAATGGTGATGACCTGG

2.4.4 Immunohistochemistry staining

Concerning the hiPSC-derived to beta cells model, after transfer to an untreated TCPS 24 wells plate, the spheroids were washed with phosphate buffer saline solution (PBS) and fixed in paraformaldehyde 4% at 4 °C overnight. In order to perform the Immunohistochemistry (IHC) staining in a 3D structure, the spheroids were permeabilized with 1% Triton X100 in PBS for 3 hours at 4°C and washed 3 times with PBS for 30 min. Then, the islets-like were blocked with a gelatin buffer for 24 hours at 4°C. Primary antibodies (Table 2.5) were incubated for 24 hours at 4°C in a BSA/PBS solution. After washing with PBS, secondary antibodies were further incubated overnight in a BSA/PBS solution at 4°C in the dark. Finally, the nuclei were stained with DAPI (342-07431, Dojindo) at 1/1000 for 30 min at room temperature (RT) in the dark. All the incubations and washing steps are carried out using a shaker.

The IHC staining of the 2D monoloyer beta-cells followed similar protocol in which the period of permeabilization, first antibody incubation and second antibody incubation were reduced to 15'min at RT, overnight at 4°C and 2 hours at RT respectively. The primary and secondary antibodies used are listed in Table 2.5.

Table 2.5: Primary and secondary antibodies used for islets and hepatocytes immunostaining[*]

Immunostaining	Primary antibody	Secondary antibody
Insulin	*Mouse anti-insulin (ab6995)* ***Abcam***	*Goat anti-Mouse Alexa Fluor® 594 (ab150116)* ***Abcam***
Glucagon	*Sheep anti-glucagon (ab 36232)* ***Abcam***	*Donkey anti-sheep Alexa Fluor 647 (ab 150179)* ***Abcam***
MAFA	*Rabbit anti-MAFA (ab26405)* ***Abcam***	*Goat Anti-rabbit Alexa Fluor® 680 (A-21109)* ***ThermoFisher***
PDX1	*Goat anti-PDX1 (ab347383)* ***Abcam***	*Donkey Anti-goat Alexa Fluor® 488 (ab150129)* ***Abcam***

[*] All antibodies were diluted in the range recommended by the manufacturers.

Concerning the rat experiments, the islets were transferred to an untreated TCPS 24-wells plate. The hepatocytes immunostaining was performed in the biochip. The islets and hepatocytes were washed with phosphate buffer saline solution (PBS, Gibco) and fixed in paraformaldehyde 4% at 4 °C for 24h. In order to perform the immunostaining in a 3D structure, the islets were permeabilized with 1% Triton X100 in PBS for 3h at 4°C and washed 3 times with PBS for 30 min, while the hepatocytes were permeabilized with 0.1% Triton X100 in PBS for 15 min. Then, both islets and hepatocytes were blocked with a gelatin buffer for 24h at 4°C. Primary antibodies were incubated at 4°C in a BSA/PBS solution for 48h and overnight for the pancreatic islets and hepatocytes, respectively. After several washing steps, secondary antibodies were incubated in a BSA/PBS solution at 4°C in the dark (24h for islets and overnight for hepatocytes). Actin filaments were stained with Phalloidin-iFluor488 Reagent (abcam). Finally, the nuclei were stained with DAPI or Hoechst 33342 (H342, Dojindo) at 1/800 for 30 min at room temperature in the dark. The rat antiboides are given in table 2.6.

*Table 2.6: Primary and secondary antibodies used for islets and hepatocytes immunostaining**

Immunostaining	Primary antibody	Secondary antibody
Insulin	*Mouse anti-insulin (ab6995)* ***Abcam***	*Goat anti-Mouse Alexa Fluor® 594 (ab150116)* ***Abcam***
Glucagon	*Rabbit anti-glucagon (ab167078)* ***Abcam***	*Goat anti-rabbit Alexa Fluor 680 (A-21109)* ***ThermoFisher***
INSR	*Mouse anti-insulin receptor Rβ (sc-57342)* ***Santa Cruz***	*Donkey Anti-Mouse Alexa Fluor® 647 (ab150107)* ***Abcam***
GLUT2	*Rabbit anti- Glucose transporter type 2 (E-AB-65640)* ***Elabscience***	*Goat Anti-Rabbit Alexa Fluor® 488 (ab150077)* ***Abcam***
CK18	*Mouse anti-Cytokeratin 18 (sc-32329)* ***Santa Cruz***	*Goat anti-Mouse Alexa Fluor® 594 (ab150116)* ***Abcam***
CYP3A2	Rabbit anti- Cytochrome P450 type 3A2 (ab195627) ***Abcam***	Goat anti-rabbit Alexa Fluor 680 (A-21109) ***ThermoFisher***

GCK	anti-glucokinase (sc-17819)	anti-mouse Alexa Fluor 647 (ab150107)
	Santa Cruz	***Abcam***

* All antibodies were diluted in the range recommended by the manufacturers.

All the incubations and washing steps were carried out using a shaker for the islets of Langerhans immunostaining process. For the hepatocytes, the biochips were cut with a scalpel to remove the PDMS top layer in order to increase the resolution of the image.

All observations were made with an Olympus IX-81 confocal laser-scanning microscope. The primary and secondary antibodies used are presented in Table S3 (supplementary file). The quantitative assessment of fluorescence intensity was performed by grey value intensity analysis (ImageJ software; NIH, Bethesda, Maryland) using the collected images.

2.4.5 Insulin, glucagon, C-peptide and albumin measurements by ELISA

The hormones and albumin released into the culture medium samples from the different culture conditions were assessed using ELISA assays, following the manufacturer's protocol. The following kits were used: insulin (rat Insulin ELISA kit, 10-1250-01, human insulin ELISA kit, 10-1113-01, Mercodia), glucagon (Glucagon DuoSet ELISA kit, DY1249 and DuoSet ELISA Ancillary Reagent Kit 2, DY008, R&D Systems), C-peptide (rat C-Peptide ELISA kit, 10-1172-01, human C-peptide ELISA kit, 10-1136-01, Mercodia) and albumin (Rat Albumin ELISA quantification set E110-125 from Bethyl, combined with the Enzyme Substrate, TMB, E102). The results were obtained with an iMark microplate reader (Bio-Rad, Osaka, Japan) set to a wavelength of 450nm.

2.4.6 Glucose and lactate measurements

Glucose and lactate were measured using a YSI 2950 Biochemistry Analyzer. To do so, 160 µL of culture medium were inserted into the analyzer. Measurements were based on a direct reading of L-lactate (L-lactic acid) and glucose in the culture medium by the YSI enzyme sensors, as the enzymes L-lactate oxidase, and glucose oxidase are respectively immobilized in the lactate and glucose sensors.

2.4.7 Glucose-stimulated insulin secretion (GSIS)

At the end of culture, we performed a low /high glucose stimulation to check insulin production. In biochips, the culture medium was removed from the bubble trap and the perfusion circuits with the culture chamber containing the spheroids were washed with a 0-glucose solution (DMEM, No Glucose, Wako) for 2 hours. Then, the washing 0-glucose solution was removed from

the bubble trap and 1 mL of fresh 0-glucose was added and perfused for 2 additional hours. After this low glucose perfusion, the spheroids were exposed to a high glucose culture medium for 2 hours (DMEM, 25 mM high Glucose, Wako). For that purpose, the low glucose solution was removed from the bubble trap and replaced by 1mL of high glucose. In Petri this protocol led to 2h 0-glucose exposure (washing), followed by another 2h 0-glucose exposure and finally 2h of high glucose stimulation. At the end of the assays, basal media was reestablished for all conditions. A similar protocol was performed in 3D spheroid honeycomb static cultures for comparative purposes.

2.4.8 Statistical analysis

All experiments were repeated at least three times. The data are presented as the mean ± standard deviations (SD) of 9 biochips (3 biochips from 3 different experiments, n=3x3). The data were statistically analyzed using GraphPad prism 8 software (San Diego, USA). The Kruskal Wallis test was performed to determine the significant differences among the samples (*P* values < 0.05 were identified as statistically significant).

2. 5 References

1. Baudoin R, Alberto G, Paullier P, Legallais C, Leclerc E. Parallelized microfluidic biochips in multi well plate applied to liver tissue engineering. *Sensors Actuators, B Chem*. 2012;173:919-926. doi:10.1016/j.snb.2012.06.050

2. Baudoin R, Prot JM, Nicolas G, et al. Evaluation of seven drug metabolisms and clearances by cryopreserved human primary hepatocytes cultivated in microfluidic biochips. *Xenobiotica*. 2013;43(2):140-152. doi:10.3109/00498254.2012.706725

3. Baudoin R, Alberto G, Legendre A, et al. Investigation of expression and activity levels of primary rat hepatocyte detoxication genes under various flow rates and cell densities in microfluidic biochips. *Biotechnol Prog*. 2014;30(2):401-410. doi:10.1002/btpr.1857

4. Yonekawa Y, Okitsu T, Wake K, et al. A New Mouse Model for Intraportal Islet Transplantation with Limited Hepatic Lobe as a Graft Site. *Transplantation*. 2006;82(5):712-715. doi:10.1097/01.tp.0000234906.29193.a6

5. Kiba T, Tanemura M, Yagyu K. High-quality RNA extraction from rat pancreatic islet. *Cell Biol Int Rep*. 2013;20(1):1-4. doi:10.1002/cbi3.10002

6. Tanioka Y, Sutherland DER, Kuroda Y, et al. Excellence of the two-layer method (University of Wisconsin solution/perflu-orochemical) in pancreas preservation before islet isolation. In: *Surgery*. Vol 122. Mosby Inc.; 1997:435-442. doi:10.1016/S0039-6060(97)90037-4

7. Kimura Y, Okitsu T, Xibao L, et al. Improved hypothermic short-term storage of isolated mouse islets by adding serum to preservation solutions. *Islets*. 2013;5(1):45-52. doi:10.4161/isl.24025

8. Seglen PO. Preparation of Isolated Rat Liver Cells. *Methods Cell Biol*. 1976;13(C):29-83.

doi:10.1016/S0091-679X(08)61797-5

9. Shinohara M, Kimura H, Montagne K, Komori K, Fujii T, Sakai Y. Combination of microwell structures and direct oxygenation enables efficient and size-regulated aggregate formation of an insulin-secreting pancreatic β-cell line. *Biotechnol Prog*. 2014;30(1):178-187. doi:10.1002/btpr.1837

10. Rizki-Safitri A, Shinohara M, Miura Y, et al. Efficient functional cyst formation of biliary epithelial cells using microwells for potential bile duct organisation in vitro. *Sci Rep*. 2018;8(1):1-11. doi:10.1038/s41598-018-29464-w

Chapter III: Microwell-based pancreas-on-chip model enhances genes expression and functionality of rat islets of Langerhans

In this section, we will present the pancreas-on-chip model using the microwells-based biochip and rat islets of Langerhans. This work was published as:

Essaouiba A, Okitsu T, Jellali R, Shinohara M, Danoy M, Tauran Y, Legallais C, Sakai Y, Leclerc E, Microwell-based pancreas-on-chip model enhances genes expression and functionality of rat islets of Langerhans, Molecular and Cellular Endocrinology, Volume 514, 20 August 2020, https://doi.org/10.1016/j.mce.2020.110892

The paper abstract is presented as a short summary of the chapter 3. The material and methods of the paper correspond to a short version of the previous chapter II. As a result, the materials and methods are not included in the following pages. The supplementary files of the paper are provided at the end of this chapter. The overall published paper is presented in annex of the thesis manuscript.

Summary

Organ-on-chip technology is a promising tool for investigating physiological in vitro responses in drug screening development, and in advanced disease models. Within this framework, we investigated the behavior of rat islets of Langerhans in an organ-on-chip model. The islets were trapped by sedimentation in a biochip with a microstructure based on microwells, and perfused for 5 days of culture. The live/dead assay confirmed the high viability of the islets in the biochip cultures. The microfluidic culture leads to upregulation of mRNA levels of important pancreatic islet genes: *Ins1, App, Insr, Gcgr, Reg3a* and *Neurod*. Furthermore, insulin and glucagon secretion were higher in the biochips compared to the Petri conditions after 5 days of culture. We also confirmed glucose-induced insulin secretion in biochips via high and low glucose stimulations leading to high/low insulin secretion. The high responsiveness of the pancreatic islets to glucagon-like peptide 1 (GLP-1) stimulation in the biochips was reflected by the upregulation of mRNA levels of *Gcgr, Reg3a, Neurog3, Ins1, Ins2, Stt* and *Glp-1r* and by increased insulin secretion. The results obtained highlighted the functionality of the islets in the biochips and illustrated the potential of our pancreas-on-chip model for future pancreatic disease modeling and anti-diabetic drugs screening.

Keywords: pancreas, islets of Langerhans, microfluidic biochips, glucose homeostasis, glucagon, insulin

Chapter III: Microwell-based pancreas-on-chip model enhances genes expression and functionality of rat islets of Langerhans

3.1 Introduction

The pancreas is a gland organ that plays a key role in endocrine regulation. The functional units of the endocrine system are the islets of Langerhans. These islets are clusters of cells whose size varies between 20 and 500 µm, with five different cell types: α, β, δ, ε, and γ cells (Jouvet and Estall, 2017; Kumar and Melton, 2003). The most abundant cells are the glucagon-producing α cells and insulin-producing β cells. Blood glucose levels are obtained through the interaction of two antagonistic hormones secreted by pancreatic α and β cells. During a period of starvation, when glucose levels are low, glucagon is released by alpha cells to promote glycogenolysis and gluconeogenesis in the liver in coordination with cortisol (a hormone secreted by the adrenal gland). In contrast, insulin secretion from β cells is stimulated by elevated glucose levels and activates glycogenesis in the liver and glucose uptake by muscles and adipose tissues, thereby decreasing postprandial blood sugar levels (Baker 2016; Jellali et al., 2020).

Diabetes mellitus is the most significant endocrine system dysfunction in the pancreas. According to the latest estimates by the International Diabetes Federation (IDF), 1 in 11 adults are living with diabetes in 2019 (463 million people worldwide, IDF official web site, 2019). The incidence of diabetes is increasing dramatically, and is predicted to reach more than 700 million people by 2045 (IDF official web site, 2019). Type 1 diabetes mellitus (T1DM) is an autoimmune disorder which leads to the destruction of insulin-secreting β cells, resuting a lack of insulin production (Jellali et al., 2020; Rogal et al., 2019). This pathology affects about 10% of diabetic patients, mostly the young population (Aghamaleki et al., 2019; IDF official web site, 2019). The daily insulin administration is currently the most common treatment of T1DM (King and Bowe 2016). Type 2 diabetes mellitus (T2DM) is the most prevalent form of diabetes, accounting for 90% of all adult diabetic patients, i.e. 20-79 years old (Sardu et al., 2019; IDF official web site, 2019). T2DM is a metabolic disorder characterized by insulin resistance coupled to impaired insulin secretion from the pancreatic β cells (Jun et al., 2019; Zbinden et al., 2020). Insulin resistance is the organs incapacity to respond properly to normal insulin levels (mainly the liver, muscles and adipose tissue, Rogal et al., 2019). The treatment of T2DM involves lifestyle adjustments and drug therapy such as metformin, sulphonylureas, glitazones and GLP-1 receptor agonists (Rogal et al., 2019; Zbinden et al., 2020).

Nowadays, Diabetes is one of the most prevalent chronic diseases (Silva et al., 2018). This raises a need for developing pancreatic models to increase knowledge of the underlying mechanisms of diabetes and to screen and identify new anti-diabetic drugs. Pancreatic disease

modeling and pertinent models for pancreatic drug screening involve considering the pancreas and its interaction with other organs, such as the liver, muscle, adipose tissues, kideney and gut (Efanov et al., 2004; Artunc et al., 206; Bauer et al., 2017; Rogal et al., 2019). This is the reason why the disease models involve transgenic and knockout animals (King and Bowe 2016). However, animal experimentation is ethically controversial, and often, the animal models developed in other species lose relevance when extrapolating the results to humans (Ghaemmaghami et al., 2012; Merlier et al., 2017; Rogal et al., 2019). Concerning in vitro models, the cell cultures used for drug screening and biomarker discovery are mainly performed in static 2D cultures using conventional Petri dishes or multi-well plates. Although these models have significantly contributed to medical research and drugs screening, they present certain limitations. Today, it seems clear that 2D cultures are poorly representative of human *in vivo* physiology, metabolism and toxicity, due to the physiological gap between the cells cultivated in static 2D mode and human cells as they exist in their native state (3D, dynamic mode) and the lack of physiological integration between cells and organs (Merlier et al., 2017). As a result, it is essential to improve these basic plate cultures to understand and model metabolic processes and human disorders. This is why many groups are developing tissue-engineering and 3D culture processes in order to provide a more appropriate micro-environment for tissue maintenance and development. This environment must reproduce, as closely as possible, the characteristics found *in vivo*.

The organ-on-chip approach is one way of mimicking organ physiology to help in the development of therapeutic solutions and pharmacological studies (Huh et al., 2012; Bathia and Ingber 2014). This approach has many advantages to reproduce the characteristics of physiological microenvironments, including three-dimensional architectures, cell-cell interactions and dynamic flow that ensures the transport and exchange of culture medium, hormones, metabolic waste and other chemicals (merlier et al., 2017; Lee et al., 2018; Zbendin et al., 2020). Unlike the static cultures in Petri dishes, organ-on-chip approch provides the possibility to perform co-cultures, where the different cell types can be cultivated in separated microbioreactors and the cell-cell interactions are ensured by soluble factors exchange (Merlier et al., 2107). The co-culture of two or more organ is a promising tool to study multi-organs diseases such as T2DM (Rogal et al., 2019). In the last years, organ-on-chip technology has been used to reproduce pancreas *in vitro* models (Schulze et al., 2017; Li et al., 2017; Brooks et al., 2016; Lee et al; 2018; Jun et al., 2020). A literature review highlighted that most of the current microfluidic platforms have been designed mainly for islet quality assessment for subsequent *in vivo* implantation (Rogal et al 2019). In parallel, some recent works have also demonstrated the potential of organ-on-chip technology for more complex pancreatic physiopathology analysis (Bauer et al., 2017; Zbinden et al., 2020).

In this work, we developed a simple microfluidic biochip for assessment of pancreatic islet function and long-term cultures. We also presented and demonstrated that the islets functionality was maintained in microfluidic biochips when compared to conventional islet cultures inside polystyrene (TCPS) dishes.

3.2 Results

3.2.1 Characterization of islet biochip cultures when compared to Petri dish cultures

3.2.1.1 Viability assay showed highly viable islets in the biochip

After extraction (Fig. 3.1A), the islets were cultivated in Petri dishes (Fig. 3.1B) and in biochip dynamic culture for 5 days (Fig. 3.1C). In the device, the islets sedimented into the microwells located at the bottom of the culture chamber. Then, we confirmed that the islets had not been washed away by the flow rate after 5 days of perfusion. Indeed, the number of islets seeded at the beginning of the experiments and collected at the end of the perfusion remained similar, as shown in Fig. 3.1.D. In addition, the islets presented a round shape at the end of the perfusion (Fig. 3.1B, 3.1.C and Fig.3.S1, supplementary file). The typical size of the islets was about 150 ± 50 microns.

The fluorescent images of islets stained with calcein AM/PI are presented in Fig. 3.1.E. We found a different size to the necrotic core of the islets between static and dynamic conditions after 5 days of culture. Nevertheless, the viability was higher in the islets cultivated in the biochips inasmuch as the IP staining was weaker when compared to Petri situations. The quantification of the necrotic core showed that the proportion of dead cells in dynamic biochip was significantly lower when compared to the Petri culture. The normalized size of necrotic core was of 0.34±0.15 and 0.12±0.03 for islets cultivated in Petri and biochip, respectively (Fig.3.S2, supplementary file).

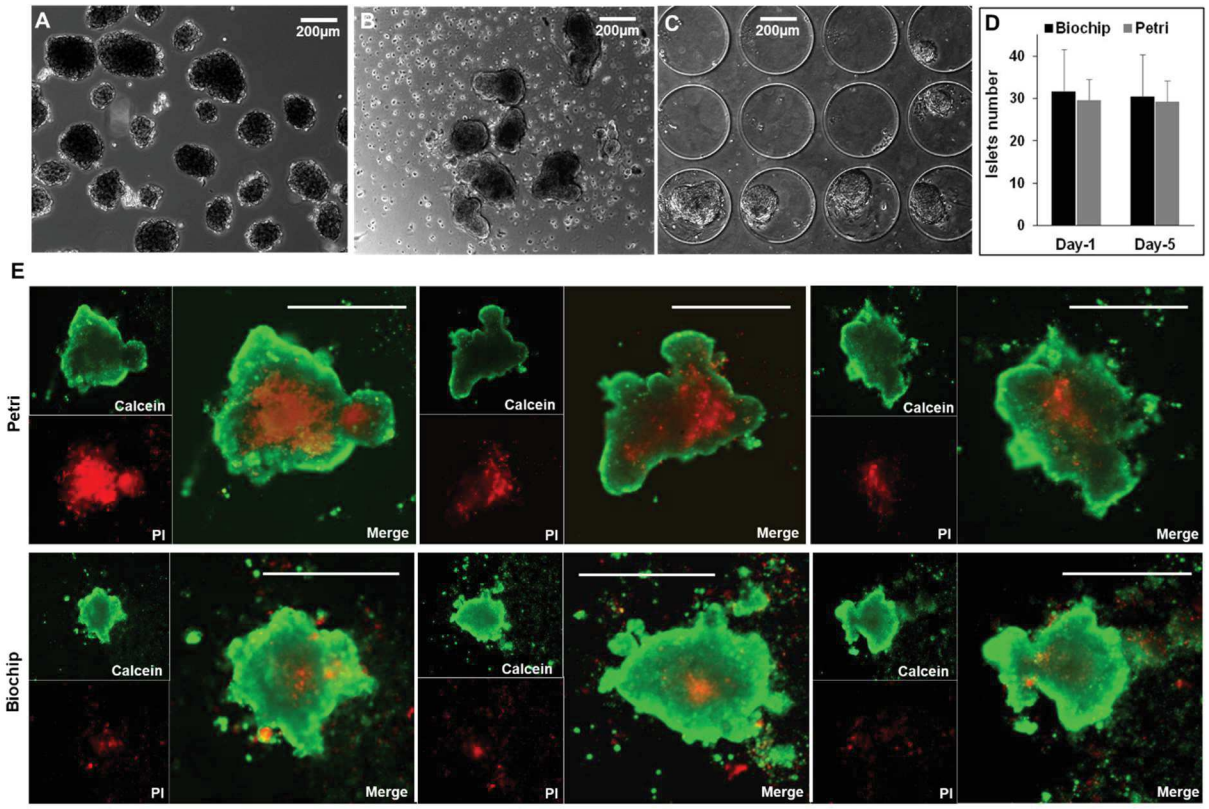

Figure 3.1 : Morphology of islets after extraction (A), after 5 days of culture in Petri (B) and after 5 days of culture in biochip (C); number of islets at days 1 and 5 in biochip and Petri (D); and calcein AM/propidium iodide staining of islets after 5 days of culture in Petri and biochip (E, PI: propidium iodide, scale bar: 100 µm).

3.2.1.2 RTqPCR analysis revealed higher mRNA levels of pancreatic islets markers in biochip cultures

At the end of the experiments, we compared the mRNA levels of the cells in the islets cultivated in biochips and Petri dishes (Fig. 3.2). The markers related to maintaining islet differentiation, such as *Reg3a* and *Neurod*, were upregulated in the biochips when compared to the Petri cultures (fold change, FC, of 190 and 13, respectively). In addition, the markers related to islet functions such as *App* (4.3 FC), *Ins1* (1.7 FC), *Sst* (2.8 FC) and *Gcg* (2.1 FC) were also upregulated in the biochips. Finally, the levels of several receptors and transporters such as *Gcgr*, *Insr*, and *Glut2* were 3.2 to 5.5 times higher in the biochip compared to the Petri dishes (Fig. 3.2).

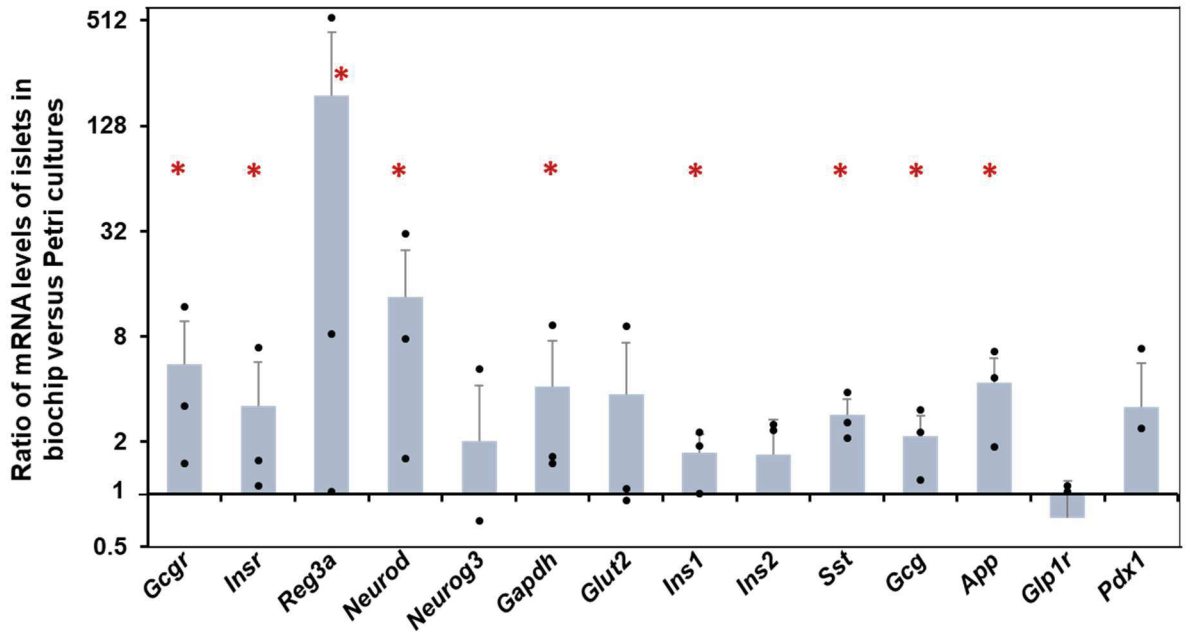

*Figure 3.2 : Ratio (biochip/Petri) of mRNA levels of selected important pancreatic islets genes after 5 days of culture. *P < 0.05, mRNA level significantly different between biochip and Petri cultures (each dot correspond to one experiment (mean of 3 biochips/Petri); n = 3x3 = 9).*

3.2.1.3 Immunostaining confirmed the expression of pancreatic islets markers and glucose regulators in both biochips and Petri dishes

The immunostaining of the islets, prior to inoculation in the biochips, demonstrated that the islets were positive for insulin and glucagon (day 0, Fig. 3.3A and Fig. S3 in supplementary file). At the end of the experiments, the islets from the Petri dishes and biochips were positive for insulin and glucagon as shown in Fig. 3.3A and Fig. S3 (supplementary file). We observed three types of cell populations, insulin positive cells, glucagon positive cells and a third subpopulation expressing both insulin and glucagon (those bihormonal cells may reflect a partial switch from β-cells to β-cells, supplementary file). We confirmed also that the islets in both culture modes were positive for GCK (Fig. 3.3B and Fig. S4 in supplementary file), consistently with the composition of the culture medium containing 10 mM of basal glucose (nb: GCK, in the pancreas, plays a role in glucose-stimulated insulin secretion).

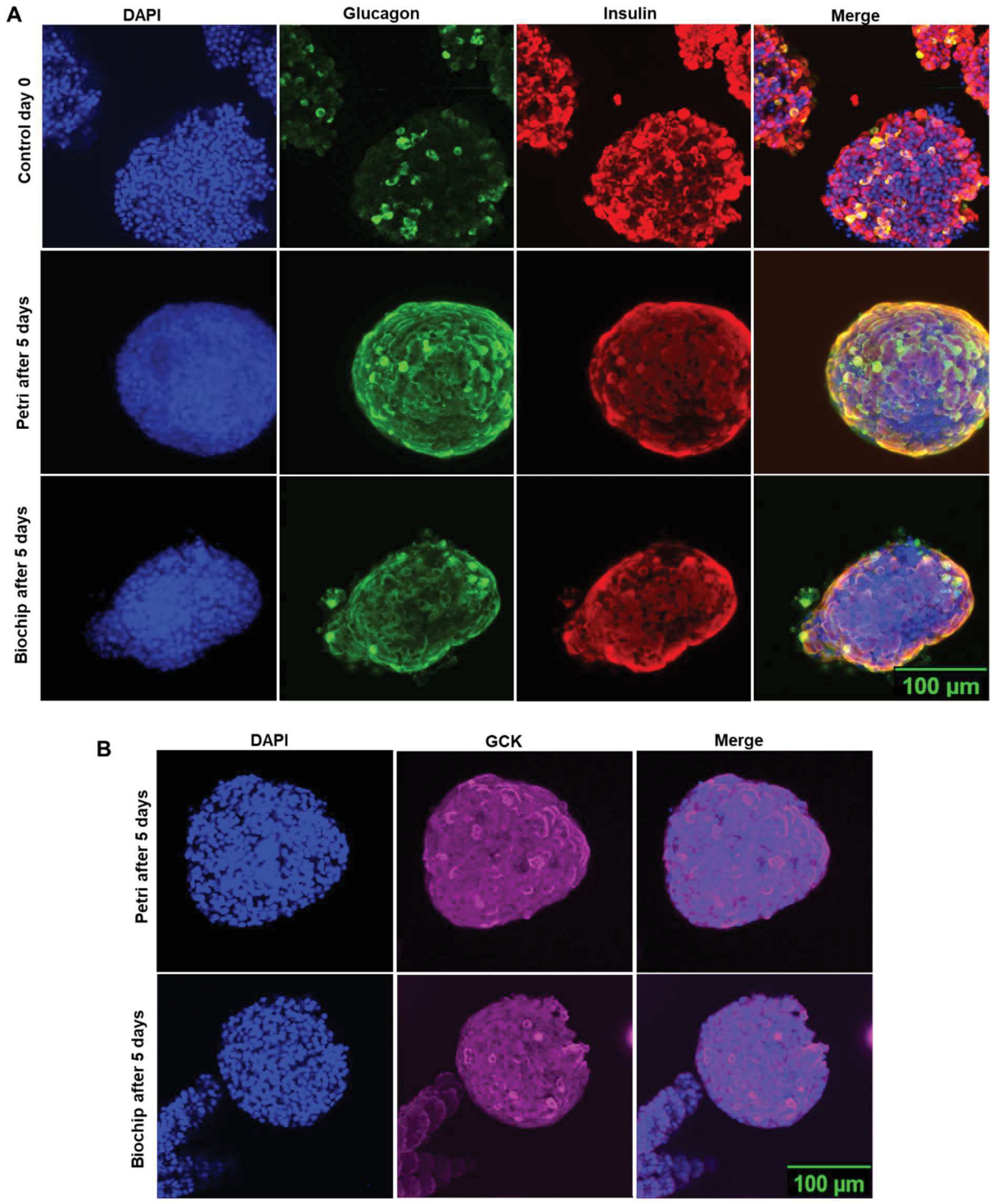

Figure 3.3 : Islets immunostainings: (A) DAPI, glucagon, insulin and merge at day 0 and after 5 days of culture in biochip and petri; (B) DAPI, GCK and merge after 5 days of culture in biochip and Petri.

3.2.1.4 Functional assays revealed higher insulin secretion in the islets in the biochips

The basal functionality of the islets was demonstrated by measuring insulin, C-peptide and glucagon secretion. At the end of each experiment, the islets were counted to normalize the data. We found that the insulin concentration in the culture medium decreased in both biochips and Petri dishes. However, the biochip cultures contributed to maintaining relatively high levels for all experiments until day 4, whereas a drop occur between day 3 and day 4 in Petri (Fig 3.4.A). Biochip cultures contributed to maintaining insulin secretion close to 130 ng/islet/day until day 4, and decreasing to 44 ng/islet/day at day 5. In the Petri dishes, we found a significant reduction in days 3 and 4, leading to measured secretion close to 30 ng/islet/day before dropping to 17 ng/islet/day at day 5. We also observed higher secretion of C-peptide in the biochips when compared to the Petri dish cultures, as shown in Fig 3.4.B. Secretion was about 5 times higher in the biochip from days 3 to 5. C-peptide secretion in Petri dish decreased significantly since day 2, whereas it decreased only at day 5 in the biochips.

The glucagon levels were higher in the biochips than in the Petri dishes, as shown in Fig. 3.4.C. Furthermore, the levels remained constant in the biochip cultures for 4 days of culture, close to 1000 pg/islet/day, before decreasing to 500 pg/islet/day on day 5. In the Petri dishes, glucagon secretion decreased from day 3 to day 4 and leading to a drop from 560 to 180 pg/islet/day between day 2 to day 5. The ratio between insulin and glucagon secretion is shown in Fig 3.4.D. In the biochips, the ratio increased from 130 to 250 between days 2 and 4, before dropping to 85 on day 5. In the Petri dishes, the ratio decreased continuously from 380 to 80, but with high intra and extra experiment variability.

Finally, glucose and lactate levels were measured during culture. As the culture medium was frequently changed during the experiments, we observed that glucose levels remained relatively stable and very high in our experiments. Both in the Petri dishes and biochips, we were

unable to detect any significant glucose depletion (Fig 3.4.E). Furthermore, lactate production was higher in the biochips than in the Petri dishes (Fig 3.4.E).

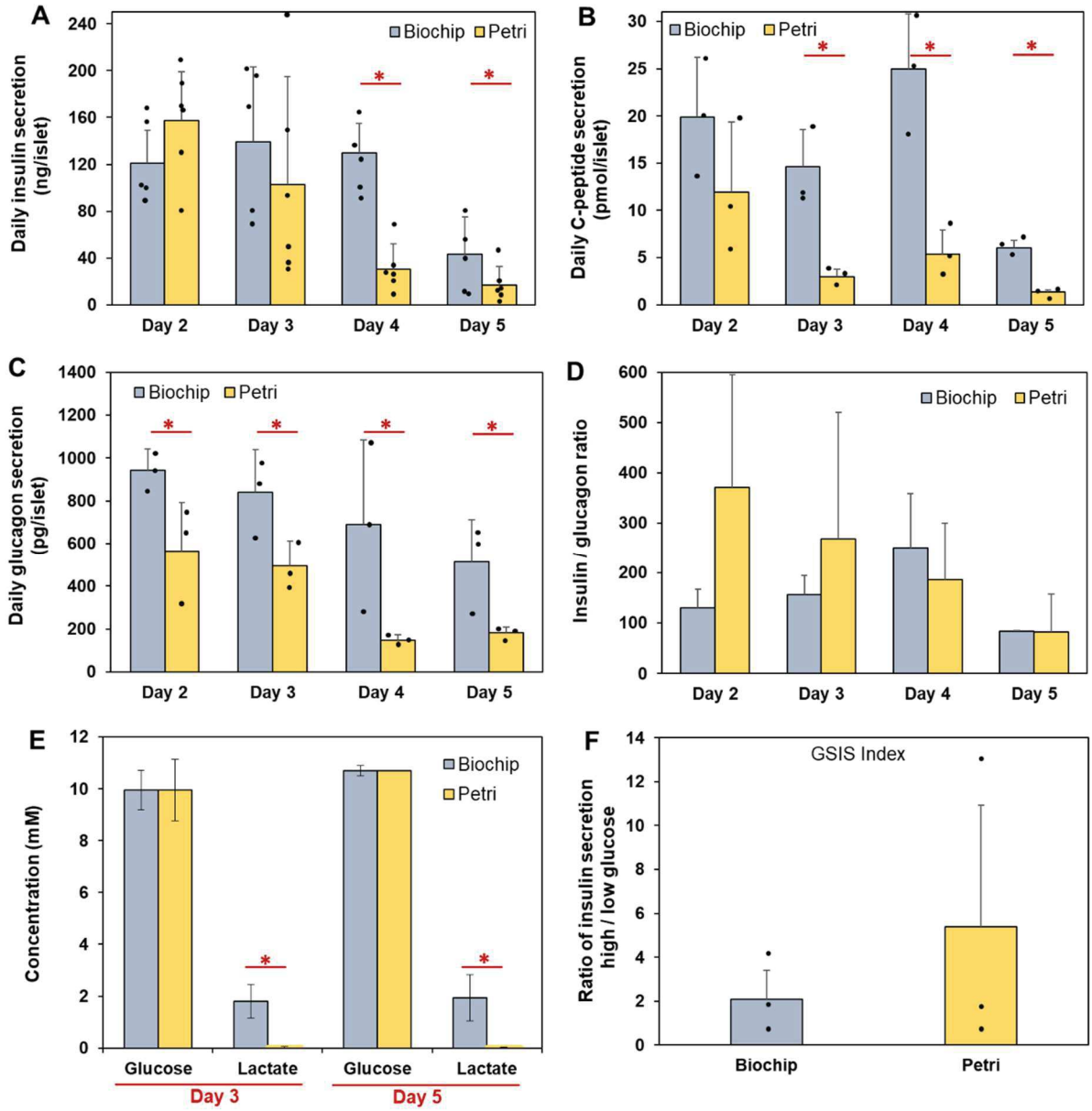

*Figure 3.4 : (A) Insulin, (B) C-peptide and (C) glucagon secretion during 5 days of culture in biochip and Petri (n = 6 for insulin and n = 3 for C-peptide and glucagon, *P < 0.05); (D) insulin/glucagon ratio; (E) glucose and lactate production in Petri and biochip after 3 and 5 days of culture (n = 3, *P < 0.05) and (F) ratio of insulin production (high/low, GSIS index) in biochip and Petri after high/low glucose stimulations (n = 3, *P < 0.05). GSIS: glucose-stimulated insulin secretion.*

3.2.2 Pancreatic islet response to stimulations demonstrated functional and active biochip culture conditions

3.2.2.1 Low-high glucose stimulations

After 4 days of culture, we performed a low-high glucose stimulation. The islets demonstrated lower insulin secretion in low glucose stimulation when compared to high glucose stimulation. To evaluate islets responsiveness to low/high glucose stimulation, we calculated the GSIS (glucose-stimulated insulin secretion) index by dividing insulin measured in high-glucose and low-glucose media (Fig. 3.4.F). The GSIS index values were of 5 and 2.1 in the Petri dishes and biochip, respectively. These results indicate that glucose response of islets was maintained in both culture modes. However, we should mention that we observed wide variability in this assay inasmuch as some Petri dishes or biochips were not induced, thus leading to a significant error bar and dispersion.

3.2.2.2 Effect of glucagon-like peptide-1 (GLP-1)

The GLP-1 stimulation contributed to the modification of mRNA levels, both in Petri dishes and biochips (Fig 3.5A). GLP-1 increased the mRNA levels of the receptors *Glp-1r*, *Gcgr*, and of the *Reg3a*, *Ins1*, *Ins2* and *Stt* genes in the biochips (when compared to non-treated biochip controls) and downregulated *Neurod*. In Petri dishes, we also found upregulation of *Gcgr*, *Insr, Ins2*, and downregulation of *Neurod* (Fig. 3.S5, supplementary file). Furthermore, the mRNA levels in the GLP-1-treated biochips were upregulated when compared to GLP-1-treated Petri dishes (data not shown).

Fig. 3.5.B shows the insulin immunostaining of islets treated by GLP-1. The data demonstrated high fluorescence intensity in GLP-1-treated Petri and biochip. We also found that the levels of the GCK protein in the islets were not over-expressed by the GLP-1 treatment (Fig. 3.5.B). At the functional levels, insulin secretion was increased in both Petri dishes and biochips by the GLP-1 treatments (Fig 3.6.A). On days 2, 3 and 4, the levels of insulin in the biochips were up to 3 times higher than those attained in control. However, after 5 days, this induction was weaker (2 times). We then performed the low-high glucose stimulation tests after pre-treatment with GLP-1. As expected, GLP-1 did not inhibit the effect of the high / low glucose stimulations and maintained a high level of insulin production in the biochips under high glucose stimulation (Fig 3.6.B). In this assay, the low / high glucose stimulation led to an insulin over production of 2.2 and 4 in biochips and Petri, respectively (GSIS index of 2.24 and 4, respectively). Furthermore, we did not observe variability in the assay when compared to the untreated conditions (cf. Fig 3.4.F).

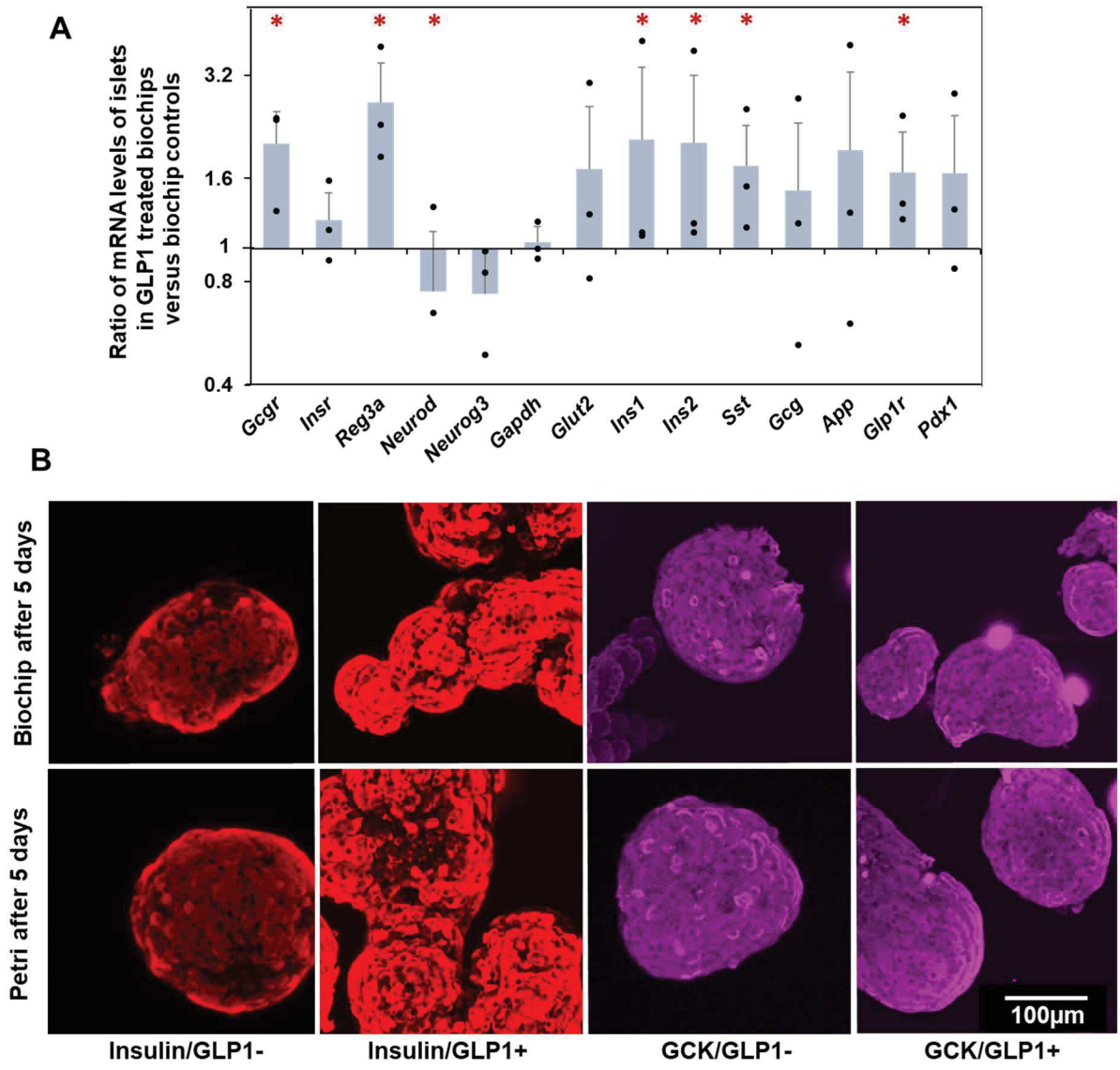

*Figure 3.5 : (A) Ratio of mRNA levels (GLP1 treated biochip/control biochip) of selected pancreatic islets genes after GLP1 stimulation; and (B) insulin and GCK immunostainings in controls and GLP1 treated biochip/Petri. *P < 0.05, mRNA level significantly different between GLP1 treated biochip and control biochip (each dot correspond to one experiment (mean of 3 biochips/Petri); n = 3x3 = 9).*

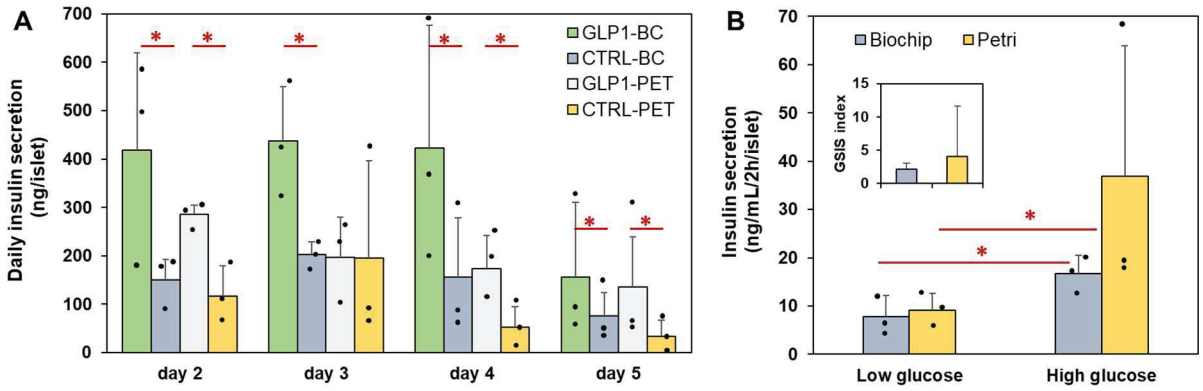

*Figure 3.6 : (A) Insulin secretion in controls and GLP1 treated biochip and Petri during 5 days of culture (n = 3, *P < 0.05); and (B) insulin secretion and GSIS index in GLP1 treated biochip and Petri during high/low glucose stimulations (n = 3, *P < 0.05). GSIS: glucose-stimulated insulin secretion.*

3.3 Discussion

In this study, we investigated the performance of islets of Langerhans in a closed loop microfluidic system. Several investigations have reported microfluidic techniques for keeping islet or spheroid cultures on chip, including the pancreas (Tan and Takeuchi 2007; Zbinden et al., 2020; Lee et al., 2018; Mohammed et al., 2009). Those devices are based on a flow trapping process (Tan and Takeuchi 2007; Zbinden et al., 2020). We built a simple culture biochip where the pancreatic islets can be trapped by sedimentation in the bottom microstructure. This type of trapping was also reported by Lee et al., 2018. In our biochip, the microstructure contributed to create an array of 600 microwells allowing to trap an important quantity of islets. The depth of microwells made it possible to protect the islets from flow circulation and thus prevent them from being washed away and from mechanical damage. As a result, we maintained a constant number of islets between the beginning and the end of the perfusion. Furthermore, due to sedimentation in the microwells, the islets were protected from the fluid shear stresses created by the laminar flow.

In biochip, we observed higher viability for the cells located in the center of the pancreatic islets when compared to the Petri dish cultures. This was illustrated by the viability assay in which a larger number of dead cells was observed in the center of the islets when they were cultivated in Petri dishes. Central necrosis and apoptosis in pancreas islets are due mainly to the high density of the tissue and the lake irrigation as has been widely reported in literature (Giuliani et al., 2005, Moritz et al., 2002). Several hypotheses are proposed to explain central necrosis and apoptosis in pancreatic islets (and also in cell spheroids), including deprivation of oxygen, nutrients and serum as a result of limited diffusion (Giuliani et al, 2005). In the case of the pancreatic islets, the blood micro-vessels usually reach the center of the structure *in vivo* but the microvasculature gets closed in *ex vivo* tissue (Jansson et al. 2016). In parallel, microfluidic cultures have been shown to improve the viability of spheroid tissue by reducing the central necrotic core thanks to

control of local glucose concentrations and local oxygenation through the dissolved oxygen provided by the medium flows (Barisam et al., 2018, Baye et al., 2017). As a result, those literature reports appeared consistent with our findings.

In our investigation, we found that the microfluidic culture maintained and improved pancreatic regeneration and maturation markers of the rat islet cells. This was illustrated by higher levels of mRNA in important pancreatic islet markers, including receptor genes (*Gcr* and *Insr*), hormone secretion-related genes (*App*, *Sst* and *Ins1*) and differentiation genes (*Neurod* and *Reg3a*). More particularly, we found a 190-fold upregulation of *Reg3a*, which is an islet regeneration marker (Coffey et al., 2014) involved in the pro-islet gene cascade and their protection against induced diabetes mellitus (Xiong et al., 2011). In addition, *Neurod* was 13 times higher in the biochips compared to Petri dish levels. *Neurod* is an important gene (an insulin trans activator) required to maintain functional maturity in pancreatic beta cells, including insulin production through *Ins1* (Gu et al., 2010). We also consistently found upregulation of the *Ins1* gene in the biochips, which is consistent with *Ins1* silencing in *Neurod* KO mice (Gu et al., 2010). *Neurod* KO-mice expressed the *Ins2* gene and were thus able to produce insulin in a glucose stimulation test, which also appeared consistent with our findings in which *Ins2* was commonly expressed in both the Petri dishes and the biochips (Gu et al., 2010).

In parallel, an over-expression of the insulin receptor *Insr* was observed. *Insr* is involved in controlling glucose-stimulated insulin secretion *via* its relationship with insulin gene expression, *Glut2* and *Pdx1* (Wang et al., 2018). We consistently observed a tendency for higher mRNA levels in the *Glut2* and *Pdx1* genes in the biochips. The upregulation of *Gcgr*, the glucagon receptor, in the biochips also indicated a probable beneficial effect of the microfluidic cultures on the alpha cells inasmuch as the lack of glucagon receptors is correlated with several pancreas disorders and alteration to glucose homeostasis, such as hyperplasia and hyperglucagonemia (Charron et al., 2015).

At the functional level, we analyzed the performances of the pancreas islets when they were cultivated in the biochips. At first, this was illustrated by the kinetics of the secretion of insulin in the culture medium. Although the overall secretion decreased between the first day and fifth day of culture in both culture conditions, the biochip levels remained higher when compared to those of the Petri dishes. Secondly, the high/low glucose stimulation assay demonstrated that islet response to stimuli was preserved in our biochip culture. However, in the biochips, the protocol required an extended washing process to remove the insulin and remaining glucose from the basal culture medium in the perfusion circuit (mainly due to the dilution of high glucose solution in washing solution that would lead to bias stimulation). This need of washing process synchronization in the biochips, when compared to conventional Petri dishes, has already been reported in pancreas-on-chip investigations (Zbinden et al., 2020).

Nevertheless, enhancements of basal islets functions such as insulin secretion and glucose-induced insulin secretion in microfluidic devices have been observed consistently in the literature (Sankar et al., 2011). In our dataset, this over-secretion of insulin was not correlated with over-expression of *Gck*, as demonstrated by the immunostaining. The glucose-stimulated insulin secretion was regulated by the rate of glucose metabolism within β cells, and a key event in this process is the phosphorylation of glucose by glucokinase (the coding gene is *Gck*, Wu et al., 2004). Although we worked in a closed loop perfusion circuit, the flow rate led to continuously renewing the culture medium locally in the biochips. Furthermore, the level of glucose remained high in the medium, probably due to the number of islets. The microfluidic culture completely modulated the chemical cellular microenvironment (*via* a complex gradient of molecules, a balance between diffusion and convection, cellular consumption) leading to complex signals (Young et al., 2010, Halldorson et al., 2015). In parallel, the microwells almost certainly influenced the local nutrient islets' microenvironment (a balance between glucose consumption, glucose renewal, secreted insulin concentration, etc…). As a result, additional local measurements (*via* integrated sensors) and numerical simulations are needed to understand the complex kinetics of insulin secretion in relation to local glucose concentrations in our biochips.

Finally, we tested the effect of the glucagon-like peptide-1 (GLP-1) in both culture conditions. GLP-1 physiologically induces glucose-dependent insulin secretion from β-cells and GLP-1 analogues improve hyperglycemia in T2D patients (Drucker et al., 2006; DeFronzo et al., 2005, Vilsbol et al., 2007). Furthermore, GLP-1 treatment increases *Gck* activity (Ding et al., 2011). However, long term GLP-1 exposure (about 18h) also resulted in the promotion of the metabolic reprogramming of β-cells through mTOR-dependent HIF signaling, and independently of *Gck* post-translational activation (Carlessi et al., 2017). In the present study, GLP-1 stimulation clearly upregulated several pancreatic islet genes such as *Glp-1r* and *Gcgr,* in both Petri dishes and biochips. In addition, those mRNA levels were upregulated in the biochips compared to the Petri dishes when the GLP-1 was loaded. At the functional level, GLP-1 induced an increase in insulin secretion in both culture modes (as confirmed by the immunostaining of insulin and the insulin extracellular concentrations in the medium). The secretion levels in the culture medium were found to be higher in the biochips. However, we did not find any of the inhibitory effect we expected in the alpha cells of the islets of Langerhans (glucagon secretion) (Tudori et al. 2016). In our biochips, we found mRNA *Glut2* over-expression compared to the Petri dishes, leading to the suspicion of higher glucose transport, and thus metabolism, in the islets. We did not find an effect of GLP-1 on the *Gck* at the immunostaining fluorescent level. Although these findings seems consistent with the observations made by Carlessi et al., 2017, more extensive investigations are needed to confirm the underlying mechanism in biochips.

3.4 Conclusion

In this work, we studied the behavior of rat islets of Langherans when cultivated in microfluidic biochips or in Petri dishes. The microfluidic biochips cultures maintained high islet viability throughout the 5 days of culture. More particularly, several important pancreatic islet genes, including *Reg2a*, *Neurod*, *Insr*, *Gcgr*, *Glut2*, *Ins1*, *App* and *Stt* were overexpressed in biochips cultures (compared to islets cultivated in Petri). The islets were able to secrete insulin and glucagon, as well as to respond to GLP-1 stimulation and high-low glucose test. Furthermore, the levels of insulin secretion appeared higher in biochips when compared to the Petri dishes. Our dataset illustrated the fact that the microfluidic culture is beneficial for maintaining *in vitro* maturation and functionality of islets of Langerhans. We believe that our results are encouraging for the development of functional pancreas *in vitro* models using the advantages of organ-on-chip technology.

3.5. Supplementary figures

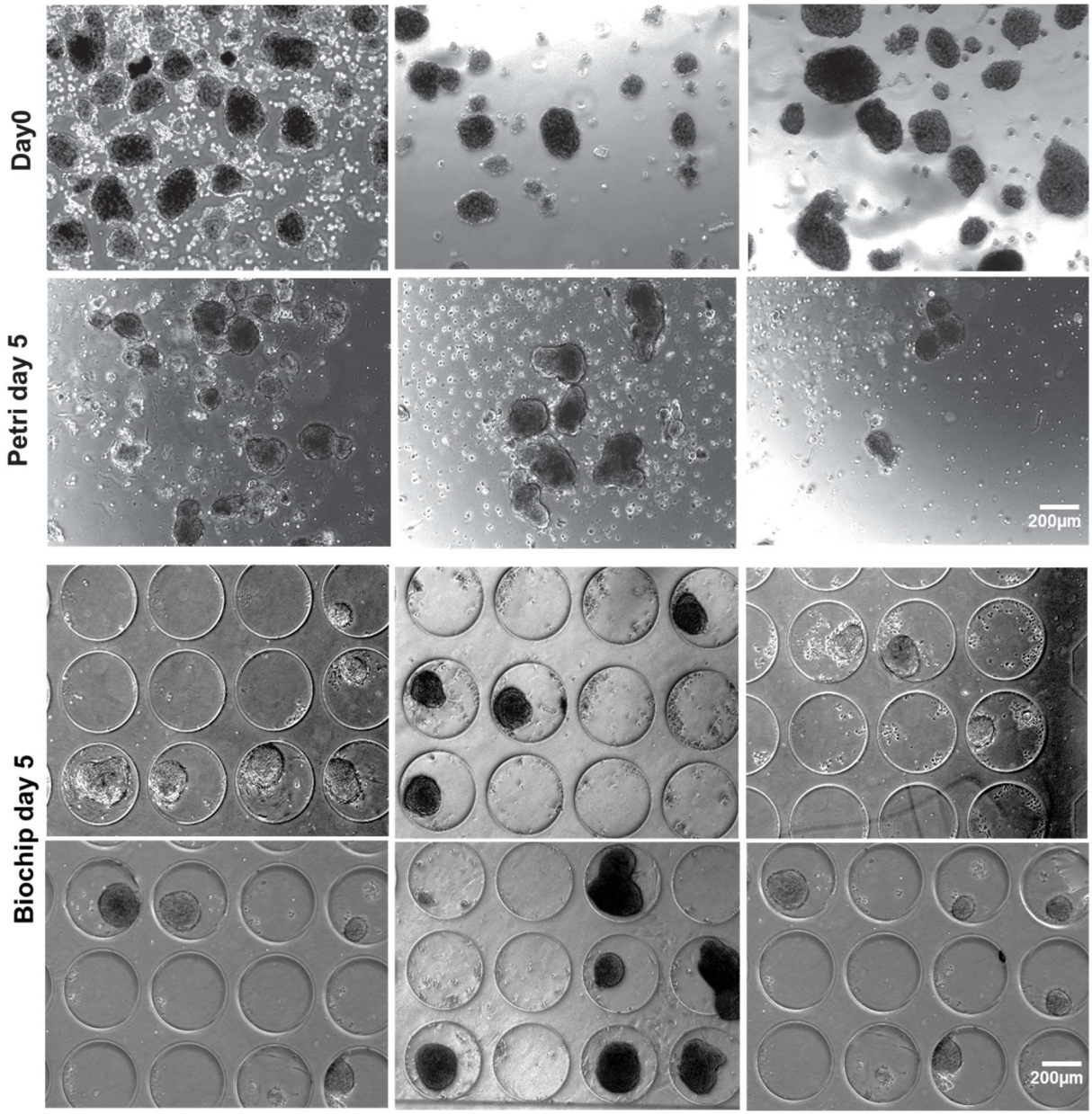

Figure 3.S1: Morphology of the islets before seeding (day 0) and after 5 days of culture in biochip and in Petri dish.

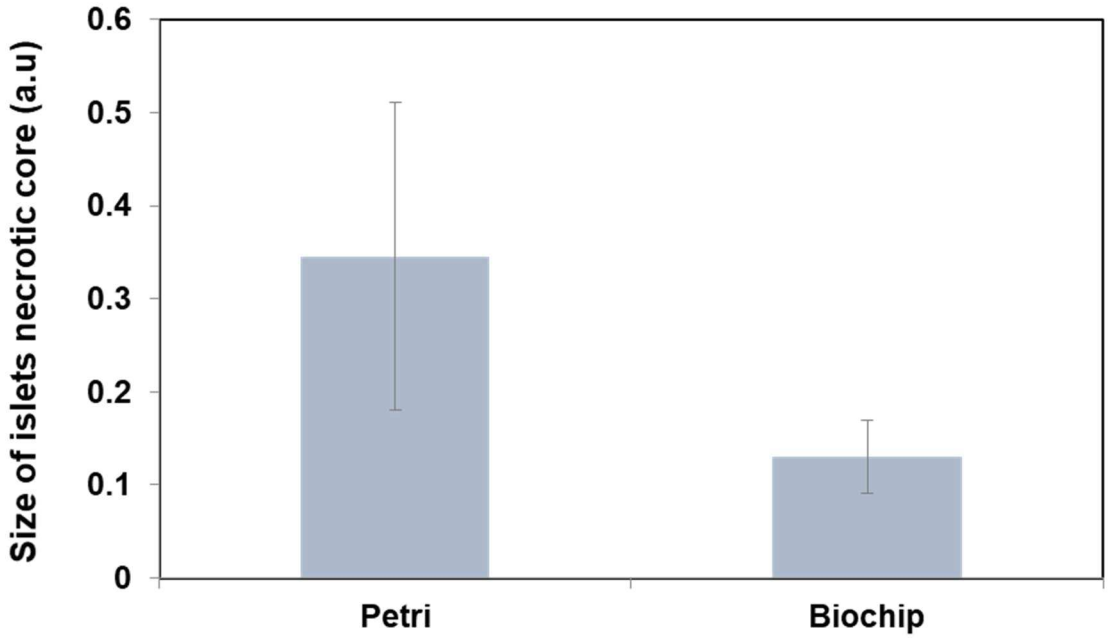

Figure 3.S2: Size of necrotic core of islets cultivated in Petri and in biochip after 5 days (quantification by ImageJ software using the fluorescent images of live/dead assay).

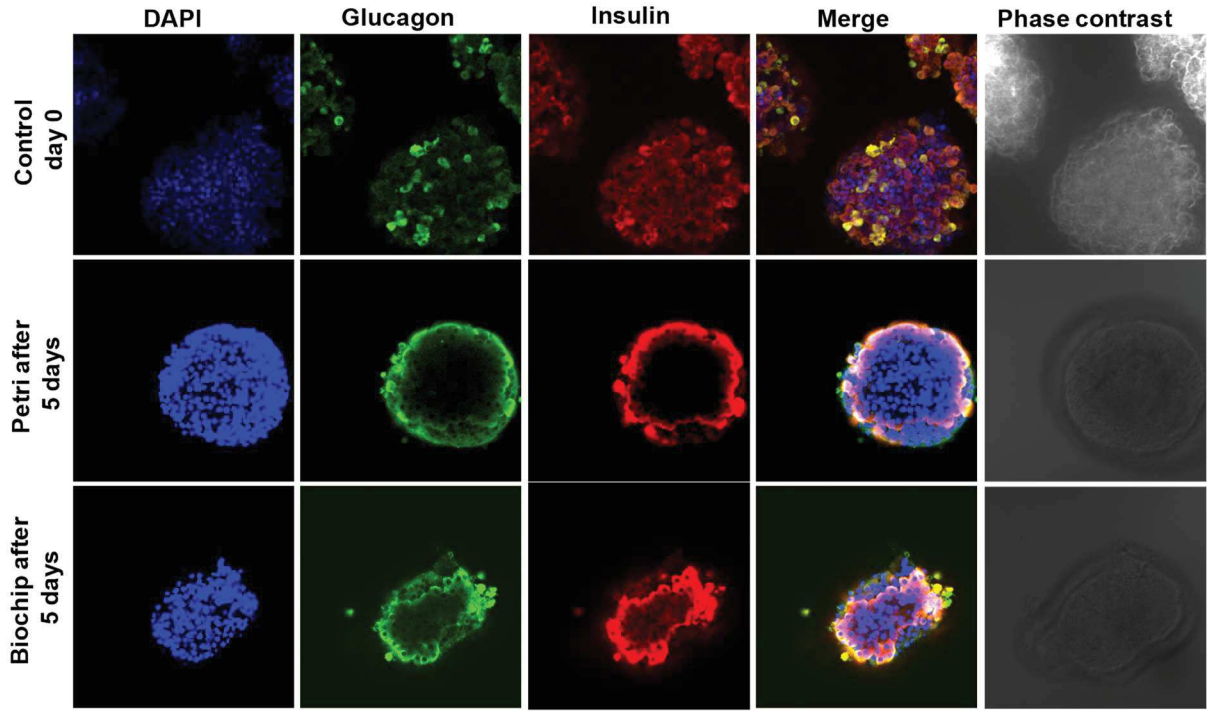

Figure 3.S3: Islets immunostainings (DAPI, glucagon, insulin, and merge) and phase contrast images of islets at day 0 and after 5 days of culture in biochip and Petri.

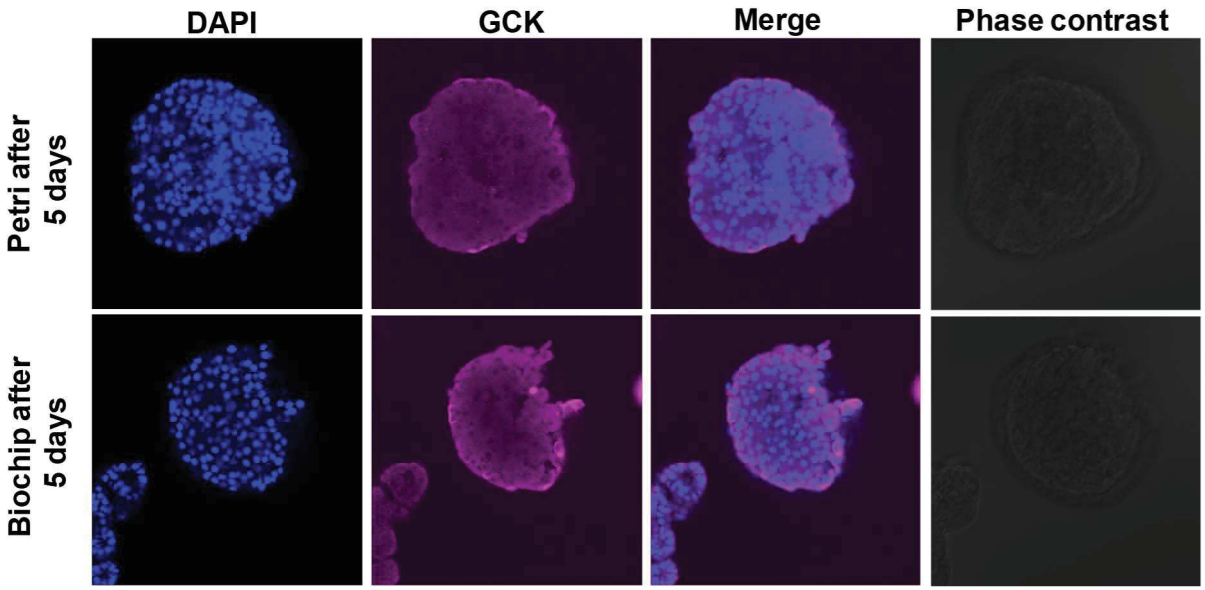

Figure 3.S4: Islets immunostainings (DAPI, GCK and merge) and phase contrast images of islets after 5 days of culture in biochip and Petri.

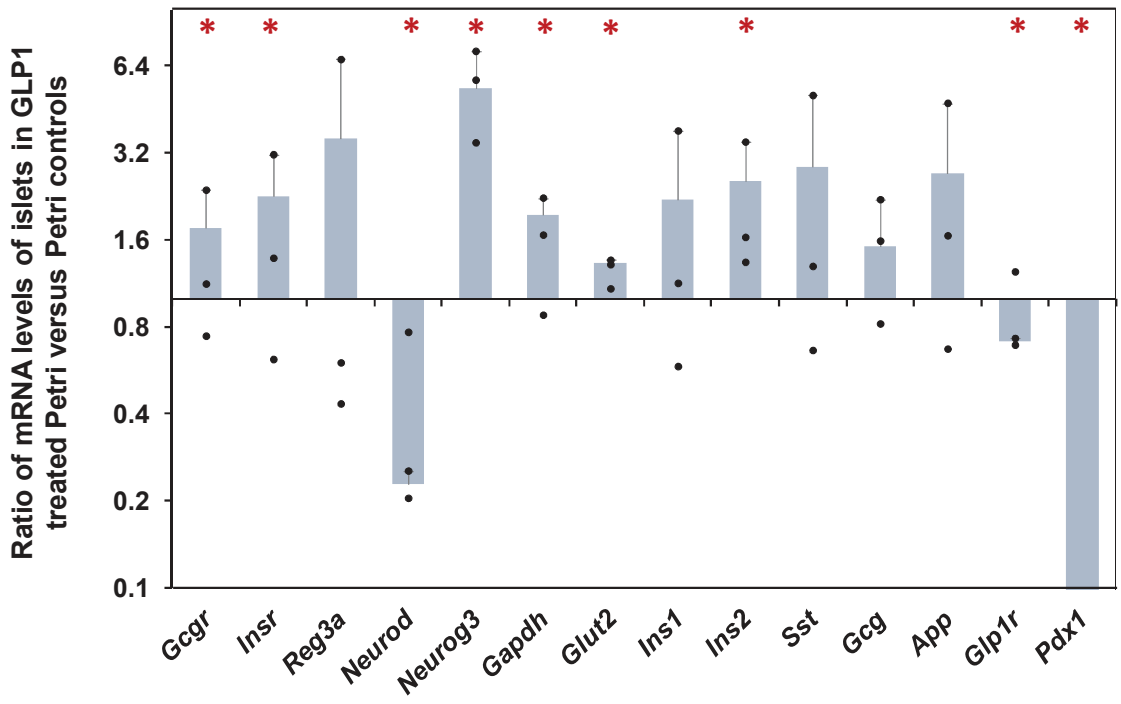

*Figure 3.S5: Ratio of mRNA levels (GLP1 treated Petri/control Petri) of selected pancreatic genes after GLP1 stimulation. *P < 0.05, mRNA level significantly different between GLP1 treated Petri and control Petri.*

3.6 References

Aghamaleki, M.A., Hajiahmadi, M., Pornasrollah, M., Oruji, Z., Aghajanpour, F., 2019., Effect of vitamin D supplementation on pancreatic B -cell function in patients with Type 1 Diabetes Mellitus and vitamin D deficiency: A clinical trial study. Int. J. Pediatr. 7, 8977-8984.

Artunc, F., Schleicher, E., Weigert, C., Fritsche, A., Stefan, N., Häring, H.U., 2016. The impact of insulin resistance on the kidney and vasculature. Nat. Rev. Nephrol. 12, 721-737.

Baker, K., 2016. Comparison of bioartificial and artificial pancreatic transplantation as promising therapies for Type I Diabetes Mellitus. Biosci. Horizons 9, hzw002.

Barisam, M., Saidi, M.S., Kashaninejad, N., Nguyen, N.T., 2018. Prediction of necrotic core and hypoxic zone of multicellular spheroids in a microbioreactor with a U-shaped barrier. Micromachines 9, 94.

Bauer, S., Wennberg Huldt, C., Kanebratt, K., Durieux, I., Gunne, D., Andersson, S., Ewart, L., Haynes, W., Maschmeyer, I., Winter, A., Ämmälä, C., Marx, U., Andersson, T., 2017. Functional coupling of human pancreatic islets and liver spheroids on-a-chip: Towards a novel human ex vivo type 2 diabetes model. Sci Rep. 7, 14620.

Baye, J., Galvin, C., Shen, A.Q., 2017. Microfluidic device flow field characterization around tumor spheroids with tunable necrosis produced in an optimized off-chip process. Biomed. Microdevices. 19, 59.

Bhatia, S.N., Ingber, D.E., 2014. Microfluidic organs-on-chips. Nat. Biotechnol. 32, 760-772.

Brooks, J.C., Ford, K.I., Holder, D.H., Holtan, M.D., Easley, C.J., 2016. Macro-to-micro interfacing to microfluidic channels using 3D-printed templates: application to time-resolved secretion sampling of endocrine tissue. Analyst 141, 5714-5721.

Carlessi, R., Chen, Y., Rowlands, J., Cruzat, V.F., Keane, K., Egan, L., Mamotte, C., Stokes, R., Gunton, J., Homem de Bittencourt, P.I., Newsholme, P., 2017. GLP-1 receptor signalling promotes β-cell glucose metabolism via mTOR-dependent HIF-1α activation. Sci. Rep. 7, 2661.

Charron, M.J., Vuguin, P.M., 2015. Lack of glucagon receptor signaling and its implications beyond glucose homeostasis. J. Endocrinol. 224, R123-R130.

Coffey, R., Nam, H., Knutson, M., 2014. Microarray analysis of rat pancreas reveals altered expression of Alox15 and regenerating islet-derived genes in response to iron deficiency and overload. PLoS One. 9, e86019.

DeFronzo, R.A., Ratner, R.E., Han, J., Kim, D.D., Fineman, M.S., Baron, A.D., 2005. Effects of exenatide (exendin-4) on glycemic control and weight over 30 weeks in metformin-treated

patients with type 2 diabetes. Diabetes care 28, 1092-1100.

Ding, S.Y., Nkobena, A., Kraft, C., Markwardt, M., Rizzo, M.A., 2011. Glucagon-like peptide 1 stimulates post-translational activation of glucokinase in pancreatic cells, J. Biol. Chem. 286, 16768-16774.

Drucker, D.J., Nauck, M.A., 2006. The incretin system: glucagon-like peptide-1 receptor agonists and dipeptidyl peptidase-4 inhibitors in type 2 diabetes. Lancet 368, 1696-1705.

Efanov, A.M., Sewing, S., Bokvist, K., Gromada, J., 2004. Liver X Receptor Activation Stimulates Insulin Secretion via Modulation of Glucose and Lipid Metabolism in Pancreatic Beta-Cells. Diabetes 53, S75-S78.

Ghaemmaghami, A.M., Hancock, M.J., Harrington, H., Kaji, H., Khademhosseini, A., 2012. Biomimetic tissues on a chip for drug discovery. Drug. Discov. Today. 17, 173-181.

Giuliani, M., Moritz, W., Bodmer, E., Dindo, D., Kugelmeier, P., Lehmann, R., Gassmann, M., Groscurth, P., Weber, M., 2005. Central necrosis in isolated hypoxic human pancreatic islets: evidence for postisolation ischemia. Cell Transplant. 14, 67-76.

Gu, C., Stein, G., Pan, N., Goebbels, S., Hörnberg, H., Nave, K.A., Herrera, P., White, P., Kaestner, K., Sussel, L., Lee, J., 2010. Pancreatic β cells require NeuroD to achieve and maintain functional maturity. Cell Metab. 11, 298-310.

Halldorsson, S., Lucumi, E., Gómez-Sjöberg, R., Fleming, R.M.T., 2015. Advantages and challenges of microfluidic cell culture in polydimethylsiloxane devices. Biosens. Bioelectron. 63, 218-231.

Huh, D., Torisawa, Y.S., Hamilton, G.A., Kim, H.J., Ingber, D.E., 2012. Microengineered physiological biomimicry: organs-on-chips. Lab Chip. 12, 2156-2164.

International Diabetes Federation official web site: https://www.idf.org/.

Jellali, R., Essaouiba, A., Leclerc, E., Legallais, C., 2020. Chapter 4 - Membrane bioreactors for bio-artificial pancreas, in: Basile, A., Annesini, M.C., Piemonte, V., Charcosset, C., (Eds.), Current Trends and Future Developments on (Bio-) Membranes, Elsevier, pp. 77-108.

Jouvet, N., Estall, J.L., 2017. The pancreas: Bandmaster of glucose homeostasis. Exp. Cell Res. 360, 19-23.

Jun, Y., Lee, J., Choi, S., Yang, J.H., Sander, M., Chung, S., Lee, S.H.,2019. In vivo-mimicking microfluidic perfusion culture of pancreatic islet spheroids. Sci Adv. 5, eaax4520.

Kiba, T., Tanemura, M., Yagyu, K., 2013. High-quality RNA extraction from rat pancreatic islet. Cell Biol. Int. Rep. 20, 1-4.

Kimura, Y., Okitsu, T., Xibao, L., Teramae, H., Okonogi, A., Toyoda, K., Uemoto, S., Fukushima, M., 2013. Improved hypothermic short-term storage of isolated mouse islets by adding serum to preservation solutions. Islets 5, 45-52.

King, A., Bowe, J., 2016. Animal models for diabetes: Understanding the pathogenesis and finding new treatments. Biochem. Pharmacol. 99, 1-10.

Kneteman, N.M., Warnock, G.L., Evans, M.G., Dawidson, I., Rajotte, R.V., 1990. Islet isolation from human pancreas stored in UW solution for 6 to 26 hours. Transplant. Proc. 22, 763-764.

Kumar, M., Melton, D., 2003. Pancreas specification: a budding question. Curr. Opin. Genet. Dev. 13, 401-407.

Lee, S.H., Hong, S., Song, J., Cho, B., Han, E.J., Kondapavulur, S., Kim, D., Lee, L.P., 2018. Microphysiological analysis platform of pancreatic islet β-cell spheroids. Adv. Healthc. Mater. 7, 1701111.

Li, X., Brooks, J.C., Hu, J., Ford, K.I., Easley, C.J., 2017. 3D-templated, fully automated microfluidic input/output multiplexer for endocrine tissue culture and secretion sampling. Lab Chip. 17, 341-349.

Mohammed, J.S., Wang, Y., Harvat, T.A., Oberholzer, J., Eddington, D.T., 2009. Microfluidic device for multimodal characterization of pancreatic islets. Lab Chip 9, 97-106.

Moritz, W., Meier, F., Stroka, D.M., Giuliani, M., Kugelmeier, P., Nett, P.C., Lehmann, R., Candinas, D., Gassmann, M., Weber, M., 2002. Apoptosis in hypoxic human pancreatic islets correlates with HIF-1alpha expression. FASEB J. 16, 745-747.

Rogal, J., Zbinden, A., Schenke-Layland, K., Loskill, P., 2019. Stem-cell based organ-on-a-chip models for diabetes research. Adv. Drug. Deliv. Rev. 140, 101-128.

Sankar, K.S., Green, B.J., Crocker, A.R., Verity, J.E., Altamentova, S.M., Rocheleau, J.V., 2011. Culturing pancreatic islets in microfluidic flow enhances morphology of the associated endothelial cells. Plos One 6, e24904.

Sardu, C., De Lucia, C., Wallner, M., Santulli, G4., 2019. Diabetes mellitus and its cardiovascular complications: New insights into an old disease. J. Diabetes Res. 2019, 1905194.

Schulze, T., Mattern, K., Früh, E., Hecht, L., Rustenbeck, I., Dietzel, A., 2017. A 3D microfluidic perfusion system made from glass for multiparametric analysis of stimulus-secretion coupling in pancreatic islets. Biomed. Microdevices 19, 47.

Silva, J.A.D., Souza, E.C.F., Echazú Böschemeier, A.G., Costa, C.C.M.D., Bezerra, H.S., Feitosa, E.E.L.C., 2018. Diagnosis of diabetes mellitus and living with a chronic condition: participatory study. BMC Public Health 18, 699.

Tan, W.H., Takeuchi, S., 2007. A trap-and-release integrated microfluidic system for dynamic microarray applications. Proc. Natl. Acad. Sci. USA. 104, 1146-1151.

Vilsbøll, T., Zdravkovic, M., Le-Thi, T., Krarup, T., Schmitz, O., Courrèges, J.P., Verhoeven, R., Bugánová, I., Madsbad, S., 2007. Liraglutide, a long-acting human glucagon-like peptide-1 analog, given as monotherapy significantly improves glycemic control and lowers body weight without risk of hypoglycemia in patients with type 2 diabetes. Diabetes care 30, 1608-1610.

Wang, J., Gu, W., Chen, C., 2018. Knocking down insulin receptor in pancreatic Beta cell lines with lentiviral-small hairpin RNA reduces glucose-stimulated insulin secretion via decreasing the gene expression of insulin, GLUT2 and Pdx1. Int. J. Mol. Sci. 19, 985.

Wu, L., Nicholson, W., Knobel, S.M., Steffner, R.J., May, J.M., Piston, D.W., Powers, A.C., 2004. Oxidative stress is a mediator of glucose toxicity in insulin-secreting pancreatic islet cell lines. J. Biol. Chem. 279, 12126-12134.

Xiong, X., Wang, X., Li, B., Chowdhury, S., Lu, Y., Srikant, C.B., Ning, G., Liu, J.L., 2011. Pancreatic islet- specific overexpression of Reg3beta protein induced the expression of pro-islet genes and protected the mice against streptozotocin-induced diabetes mellitus. Am. J. Physiol. Endocrinol. Metab. 300, E669-680.

Yonekawa, Y., Okitsu, T., Wake, K., Iwanaga, Y., Noguchi, H., Nagata, H., Liu, X., Kobayashi, N., Matsumoto, S., 2006. A new mouse model for intraportal islet transplantation with limited hepatic lobe as a graft site. Transplantation 82, 712-715.

Young, E.W.K., Beebe, D.J., 2010. Fundamentals of microfluidic cell culture in controlled microenvironments. Chem. Soc. Rev. 39, 1036-1048.

Zbinden, A., Marzi, J., Schlünder, K., Probst, C., Urbanczyk, M., Black, S., Brauchle, E.M., Layland, S.L., Kraushaar, U., Duffy, G., Schenke-Layland, K., Loskill, P., 2020. Non-invasive marker-independent high content analysis of a microphysiological human pancreas-on-a-chip model. Matrix Biol. 85-86, 205-220.

Chapter IV: Development of a pancreas-liver organ-on-chip coculture model for organ-to-organ interaction studies

In this chapter, we present the functional coupling of rat hepatocytes and pancreatic islets of Langerhans on-a-chip model. This work was published as:

Essaouiba A, Okitsu T, Kinoshita R, Jellali R, Shinohara M, Danoy M, Legallais C, Sakai Y, Leclerc E, Development of a pancreas-liver coculture model for organ-to-organ interaction studies, Biochemical Engineering Journal, Volume 164, 15 December 2020, https://doi.org/10.1016/j.bej.2020.107783

The paper abstract is presented below as a short summary of the chapter. The material and methods of the paper correspond to a short version of the previous chapter II. As a result, the materials and methods are not included in the following pages. The supplementary files of the paper are provided at the end of this chapter. The overall published paper is presented in annex of the thesis manuscript.

Summary

Type 2 diabetes mellitus (T2DM) is a widespread chronic disease with a high prevalence of comorbidity and mortality. The exponential increase of TD2M represents an important public health challenge and leads a strong demand for the development of relevant *in vitro* models to improve mechanistic understanding of diabetes and identify new anti-diabetic drugs and therapies. These models involve considering the multi-organ characteristic of T2DM. The organ-on-chip technology has made it possible to connect several organs thanks to dedicated microbioreactors interconnected by microfluidic network. Here, we developed pancreas-liver coculture model in a microfluidic biochip, using rat islets of Langerhans and hepatocytes. The behavior and functionality of the model were compared to islets and hepatocytes (with/without insulin) monocultures. Compared to monoculture, the islets coculture presented high C-peptide and insulin secretions, and downregulation of *Pdx1*, *Glut2*, *App*, *Ins1*, *Neurod*, *Neurog3* and *Gcgr* genes. In the hepatic compartment, the monocultures without insulin were negative to CK18 staining and displayed a weaker albumin production, compared to monoculture with insulin. The hepatocytes cocultures were highly positive to INSR, GLUT2, CK18 and CYP3A2 immunostaining and allowed to recover mRNA levels similar to monocultures with insulin. The result showed that islets could produce insulin to supplement the culture medium and recover hepatic functionality. This model illustrated the potential of organ-on-chip technology for reproducing crosstalk between liver and pancreas.

Keywords: Organ-on-chip, Islets of Langerhans, hepatocytes, coculture, glucose homeostasis, diabetes

Chapter IV: Development of a pancreas-liver organ-on-chip coculture model for organ-to-organ interaction studies

4.1. Introduction

Diabetes mellitus (DM) is a chronic metabolic disorder characterized by deregulation of glucose homeostasis that results from insulin deficiency or systemic insulin resistance [1]. DM is one of the most prevalent and costly diseases in the world, affecting approximately 463 million people worldwide (1 in 11 adults), according to the latest International Diabetes Federation (IDF) estimation [2]. In 2016, the World Health Organization (WHO) estimated that 1.6 million deaths were directly caused by diabetes [3]. The complications of diabetes are also associated with multiple medical problems such as blindness, kidney failure, cardiovascular diseases, sexual dysfunction, neuropathy, and peripheral vascular disease [4, 5]. Type 2 diabetes mellitus (T2DM, known as insulin-independent diabetes) is the most common form of diabetes, representing 90% of diabetic patients (415 million people worldwide) [2, 6]. T2DM is caused by the insensitivity of target-tissues to insulin, and impaired insulin secretion [4]. Currently, there is no curative treatment for T2DM. Most treatments help patients control the disease and include lifestyle adjustments and drug therapy such as metformin, sulphonylureas, glitazones and GLP-1 receptor agonists [4, 7].

T2DM is a complex disease involving interactions between several organs, including the pancreas, liver, muscle, adipose tissues, kidneys, and gut [4]. One of the key features of T2DM is the insulin resistance state characterized by a drop-down of glucose uptake by the skeletal muscle, fatty tissue, and liver [5]. In the pancreas, the state of hyperglycemia triggers the increase in insulin secretion, which can lead to hyperinsulinemia and beta cell proliferation as a compensatory effect for the insulin resistance state. T2DM occurs when the pancreas fails to adapt to increased blood glucose levels [4, 8]. The liver is one of the first organs to be severely affected by insulin resistance. The liver responds to chronic systemic hyperglycemia by increasing gluconeogenesis. In the diabetic state, gluconeogenesis is increased because of the decreased insulin released by the beta cells and/or the suppressed insulin action on the liver [4]. TD2M is associated with high prevalence of hepatic comorbidities, such as non-alcoholic fatty liver disease (NAFLD) [9]. NAFLD is a rapidly-growing disease affecting 30 % of the general population and around 90% of T2DM patients [10]. Furthermore, it is still controversial whether NAFLD is a consequence or a cause of pancreas disorders. The relevant pathophysiological models involving organ-to-organ interactions are critical for extracting the relevant biomarkers and therapeutic solutions. As a result, it is of crucial importance to reproduce the physiology of both the liver and the pancreas to control and properly identify the interaction with the development of diabetes and its systemic relationship with the liver.

New, advanced *in vitro* technologies can create ample opportunities for a more modern approach to toxicology and pharmacology, replacing the traditional "black box" of animal-based and conventional 2D *in vitro*-based paradigms. Animal models fail to faithfully reproduce the human condition and lose relevance when extrapolating the results to humans [11, 12]. *In vitro* cell cultures are mainly performed in static 2D cultures using conventional multi-well plates, which do not accurately reflect the physiological *in vivo* micro-environment [12, 13]. Consequently, it is essential that those basic plate cultures be improved in order to reproduce the characteristics found *in vivo* as closely as possible. This is why many groups are developing tissue-engineering 3D culture (spheroids, culture in 3D hydrogel and organoid), dynamic organ-on-chip culture and coculture models in order to provide a more appropriate micro-environment for tissue maintenance and development [14].

Of those *in vitro* complex models, organ-on-chip technology seems to be one of the suited methods for reproducing the behavior of an organ or a group of organs, as well as the controlled physiological micro-environment [12, 15]. Microfluidic organ-on-chip culture improve the exchange and transport of nutrients, oxygen, metabolic waste, hormones and other chemical, and creates "physiological-like" situations such as the liver zonation, shear stress and chemical gradients [12, 14]. In particular, organ-on-chip technology allows the cocultures of two or more organs in separated microbireactors and connected by soluble factors exchange through the microfluidic network [12]. In recent years, several teams have proposed organ-on-chip devices that reproduce diverse behaviors of various organs and tissues including the liver, kidneys, gut, lung, heart, and intestines [15, 16]. While many organ-on-chip technologies have been developed and advanced for the liver, only a few studies have focused on the pancreas, and even less, to our knowledge, on liver-pancreas interactions. Of these studies, organ-on-chip technology has been used to reproduce an *in vitro* pancreas-on-chip model [17-22]. However, most of the current microfluidic platforms have mainly been designed for the quality assessment of islets for subsequent *in vivo* implantation [14]. In parallel, a few recent works have also demonstrated the potential of organ-on-chip technology for complex pancreatic analysis and pancreatic islet-liver crosstalk studies [18, 23]. Therefore, it was demonstrated the potential of technology for liver and pancreas interaction via the insulin – glucose regulation [23].

In this paper we propose an alternative design of coculture organ-on-chip microfluidic technology making long-term culture of hepatocytes and pancreatic islets possible. We represented the hepatic disturbance by removing the insulin from the culture medium. Then, we investigated the restoration of hepatic function thanks to the interaction between the liver and endocrine pancreas through the circulating hormones and cofactors in the coculture configuration. We also included new features by investigating mRNA response of important liver

and pancreas gene marker (differentiation and functional pattern) during the glucose-insulin regulation.

4.2 Results

4.2.1 Cell morphology analysis

The hepatocytes were successfully attached in the collagen-coated biochip after a few hours of culture. They were kept under static conditions in an incubator. After 24h, the hepatocytes created a confluent tissue and displayed typical cuboidal hepatocyte phenotypes (Fig. 4.S1, supplementary file).

The hepatocytes morphology at the end of the experiments (24h in static conditions and 6 days of perfusion) is presented in Fig.4.1. The hepatocytes monoculture with insulin (hepatocytes monoculture ITS +) displayed typical hepatic monolayer cultures (cells with the typical cuboid shape). The cell monolayer was maintained over 7 days of culture, including 24h at rest and 6 days in perfusion (Fig. 4.1A). Without insulin (hepatocytes monoculture ITS -), the hepatocytes cultures were heterogeneous from one biochip to another. A few hepatic cultures in the biochips without insulin presented similar morphologies when compared to the hepatic culture with insulin (Fig. 4.1B). In most of the biochips, the hepatocytes formed some aggregated structures or degraded tissue (Fig. 4.1C). Finally, in the hepatocytes/islets biochips coculture, the typical hepatic phenotypes (similar to hepatocytes monoculture ITS +) were recovered, as shown in Fig. 4.1D.

Concerning islets cultures, we did not detect any modification in the morphologies of the pancreatic islets when we compared the islets monoculture and the islets/hepatocytes coculture. The islets were trapped in the microwells of the pancreas biochips and displayed the typical spheroid shapes of islets of Langerhans (Fig. 4.1E and F). Furthermore, we counted the number of islets at the end of the experiments (5 days of perfusion). The result showed that the number of islets collected at the end of the perfusion remained similar to the number of islets seeded.

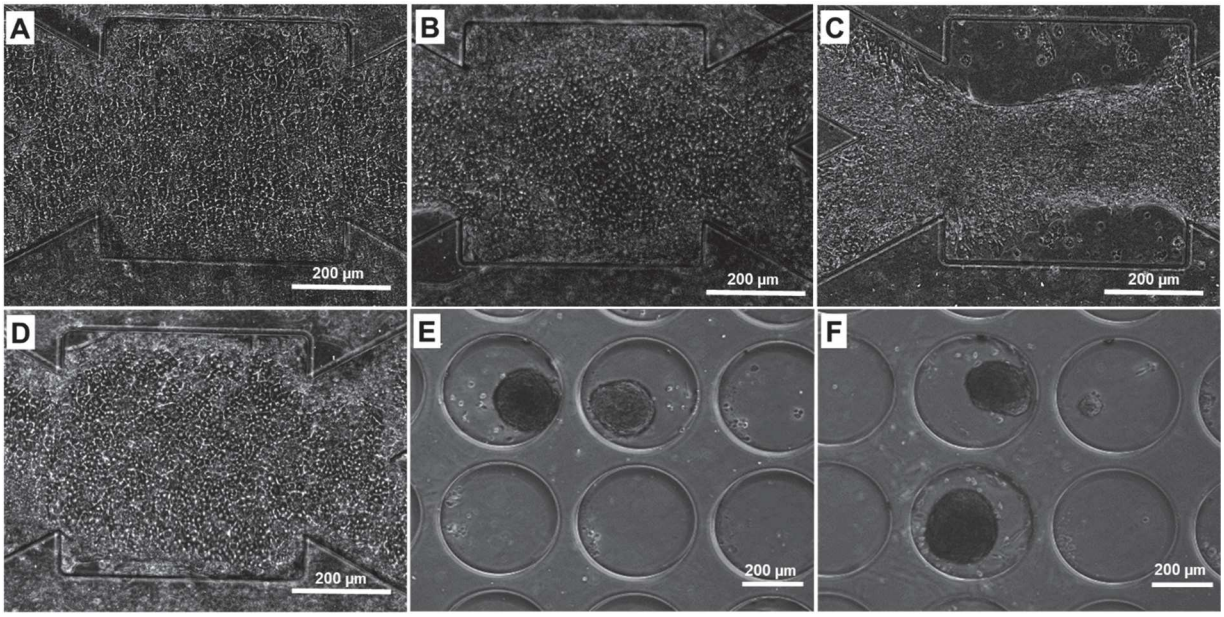

Figure 4.1 : Hepatocytes and islets morphologies at the end of the experiments: (A) hepatocytes monoculture with insulin (ITS+), (B) and (C) hepatocytes monoculture without insulin (ITS-), (D) hepatcytes in coculture with islets, (E) islets monocultures and (F) islets in cocultre with hepatocytes.

4.2.2 Immunostaining analysis

Immunofluorescence staining was performed at the end of the experiment (days 5 and 7 for islets and hepatocytes, respectively). For hepatocytes, we chose to stain several hepatic markers: CYP3A2 (one of the most abundant cytochrome P450 in the liver), CK18 (differentiation marker), INSR (insulin receptor) and GLUT2 (glucose transporter). We also stained two important markers in the pancreatic islets: insulin and glucagon, which are markers of β-cells and α-cells, respectively.

The immunostaining of the hepatic cells on day 7 is presented in Fig. 4.2. The immunostaining demonstrated that the hepatocytes monoculture with insulin and the hepatocytes/islets coculture led to positive cell populations expressing CYP3A2 and CK18. These results illustrate that the differentiation of hepatocytes in both types of culture was maintained. On the contrary, the CK18 was not expressed and the CYP3A2 was moderately expressed in hepatocytes monoculture without insulin (Fig. 4.2A). The quantification of staining intensity revealed that CK18 level was around 13 in coculture and monoculture with insulin, and close to zero for monoculture without insulin. The intensities of CYP3A2 staining were of 30, 32 and 26 for coculture, monoculture with insulin and monoculture without insulin, respectively (Fig. 4.S3, supplementary file). In parallel, the hepatocytes monoculture with insulin and the hepatocytes/islets coculture showed an intense positive cell population for INSR (intensity level at 14.5 and 14, respectively) and GLUT2 (staining intensity around 35 for both cultures). Whereas

the expressions of those markers were weaker in hepatocytes without insulin (Fig. 4.2B). The fluorescence intensities were of 6 and 27 for INSR and GLUT2, respectively (Fig. 4.S3, supplementary file).

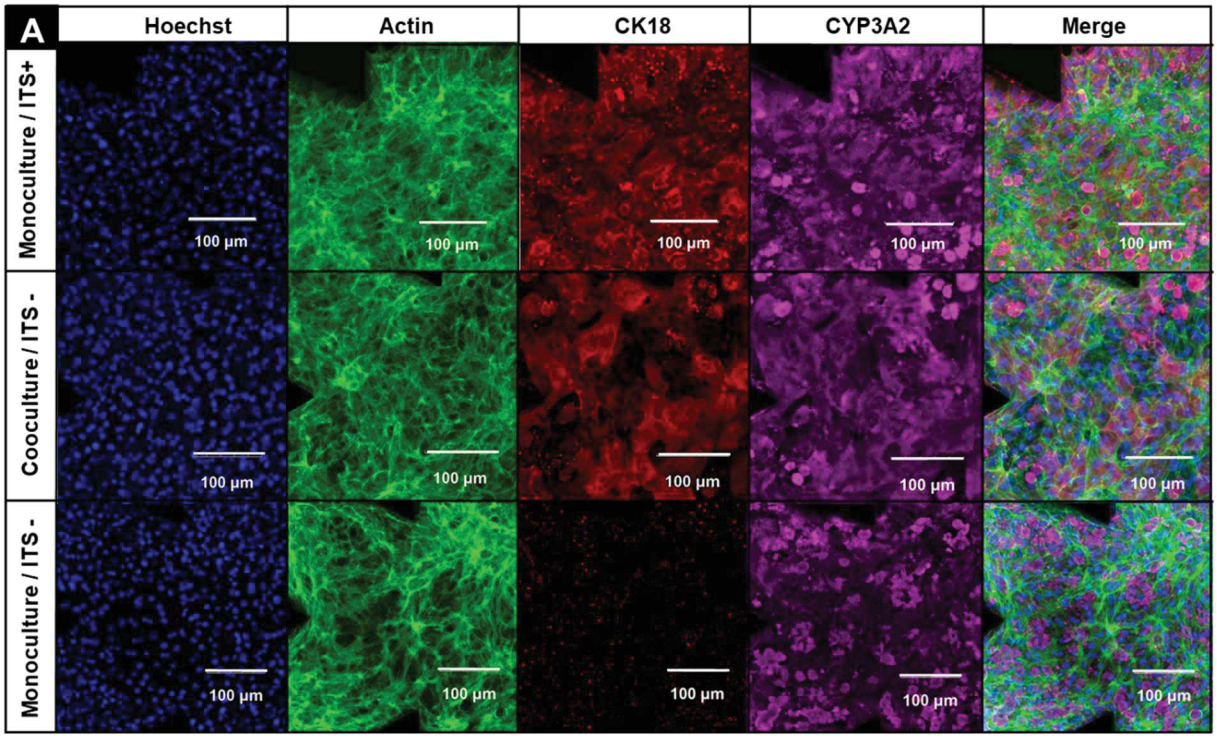

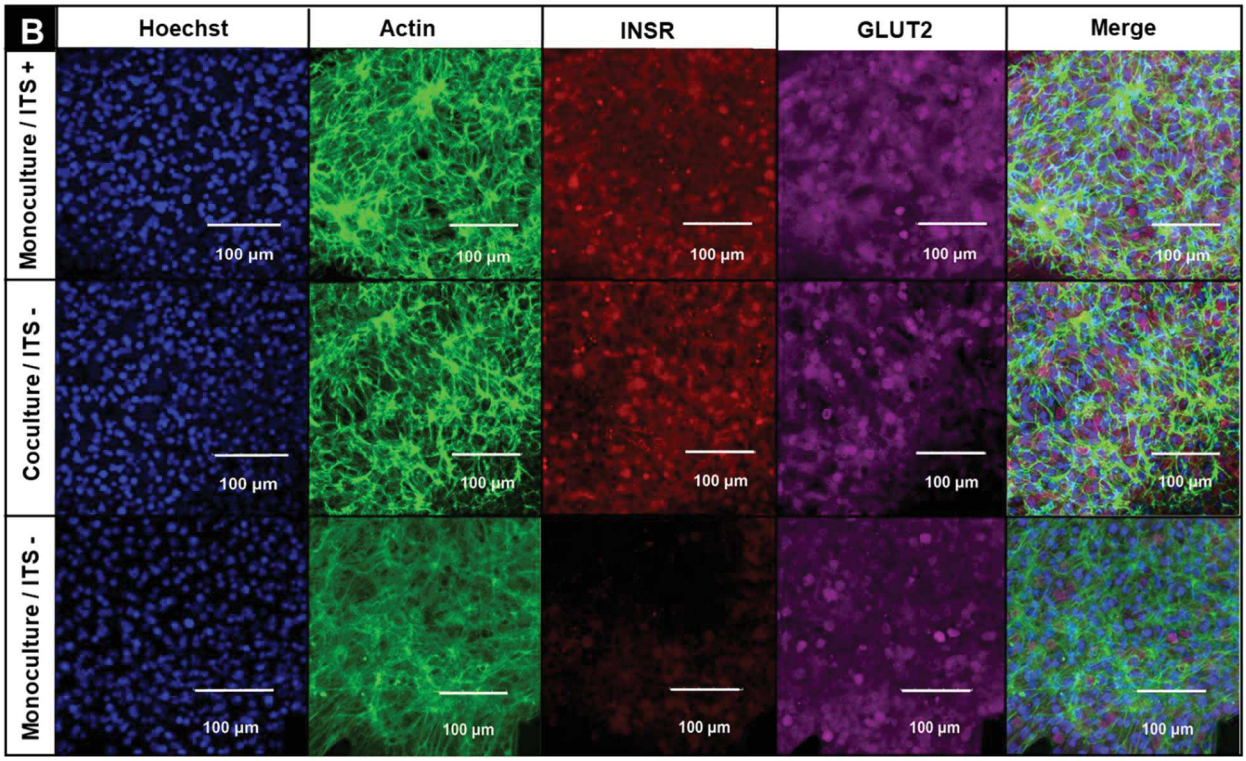

Figure 4.2 : Immunostainings of hepatocytes in monoculture with insulin, without insulin and coculture with islets at the end of the experiments: (A) DAPI, actin, CK18, CYP3A2 and merge; (B) INSR, GLUT2 and merge with DAPI and actin.

In the case of pancreatic islets, the level of insulin and glucagon expression inside the islets after extraction (day 0) appeared variable from one rat to another, probably due to the rat fed state at the moment of the extractions (Fig. 4.S2, supplementary file). Then, in the pancreatic islets monoculture and islets of pancreas/liver coculture, we found an expression of both glucagon and insulin hormones at the end of the experiments (Fig. 4.3). Furthermore, the levels of insulin appeared over-expressed in coculture when compared to the islets monoculture levels (2 times higher in coculture; Fig. 4.S3, supplementary file). The glucagon was similarly expressed, in both monoculture and coculture of islets, and we did not detect any difference between the immunostaining images.

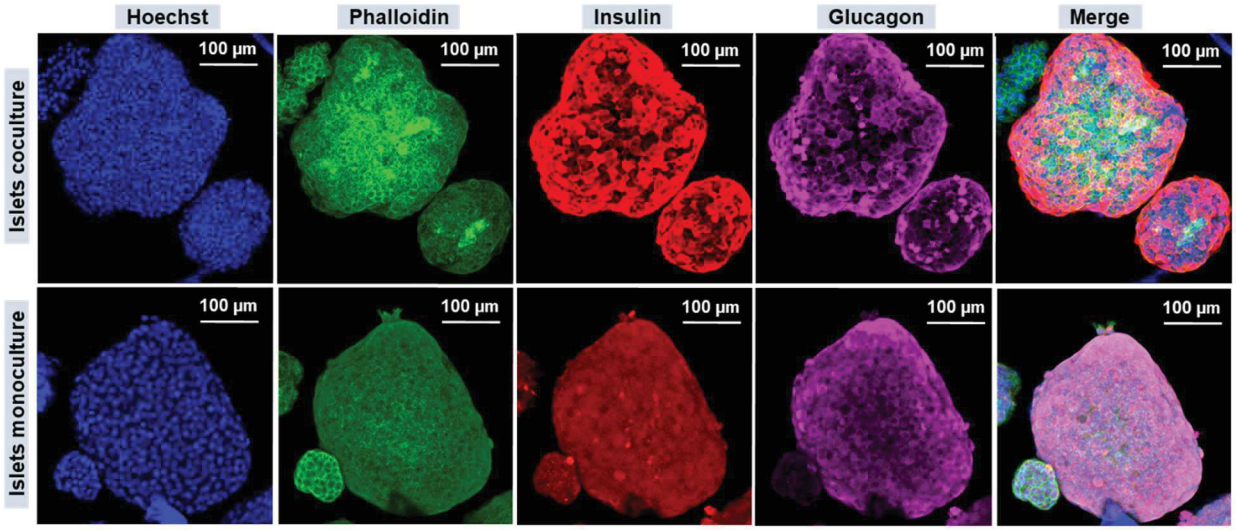

Figure 4.3: DAPI, phalloidin, insulin, glucagon and merge immunostainings of islets cultivated in monoculture and coculture with hepatocytes (at end of the experiments).

4.2.3. RTqPCR analysis

At the end of the experiments, we analyzed the expression levels of selected hepatic genes in the different culture conditions (monoculture ITS+, monoculture ITS- and coculture). The comparison of the mRNA levels between the hepatocytes cultivated in monoculture without insulin and with insulin is presented in Fig. 4.4 (ratio of mRNA levels in monoculture ITS- versus monoculture ITS+). We found that the mRNA level of *Alb* was downregulated in monoculture without insulin (fold change, FC of 0.55). On the contrary, the expression levels of *Hnf4a* (FC 40), *Insr* (FC 4.5), *Igfbp1* (FC 2.5) and *Pck1* (FC 10) were significantly increased. Considerable variability in the levels of *Gcgr*, *Glut2* and *Cyp3a2* in the monoculture without insulin was measured, which led to no statistical difference between the two culture conditions for those genes.

The comparison was then performed for gene expression in the hepatocytes cultivated in coculture with pancreatic islets and the hepatocytes monoculture with insulin. As shown in Fig. 4.4, the coculture contributed to recovering similar mRNA levels regarding *Gcgr*, *Insr*, *Hnf4a*, *Igfbp1* and *Alb* when compared to the monoculture of hepatocytes with insulin. However, the mRNA level of *Cyp3a2*, *Cyp1a2* appeared lower when compared to monoculture with insulin (FC of 0.1 and 0.35 respectively). Conversely, the mRNA level of *Pck1* remained high in coculture when compared to the hepatocytes with insulin monoculture, and at similar levels when compared to hepatocytes monoculture without insulin.

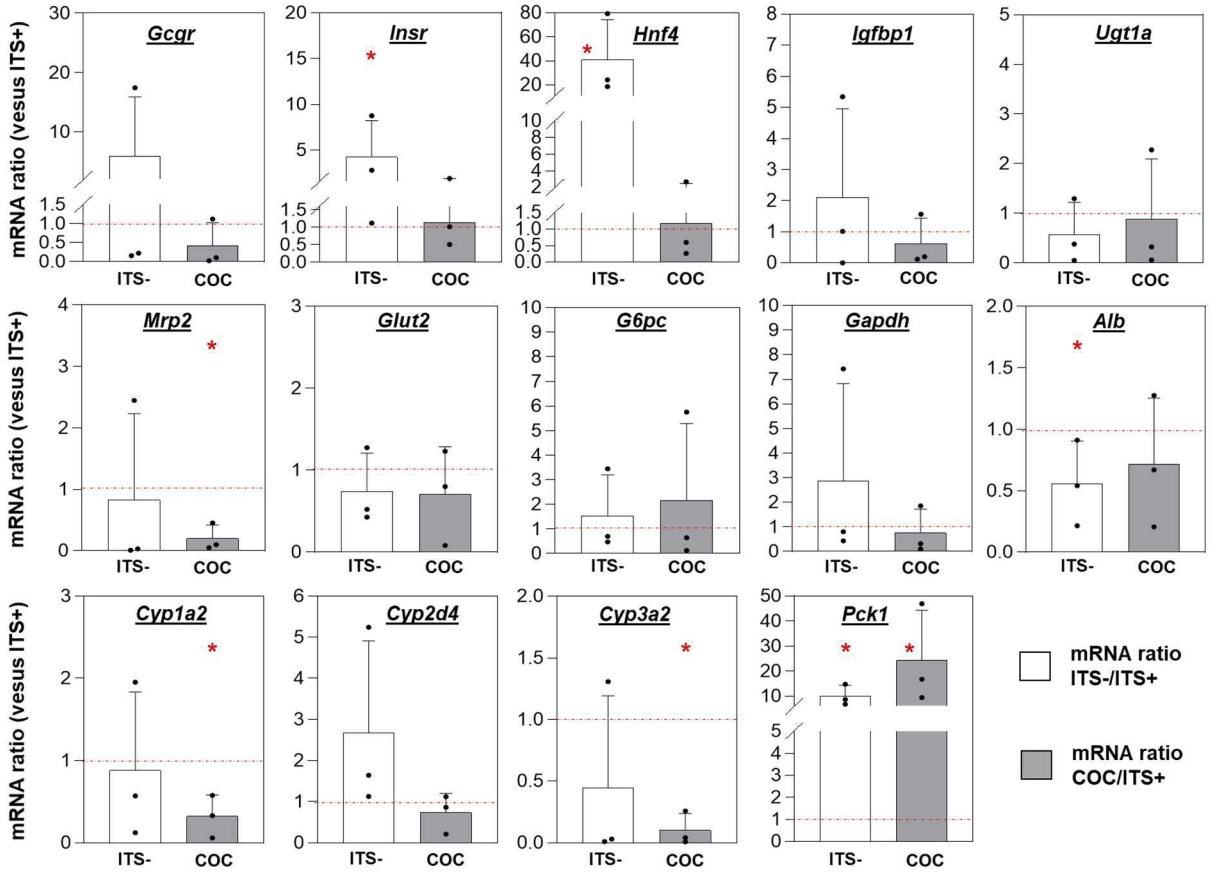

*Figure 4.4: Ratio of mRNA levels of selected hepatic genes after 7 days of culture. White bars: hepatocytes monoculture without insulin (ITS -) versus hepatocytes monoculture with insulin (ITS +), and gray bars: hepatocytes in coculture with islets (COC) versus hepatocytes monoculture with insulin (ITS +). *P < 0.05, mRNA level significantly different when compared to monoculture (ITS +); each dot corresponds to one independent experiment (one independent rat; mean of 3 biochips).*

Finally, we investigated the effect of coculture with hepatocytes on expression levels of pancreatic islet-specific genes. The comparison of the mRNA levels is shown in Fig. 4.5 (ratio of mRNA levels in coculture versus islet monoculture). We found that the coculture with the hepatocytes contributed to downregulate the levels of *Gcgr*, *Neurod*, *Neurog3*, *Glut2*, *Ins1*, *Gcg*, *App* and *Pdx1* (FC between 0.1 and 0.36). In contrast, expression of *Reg3a*, *Ins1* and *Glp1r* was 5 to 15.5 times higher in the coculture compared to the islet monoculture. However, wide variability was found for *Ins1* and *Glp1r* in both culture conditions.

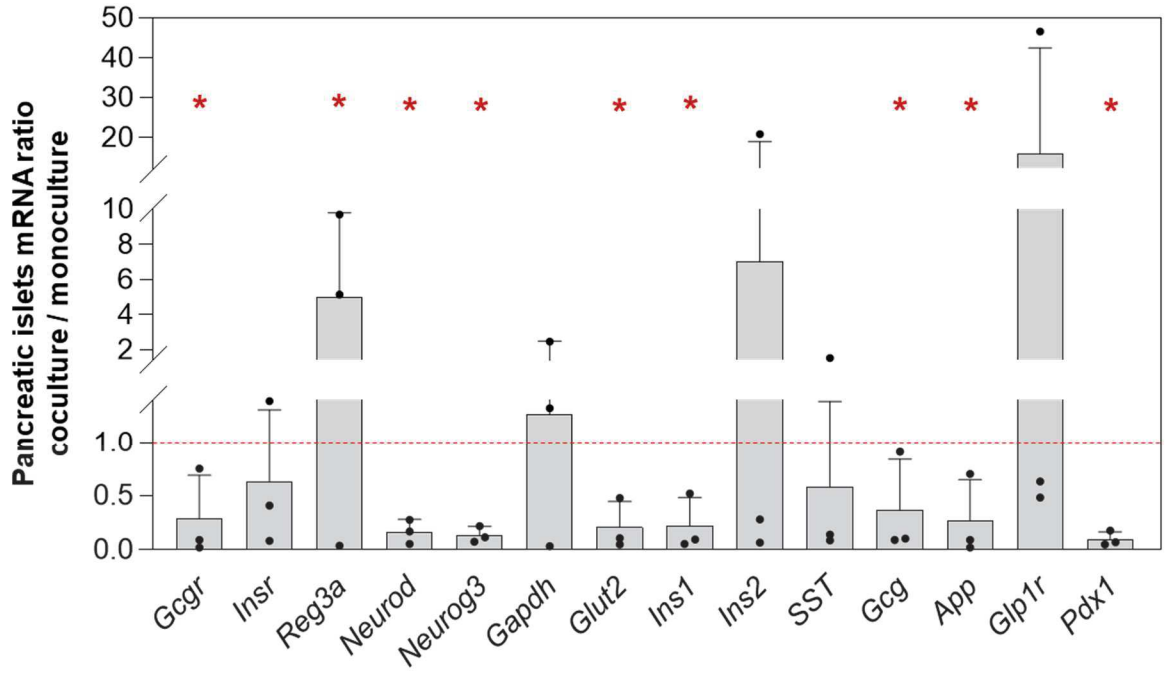

*Figure 4.5: Ratio of mRNA levels of selected pancreatic islets genes after 5 days of culture (islets coculture versus islets monoculture). *P < 0.05, mRNA level significantly different between islets monoculture and coculture; each dot corresponds to one independent experiment (one independent rat; mean of 3 biochips).*

4.2.4. Functional assays revealed higher insulin and C-peptide secretions in the islets in coculture with hepatocytes when compared to islet monoculture

The basal functionality of the pancreatic islets in both culture modes (islet monoculture and coculture with hepatocytes) was investigated by measuring the levels of insulin, C-peptide and glucagon secretions. The daily secretions of the three hormones on days 3 and 5 (end of the experiment) are presented in Fig.4.6.

We found that the insulin concentration in the culture medium decreased between days 3 and 5, in both culture conditions (monoculture and coculture). However, the coculture with hepatocytes contributed to maintaining relatively high levels of secretion when compared to monoculture (Fig.4.6A). Especially on day 5, we found a secretion of 0.4 µg/mL/day and 2 µg/mL/day in monoculture and coculture, respectively. Similarly, we measured higher production of C-peptide in coculture when compared to monoculture. The secretion was about 1.5 (245 pmol/mL/day) and 5 (340 pmol/mL/day) times higher in the islets coculture with hepatocytes on days 3 and 5, respectively (Fig. 4.6B and D). The levels of glucagon remained constant in the coculture during the 5 days of the experiment, close to 10 ng/mL/day, but with wide dispersion on day 3 (Fig.4.6C). Conversely, the level of glucagon in islets monoculture dropped from 9 to 5 ng/mL/day between days 3 and 5 of culture. Finally, the pancreatic compartment (islets

monoculture) was responsive to the high/low glucose stimulations (GSIS stimulation). Indeed, the high glucose stimulation lead to a 2-3 fold higher insulin production when compared to the low glucose condition (GSIS index, results not shown).

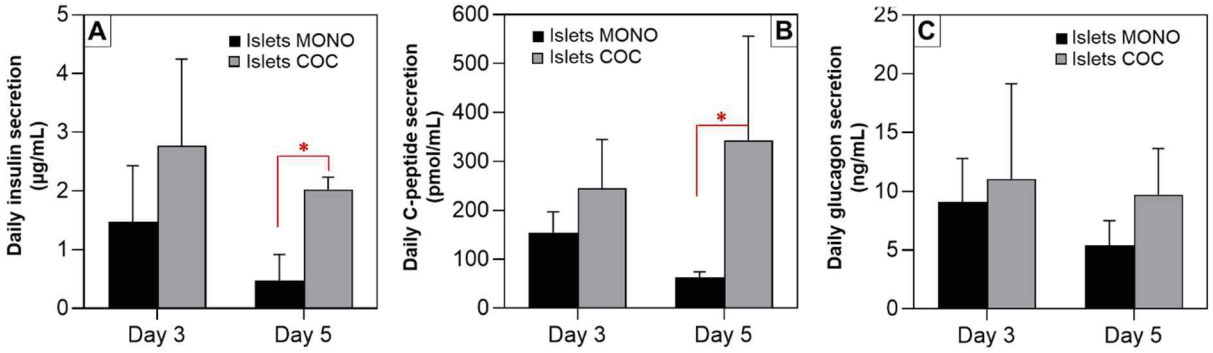

D

	Ratio of hormone secretion (islets coculture / islets monoculture)		
	Insulin	C-peptide	Glucagon
Day 3	1.88±1.53	1.58±1.08	1.21±1.3
Day 5	4.24±1.47	5.48±4.24	1.8±1.39

*Figure 4.6; (A) Insulin, (B) C-peptide, (C) glucagon daily secretions after 3 and 5 days of islets culture in monoculture and coculture with hepatocytes (*P < 0.05) and (D) ratio of hormones (insulin, C-peptide and glucagon) secretion between islets coculture and islets monoculture .*

Hepatocytes functionality was assessed by measuring the levels of albumin in the three culture modes (monoculture ITS+, monoculture ITS- and coculture). The hepatocytes in monoculture with insulin and in coculture with pancreatic islets produced similar quantities of albumin (constant over time, from days 3 to 7, till the end of the experiment). Conversely, without insulin in the culture medium, the hepatocytes monoculture presented a drop in albumin production between days 3 and 7, as shown in Fig.4.7A. This led to attaining albumin production of close to 750±100 µg/10^6 cells in hepatocytes/islets biochip coculture and the liver biochip monoculture with insulin, whereas the values dropped to close to 440±230 µg/10^6 cells in the liver biochip monoculture without insulin (Fig.4.7A).

Finally, we measured glucose and lactate levels during the cultures in the different conditions (Fig.4.7B, C and Table 4.S1, supplementary file). The data showed wide dispersion, but the tendency illustrated higher glucose consumption in coculture compared to liver monoculture conditions with and without insulin. Furthermore, this consumption (in hepatocytes/islets coculture) seemed to be constant between days 3 and 7 (Fig.4.7B). Concerning lactate production, we could not distinguish any significant difference between the different culture conditions, with lactate production of around 0.6-0.8 mmol/L (Fig.4.7C).

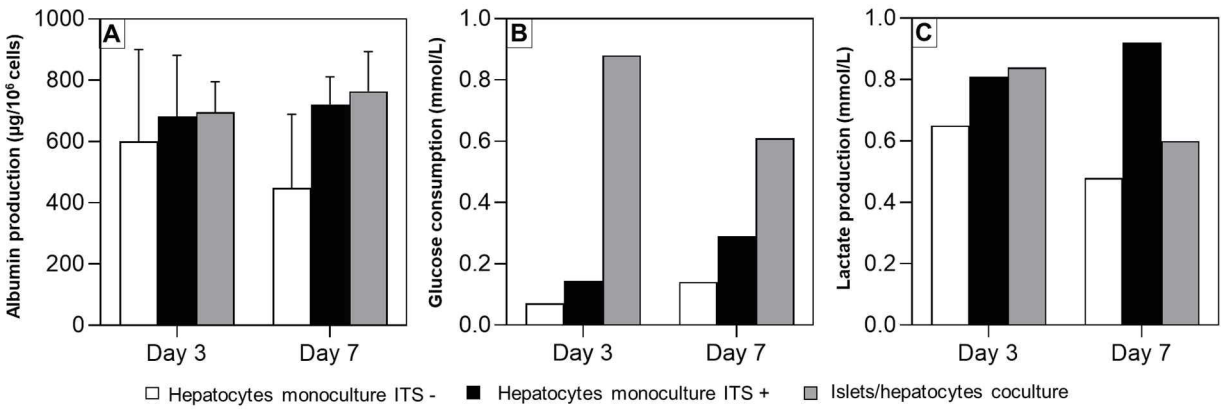

Figure 4.7 : (A) Albumin production; (B) glucose consumption and (C) lactate production in hepatocytes monoculture without insulin (ITS -), monoculture with insulin (ITS +) and coculture with islets after 3 and 7 days.

4.3 Discussion

We developed a coculture model for rat hepatocytes with rat islets of Langerhans, using organ-on-chip technology. The liver biochip was the result of our previously developed liver-on-chip technology that had already been successfully applied to rat and human primary hepatocytes [33-36]. We coupled this liver-on-chip model, with a recent update to our technology, to a pancreas-on-chip model [24]. The interconnection of both organ-on-chip technologies produced a new model of interaction between the organs: the liver and the pancreas. The coculture of two cell/tissue types required an adapted coculture medium capable of maintaining their characteristics. Preliminary tests (data not shown) were carried out to define the culture medium adapted to islets/hepatocytes coculture: i) hepatocytes monoculture in William's E medium (the standard medium for rat hepatocytes culture) and in a 1:1 mixture of William's E/RPMI 1640; ii) islets monoculture in RPMI 1640 medium (the standard medium for islets culture) and in a 1:1 mixture of William's E/RPMI 1640. The analyses performed (viability, morphology, gene expression of selected markers, albumin and insulin secretion) showed that islets and hepatocytes monoculture in a mixture of William's E and RPMI 1640 maintained their characteristics (when compared to islets and hepatocytes cultivated in their standard medium). Consequently, a 1:1 mixture of William's E/RPMI 1640 medium was chosen for the islets/hepatocytes coculture experiments.

In this study, the suppression of insulin in hepatocytes monoculture led to a downregulation of the *Alb* mRNA (Fig.4.4) and to weaker albumin production (Fig. 4.7) in culture medium, compared to monoculture with insulin. The decrease in albumin production and *Alb* gene expression with the lack of insulin has already been reported in the literature on *in vitro* data in rats and *in vivo* in mice [37-39]. The lack of insulin also led to weaker CYP3A2 expression and to the lack of CK18 expression at the protein level (Fig. 4.2, the *Cyp3a2* was also

downregulated at the mRNA level, Fig. 4.4). Both markers are hepatic differentiation markers. It is reported that rat hepatocytes presented a reduction of about 30% in the mRNA level of *Cyp3a* in the absence of insulin [40]. Although there is no literature showing the results of the effect of insulin on CK18 immunostaining, various reports have mentioned the crosstalk between CK18 and insulin resistance as in diabetic patients or patients with non-alcoholic steatohepatitis, in which CK18 fragments are elevated in plasma [41, 42]. The HNF4 transcription factor is involved in the mechanism of liver differentiation *via* the HNF1, HNF4, PXR and CYP450 axis, but it is also involved in glucose homeostasis, liver-pancreas interactions and diabetes [43-45]. HNF4 is targeted and repressed by insulin in hepatocytes, which was consistent with our result in as much as *Hnf4a* was upregulated without insulin [46, 47].

The hepatocytes monoculture without insulin also presented modulation of *Igfpb1* (Insulin-like growth factor binding proteins, upregulation of mRNA levels), *Insr* (lower expression of the protein in the immunostaining and gene upregulation), and *Pck1* (gene upregulation, Fig. 4.3). Interestingly, our results are consistent with the literature reporting that insulin inhibits *Igfpb1* in the liver [48]. *Pck1* catalyzes the first step in gluconeogenesis. By silencing *Pck1* in mice, insulin signaling improved in the liver [49]. Conversely, insulin is also reported as reducing the expression of *Pck1* [50]. Once more, these data appeared consistent with our biochip findings. Finally, the overall hepatic biochip culture without insulin illustrated a consistent behavior when compared to the literature.

The pancreatic islets in coculture were able to produce insulin to counterbalance the suppression of ITS. However, the level of insulin detected (about 3000 µg/L) was lower than the insulin level used in "conventional" hepatocytes culture models (in the present experiment, the hepatocytes monoculture with insulin were performed at 10 mg/L of insulin via ITS supplementation in the medium). This could explain why, at the mRNA level, the hepatic markers (Alb and Cyp3a2) remained lower in the hepatocytes coculture (when compared to hepatocytes monoculture with insulin, Fig. 4.4). Furthemore, *Pck1* remained higher than the level in the hepatocytes monoculture with insulin [37-40, 50]. Nevertheless, at the protein level, the expression of CYP3A2, CK18 and the production of albumin were restored in coculture (Fig. 4.3). The expression of insulin-related genes such as *Igfbp1* and *Insr* were also restored, including *Hnf4a* (Fig. 4.4). In addition, the protein expression of Insr and Glut2 appeared similar in the immunostaining in both hepatocytes monoculture with insulin and in islets/hepatocytes coculture (Fig. 4.2). These data illustrate the functional crosstalk between the pancreas and the liver. They also demonstrate the partial restoration of the expected effect of insulin on hepatocytes. Nevertheless, additional experiments, involving tuning the number of islets to increase the production of insulin, are needed to confirm the full recovery of *Pck1* and *Cyp3a2* mRNA levels.

High glucose levels normally lead to high production of insulin. In the present culture conditions, the glucose level in the medium was 9.1-9.8 mM and did not decrease significantly between the two time points of culture medium change (*nb* a similar glucose concentration was used in all culture modes). This led to continuous stimulation for insulin secretion in the pancreatic islets monoculture and during the islets/hepatocytes coculture (and thus contributes to restore the hepatic functions in the coculture by insulin secretion stimulated by glucose). Regarding the effect of hepatocytes coculture on the pancreatic islets, we found that the coculture downregulated *Gcgr*, *Glut2*, *Ins1*, *Neurod*, *Neurog3*, *App*, *Gcg*, *Pdx1* and upregulated *Glp1r* at the mRNA level (Fig. 4.5). *Pdx1*, *Neurod* and *Neurog3* are important markers in the differentiation of islets [51, 52]. *Neurod* is an important gene (an insulin trans activator) required to maintain functional maturity in pancreatic beta cells, including insulin production through *Ins1* [51]. We consistently found both downregulation of *Ins1* and *Neurod* in coculture biochips (which is consistent with *Ins1* silencing in *Neurod* KO mice [51]). *Neurod* KO-mice express the *Ins2* gene and are thus able to produce insulin in glucose tolerance tests, which also appeared consistent with our findings in which *Ins2* was over-expressed in pancreas biochip cocultures [51]. *Pdx1* is a pivotal important gene in β-cells. *Pdx1* is a homeobox-containing transcription factor that plays a key role in pancreatic development and adult β cell function [53]. Depletion of *Pdx1* leads to hyperglycemia in mice, cell reprogramming in mice islets and glucagon over-expression in Min6 β cells [53]. Furthermore, *Pdx1*-deficient β cells led to a reduction in the transcript levels of *Pdx1*, *Ins1* and *Glut2*, and the maintenance of glucagon levels [53]. This result was partially consistent with our dataset, in which we found a concomitant downregulation of *Pdx1*, *Ins1* and *Glut2* genes in coculture. However, as *Neurod* and *Pdx1* are also marker of islets health, additional investigation would be required to fully understand the crosstalk between the liver and pancreas.

Glucagon is produced during hypoglycemia to stimulate hepatic glucose output. In our study, the glucose concentration remained high in the culture medium, leading to a high insulin/glucagon ratio being detected, which is consistent with the downregulation of the levels of *Gcg* (glucagon) and *Gcgr* (glucagon receptor) mRNA. However, we also measured high levels of *Glp1r* mRNA. It is reported that paracrine glucagon stimulates insulin secretion through both *Gcgr* and *Glp1r*. More particularly, the activity of glucagon and GLP-1 receptors was reported as being essential for β cell secretory responses *via* paracrine intra-islet glucagon actions for maintaining appropriate insulin secretion [54], which is consistent with our findings in coculture. Although we described those behaviors in the pancreatic tissue as a result of the hepatic coculture, we did not clearly identify the underlying mechanisms or the endocrine liver signaling that drives such crosstalk. As a result, additional analysis is needed to complete our investigation, including metabolome and proteome analysis.

4.4 Conclusion

In this study, we proposed a new liver/pancreas interaction model in biochips to investigate the crosstalk between the two organs. The characteristic functions of the hepatocytes/islets coculture model were evaluated, comparing them with those of islets or hepatocytes (with and without insulin) monoculture. The hepatocytes monoculture without insulin led to modulation of both glucose homeostasis targets and hepatic differentiation markers. Conversely, the coculture with pancreatic cells producing insulin helped recover the hepatic function, illustrating the benefits of the two-organ model. For pancreatic functions, the presence of the hepatocytes in the coculture model helped modify the islets response via the increase in insulin secretion and the modification of the expression of the gene involved in insulin/glucagon homeostasis. The pancreas-liver organ-on-chip model presented here was capable of reproducing several physiological responses and demonstrated the potential of our approach to reproduce and investigate complex *in vivo* patterns using alternative *in vitro* method

4.5 Supplementary figures

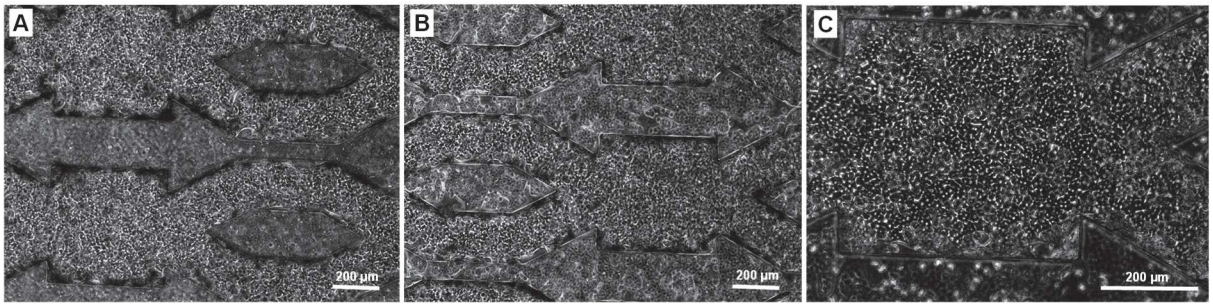

Figure 4.S1. Hepatocytes morphology after 24h of adhesion at static condition (A, B: magnification X10 and C: magnification X20).

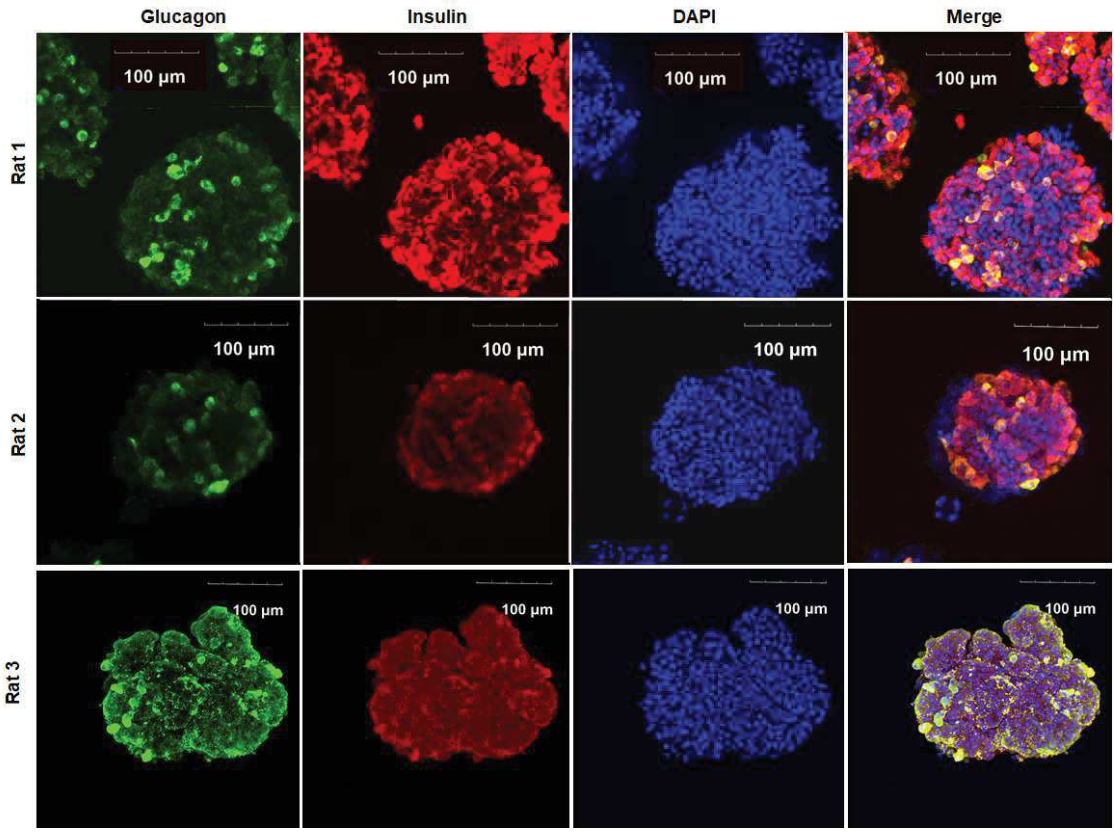

Figure 4.S2. Islets immunostainings (DAPI, glucagon, insulin, and merge) at day 0 (post-extraction) for two different rats.

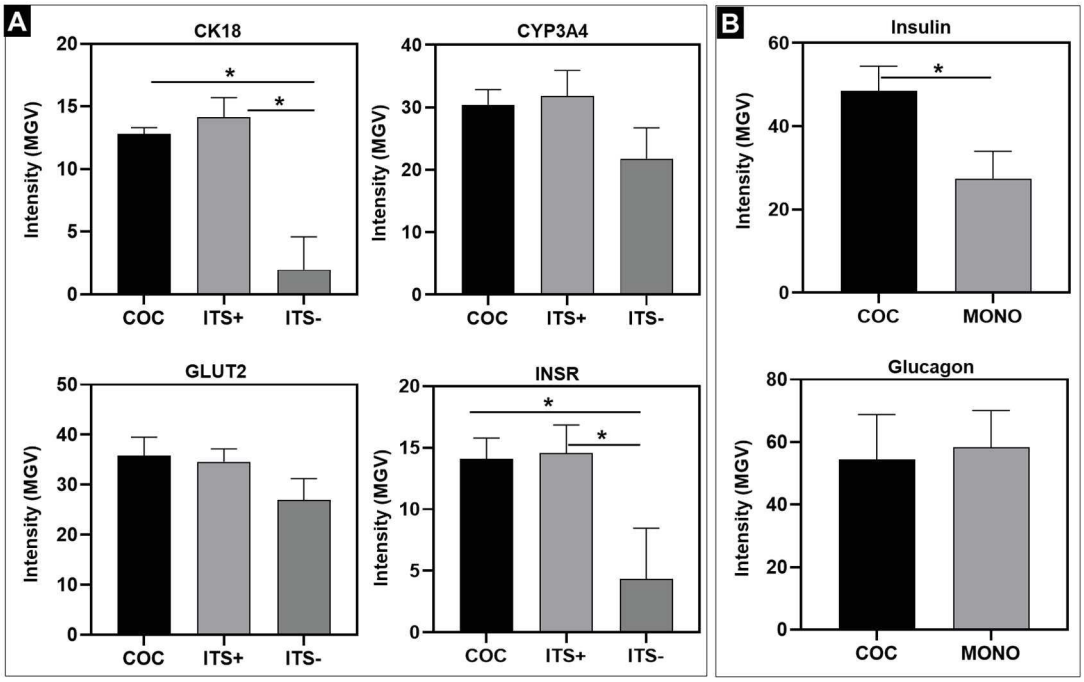

Figure 4.S3. Quantification of staining intensity (mean gray value: MGV) of hepatic (A) and pancreatic islets (B) markers. Quantification by ImageJ software using the fluorescent images.

Table 4.S1. glucose consumption and lactate production in hepatocytes monoculture without insulin (ITS -), monoculture with insulin (ITS +) and coculture with islets after 3 and 7 days.

	Glucose consumption		Lactate production	
	Day 3	Day 7	Day 3	Day 7
Monoculture ITS-	0.07±1	0.14±1.2	0.65±0.4	0.48±0.41
Monoculture ITS+	0.145±0.6	0.29±1	0.81±0.18	0.92±0.11
Coculture with islets	0.88±0.5	0.61±0.78	0.84±1	0.6±0.8

4.6 References

[1] W. Fan, Epidemiology in diabetes mellitus and cardiovascular disease, Cardiovasc. Endocrinol. 6 (2017) 8-16.

[2] International Diabetes Federation, IDF Diabetes Atlas, 9th edn. 2019. https://www.diabetesatlas.org/en/ (accessed may 2020).

[3] World Health Organization official web site: http://www.who.int/diabetes/en/(accessed may 2020).

[4] R.A. DeFronzo, E. Ferrannini, L. Groop, R.R. Henry, W.H. Herman, J.J. Holst, F.B. Hu, C.R. Kahn, I. Raz, G.I. Shulman, D.C. Simonson, M.A. Testa, R. Weiss, Type 2 diabetes mellitus, Nat. Rev. Dis. Primers. 1 (2015) 15019.

[5] J.M. Forbes, M.E. Cooper, Mechanismes of diabetic complications, Physiol. Rev. 93 (2013) 137-188.

[6] C. Sardu, C. De Lucia, M. Wallner, G. Santulli, Diabetes mellitus and its cardiovascular complications: New insights into an old disease, J. Diabetes Res. 2019 (2019) 1905194.

[7] A. King, J. Bowe, Animal models for diabetes: Understanding the pathogenesis and finding new treatments, Biochem. Pharmacol. 99 (2016) 1-10.

[8] D. Tripathy, A.O. Chavez, Defects in insulin secretion and action in the pathogenesis of type 2 diabetes mellitus, Curr. Diab. Rep. 10 (2010) 184-191.

[9] R.J. Perry, V.T. Samuel, K.F. Petersen, G.I. Shulman, The role of hepatic lipids in hepatic insulin resistance and type 2 diabetes, Nature. 510 (2014) 84-91.

[10] C. Saponaro, M. Gaggini, A. Gastaldelli, Nonalcoholic fatty liver disease and type 2 diabetes: common pathophysiologic mechanisms, Curr. Diab. Rep. 15 (2015) 607.

[11] A.M. Ghaemmaghami, M.J. Hancock, H. Harrington, H. Kaji, A. Khademhosseini, Biomimetic tissues on a chip for drug discovery, Drug. Discov. Today. 17 (2012) 173-181.

[12] F. Merlier, R. Jellali, E. Leclerc, Online hepatic rat metabolism by coupling liver biochip and mass spectrometry, Analyst. 142 (2017) 3747-3757.

[13] A.K. Capulli, K. Tian, N. Mehandru, A. Bukhta, S.F. Choudhury, M. Suchyta, K.K. Parker, Approaching the in vitro clinical trial: engineering organs on chips, Lab Chip. 14 (2014) 3181-3186.

[14] J. Rogal, A. Zbinden, K. Schenke-Layland, P. Loskill, Stem-cell based organ-on-a chip models for diabetes research, Adv. Drug Del4. Rev. 140 (2019) 101-128.

[15] H. Kimura, Y. Sakai, T. Fujii, Organ/body-on-a-chip based on microfluidic technology for drug discovery, Drug Metab. Pharmacokinet. 33 (2018) 43-48.

[16] A. Polini, L. Prodanov, N.S. Bhise, V. Manoharan, M.R. Dokmeci, A. Khademhosseini, Organs-on-a-chip: a new tool for drug discovery, Expert Opin. Drug Discov. 9 (2014) 335-352.

[17] Y. Jun, J. Lee, S. Choi, J.H. Yang, M. Sander, S. Chung, S.H. Lee, In vivo-mimicking microfluidic perfusion culture of pancreatic islet spheroids, Sci. Adv. 5 (2019) eaax4520.

[18] A. Zbinden, J. Marzi, K. Schlünder, C. Probst, M. Urbanczyk, S. Black, E.M. Brauchle, S.L. Layland, U. Kraushaar, G. Duffy, K. Schenke-Layland, P. Loskill, Non-invasive marker-independent high content analysis of a microphysiological human pancreas-on-a-chip model, Matrix Biol. 85-86 (2020) 205-220.

[19] T. Schulze, K. Mattern, E. Früh, L. Hecht, I. Rustenbeck, A. Dietzel, A 3D microfluidic perfusion system made from glass for multiparametric analysis of stimulus-secretion coupling in pancreatic islets, Biomed. Microdevices 19 (2017) 47.

[20] S.H. Lee, S. Hong, J. Song, B. Cho, E.J. Han, S. Kondapavulur, D. Kim, L.P. Lee, Microphysiological analysis platform of pancreatic islet β-cell spheroids, Adv. Healthc. Mater. 7 (2018) 1701111.

[21] X. Li, J.C. Brooks, J. Hu, K.I. Ford, C.J. Easley, 3D-templated, fully automated microfluidic input/output multiplexer for endocrine tissue culture and secretion sampling, Lab Chip. 17 (2017) 341-349.

[22] J.C. Brooks, K.I. Ford, D.H. Holder, M.D. Holtan, C.J. Easley, Macro-to-micro interfacing to microfluidic channels using 3D-printed templates: application to time-resolved secretion sampling of endocrine tissue, Analyst 141 (2016) 5714-5721.

[23] S. Bauer, C. WennbergHuldt, K.P. Kanebratt, I. Durieux, D. Gunne, S. Andersson, L. Ewart, W.G. Haynes, I. Maschmeyer, A. Winter, C. Ämmälä, U. Marx, T.B. Andersson, Functional coupling of human pancreatic islets and liver spheroids on-a-chip: Towards a novel human ex vivo type 2 diabetes model, Sci. Rep. 7 (2017) 14620.

[24] A.Essaouiba, T.Okitsu, R.Jellali, M. Shinohara, M.Danoy, Y.Tauran, C.Legallais, Y. Sakai, E.Leclerc, Microwell-based pancreas-on-chip model enhances genes expression and functionality of rat islets of Langerhans, Mol. Cell Endocrinol. 514 (2020) 110892.

[25] R. Jellali, M.J. Fleury, P. Paullier, E. Leclerc, Liver and kidney cells cultures in a new perfluoropolyether biochip, Sens. Actuator B-Chem. 229 (2016) 396-407.

[26] R. Baudoin, L. Griscom, J.M. Prot, C. Legallais, E. Leclerc E, Behaviour of HepG2/C3a cell culture in a microfluidic bioreactor, Biochem. Eng. J. 53 (2011) 172-181.

[27] Y. Yonekawa, T. Okitsu, K. Wake, Y. Iwanaga, H. Noguchi, H. Nagata, X. Liu, N. Kobayashi, S. Matsumoto, A new mouse model for intraportal islet transplantation with limited hepatic lobe as a graft site, Transplantation. 82 (2006) 712-715.

[28] T. Kiba, M. Tanemura, K. Yagyu, High-quality RNA extraction from rat pancreatic islet, Cell. Biol. Int. Rep. 20 (2013) 1-4.

[29] N.M. Kneteman, G.L. Warnock, M.G. Evans, I. Dawidson, R.V. Rajotte, Islet isolation from human pancreas stored in UW solution for 6 to 26 hours, Transplant. Proc. 22 (1990) 763-764.

[30] P.O. Seglen, Preparation of isolated rat liver cells, Methods Cell Biol. 13 (1976) 29-83.

[31] A. Rizki-Safitri, M. Shinohara, M. Tanaka, Y. Sakai, Tubular bile duct structure mimicking bile duct morphogenesis for prospective in vitro liver metabolite recovery, J. Biol. Eng. 14:11 (2020).

[32] W. Xiao, G. Perry, K. Komori, Y. Sakai, New physiologically-relevant liver tissue model based on hierarchically cocultured primary rat hepatocytes with liver endothelial cells, Integr. Biol. 7(2015) 1412-1422.

[33] R. Baudoin, G. Alberto, A. Legendre, P. Paullier, M. Naudot, M.J. Fleury, S. Jacques, L. Griscom, E. Leclerc, Investigation of the levels of expression and activity of detoxication genes of primary rat hepatocytes under various flow rates and cell densities in microfluidic biochips, Biotechnol. Prog. 30 (2014) 401-410.

[34] R. Jellali, T. Bricks, S. Jacques, M.J. Fleury, P. Paullier, F. Merlier, E. Leclerc, Long term human primary hepatocyte cultures in a microfluidic liver biochip show maintenance of mRNA levels and higher drugs metabolisms when compared to Petri cultures, Biopharm. Drug. Dispo. 37 (2016) 264-275.

[35] T. Bricks, J. Hamon, M.J. Fleury, R. Jellali, F. Merlier, Y.E. Herpe, A. Seyer, J.M. Regimbeau, F. Bois, E. Leclerc, Investigation of omeprazole and phenacetin first-pass metabolism in humans using a microscale bioreactor and pharmacokinetic models, Biopharm. Drug. Dispo. 36 (2015) 264-275.

[36] A. Legendre, R. Baudoin, G. Alberto, P. Paullier, M. Naudot, T. Bricks, J. Brocheton, S. Jacques, J. Cotton, E. Leclerc, Metabolic characterization of primary rat hepatocytes cultivated in parallel microfluidic biochips, J. Pharm. Sci. 102 (2013) 3264-3276.

[37] S.R. Kimball, R.L. Horetsky, L.S. Jefferson, Hormonal regulation of albumin gene expression in primary cultures of rat hepatocytes, Am. J. Physiol. 268 (1995) E6-14.

[38] K.E. Flaim, S.M. Hutson, C.E. Lloyd, J.M. Taylor, R. Shiman, L.S. Jefferson, Direct effect of insulin on albumin gene expression in primary cultures of rat hepatocytes, Am. J. Physiol. 249 (1985) E447-453.

[39] Q. Chen, M. Lu, B. Monks, M. Birnbaum, Insulin is required to maintain albumin expression by inhibiting forkhead box O1 protein, J. Biol. Chem. 291 (2016) 2371-2378.

[40] K.J. Woodcroft, R.F. Novak, Insulin differentially affects xenobiotic-enhanced, cytochrome P-450 (CYP)2E1, CYP2B, CYP3A, and CYP4A expression in primary cultured rat hepatocytes, J. Pharmacol. Exp. Ther. 289 (1999) 1121-1127.

[41] M. Civera, A. Urios, M.L. Garcia-Torres, J. Ortega, J. Martinez-Valls, N. Cassinello, J. del Olmo, A. Ferrandez, J. Rodrigo, C. Montoliu, Relationship between insulin resistance, inflammation and liver cell apoptosis in patients with severe obesity, Diabetes Metab. Res. Rev. 26 (2010) 187-192.

[42] M. Kitade, H. Yoshiji, R. Noguchi, Y. Ikenaka, K. Kaji, Y. Shirai, M. Yamazaki, M. Uemura, J. Yamao, M. Fujimoto, A. Mitoro, M. Toyohara, M. Sawai, Y. Yoshida, C. Morioka, T. Tsujimoto, H. Kawaratani, H. Fukui, Crosstalk between angiogenesis, cytokeratin-18, and insulin resistance in the progression of non-alcoholic steatohepatitis, World J. Gastroenterol. 15 (2009) 5193-5199.

[43] J. Chiang, Hepatocyte nuclear factor 4α regulation of bile acid and drug metabolism, Expert Opin. Drug Metab. Toxicol. 5 (2009) 137-147.

[44] M. Stoffel, S.A. Duncan, The maturity-onset diabetes of the young (MODY1) transcription factor HNF4 alpha regulates expression of genes required for glucose transport and metabolism, Proc. Natl. Acad. Sci. USA. 94 (1997) 13209-13214.

[45] H.H. Lau, N.H.J. Ng, L.S.W. Loo, J.B. Jasmen, A.K.K. Teo, The molecular functions of hepatocyte nuclear factors – In and beyond the liver, J. Hepatol. 68 (2018) 1033-1048.

[46] K. Hirota, H. Daitoku, H. Matsuzaki, N. Araya, K. Yamagata, S. Asada, T. Sugaya, A. Fukamizu, Hepatocyte nuclear factor-4 is a novel downstream target of insulin via FKHR as a signal-regulated transcriptional inhibitor, J. Biol. Chem. 278 (2003) 13056-13060.

[47] X. Xie, H. Liao, H. Dang, W. Pang, Y. Guan, X. Wang, J. Shyy, Y. Zhu, F. Sladek, Down-regulation of hepatic HNF4α gene expression during hyperinsulinemia via SREBPs, Mol. Endocrinol. 23 (2009) 434-43.

[48] D.R. Powell, A. Suwanichkul, M.L. Cubbage, L.A. DePaolis, M.B. Snuggs, P.D. Lee, Insulin inhibits transcription of the human gene for insulin-like growth factor-binding protein-1, J. Biol. Chem. 266 (1991) 18868-18876.

[49] A.G. Gómez-Valadés, A. Méndez-Lucas, A. Vidal-Alabró, F.X. Blasco, M. Chillon, R. Bartrons, J. Bermúdez, J.C. Perales, Pck1 gene silencing in the liver improves glycemia control, insulin sensitivity, and dyslipidemia in db/db mice, Diabetes. 57 (2008) 2199-2210.

[50] Y. Zhang, W. Chen, R. Li, Y. Li, Y. Ge, G. Chen, Insulin-regulated Srebp-1c and Pck1 mRNA expression in primary hepatocytes from zucker fatty but not lean rats is affected by feeding conditions, PLoS One. 6 (2011) e21342.

[51] C. Gu, G. Stein, N. Pan, S. Goebbels, H. Hörnberg, K.A. Nave, P. Herrera, P. White, K. Kaestner, L. Sussel, J. Lee, Pancreatic β cells require NeuroD to achieve and maintain functional maturity, Cell Metab. 11 (2010) 298-310.

[52] P. McGrath, C. Watson, C. Ingram, M. Helmrath, J. Wells, The basic Helix-Loop-Helix transcription factor NEUROG3 is required for development of the human endocrine pancreas, Diabetes. 64 (2015) 2497-2505.

[53] T. Gao, B. McKenna, C. Li, M. Reichert, J. Nguyen, T. Singh, C. Yang, A. Pannikar, N. Doliba, T. Zhang, D. Stoffers, H. Edlund, F. Matschinsky, R. Stein, B. Stanger, Pdx1 maintains β-cell identity and function by repressing an α-cell program, Cell Metab. 19 (2014) 259-271.

[54] B. Svendsen, O. Larsen, M.B.N Gabe, C.B. Christiansen, M.M. Rosenkilde, D.J. Drucker, J.J. Holst, Insulin secretion depends on intra-islet glucagon signaling, Cell Rep. 25 (2018) 1127-1134.

Chapter V: Analysis of the behavior of 2D monolayers and 3D spheroid human pancreatic beta cells derived from induced pluripotent stem cells in a microfluidic environment

In this chapter, we present a novel pancreas-on-chip model using beta-cell spheroids differentiated from human induced pluripotent stem cells. This work is being reviewed for publication in *Journal of Biotechnology* as:

Amal Essaouiba, Rachid Jellali, Marie Shinohara, Benedikt Scheidecker, Cécile Legallais, Yasuyuki Sakai, Eric Leclerc, Analysis of the behavior of 2D monolayers and 3D spheroid human pancreatic beta cells derived from induced pluripotent stem cells in a microfluidic environment, SUBMITTED. (in 2nd review)

The paper abstract is presented below as a short summary of the chapter. The material and methods of the paper correspond to a short version of the previous chapter II. As a result, the materials and methods are not included in the following pages. The supplementary files of the paper are provided at the end of this chapter. The overall published paper is presented in annex of the thesis manuscript.

Summary

The limited availability of primary human β-cells/islets and their quality (due to donor diversity) restrict the development of in vitro models for diabetes research. Human induced pluripotent stem cells (hiPSCs) may be a promising cell-source for diabetes studies, anti-diabetic drug screening and personalized therapies. However, achieving levels of maturity/functionality that are comparable to the in vivo situation and islets rebuilt from iPSCs is still challenging. Here, we compare and discuss two strategies for culturing human pancreatic β-cells derived from hiPSCs in microfluidic biochips. First, we confirmed that the protocol in conventional Petri 2D monolayer led to insulin, PDX1 and MAFA positive staining, to C-Peptide productive cells, and to tissue responsive to high/low glucose and GLP-1 stimulation. This protocol and its subsequent modifications (including extracellular matrix coating, cell adhesion time, cell inoculation density, flow rate) was not successful in the 2D biochip culture. We proposed a second strategy using 3D spheroids created from honeycomb static cultures. Spheroids in static experiments carried out over 14 days demonstrated that they expressed high levels of β-cell markers (INS mRNA) and higher α-cell markers (GCG mRNA and glucagon positive staining), when compared to Petri 2D cultures. Furthermore, the 3D spheroids were specifically able to secrete insulin in response to both high/low glucose stimulation and GLP-1 exposure. The spheroids were successfully inoculated into biochips and maintained for 10 days in perfusion. The 3D biochip cultures increased mRNA levels of GCG and maintained high levels of β-cell markers and responsiveness to both high/low glucose and GLP-1 stimulation. Finally, C-peptide and insulin secretion were higher in biochips when compared to static spheroids. These results illustrate the promising potential for hiPSCs derived β-cells and their spheroid-based pancreas-on-chip model for pancreatic disease/diabetes modeling and anti-diabetic drug screening.

Keywords: human induced pluripotent stem cells, β-pancreatic cells, microfluidic culture, 3D spheroids.

Chapter V: Analysis of the behavior of 2D monolayers and 3D spheroid human pancreatic beta cells derived from induced pluripotent stem cells in a microfluidic environment

5.1 Introduction

Pancreatic β-cells play an essential role in maintaining blood glucose homeostasis by insulin action. β cells act also as glucose sensors to detect elevated blood glucose (Webb et al., 2000). Increasing level of glucose in bloodstream stimulate insulin production and release by β-cells. Insulin is synthesized from proinsulin by cleavage of C-peptide, which is released in amounts equimolar with those of insulin (Wahren et al., 2000). Insulin activates glycogenesis in the liver and glucose uptake by muscles and adipose tissues, thereby decreasing blood sugar levels (Rogal et al., 2019). Disturbances in β-cell development or function result diabetes mellitus (DM). There are two main types of DM: type 1 DM (T1DM) is characterized by autoimmune destruction of β-cells, while type 2 DM (T2DM) T2DM is caused by the insensitivity of target tissues to insulin and impaired insulin secretion (DeFronzo et al., 2015; Jellali et al., 2020). Diabetes treatment consists of daily insulin administration or oral antidiabetic agents with lifestyle adjustment for TDM1 and TDM2, respectively (Galderisi et al., 2017; Kahraman et al., 2016). In 2019, 466 million people worldwide have diabetes mellitus (DM) and the predictions are worrying, with 700 million people affected by 2047 (IDF Diabetes Atlas, 2019).

Several animal models (in particular rodents) with the characteristics of T1DM and T2DM have been used for DM studies (King and Bowe 2016). However, animal models have their limitations because of species differences, resulting in poor extrapolation from animal to human (Cota-Coronado et al., 2019; Merlier et al., 2017). With the development of tissue-engineering 3D cultures, dynamic organ-on-chip cultures, and co-culture models, *in vitro* cell-based models have the potential to provide relevant models for diabetes modelling. The type of cells and their source are a key factor for the development of *in vitro* models (Rogal et al., 2019). Primary human β-cells or islets are considered a gold standard for *in vitro* models in DM research (Kaddis et al., 2009). However, the limited availability, the high cost of islet isolation and inter-donor differences remain major limitations to using primary islets/β-cells (Balboa et al., 2019; Amirruddin et al., 2020). Furthermore, primary islets rapidly lose their specific functions when cultured *in vitro* (Rogal et al., 2019). β-cell lines are a potential alternative to primary β-cells as they have an infinite life span, low cost and have reduced variability (Scharfmann et al., 2019). Nevertheless, these cells have limited functionality, lack plasticity and there are differences in the gene expression of β-cell markers when compared to primary cells (Amirruddin et al., 2020; Bakhti et al., 2019).

In 2007, Takahashi et al., achieved a major breakthrough by reprogramming patient somatic cells into human induced pluripotent stem cells (hiPSCs) (Takahashi et al., 2007). The availability of these cells, along with their ability to both self-renew indefinitely *in vitro*, and generate different cell types, provide great insight for investigating the pathogenic mechanisms of diseases and for contributing to cell therapies and drug development (Balboa et al., 2019; Amirruddin et al., 2020). Furthermore, unlike human embryonic stem cells (hESCs), hiPSCs do not raise any ethical problems and offer the possibility of developing patient-specific models (Balboa et al., 2019). It is currently assumed that hiPSCs can be differentiated into pancreatic β-like cells (Hosoya, 2012; Zhu et al., 2016; Kahraman et al., 2016; Hohwieler et al., 2019). However, attaining levels of maturity and functionality comparable to those of the primary human β-cell is still challenging.

Organ-on-chip is one of the more promising techniques for investigating complex human diseases (Esch et al., 2015). These microfluidic platforms improve the exchange and transport of nutrients, oxygen, metabolic waste and hormones, and create "physiological-like" situations such as cell-cell interaction, shear stress and chemical gradients (Merlier et al., 2017; Rogal et al., 2019). Previous studies have reported that perfused microfluidic cultures enhance the long-term viability and functionality of pancreatic islets and β-cell spheroids (Jun et al., 2019; Bakhti et al., 2019). Last but not least, organ-on-chip technology makes possible the co-cultures of two or more organs in separate micro-bireactors, connected by soluble factors exchanged through the microfluidic network (Merlier et al., 2107). This system can be used to study inter-organ crosstalk such as interactions between pancreatic islets and hepatic cells (Bauer et al., 2019; Essaouiba et al., 2020b). The co-culture of two or more organs is a powerful tool for modulating multi-organ diseases such as diabetes. Although organ-on-chip technology has been used to reproduce *in vitro* pancreas-on-chip models using pancreatic islets or β-cell spheroids (Jun et al., 2019; Lee et al., 2018; Li et al., 2017; Mohammed et al., 2009; Bauer et al., 2017; Schulze et al., 2017; Zbinden et al., 2020), only very few studies have already coupled iPSC derived pancreatic-like cells with organ-on-chip technology (Rogal et al., 2019; Hirano et al., 2017; Tao et al., 2019).

Our group has developed organ-on-chip technology contributing to investigations into human liver metabolism (Prot et al., 2011; Jellali et al., 2016), the human liver regeneration process (Danoy et al., 2019), as well as crosstalk and synergy between different organs such as the liver's interaction with the intestine and kidneys (Bricks et al., 2014; Choucha-Snouber et al., 2013). Recently, we have investigated the behavior of rat islets of Langerhans and their interaction with hepatocytes in microfluidic biochips (Essaouiba et al., 2020a; Essaouiba et al., 2020b). In this paper, we propose extending those microfluidic developments to pancreatic human β-cells derived from induced pluripotent stem cells. We investigated and compared several protocols for biochip cultures, as well as 2D and 3D culture configurations.

5.2 Results

5.2.1 The 2D monolayer strategy derived β-cells in Petri dishes but failed in biochips

The protocol recommended by Cellartis (cells plated in Petri 2D) led to successful cells adhesion and 16 days of cell culture (Fig. 5.3 A-C). The β-cells profile, at the protein level, was confirmed by the expression of PDX1, MAFA and insulin, as demonstrated by the immunostaining in Fig. 5.3 D. The RTqPCR analysis illustrated successful β -cells differentiation in Petri dishes, as demonstrated by the upregulation of the mRNA levels of *INS*, *PDX1*, *NGN3*, *NKX6.1* and *NKX2.2* at the end of the differentiation, when compared to the first day of culture and to the iPSCs standard (Fig. 5.3E). Finally, the functionality of the cells was confirmed by the secretion of the C-peptide (Fig. 5.3F). Secretions reached 4.5±0.5 pmol/10^5 of inoculated cells (8600 pmol/L/10^5 cells). The β-cells culture was also responsive to high / low glucose stimulation, leading to a 2.6±0.9 (n=4 assays) times more insulin secretion in high glucose stimulation when compared to low glucose stimulation (data not shown). Finally, glucagon production was not detected (either by ELISA, or by immunostaining, Fig. 5.3D). This set of results confirmed that the β-cells differentiated in 2D Petri conditions.

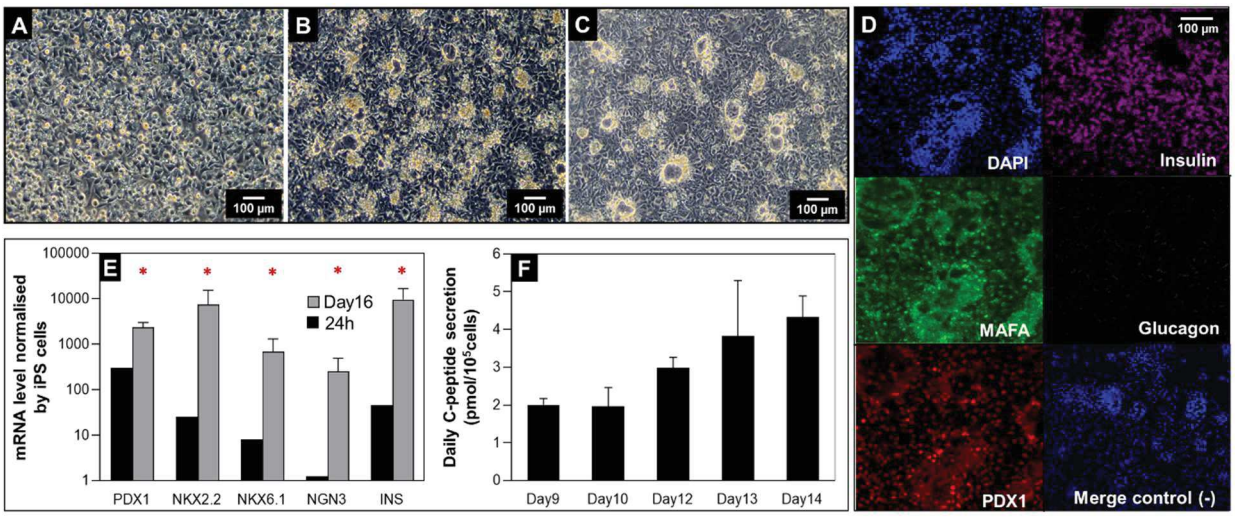

*Figure 5.1: hiPSC derived β-cells cultures in static Petri (monolayer). (A-C) morphologies after 5 h, 12 and 16 days, respectively; (D-G) immunostainings of β-cells at the end of the experiment: DAPI, MAFA, PDX1 and insulin, respectively; (H) ratio of mRNA levels (iPSC derived β-cells/iPSC) of selected genes after 24h and 16 days of culture, *P < 0.05 mRNA level significantly different when compared to iPSC; (I) daily C-peptide secretion.*

The same strategy was investigated in the biochips by directly seeding the hiPS β-cells, after thawing, inside the 2D biochips. To try to attach the cells to the bottom surface of biochips, we investigated several conditions including (i) the extracellular matrix coating; (ii) the presence of a rock inhibitor in the seeding medium; (iii) adjusting oxygen concentrations during the

adhesion phase; (iv) and the density of the seeded cells. The complete set of parameters tested is summarized in Table S1 (supplementary file). After 24h of adhesion, the cells were not able to attach in most of the conditions tested. The typical morphology is presented in Fig. 5.4A (24h after seeding, ↓ density). When using the high cell density, few cells managed to attach but they quickly formed aggregates, as shown in Fig. 5.4A (24h after seeding, ↑ density). Then, once the perfusion was launched, the cells were detached after 5h of culture (Fig. 5.4A, 5h after perfusion, ↑ density). Finally, no optimized condition was found to make successful 2D monolayer biochip cultures possible (n=3 cryotubes used in 3 independent experiments, leading to 26 biochips).

Table 5.1 : Matrix of tested conditions to plate the β-cell in biochips after thawing. Data results from 3 cryotubes of cellartis ChiPSC12 kit, n is the number of biochips per conditions, k is the cryotube number. K1 and K2 cryotubes were used to generate biochips and Petri 2D cultures, K3 was used only for biochip experiments due to larger inoculation density.

2D Biochip tests	Modification compared to Petri	status
Condition-1, n=5, k1	None (ECM-1h coating, low cell density)*	Adhesion failed (100%)
Condition-2, n=3, k2	ECM-4h coating (low cell density)	Adhesion failed (100%)
Condition-3, n=3, k2	ECM-24h coating (low cell density)	Adhesion failed (100%)
Condition-4, n=3, k2	ECM-4h+high cell density**	Adhesion failed (100%)
Condition-5, n=4, k3	ECM-24h+high cell density	Form aggregates (50%)
Condition-6, n=4, k3	ECM-24h+high cell density+rock inhibitor	Form aggregates (50%)
Condition-7, n=2, k3	ECM-24h+high cell density+rock inhibitor+low oxygen incubator	Adhesion failed (100%)
Condition-8, n=4, k3	Conditions 5 and 6 with aggregates + 10mL/min	Perfusion failed (100%)

* Low cell density = $2x10^5$ cells/cm^2

** High cell density = $6x10^5$ cells/cm^2

5.2.2. 3D spheroid strategy in static honeycombs

As the biochip cultures failed with the monolayer of β-cells, we cultured the cells into spheroids to create aggregates and allow us to seed them in the biochips with crescent-shaped microstructures. The 3D spheroids were created using honeycomb microwells. Two cell densities, $0.6x10^6$ and $0.2x10^6$ cells per well, were tested (Fig. 5.4B). The aggregates were formed after 7 hours of culture but still presented a rough circumference (Fig.5.4B, 7h after seeding). They started to present a round shape after 3 to 4 days of culture. The highest density led to spheroids of 90±15 µm in diameter (Fig. 5.4B, 14 days). The lowest density led to smaller spheroids, of 50±25 µm in diameter, but with greater dispersion (Fig. 5.4B and Fig.S2 in supplementary file, 14 days). Based on the number of honeycombs (6750), we estimated about 30 and 90 cells/spheroid in low- and high-density, respectively.

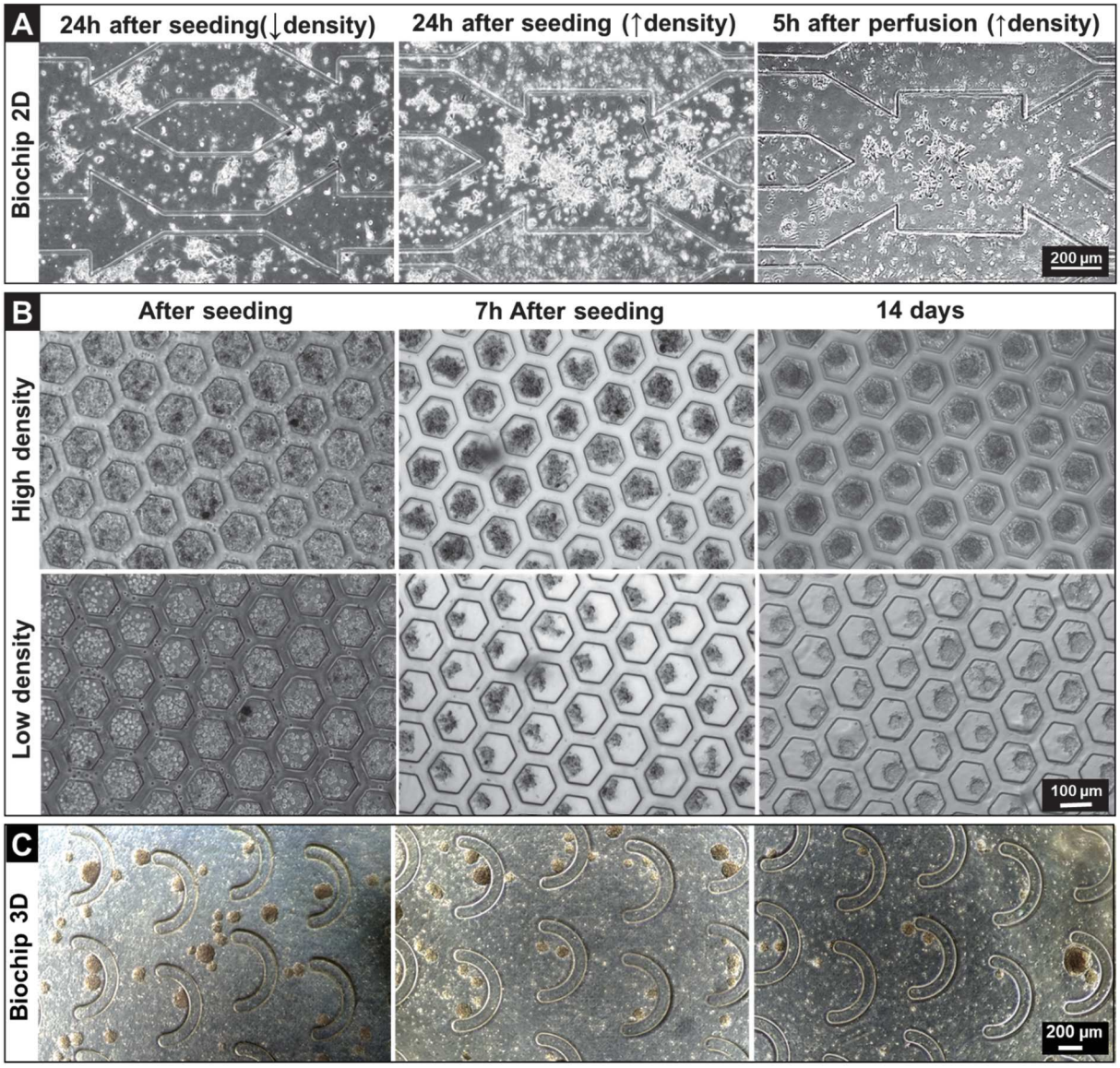

Figure 5.2 : Morphology of hiPSC derived β-cells cultivated in honeycomb wells and microfluidic biochips. (A) 2D (monolayer) dynamic culture in biochip; (B) 3D (spheroids) static culture in honeycomb wells seeded at low- and high-density of cells; (C) 3D (spheroids) dynamic culture in biochip after 14 days of culture (4 days in static honeycomb and 10 days in biochip).

The immunostainings are presented in Fig.5 for both types of spheroid. They confirmed that the spheroids were positive for β-cell markers: insulin, MAFA and PDX1. When compared to 2D cultures, the spheroids appeared to be positive for glucagon (in both high- and low-density).

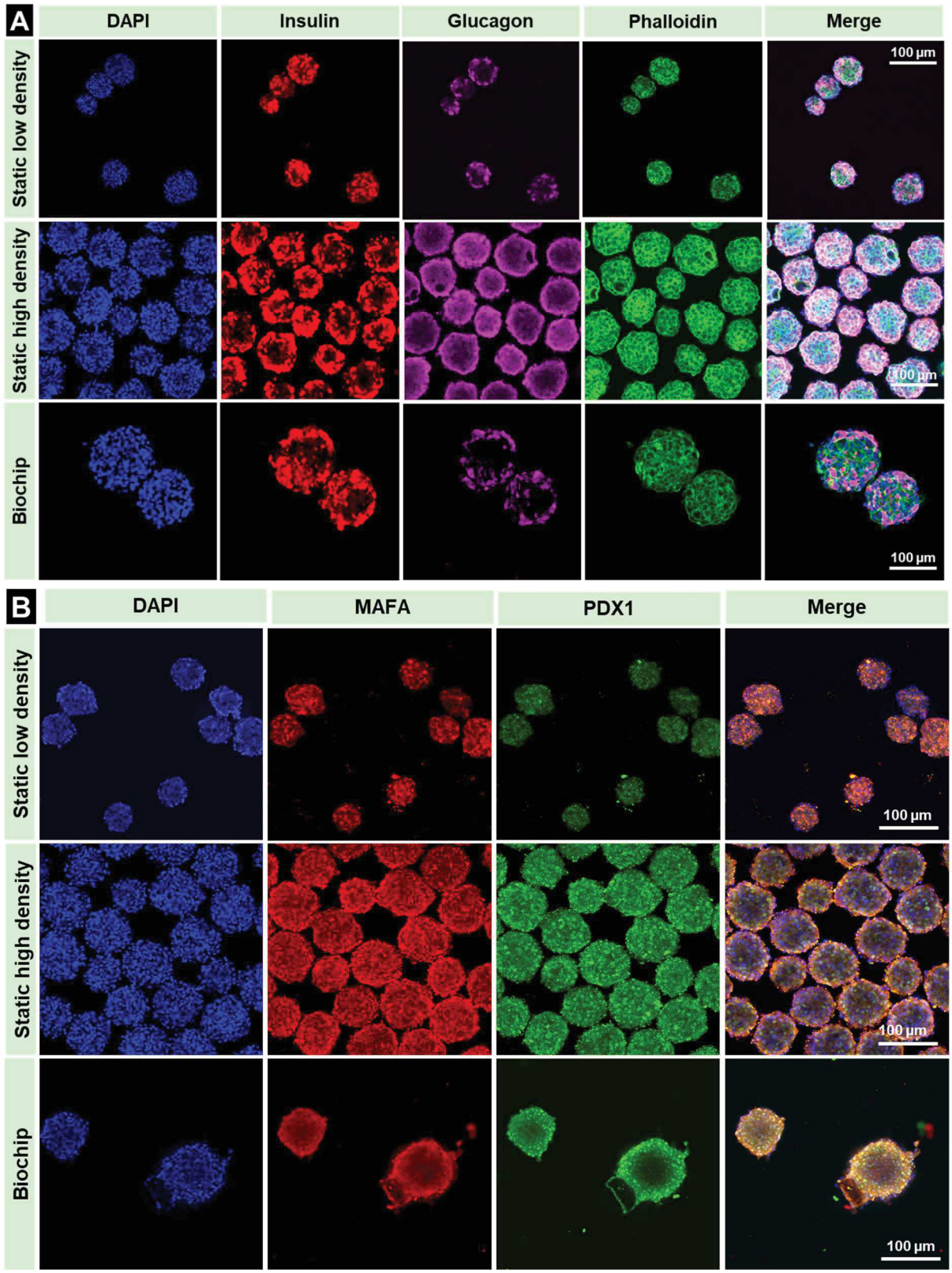

Figure 5.3: Immunostainings (end of the experiments) of hiPSC derived β-cells spheroids cultivated in honeycomb wells and biochips (A) DAPI, insulin, glucagon, phalloidin and merge; (B) DAPI, MAFA, PDX1 and merge. Negative controls (secondary antibodies without primary antibodies) are presented in Fig.S3 in supplementary file.

The β-cells spheroids led to positive C-peptide secretion, as shown in Fig. 5.6 A. When normalized by the number of seeded cells, we found that the secretion of C-peptide was similar in both high- and low-density experiments (Fig. 5.6A). Peak concentrations of around 5 pmol/10^5 inoculated cells were achieved after 13 days of culture. At the end of the experiment (day 14), we detected higher secretion of insulin in the low-density spheroids cultures (210±65 pmol/10^5 cells) when compared to the high-density spheroids cultures (98±20 pmol/10^5 cells), as shown in Fig. 5.6C. Furthermore, we found glucagon secretion during the differentiation (Fig. 5.6B). The low-density spheroids produced higher levels of glucagon, about 1.5-fold higher values than high-density spheroids. Both culture modes were responsive to the high/low glucose stimulations (Fig. 5.6D). Namely, the high glucose stimulation led to 4.5±1.3 times more insulin production when compared to the low glucose condition in high-density spheroids (GSIS index). In the low-density spheroid cultures, the GSIS index was 11.5±5. Finally, both types of spheroid were also responsive to GLP-1 drug stimulation, leading to double the insulin secretion (Fig. 5.6E). The ratios of insulin secretion (GLP-1 treated/control) were 1.96 and 1.6 in high- and low-density, respectively.

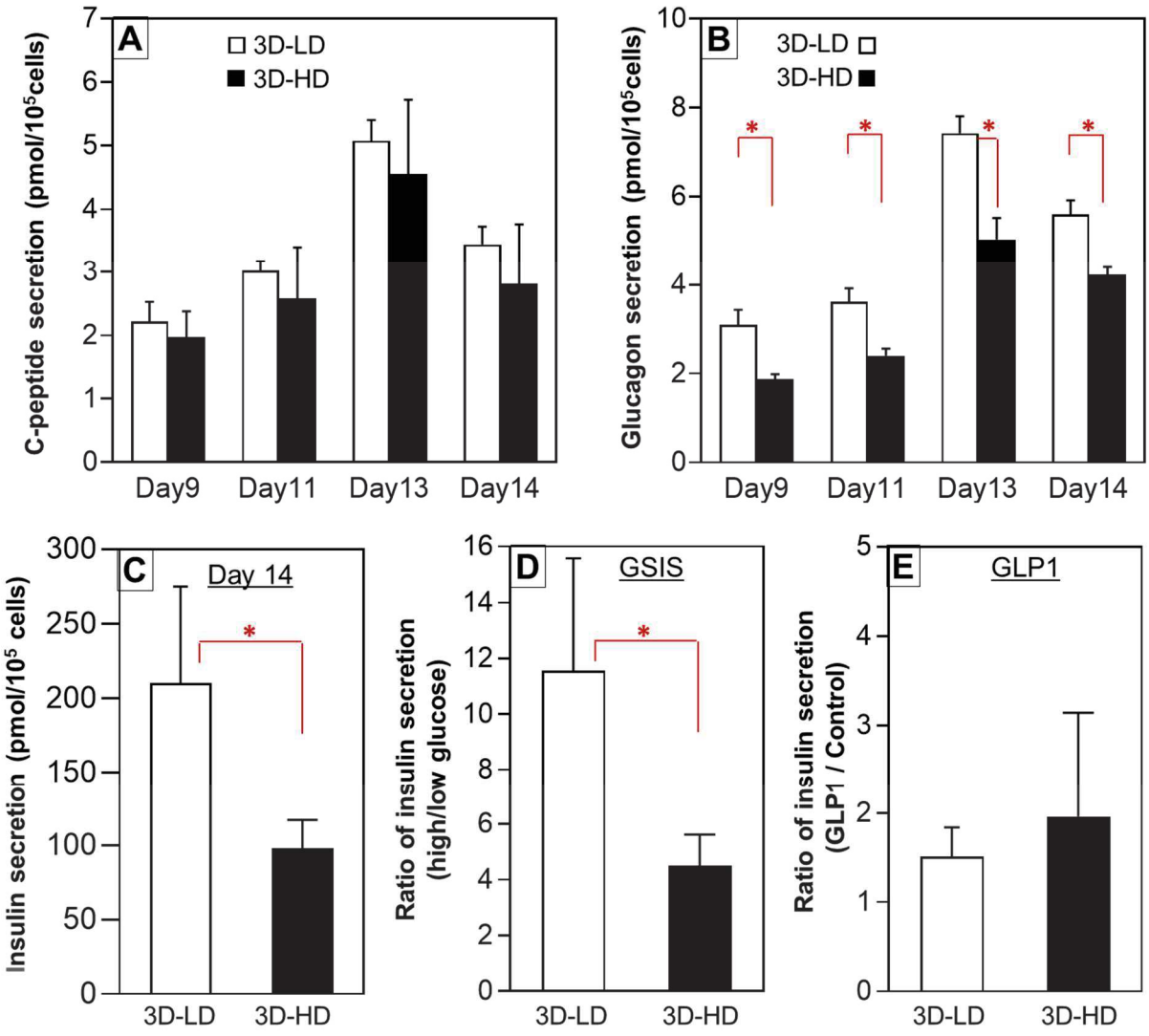

*Figure 5.4: hiPSC derived β-cells spheroids cultivated at high- and low-density in static honeycomb wells. (A and B) daily c-peptide and glucagon secretion between day 9 and day 14; (C) daily insulin secretion at day 14; (D) ratio of insulin secretion (high/low, GSIS index) after high/low glucose stimulations (GSIS: glucose-stimulated insulin secretion); (E) ratio (GLP-1/control) of insulin secretion after GLP-1 treatment. *P < 0.05, level significantly different between low (3D-LD) and high (3D-HD) density spheroids.*

5.2.3. Critical transfer of 3D β-cells spheroids into microfluidic biochips

After 4 days of culture in the honeycomb, once the spheroids had presented a round shape, they were collected and inoculated into the 3D biochips. The low-density spheroids were very fragile, and we were not able to collect the spheroids without damaging them (loss during pipetting, loss during centrifugation, spheroids destroyed during handling, n=6 honeycomb microwell dishes were tested for transfer). As a result, we only transferred the high-density spheroids into the biochips.

Although it was possible to inject the high-density spheroids, we still noticed significant loss: we counted only 150±50 spheroids entering the biochips. As we used one honeycomb Petri to fill 6 biochips, this led to about 82% - 91% of spheroids lost (600/6750 – 1200/6750, this will be discussed below). The perfusion was started for 10 additional days, leading to 14 days of culture (4 days in static conditions to create the spheroids and 10 days of dynamic culture). At the end of the perfusion, we confirmed the presence of the spheroids (number similar to the inoculation density, about 160±66 spheroids), illustrating successful perfusion culture as shown by their morphologies, which are presented in Fig. 5.4C. The typical size of the spheroids was about 98 ± 42 microns (Fig.S2 in supplementary file).

5.2.4. High functionality of the 3D pancreatic spheroids in microfluidic biochips

Analyzing the mRNA levels revealed major modifications to the profile of the cells when we compared the 2D Petri, 3D Petri honeycomb (3D-HD) and the 3D biochip cultures (Fig.V.5). The spheroid culture, in 3D Petri, appeared to increase the gene expression of β-cell markers such as *PDX1*, *NKX2.2*, *NKX6.1* and *INS* (Fold change, FC of 3.3, 2.6, 3 and 3.8, respectively when compared to Petri 2D). In parallel, alpha or delta cell markers such as *GCG* (FC 2.6), *SST* (FC 6.6) and glucose transporter *GLUT2* (FC 19) were higher in static 3D spheroid conditions than in 2D Petri conditions. Finally, *GCK, UCN3* and *NGN3* were downregulated in static 3D spheroids (in comparison with Petri 2D).

Once cultivated in the biochip, we found an increase in mRNA levels of alpha cells markers (*GCG*, FC 6.8), delta cell markers (*SST*, FC 3.5) and glucose metabolism markers (*GLUT2*, FC 12.7), when compared to 2D cultures (Fig. 5.7). Furthermore, we found clear upregulation of *GCG* when compared to the 3D Petri cultures. Although β-cells markers such as *NKX6.1* and *NKX2.2* were 2.5-2.7 times higher in the biochips when compared to 2D (and similar to 3D Petri levels), the levels of *PDX1* and *INS* mRNA were similar in the 2D cultures and biochips. Finally, *MAFA* (FC 0.42), *GCK* (FC 0.11), *UCN3* (FC 0.12) and *NGN3* (FC 0.08) were lower in the biochips, when compared to 2D cultures.

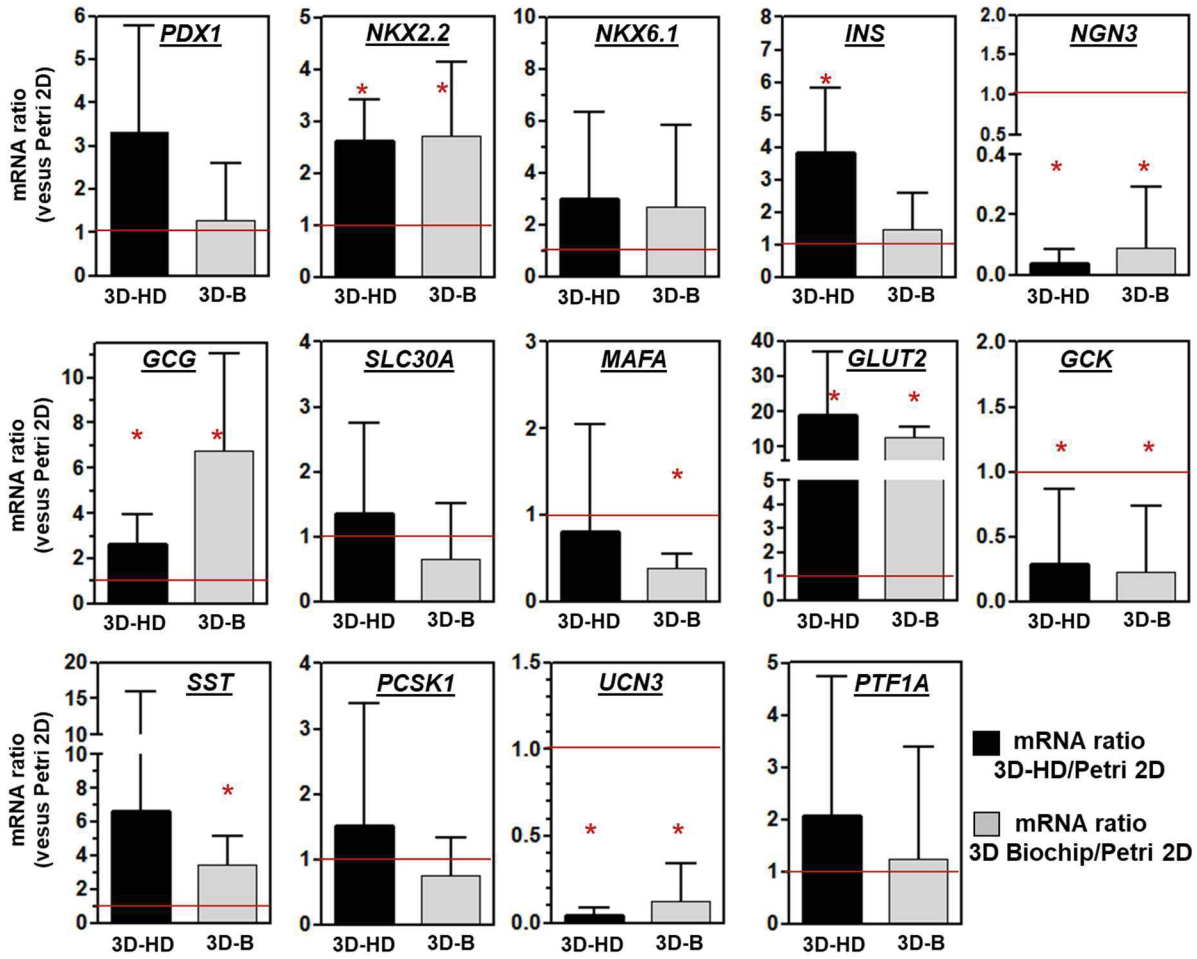

*Figure 5.5: Ratio of mRNA levels of selected genes at the end of culture. black bars: β-cells spheroids cultivated at high-density in static honeycomb wells versus β-cells cultures in static Petri (2D monolayer) and gray bars: β-cells spheroids cultivated in dynamic biochip versus β-cells cultures in static Petri (2D monolayer). *P < 0.05, mRNA level significantly different when compared to static Petri (2D monolayer.*

Immunostaining confirmed that the spheroids cultures in biochips expressed typical β-cells markers, as illustrated by the detection of insulin, MAFA and PDX1 positive cells (Fig. 5.3.A). However, we also found cells positive for glucagon, demonstrating the presence of alpha-like cells as well. As mentioned above, in the 2D Petri cultures, we never detected glucagon positive cells.

The kinetics of C-peptide secretion in biochips presented in Fig. 5.6.A demonstrates the functionality of the spheroids. To be able to compare the dataset in biochips and honeycombs (3D-HD), we normalized by number of spheroids at the end of the experiments. When normalized by the number of spheroids, C-peptide secretion in the biochips was measured at around 0.02-0.05 pmol/islet between day 9 and the end of the perfusion (day 14, Fig. 5.6.A). Furthermore, we detected higher quantities of C-peptide in biochip cultures when compared to 3D honeycombs

(about 10-30 times higher). We also observed higher secretions of insulin in the biochip spheroids cultures when compared to the static spheroids cultures (3D-HD), as shown in Fig. 5.6.B. Insulin secretion was about 2.55 times higher in the biochips at the end of the experiment (day 14).

The functional assays performed using high/low glucose stimulation (glucose-stimulated insulin secretion, GSIS) and GLP-1 stimulation demonstrated that the biochip spheroids were able to adapt their insulin response, as shown in Fig. 5.6.C and Fig. 5.8.D, respectively. However, in terms of the induction ratio itself, no difference between the biochip and the static honeycomb cultures was observed. The GSIS index (glucose-stimulated insulin secretion: insulin measured in high-glucose divided by insulin in low-glucose) values were of 3.2±1.1 and 4.5±1.2 in the biochip and static honeycomb, respectively (Fig. 5.6.C). Concerning the GLP-1 effect, the levels of insulin were 1.5 (static spheroids) and 2 (biochip spheroids) times higher after GLP-1 stimulation, when compared to the control (Fig. 5.6.D).

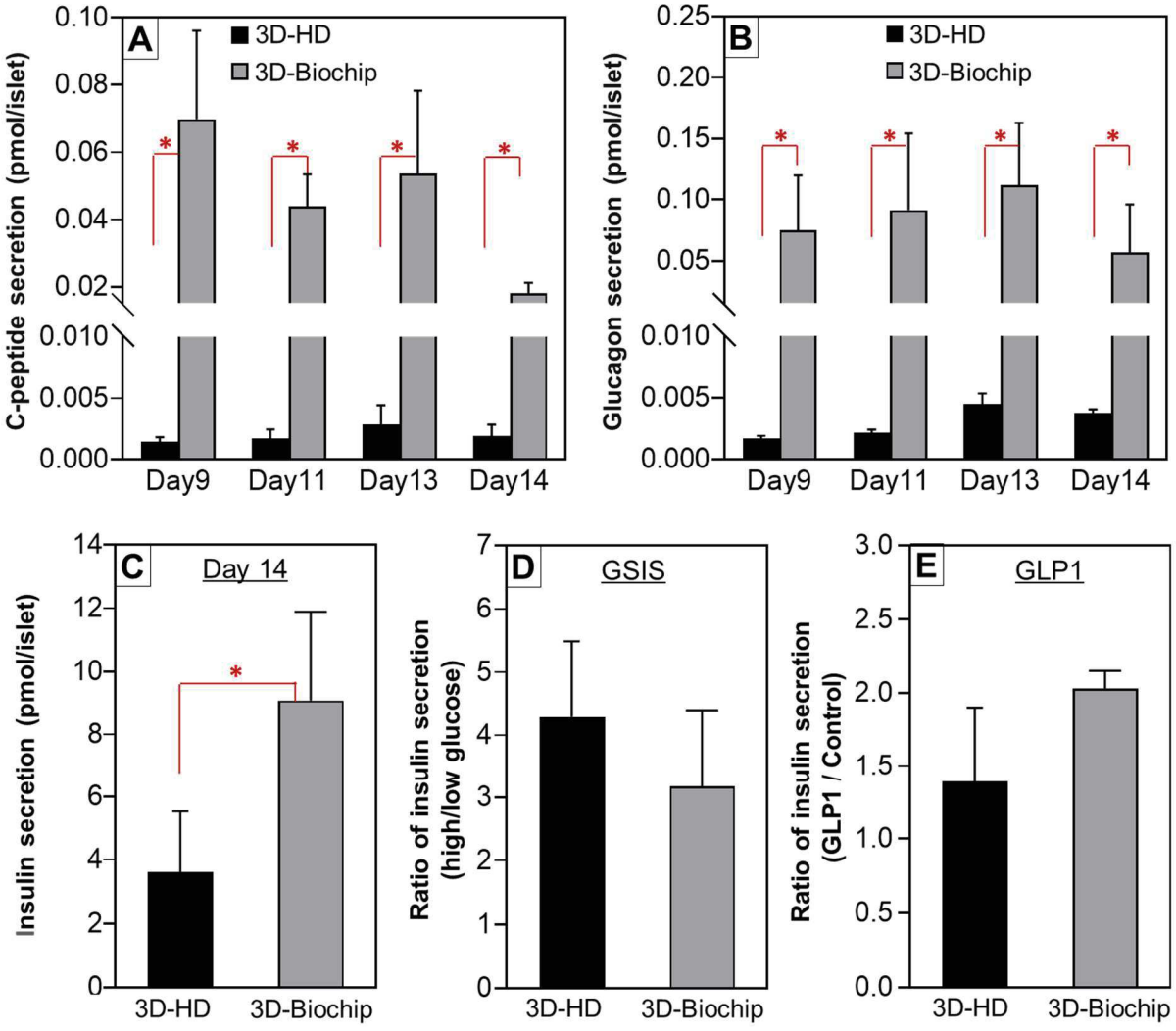

*Figure 5.6: hiPSC derived β-cells spheroids cultivated in honeycomb wells (high-density) and biochips. (A and B) daily c-peptide and glucagon secretion between day 9 and day 14; (C) daily insulin secretion at day 14 (*P < 0.05); (D) ratio of insulin secretion (high/low, GSIS index) after high/low glucose stimulations (GSIS: glucose-stimulated insulin secretion); (E) ratio (GLP1/control) of insulin secretion after GLP1 treatment. *P < 0.05, level significantly different between low (3D-LD) and high (3D-HD) density spheroids.*

5.3. Discussion

In this work we investigated the behaviors of pancreatic β-cells derived from human induced pluripotent stem cells. The 2D cultures in Petri dishes confirmed the functionality of the derived tissue as a pancreatic-like β-cells. This was illustrated by C-peptide production, the positive staining for insulin, negative staining for glucagon, and insulin secretion in response to low/high glucose stimulation. Other 2D protocols for iPSCs derived pancreatic β-cells, including different growth factor sequences, iPS cell lines and sources, have also reported successful insulin and C-peptide functional tissues (Yabe et al., 2017; Southard et al., 2018; Pelligrini et al., 2018). Those works attained C-peptide production of up to 5000 pmol/L/2x10^6 cells after 23 days of

culture (Yabe et al., 2017), and ranging from 700 to 1500 pmol/L/6.4x10^4 of plated cells after 28 days of culture (Southard et al., 2018). Our differentiation took place over 16 days after stage 1 of the Cellartis protocol (Fig 1), corresponding to 37 days overall of differentiation from undifferentiated iPSCs. As we reached a peak of 8600 pmol/L/10^5 of plated cells (4.5 pmol/10^5 of cells) after 35 days, our results appeared consistent with the data in the literature.

Although the 2D Petri cultures were encouraging, we failed to create 2D cultures of β-cells in our microfluidic devices (our primary goal). This strategy was first investigated because the Cellartis ChiPSC12 kit is recommended for use in monolayers. We could not identify the key parameters leading to this failure. First the cell adhesion, and then the cell monolayer could not be created in the biochips even though we tested several conditions, including the initial cell density, extracellular matrix coating and oxygen adhesion conditions (see Table S1, supplementary file). Several hypotheses can be formulated: (i) the first is related to choosing the extracellular matrix and its protocol of coating on PDMS. PDMS is a hydrophobic material that needs an appropriate coating of ECM to make cell adhesion possible. The Cellartis recommended ECM, when coated on PDMS, may require higher concentrations of ECM compounds and longer incubation times on the surface compared to the recommended protocol for polystyrene Petri cultures; it may also require other components, such as Matrigel (suitable for iPSC hepatocytes on PDMS for instance, Danoy et al., 2019) (ii) in addition, during the adhesion phase of cells in biochips, and the first hours of perfusion, our previous experiments (with cell lines) demonstrated that there was significant glucose consumption by the cells (Prot et al., 2011). As the biochip volume was 30 µL, leading to a cell/volume ratio of 6 600 000 cells/mL in the biochip (200 000 cells/cm^2 in 30 µL) and 400 000 cells/mL in Petri dishes (200 000 cells/cm^2 in 0.5 mL), we can hypothesize that there was a local shortage of a critical nutrient at the density inoculation tested. In this context, several reviews to help obtain successful microfluidic cultures have been proposed in the literature, exploring other 2D strategies (Yu et al., 2007, Young and Beebe 2010); (iii) we also previously reported some ROS production during the adhesion stage of cell culture in a microfluidic environment and during the first hours of perfusion (Leclerc et al., 2015). To avoid potential apoptosis, we tested the effects of a ROCK inhibitor, as it is used in several iPSC protocols during the plating stage after thawing (Emre et al., 2010; Watanabe et al., 2007), but it did not lead to improved adhesion. As a result, more extensive investigations are needed to solve the issues with the 2D biochip cultures.

As an alternative to the 2D biochip culture strategy, we proposed a 3D spheroid protocol. In honeycomb static cultures, our spheroid protocol contributed to generating β-cells-based spheroids secreting C-peptide and insulin. We found that low cell density spheroids generated smaller spheroids (50 µm) compared to high cell density ones (100 µm), although they produced similar levels of C-peptide. The effects of cell density and spheroid diameter on functionality were

documented with β-cells line (Shinohara et al., 2014; Bernard et al., 2012). Microwells of 100 to 300 µm in diameter led to insulin levels close to 75ng/1000 cells in Min-6 (Bernard et al., 2012). In our honeycomb geometry, previous works with Min-6 spheroids ranging from 60 to 150 µm in diameter produced levels of insulin close to 60 ng/ng-DNA (Shinohara et al., 2014). Furthermore, *in vitro* secretion of insulin from derived iPSCs β-cells spheroids is reported as ranging from 1.6 to 2 µUI/10^3 cells (Millman and Pagliuca 2017; Pagliuca et al., 2014, Millman et al., 2016). Based on the data in Figs. 6 and 8, our study contributed to generating β-cell-based spheroids secreting insulin around 1.8 µUI/10^3 cells in the high density spheroids used in 3D Petri (with a conversion of 0.144 µUI/mL = 1 pmol/L). Finally, insulin secretion stimulated by high glucose in primary human islets led to 4-fold induction (glucose 5.6 mM), 16-fold (16.7 mM) after one hour of exposure (Mc Donald et al., 2011) and about 10-fold at 11 mM, 20 min of stimulation (Pelligrini et al., 2018). These results appear to be in the range of our data in which the mean value of the induced insulin secretion ratio was close to 4 and 11 in the 3D high- and low-density spheroids, respectively.

We then successfully applied our 3D spheroid cultures to the microfluidic biochips. There was still a significant loss of spheroids, and a third strategy consisting of generating the islets inside the biochips, to avoid having to transfer them, needs to be investigated. Nevertheless, thanks to the biochips, we were able to improve spheroid functionality when compared to 3D Petri controls in terms of insulin and C-peptide secretion. The enhancements of basal pancreatic islets or pseudo-islets functions such as insulin secretion and glucose-induced insulin secretion under microfluidic flow have been observed consistently in the literature (Jun et al., 2019; Tao et al., 2019; Li et al., 2013; Sankar et al., 2011). We suspect that changing the continuous culture medium played a part in continuously stimulating the spheroids with high glucose stimulation, and thus insulin secretion. The spheroids in the biochip cultures were also responsive to both low/high glucose stimulation and GLP1 exposure.

Focusing on the 3D spheroids experiments, we found that the 3D spheroids had greater heterogeneity (in the 3D Petri and 3D biochip conditions), when compared to the Cellartis optimized 2D protocol. The mRNA levels and immunostaining analysis revealed partial loss of the β-cell specifications in the 3D spheroids, and the potential orientation toward pancreatic β-cells and β-cells sub-lineages. This was illustrated by the positive staining of the glucagon, upregulation of *SST* and *GCG,* and downregulation of *NGN3* in the spheroids in 3D conditions. It is reported in the literature that *PDX1*, *MAFA*, *NGN3* and *NKX6.1* play a pivotal role in β-cells differentiation, as well as in various processes within β-cell differentiation (Schaffer et al., 2010; Matsuoka et al., 2017; Zhu et al., 2016; Brissova et al., 2018). Furthermore, the *SST* gene (upregulated in the 3D Petri and 3D biochip cultures when compared to 2D Petri) is a key player in β-cell specification (Hauge Evans et al., 2009).

In parallel, modification to the differentiation pattern was concomitant with high levels of *GLUT2* and *GCG*, and low levels of *GCK* in 3D cultures. We confirmed the high level of glucose in the culture medium, even in 3D Petri and 3D biochip cultures (in the culture medium from step 2, we measured 9.5±0.5 mM, data not shown). As a result, we can hypothesize that the secretion of glucagon in the spheroids (detected by positive immunostaining) is due to local shortage of glucose inside the spheroid, and thus to a modulation of glucose transport inside the spheroid (*nb:* it has been reported that *GLUT2* is weakly expressed in β-cells and over-expressed in β-cells, leading to the way the glucose is transported being modulated, but not the fact of the transport itself, Heimberg et al., 1995). *GCK* is a glucose sensor that regulates insulin release in β-cells, and glucose homeostasis in α and β-cells (Matschinsky et al., 2019). In addition, *GCK* governs an α-cell metabolic pathway by suppressing glucose-related secretion of glucagon at/or above normoglycemic levels (Basco et al., 2018). Downregulation of *GCK* in our 3D cultures appeared consistent with glucagon secretion due to glucose shortage in the center of the spheroids. As a result, in agreement with pancreas organogenesis (Puri et al., 2015), our data suggest that there is major cell plasticity in the differentiation process of the present iPSCs in response to the 3D spheroid culture conditions. Additional investigations are now required to understand these phenomena. More particularly, it would be interesting to see whether complex physiological islet differentiation into multicellular pancreatic lineages including α,β and δ cells can occur in these 3D spheroid microfluidic cultures.

5.4. Conclusion

In summary, we investigated the behaviors of β-cells derived from hiPSCs in various culture conditions. 2D monolayer cultures generated typical β-cells profiles, as shown by C-peptide production and undetected glucagon secretion. When cultivated in 2D biochips in a monolayer, we did not find any stable protocol making their microfluidic cultures possible. When the cells were cultivated in 3D spheroids, the cells presented higher heterogeneity, as seen in the appearance of α,β and δ-cell markers at the mRNA level, and glucagon positive immunostaining, in addition to the secretion of C-peptide. The 3D spheroids were then successfully cultivated in a 3D biochip under microfluidic conditions. The microfluidic culture established contributed to increasing pancreatic maturation by improving C-peptide and insulin secretion levels. The high level GLUT2 and low level GCK in 3D static spheroids and 3D biochips, when compared to 2D Petri, suggested modulation of glucose metabolism and transport as a potential regulator of pancreatic specification during differentiation into 3D spheroids and 3D biochips. We believe that our results are encouraging for the development of functional pancreas-on-chip in vitro models using the advantages of organ-on-chip technology and hiPS cells, a promising source of cells.

5.5 Supplementary figures

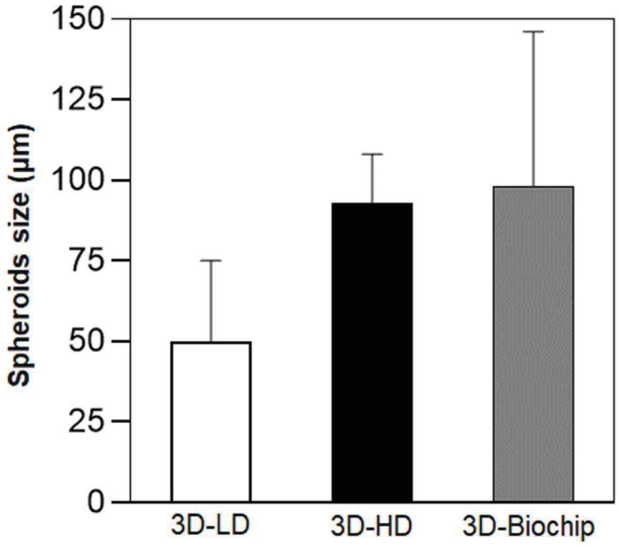

Figure 5.S1 : Spheroids size at the end of the experiments. Quantification by ImageJ software (NIH, Bethesda, Maryland) using the collected images.

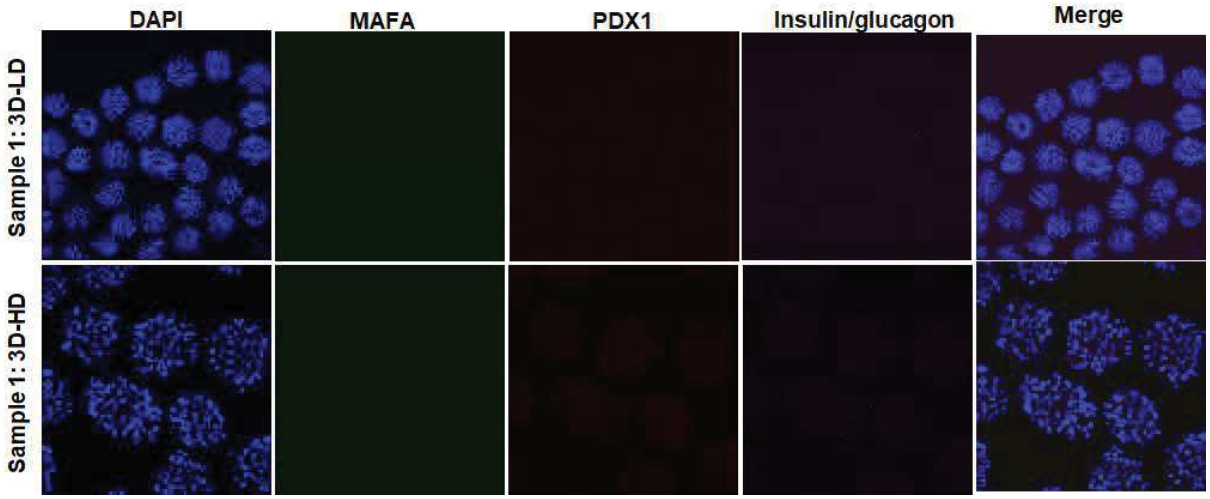

Figure 5.S2 : Spheroids immunostainings: negatives controls, samples exposed to secondary antibodies without primary antibodies.

5.6 References

Amirruddin, N.S., Low, B.S.J., Lee, K.O., Tai, E.S., Teo, A.K.K.,2020. New insights into human beta cell biology using human pluripotent stem cells. Semin. Cell Dev. Biol. 103, 31-40. https://doi.org/10.1016/j.semcdb.2019.11.004.

Bakhti, M., Böttcher, A., Lickert, H., 2019. Modelling the endocrine pancreas in health and disease, Nat. Rev. Endocrinol. 15, 155-171. https://doi.org/10.1038/s41574-018-0132-z.

Balboa, D., Saarimäki-Vire, J., Otonkoski, T., 2019. Concise Review: Human Pluripotent Stem Cells for the Modeling of Pancreatic β-Cell Pathology. Stem Cells. 37, 33-41. https://doi.org/10.1002/stem.2913.

Basco, D., Zhang, Q., Salehi, A., Tarasov, A., Dolci, W., Herrera, P., Spiliotis, I., Berney, X., Tarussio, D., Rorsman, P., Thorens, B., 2018. α-cell glucokinase suppresses glucose-regulated glucagon secretion. Nat. Commun. 9, 546. https://doi.org/10.1038/s41467-018-03034-0.

Baudoin, R., Griscom, L., Prot, J.M., Legallais, C., Leclerc, E., 2011. Behaviour of HepG2/C3a cell culture in a microfluidic bioreactor. Biochem. Eng. J. 53, 172-181. https://doi.org/10.1016/j.bej.2010.10.007.

Bauer, S., Wennberg Huldt, C., Kanebratt, K., Durieux, I., Gunne, D., Andersson, S., Ewart, L., Haynes, W., Maschmeyer, I., Winter, A., Ämmälä, C., Marx, U., Andersson, T., 2017. Functional coupling of human pancreatic islets and liver spheroids on-a-chip: Towards a novel human ex vivo type 2 diabetes model. Sci Rep. 7, 14620. https://doi.org/10.1038/s41598-017-14815-w.

Bernard, A., Lin, C., Anseth, K., 2012. A microwell cell culture platform for the aggregation of pancreatic β-cells. Tissue Eng. Part C Methods. 18, 583-592. https://doi.org/10.1089/ten.TEC.2011.0504.

Bricks, T., Paullier, P., Legendre, A., Fleury, M.J., Zeller, P., Merlier, F., Anton, P.M., Leclerc, E., 2014. Development of a new microfluidic platform integrating co-cultures of intestinal and liver cell lines. Toxicol. in Vitro. 28, 885-895. https://doi.org/10.1016/j.tiv.2014.02.005.

Brissova, M., Haliyur, R., Saunders, D., Shrestha, S., Dai, C., Blodgett, D.M., Bottino, R., Campbell-Thompson, M., Aramandla, R., Poffenberger, G., Lindner, J., Pan, F.C., von Herrath, M.G., Greiner, D.L., Shultz, L.D., Sanyoura, M., Philipson, L.H., Atkinson, M., Harlan, D.M., Levy, S.E., Prasad, N., Stein, R., Powers, A.C., 2018. α cell function and gene expression are compromised in type 1 diabetes. Cell rep. 22, 2667-2676. https://doi.org/10.1016/j.celrep.2018.02.032.

Choucha-Snouber, L., Aninat, C., Grsicom, L., Madalinski, G., Brochot, C., Poleni, P.E., Razan, F., Guguen Guillouzo, C., Legallais, C., Corlu, A., Leclerc, E., 2013. Investigation of ifosfamide nephrotoxicity induced in a liver–kidney co-culture biochip. Biotechnol. Bioeng. 110, 597-608. https://doi.org/10.1002/bit.24707.

Cota-Coronado, A., Ramírez-Rodríguez, P.B., Padilla-Camberos, E., Díaz, É.F., Flores-Fernández, J.M., Ávila-Gónzalez, D., Diaz-Martinez, N.E., 2019. Implications of human induced pluripotent stem cells in metabolic disorders: from drug discovery toward precision medicine. Drug. Discov. Today. 24, 334-341. https://doi.org/10.1016/j.drudis.2018.10.001.

Danoy, M., Lereau Bernier, M., Kimura, K., Poulain, S., Kato, S., Mori, D., Kido, T., Plessy, C., Kusuhara, H., Miyajima, A., Sakai, Y., Leclerc, E., 2019. Optimized protocol for the hepatic differentiation of induced pluripotent stem cells in a fluidic microenvironment. Biotechnol.

Bioeng. 116, 1762-1776. https://doi.org/10.1002/bit.26970.

DeFronzo, R.A., Ferrannini, E., Groop, L., Henry, R.R., Herman, W.H., Holst, J.J., Hu, F.B., Kahn, C.R., Raz, I., Shulman, G.I., Simonson, D.C., Testa, M.A., Weiss, R., 2015. Type 2 diabetes mellitus. Nat. Rev. Dis. Primers. 1, 15019. https://doi.org/10.1038/nrdp.2015.19.

Emre, N., Vidal, J.G., Elia, J., O'Connor, E.D., Paramban, R.I., Hefferan, M.P., Navarro, R., Goldberg, D.S., Varki, N.M., Marsala, M., Carson, C.T., 2010. The ROCK inhibitor Y-27632 improves recovery of human embryonic stem cells after fluorescence-activated cell sorting with multiple cell surface markers. PLoS One. 5, e12148. https://doi.org/10.1371/journal.pone.0012148.

Esch, E.W., Bahinski, A., Huh, D., 2015. Organs-on-chips at the frontiers of drug discovery. Nat. Rev. Drug. Discov. 14, 248-260. https://doi.org/10.1038/nrd4539.

Essaouiba, A., Okitsu, T., Jellali, R., Shinohara, M., Danoy, M., Tauran, Y., Legallais, C., Sakai, Y., Leclerc, E., 2020a. Microwell-based pancreas-on-chip model enhances genes expression and functionality of rat islets of Langerhans. Mol. Cell Endocrinol. 514, 110892. https://doi.org/10.1016/j.mce.2020.110892.

Essaouiba, A., Okitsu, T., Kinoshita, R., Jellali, R., Shinohara, M., Danoy, M., Legallais, C., Sakai, Y., Leclerc, E., 2020b. Development of a pancreas-liver organ-on-chip coculture model for organ-to-organ interaction studies. Biochem. Eng. J. 164, 107783. https://doi.org/10.1016/j.bej.2020.107783.

Galderisi, A., Schlissel, E., Cengiz, E., 2017. Keeping up with the diabetes technology: 2016 endocrine society guidelines of insulin pump therapy and continuous glucose monitor management of diabetes. Curr. Diab. Rep. 17, 111. https://doi.org/10.1007/s11892-017-0944-6.

Hauge-Evans, A.C., King, A.J., Carmignac, D., Richardson, C.C., Robinson, I.C., Low, M.J., Christie, M.R., Persaud, S.J., Jones, P.M., 2009. Somatostatin secreted by islet delta-cells fulfills multiple roles as a paracrine regulator of islet function. Diabetes. 58, 403-411. https://doi.org/10.2337/db08-0792.

Heimberg, H., De Vos, A., Pipeleers, D., Thorens, B., Schuit, F., 1995. Differences in glucose transporter gene expression between rat pancreatic alpha- and beta-cells are correlated to differences in glucose transport but not in glucose utilization. J. Biol. Chem. 270, 8971-8975. https://doi.org/10.1074/jbc.270.15.8971.

Hirano, K., Konagaya, S., Turner, A., Noda, Y., Kitamura, S., Kotera, H., Iwata, H., 2017. Closed-channel culture system for efficient and reproducible differentiation of human pluripotent stem cells into islet cells. Biochem. Biophys. Res. Commun. 487, 344e350. https://doi.org/10.1016/j.bbrc.2017.04.062.

Hohwieler, M., Müller, M., Frappart, P.O., Heller, S., 2019. Pancreatic progenitors and organoids

as a prerequisite to model pancreatic diseases and cancer. Stem Cells Int. 2019, 9301382. https://doi.org/10.1155/2019/9301382.

Hosoya, M., 2012. Preparation of pancreatic β-cells from human iPS cells with small molecules. Islets. 4, 249-252. https://doi.org/10.4161/isl.20856.

International Diabetes Federation, IDF Diabetes Atlas, 9th edn. 2019. https://www.diabetesatlas.org/en/ (accessed may 2020).

Jellali, R., Bricks, T., Jacques, S., Fleury, M.J., Paullier, P., Merlier, F., Leclerc, E., 2016. Long-term human primary hepatocyte cultures in a microfluidic liver biochip show maintenance of mRNA levels and higher drug metabolism compared with Petri cultures. Biopharm. drug dispos. 37, 264-275. https://doi.org/10.1002/bdd.2010.

Jellali, R., Essaouiba, A., Leclerc, E., Legallais, C., 2020. Membrane bioreactors for bio-artificial pancreas, in: Basile, A., Annesini, M.C., Piemonte, V., Charcosset, C., (Eds.), Current Trends and Future Developments on (Bio-) Membranes, Elsevier, pp. 77-108. https://doi.org/10.1016/B978-0-12-814225-7.00004-8.

Jellali, R., Fleury, M.J., Paullier, P., Leclerc, E., 2016. Liver and kidney cells cultures in a new perfluoropolyether biochip. Sens. Actuator B-Chem. 229, 396-407. https://doi.org/10.1016/j.snb.2016.01.141.

Jun, Y., Lee, J., Choi, S., Yang, J.H., Sander, M., Chung, S., Lee, S.H., 2019. In vivo-mimicking microfluidic perfusion culture of pancreatic islet spheroids. Sci Adv. 5, eaax4520. https://doi.org/10.1126/sciadv.aax4520.

Kaddis, J.S., Olack, B.J., Sowinski, J., Cravens, J., Contreras, J.L., Niland, J.C., 2009. Human pancreatic islets and diabetes research. JAMA. 2009, 301, 1580–1587. https://doi.org/10.1001/jama.2009.482.

Kahraman, S., Okawa, E.R., Kulkarni, R.N., 2016. Is transforming stem cells to pancreatic beta cells still the holy grail for type 2 diabetes? Curr. Diab. Rep. 16, 70. https://doi.org/10.1007/s11892-016-0764-0.

King, A., Bowe, J., 2016. Animal models for diabetes: Understanding the pathogenesis and finding new treatments. Biochem. Pharmacol. 99, 1-10. https://doi.org/10.1016/j.bcp.2015.08.108.

Leclerc, E., Hamon, J., Claude, I., Jellali, R., Naudot, M., Bois, F., 2015. Investigation of acetaminophen toxicity in HepG2/C3a microscale cultures using a system biology model of glutathione depletion. Cell Biol. Toxicol. 31, 173-185. https://doi.org/10.1007/s10565-015-9302-0.

Lee, S.H., Hong, S., Song, J., Cho, B., Han, E.J., Kondapavulur, S., Kim, D., Lee, L.P., 2018. Microphysiological analysis platform of pancreatic islet β-cell spheroids. Adv. Healthc. Mater. 7, 1701111. https://doi.org/10.1002/adhm.201701111.

Li, X., Brooks, J.C., Hu, J., Ford, K.I., Easley, C.J., 2017. 3D-templated, fully automated microfluidic input/output multiplexer for endocrine tissue culture and secretion sampling. Lab Chip. 17, 341-349. https://doi.org/10.1039/c6lc01201a.

Li, Z., Sun, H., Zhang, J., Zhang, H., Meng, F., Cui, Z., 2013. Development of in vitro 3D TissueFlex® islet model for diabetic drug efficacy testing. PLoS One. 8, e72612. https://doi.org/10.1371/journal.pone.0072612.

MacDonald, M.J., Longacre, M.J., Stoker, S.W., Kendrick, M., Thonpho, A., Brown, L.J., Hasan, N.M., Jitrapakdee, S., Fukao, T., Hanson, M.S., Fernandez, L.A., Odorico, J., 2011. Differences between human and rodent pancreatic islets: low pyruvate carboxylase, atp citrate lyase, and pyruvate carboxylation and high glucose-stimulated acetoacetate in human pancreatic islets. J. Biol. Chem. 286, 18383-18396. https://doi.org/10.1074/jbc.M111.241182.

Matschinsky, F.M., Wilson, D.F., 2019. The central role of glucokinase in glucose homeostasis: A perspective 50 Years after demonstrating the presence of the enzyme in islets of Langerhans. Front. Physiol. 10, 148. https://doi.org/10.3389/fphys.2019.00148.

Matsuoka, T.A., Kawashima, S., Miyatsuka, T., Sasaki, S., Shimo, N., Katakami, N., Kawamori, D., Takebe, S., Herrera, P.L., Kaneto, H., Stein, R., Shimomura, I., 2017. Mafa enables Pdx1 to effectively convert pancreatic islet progenitors and committed islet α-cells into β-cells in vivo. Diabetes. 66, 1293-1300. https://doi.org/10.2337/db16-0887.

Merlier, F., Jellali, R., Leclerc, E., 2017. Online hepatic rat metabolism by coupling liver biochip and mass spectrometry. Analyst. 142, 3747-3757. https://doi.org/10.1039/C7AN00973A.

Millman, J.R., Pagliuca, F.W., 2017. Autologous pluripotent stem cell–derived b-like cells for diabetes cellular therapy. Diabetes. 66, 11111120. https://doi.org/10.2337/db16-1406.

Millman, J.R., Xie, C., Van Dervort, A., Gürtler, M., Pagliuca, F.W., Melton, D.A., 2016. Generation of stem cell-derived b-cells from patients with type 1 diabetes. Nat. Commun. 7, 11463. https://doi.org/10.1038/ncomms11463.

Mohammed, J.S., Wang, Y., Harvat, T.A., Oberholzer, J., Eddington, D.T., 2009. Microfluidic device for multimodal characterization of pancreatic islets. Lab Chip. 9, 97-106. https://doi.org/10.1039/B809590F.

Pagliuca, F.W., Millman, J.R., Gurtler, M., Segel, M., Van Dervort, A., Hyoje, R.J., Peterson, Q.P., Greiner, D., Melton, D.A., 2014. Generation of functional human pancreatic β cells in vitro. Cell. 159, 428-439. https://doi.org/10.1016/j.cell.2014.09.040.

Pellegrini, S., Manenti, F., Chimienti, R., Nano, R., Ottoboni, L., Ruffini, F., Martino, G., Ravassard, P., Piemonti, L., Valeria Sordi, V., 2018. Differentiation of sendai virus-reprogrammed iPSC into β cells, compared with human pancreatic islets and immortalized β cell line. Cell Transplant. 27, 1548-1560. https://doi.org/10.1177/0963689718798564.

Prot, J.M., Aninat, C., Griscom, L., Razan, F., Brochot, C., Guguen Guillouzo, C., Legallais, C., Corlu, A., Leclerc, E., 2011. Improvement of HepG2/C3a cell functions in a microfluidic biochip. Biotechnol. Bioeng. 108, 1704-1715. https://doi.org/10.1002/bit.23104.

Puri, S., Folias, A.E., Hebrok, M., 2015. Plasticity and dedifferentiation within the pancreas: development, homeostasis, and disease. Cell Stem Cell. 16, 18-31. https://doi.org/10.1016/j.stem.2014.11.001.

Rogal, J., Zbinden, A., Schenke-Layland, K., Loskill, P., 2019. Stem-cell based organ-on-a chip models for diabetes research. Adv. Drug Deliv. Rev. 140, 101-128. https://doi.org/10.1016/j.addr.2018.10.010.

Sankar, K.S., Green, B.J., Crocker, A.R., Verity, J.E., Altamentova, S.M., Rocheleau, J.V., 2011. Culturing pancreatic islets in microfluidic flow enhances morphology of the associated endothelial cells. PloS One. 6, e24904. https://doi.org/10.1371/journal.pone.0024904.

Schaffer, A.E., Freude, K.K., Nelson, S.B., Sander, M., 2010. Ptf1a and Nkx6 transcription factors function as antagonistic lineage determinants in multipotent pancreatic progenitors. Dev. Cell. 18, 1022-1029. https://doi.org/10.1016/j.devcel.2010.05.015.

Scharfmann, R., Staels, W., Albagli, O., 2019. The supply chain of human pancreatic β cell lines. J. Clin. Invest. 129, 3511-3520. https://doi.org/10.1172/JCI129484.

Schulze, T., Mattern, K., Früh, E., Hecht, L., Rustenbeck, I., Dietzel, A., 2017. A 3D microfluidic perfusion system made from glass for multiparametric analysis of stimulus-secretion coupling in pancreatic islets. Biomed. Microdevices. 19, 47. https://doi.org/10.1007/s10544-017-0186-z.

Shinohara, M., Kimura, H., Montagne, K., Komori, K., Fujii, T., Sakai, Y., 2014. Combination of microwell structures and direct oxygenation enables efficient and size-regulated aggregate formation of an insulin-secreting pancreatic beta-cell line. Biotechnol. Prog. 30, 178-187. https://doi.org/10.1002/btpr.1837.

Shinohara, M., Komori, K., Fujii, T., Sakai, Y., 2017. Enhanced self-organization of size controlled hepatocytes aggregates on oxygen permeable honeycomb microwell sheets. Biomed. Phys. Eng. Express. 3, 045016. https://doi.org/10.1088/2057-1976/aa7c3d.

Southard, S.M., Kotipatruni, R.P., Rust, W.L., 2018. Generation and selection of pluripotent stem cells for robust differentiation to insulin-secreting cells capable of reversing diabetes in rodents. PloS One. 13, e0203126. https://doi.org/10.1371/journal.pone.0203126.

Takahashi, K., Tanabe, K., Ohnuki, M., Narita, M., Ichisaka, T., Tomoda, K., Yamanaka, S., 2007. Induction of pluripotent stem cells from adult human fibroblasts by defined factors. Cell. 131, 861-872. https://doi.org/10.1016/j.cell.2007.11.019.

Tao, T., Wang, Y., Chen, W., Li, Z., Su, W., Guo, Y., Deng, P., Qin, J., 2019. Engineering human islet organoids from iPSCs using an organ-on-chip platform. Lab Chip. 19, 948-958. https://doi.org/10.1039/C8LC01298A.

Wahren, J., Ekberg, K., Johansson, J., Henriksson, M., Pramanik, A., Johansson, B. L., Rigler, R., Jörnvall, H., 2000. Role of C-peptide in human physiology. Am. J. Physiol. Endocrinol. Metab. 278, E759-E768. https://doi.org/10.1152/ajpendo.2000.278.5.E759.

Watanabe, K., Ueno, M., Kamiya, D., Nishiyama, A., Matsumura, M., Wataya, T., Takahashi, J.B., Nishikawa, S., Muguruma, K., Sasai, Y., 2007. A ROCK inhibitor permits survival of dissociated human embryonic stem cells. Nat. Biotechnol. 25, 681-686. https://doi.org/10.1038/nbt1310.

Webb, G.C., Akbar, M.S., Zhao, C., Steiner, D.F., 2000. Expression profiling of pancreatic beta cells: glucose regulation of secretory and metabolic pathway genes. Proc. Nat Acad. Sci. USA, 97, 5773-5778. https://doi.org/10.1073/pnas.100126597.

Yabe, S., Fukuda, S., Takeda, F., Nashiro, K., Shimoda, M., Okochi, H., 2017. Efficient generation of functional pancreatic β-cells from human induced pluripotent stem cells. J. Diabetes. 9, 168-179. https://doi.org/10.1111/1753-0407.12400.

Young, E., Beebe, D., 2010. Fundamentals of microfluidic cell culture in controlled microenvironments. Chem. Soc. Rev. 39, 1036-1048. https://doi.org/10.1039/b909900j.

Yu, H., Alexander, C., Beebe, D., 2007. Understanding microchannel culture: parameters involved in soluble factor signaling. Lab Chip. 7, 726-30. https://doi.org/10.1039/b618793e.

Zbinden, A., Marzi, J., Schlünder, K., Probst, C., Urbanczyk, M., Black, S., Brauchle, E.M., Layland, S.L., Kraushaar, U., Duffy, G., Schenke-Layland, K., Loskill, P., 2020. Non-invasive marker-independent high content analysis of a microphysiological human pancreas-on-a-chip model. Matrix Biol. 85-86, 205-220. https://doi.org/10.1016/j.matbio.2019.06.008.

Zhu, S., Russ, H., Wang, X., Zhang, M., Ma, T., Xu, T., Tang, S., Hebrok, M., Ding, S., 2016. Human pancreatic beta-like cells converted from fibroblasts. Nat. Commun. 7, 10080. https://doi.org/10.1038/ncomms10080.

Chapter VI: Liver and pancreas co-culture model using induced pluripotent stem cells and organ-on-chip technologies

In this chapter, we present a few preliminary results of the liver-pancreas model using human induced pluripotent stem cells derived to hepatocytes and pancreatic islets-like.

Chapter VI: Liver and pancreas co-culture model using induced pluripotent stem cells and organ-on-chip technologies

6.1 Introduction

In the frame of this thesis, we have extended the rat liver pancreas model of chapter IV to a human model. For this purpose, we performed preliminary experiments of co-culture of hepatocyte like cells derived from induced pluripotent stem cells with the Cellartis pancreatic beta cells. We cannot present all the results in the manuscript because a patent application is pending regarding the liver on chip optimization. Furthermore, the COVID-19 sanitary situation stopped the experimental campaign leading to incomplete set of experiments. Nevertheless, as a general perspective of the PhD manuscript, we can introduce briefly some of the results in this short chapter VI.

The liver tissue of the human coculture model was based on the protocol of hepatocyte differentiation from hiPSC proposed by Kido et al.,[1]. In this protocol, the liver cells are differentiated in TCPS Petri dish. At the hepatic progenitor step, the cell population is sorted using the carboxypeptidase M (CPM) as a selection marker. The CPM+ cells are then plated in Petri and amplified to generate mature hepatocyte like cells. In parallel, a liver iPSC biochip technology was developed in our group by Danoy et al.,[2,3] based on a modification of the iPSC liver protocol of Si Tayeb et al.,[4]. The protocol of Danoy et al., allowed the maturation of iPSC into hepatocyte-like cells in biochips. Then, Danoy et al. extended this biochip iPSC protocol to make it compatible with the CPM+ technology. So, in our experimental setup we combined 3 different protocols: For the liver compartment (1) we used the CPM+ protocol reported by Kido et al.[1], in combination with (2) the liver iPSC biochip protocol of Danoy et al., 2019. Meanwhile, for the pancreas compartment: (3) we used the spheroids Cellartis β-cells for the pancreas-on-chip protocol reported on our chapter V.

The co-culture resulted in a liver CPM+ biochip serially connected with a pancreatic β-cells biochip. The 5 tested conditions were (i) the CPM+ liver biochip with insulin; (ii) the CPM+ liver biochip without insulin; (iii) the CPM+ liver without insulin with pancreatic beta cells (insulin producing cells); (iv) the pancreas-on-chip monoculture (as in chapter V) and (v) the CPM+ liver control (TCPS petri dish). The overall experiment length for 42 days. The dynamic co-culture started at day 35, after the specific differentiation of the liver and pancreatic β-cells. Due to patent application, no detail can be provided at this stage on those protocols and processes.

6.2 Preliminary results of liver pancreas human model

In the figure 6.1, we present the morphologies of the tissues. We observed several differences when we compared the liver configurations. The hepatocyte like cells were dense forming a multilayer tissue in the liver monoculture (Figure 6.1.B). Conversely, in liver co-culture, the tissue was less dense and monolayer like structure were observed in the biochip. The hepatic phenotypes, cuboid cells with large nucleus, were clearly detected. In both, co-culture and monoculture, we observed the pronounced hepatic phenotypes. In addition to liver phenotype, the liver monoculture led to large fibroblastic tissue along the microchannel walls, that were not observed in co-culture.

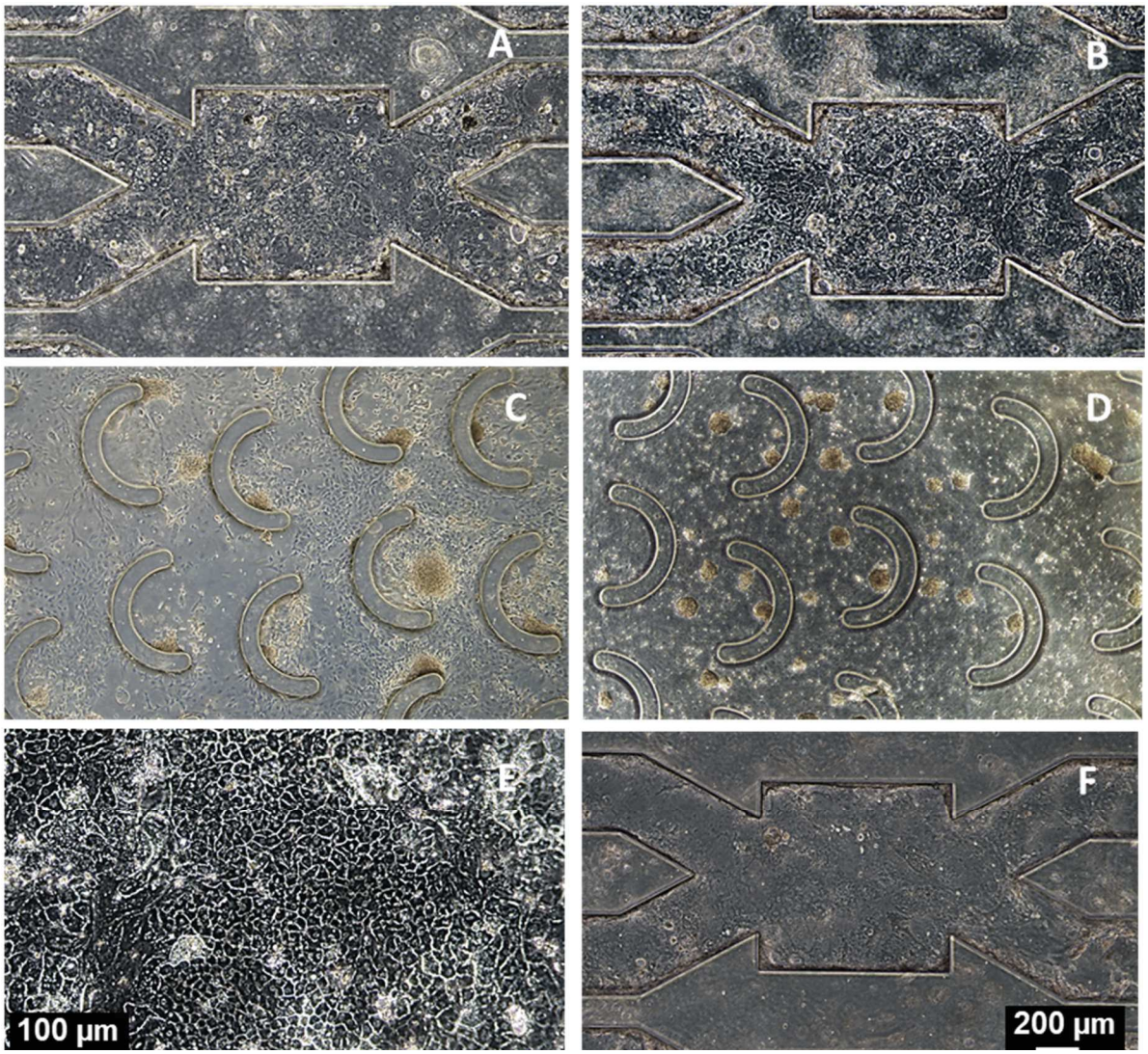

Figure 6.1: Morphology of the hepatocytes-like cells and pancreatic spheroids at the end of the experiment: (A) cells in the hepatic compartment in co-culture condition; (B) monoculture hepatocytes-like with insulin; (C) pancreatic spheroids in co-culture; (D) pancreatic spheroids in monoculture; (D) control in static of hepatocytes-like in static TCPS petri dich; ; (E) monoculture hepatocytes-like without insulin

The pancreas monoculture led to trap spheroids in a crest specific geometry. The figure 6.1 illustrate the successful dynamic culture of the spheroid at the end of the experiment. The morphology analysis also demonstrated that the co-culture condition clearly conducted to the desegregation of the pancreatic spheroids. We observed an adherent cell layer on the bottom of the pancreatic compartment of the co-culture that was not observed in the monoculture condition (figure 6.1.C). We cannot conclude if we observed a cell migration from the spheroids (and thus a destruction of the spheroids) or a cell proliferation from the spheroids. However, the spheroids shape and size of the seems to be similar in both conditions which might be indicating a cell proliferation.

On the present dataset, we could not detect any clear difference on albumin production when we compared the liver monoculture with the liver pancreas co-culture (Figure 6.2). The monoculture condition with insulin contributed to produce the highest levels of albumin in all experiments. In parallel, the monoculture without insulin and co-culture fairly led to similar results. Furthermore, we observed a significant difference between experiments 2 and 3 regarding the albumin production. The albumin was 2-fold higher in experiment 3. At the present time of the redaction of this manuscript, we did not quantify the cells number. This is critical point that can balance our discussion and conclusion considering that the morphologies clearly show a lower hepatocyte cell density in the co-culture condition. We are working on this counting as far as we have nucleus immunostaining and collect cells for protein analysis (allowing to count the total protein level). Furthermore, we need to run additional experiments to confirm the liver pancreas co-culture tendencies.

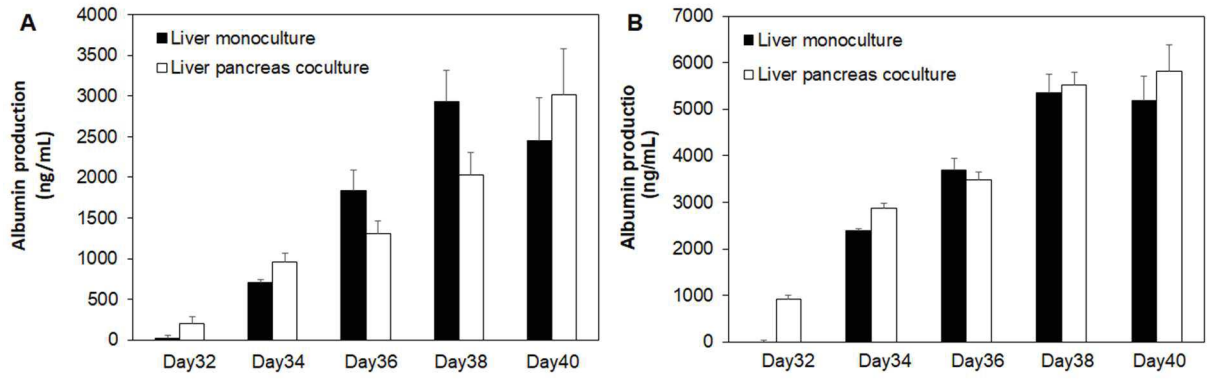

Figure 6.2 : Albumin production in ng/mL for Exp-2 and Exp-3, n = 2x4 biochips

Interestingly, in parallel, the liver CYP3A4 activity increased in co-culture condition when compared to monoculture. However, we did not detect a difference when comparing

monocultures with and without insulin (Figure 6.3.A). Then, the pancreatic C-peptide productions seemed to be increased in the co-culture when compared of the monoculture (Figure 6.3.B). The production of C-peptide reached a peak at 25 ± 10 and 49 ± 5 pmol/islet/mL in monoculture (Experiences 2 and 3 respectively) and 35 ± 10 and 192 ± 55 pmol/islet/mL in co-culture (Experiences 2 and 3 respectively). Finally, we performed immunostaining and extract the mRNA of the cells. At the time of this redaction, due to laboratory access limitation, we were not able to analyze those data.

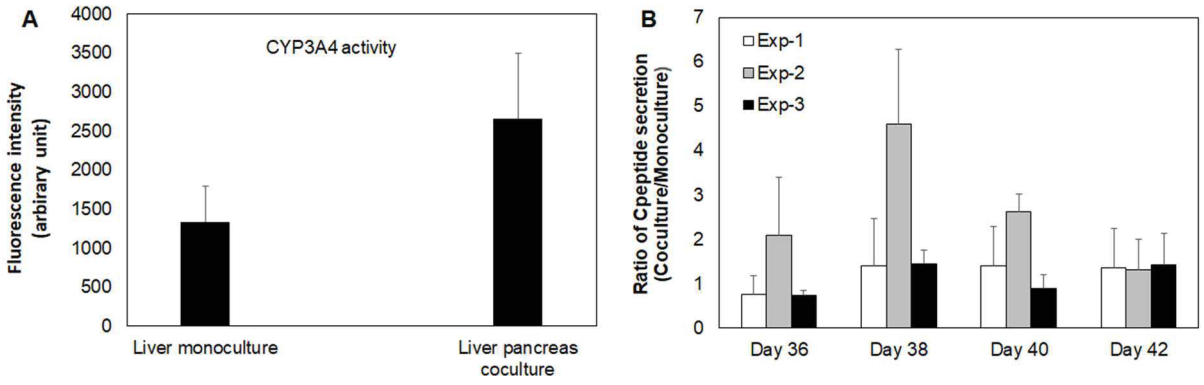

Figure 6.3 : (A) CYP3A4 activity in liver cells; (B) Ratio of C-peptide production

6.3 Conclusion

We could not finish this experimental campaign as far as at least once experimental repeat is missing. Nevertheless, those primary results demonstrated the feasibility of human co-culture models. We established a co-culture protocol based on two iPSC established protocol. However, this protocol is very long, about 42 days. The results displayed healthy tissue and functional cells. More particularly, we found a positive effect of the co-culture of pancreatic cells on CYP3A4 liver activity. In addition, the liver contributed to stimulate the C-peptide production in pancreatic spheroids. Furthermore, it is an encouraging step toward human model. We believe that those results are an encouraging step toward full human model using advanced organ on chip technology and promising cell source.

6.4 References

1. Kido T, Koui Y, Suzuki K, et al. CPM is a useful cell surface marker to isolate expandable bi-potential liver progenitor cells derived from human iPS cells. *Stem Cell Reports*. 2015;5(4):508-515. doi:10.1016/j.stemcr.2015.08.008
2. Danoy M, Bernier ML, Kimura K, et al. Optimized protocol for the hepatic differentiation

of induced pluripotent stem cells in a fluidic microenvironment. *Biotechnol Bioeng*. 2019;116(7):1762-1776. doi:10.1002/bit.26970

3. Danoy M, Poulain S, Lereau-Bernier M, et al. Characterization of liver zonation ‐ like transcriptomic patterns in <scp>HLCs</scp> derived from <scp>hiPSCs</scp> in a microfluidic biochip environment. *Biotechnol Prog*. 2020;36(5). doi:10.1002/btpr.3013
4. Si-Tayeb K, Noto FK, Nagaoka M, et al. Highly efficient generation of human hepatocyte-like cells from induced pluripotent stem cells. *Hepatology*. 2010;51(1):297-305. doi:10.1002/hep.23354

General conclusions and future perspectives

In this research work, a novel approach of co-culture has been established, based on functional coupling of pancreatic islets and hepatocytes on-a-chip. This demonstrated endocrine signaling between the pancreas and the liver presents a novel approach for drug testing and disease modeling. Microphysiological systems (MPs) have shown to be a powerful tool for cell culture that can replace conventional *in vitro* systems and eventually animal models. The achievement of the microfluidic biochip system adapted to 3D cell culture, its integration into a multi organ-on-chip system and consequent outcomes were achieved in several steps. The resulting conclusions and perspectives, for future investigations, are detailed below.

The research core was developed in a consistent part of this PhD project that was organized in tree complementary phases.

1. As a first step, after an extensive bibliographical research, we decided to tackle this subject by establishing an *in vitro* rodent model to prove its robustness before upgrading to the human model based on induced pluripotent stem cells differentiated to hepatic or pancreatic cells within a microfluidic environment. Simultaneously, it has been proven that 3D cell culture techniques recapitulate and mimic in vivo environment, we realized that to keep high functional tissues and long-term maintenance. That's why an important section of this work was devoted to the establishment of the in vitro animal model. Accordingly, as a cell source, we used primary rat hepatocytes and islets of Langerhans.
2. We have established a robust co-culture in vitro model of islets of Langerhans and hepatocytes maintaining functional responses up to 7 days in an ITS free medium. The functionality of the coupling model was demonstrated by insulin released from the rat pancreatic islets in response to a glucose stimulation and crosstalk with the liver microtissue.
3. On the other hand, we developed a series of microstructure patterns suitable for organoids and spheroids culture. We compared the trapping ability of the different biochip microstructures (microwells and inlet oriented crest) and we succeeded to reduce the islets lost in the circuit from 65% to 3%. Moreover, our system has the advantage of easy extraction of tissue without harming the cells thanks to the trapping geometry that do not relay on an extracellular matrix or a 3D hydrogel scaffold that need to be dissolved in order to harvest the cells.
4. Regarding the human induced pluripotent stem (hiPS) cells based model, we investigated the behaviors of β-cells derived from hiPSCs in various culture conditions. 2D monolayer culture generated typical β-cells profiles, as shown by C-peptide production and undetected glucagon secretion. When cultivated in 2D biochips as a monolayer, we did

not find any stable protocol making their microfluidic culture possible. When cultivated in spheroids, the cells exhibited higher heterogeneity, as seen in the appearance of α, β and δ-cell markers at the mRNA level, and glucagon positive immunostaining, in addition to the secretion of C-peptide. The spheroids were then successfully cultivated in a 3D biochip under microfluidic conditions. The established microfluidic culture contributed to increasing pancreatic maturation by improving C-peptide and insulin secretion levels. The high level GLUT2 and low level GCK in 3D static spheroids and 3D biochips, suggested modulation of glucose metabolism and transport as a potential regulator of pancreatic specification during differentiation when compared to 2D culture. We believe that our results are encouraging for the development of functional pancreas-on-chip in vitro models using the advantages of organ-on-chip technology and hiPS cells, a promising source of cells. Future studies will be oriented to explore the conclusive functional state of 3D spheroids by integrating data from proteomics, metabolomics and transcriptomics with spatial information about cell distribution from imaging techniques.

5. Finally, we hypothesized that co-culture with hepatocytes-like will improve the differentiation and function of hiPS β-cells or vice versa. Our preliminary data have shown that the coupling model seems functional when considering the CYP3A4 activity, the C-peptide and albumin secretion levels. However, an optimization of the co-culture media and some changes in the experimental setup model must be done. Specially, if we consider that most high-functioning cell types, such as human primary cells and hiPS-derived cells require highly specialized and complex media formulations. Several studies have attempted to induce β-cells differentiation from hiPS cells into a mature and functional β-cells with drug treatment, culture within a bioreactor or co-culture with other cell types. However, despite that inducing the full maturation of β-cells remains a challenge, we think that organoids and MPs are two fundamentally different yet complementary approaches with the same objective of recapitulating the complexity of human organogenesis *in vitro*. Future studies optimizing the cell/tissue proportions and co-culture duration will be helpful to determine whether the co-culture can promote the final differentiation step of hiPS cells into mature functional hepatocytes and pancreatic islets in their respective compartments.

The obtained results encourage us to exploit this model as tool for disease modeling such as type 2 diabetes (introducing modifications in the co-culture conditions) in order to unravel activated pathways and mechanisms associated with hepatic insulin resistance, steatosis and pancreatic β-cells failure. Another possibility would be the extension of the co-culture model to other organs involved in the metabolism regulation such as fat tissue or skeletal muscle. And last but not least, we need to explore our system with primary human cells or tissues for a final validation.

In order to address the automated control, high-throughput manipulation and real-time analysis of organoid culture, an important upgrade in the organ-on-chip is needed by integrating biosensors. Like many others, one of the major drawbacks of our system is the sampling procedure and the impossibility to collect real-time information about the culture conditions specially when we aim to monitor a stimulus-response test or tissue developmental process during differentiation. An embedded miniaturized biosensor in our microfluidic platform for continuous, non-invasive, and real-time monitoring of parameters of interest such like glucose or hormones metabolites concentration will allow a better assessment of the behavior and physiological functionality of the cell culture. Our project partners in Minami Laboratory at the University of Tokyo, are currently working in microfluidic system with extended - gate - type organic transistor for real - time glucose monitoring. Ideally, we could integrate different sensors in several compartments of the multi-organ MPs since each specific tissue needs to be monitored in a specific ways. For instance, we need to monitor Albumin, urea and CYP activity for the hepatic side, while it would be useful to follow the profile of insulin secretion and glucose consumption simultaneously.

Regarding the drug screening application, we explored the effect of GLP-1 and Isradipine (hypertension treatment). While the effect of GLP-1 was consistent with other studies and provides a self-explanatory interpretation of the data (in both animal and human models), the content of β-cells and insulin secretion capacity of islets of Langerhans remained unchanged under Isradipine treatment. Further studies optimizing the concentration and treatment duration are needed.

Finally, we realized how useful and helpful for the development of this project was having a global comprehension of the requirements, and the knowledge gained from the development of the bioartifical pancreas (BAPs) and bioartificial liver systems (BALs) over the last decades. Therefore, we agree that the insights from the BAL or BAP development should be considered in the organ-on-chip field despite the generation gap and lack of communication between translational research and engineering disciplines.

Annexes

CHAPTER 4

Membrane bioreactors for bio-artificial pancreas

Rachid Jellali[*,a], **Amal Essaouiba**[*,a], **Eric Leclerc**[†], **Cécile Legallais**[*]

[*]*CNRS, UMR 7338 Laboratory of Biomechanics and Bioengineering, Sorbonne Universities, Université of Technology of Compiègne, Compiègne, France* [†]*CNRS UMI 2820, Laboratory for Integrated Micro Mechatronic Systems, Institute of Industrial Science, University of Tokyo, Tokyo, Japan*

1 Introduction: The pancreas

The pancreas is a fundamental organ for coordination and regulation of body metabolism. The main functions of the pancreas are to control glucose homeostasis via endocrine hormones and produce exocrine enzymes necessary for the digestion process. Pancreatic dysfunction is responsible for many diseases including diabetes mellitus, one of the most prevalent diseases in the world. This introduction is a brief overview of the anatomy, physiology, and principal pathology associated with the pancreas.

1.1 Anatomy and physiology

The pancreas is an organ with a glandular structure located in the curve of duodenum just behind the stomach (Fig. 1). It is divided into three regions (Mahadevan, 2016): (i) the head, connected to the duodenum, is the widest and most medial region of the organ; (ii) the body is located behind the stomach; and (iii) the tapered tail region is located in the left side of the abdomen near the spleen. The vascularization of the pancreas is ensured by the anterior pancreaticoduodenal artery (head of the pancreas) and multiple branches of the splenic artery (body and tail of the pancreas). Pancreatic vein joins the splenic vein to form the hepatic portal vein together with the inferior and superior mesenteric veins.

The pancreas is a heterocrine gland involved in both exocrine and endocrine regulation. The exocrine cells of the pancreas represent more than 90% of the pancreatic tissue and are grouped in structures called acini (Fig. 1), whose function is the synthesis and secretion of enzymes implicated in the digestion process (pancreatic lipase and amylase, phospholipase, nucleases) (Jouvet & Estall, 2017). Digestive enzymes are drained by the pancreatic ductal

[a] Authors with equal contribution.

Membrane Applications in Artificial Organs and Tissue Engineering. https://doi.org/10.1016/B978-0-12-814225-7.00004-8

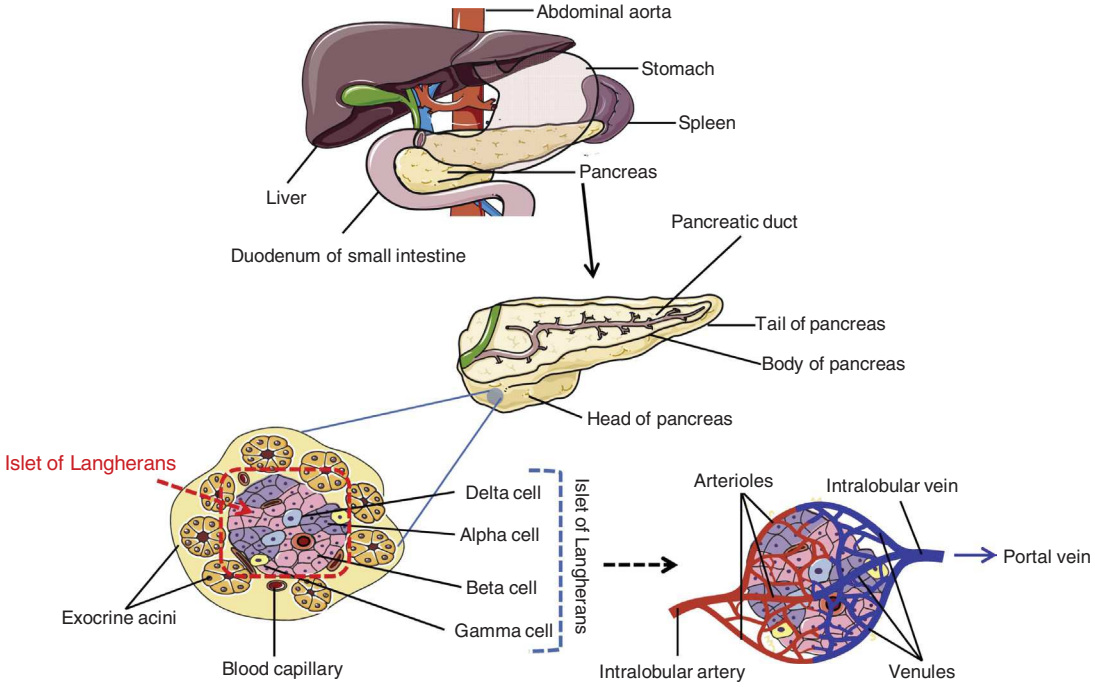

Fig. 1
Multiscale description of the systemic and local environment of islets of Langerhans.

tree into the intestine where they aid in nutrient metabolism. The functional units of the endocrine system represent approximately 2% of the pancreas (2 million cells in human adults) and are made up of pancreatic islets or islets of Langerhans. They are clusters of cells whose size varies from 20 to 500 μm, with five different cell types: α-, β-, δ-, ε-, and γ- (PP) cells (Jouvet & Estall, 2017; Kumar & Melton, 2003). The most abundant cells include the glucagon-producing α-cells and insulin-producing β-cells. The small proportion of δ-, ε-, and γ-cells secrete somatostatin, ghrelin and pancreatic polypeptides, respectively. Despite comprising only 2% of the total mass of the pancreas, the islets receive around 15% of the pancreatic blood supply, allowing their secreted hormones ready access to the circulation (Jansson et al., 2016). At the islet level, the oxygen partial pressure (PO_2) is about 40 mmHg.

1.2 Mechanisms of glycemic regulation

The control of glucose levels in the blood is carried out by the interaction of two antagonistic hormones secreted by pancreatic α and β cells. Glucagon (alpha cells) increases glucose levels in the fasting period activating the glycogenolysis and gluconeogenesis in the liver in coordination with cortisol (hormone secreted by the adrenal gland). While insulin activates the uptake and storage of glucose in the muscle, fatty tissue and most importantly the liver through glycogenesis thereby decreasing blood sugar levels in postprandial (Barrett, Barman, Boitano, & Brooks, 2015) (Fig. 2).

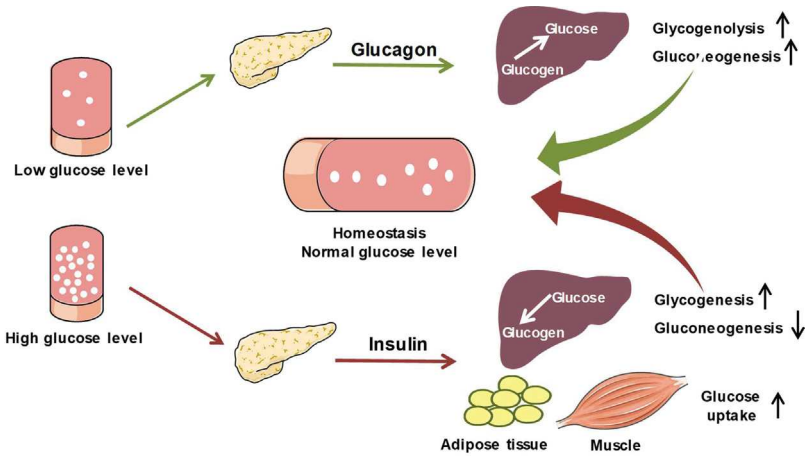

Fig. 2
Mechanisms of glycemia regulation by the pancreas and other tissues (liver, adipose tissue, muscle).

The mechanism of regulation of blood glucose begins with the stimulation of insulin secretion that intensifies when blood glucose levels increase. The beta cells of the pancreas respond in a biphasic manner to this stimulus. First there is a rapid and brief rise (in the form of a peak) of insulin release, followed by a slower but constant release of the hormone (in the form of a plateau) over time (Tortora & Derrickson, 2013).

The feedback loop that involves carbohydrates as an input signal and the synchronization of the insulin and glucagon release as an output allows the control of blood glucose and insulinemia to occur accurately and precisely (Miller, 1981).

The secretion of the two antagonist hormones is carried out in a pulsatile manner so that a simultaneous peak of insulin and glucagon would never occur. The synchronization of hormones is of great importance for the regulation of blood glucose by the liver.

1.3 Physiopathology and treatment

Diabetes mellitus is the most important dysfunction of the endocrine system of the pancreas affecting more than 425 million people worldwide, according to the International Diabetes Federation (IDF) and the World Health Organization (WHO) (IDF official web site, 2019; WHO official web site, 2019). Type I diabetes mellitus (T1DM) affects about 5%–10% of diabetes patients, mostly the young population. It is a chronic pathology occurring due to the autoimmune destruction of pancreatic beta cells. As a result, there is a disorder in blood glucose levels caused by hyperglycemia and the inability to store glucose due to the absence of insulin. It is a pathology with a complex clinical picture. The breakdown of the control mechanism of blood glucose severely affects other organs and systems on long term basis, causing blindness, kidney failure, cardiac arrest, stroke, limb amputation due to thrombosis, and even death (Amer, Mahoney, & Bryant, 2014; WHO, Global report on diabetes, 2016).

The function in need of replacement in the case of insulin dependent diabetes is thus primarily the secretion of insulin by the pancreatic islet β cells, which has four characteristics: (a) it is continuous, even in the postabsorptive state, with rapid and transient peaks during meals: (b) it undergoes automatic regulation by blood glucose levels; (c) insulin is delivered into the portal blood system; (d) the endocrine pancreas is (of course) an internal organ placed within the body.

The most widespread treatment of T1DM is the daily and scheduled administration of insulin based on previous monitoring with a glucometer (Klonoff, Ahn, & Drincic, 2017; Stephens, 2015) (Table 1). In the best cases, insulin injections, glucose levels monitoring, and a restrictive diet could successfully keep the patient safe from the risks of the extreme hyperglycemia. However, the variety of the clinical profile of the patients and the age reveals the limitations of insulin injections as a treatment. On the one hand, the production of insulin usually decreases progressively as the disease progresses, so the patient continues to produce their own insulin in small quantities. This makes it difficult to estimate the amount of exogenous insulin to be administered at each moment. On the other hand, due to the nature of the pathology, it usually manifests at an early age. This makes it difficult to control certain variables such as intake and physical exercise especially in neonates and children. In addition, to correctly apply the treatment, continuous education of the patient is required to maintain glucose in the appropriate ranges (Malik & Taplin, 2014).

Another treatment based on the same principle as insulin injections, but with some improvements is the insulin pump or also called "continuous subcutaneous therapy"

Table 1: Summary of the different treatments available for type I diabetic patients.

Treatment	Advantages	Disadvantages
Insulin injection	• Simple and relatively accessible treatment • Long-term durability in case of T1DM	• Difficult maintaining normoglycemia overnight • Requires user training • It's usually combined with a restrictive diet control
Closed-loop insulin delivery (mechanical pump)	• Ergonomic for the patient • Continuous control of blood glucose levels (overnight) • Telematic follow-up by the therapist	• Fibrosis in the catheter implant site • Slow response to sudden changes in glucose levels • Requires maintenance (battery and insulin)
Pancreas transplantation	• Durability • Full control of normoglycemia	• Quite complex surgery • Donor shortage • Requires immunosuppressants for life
Clinical islets transplantation	• Full control of normoglycemia • Minimally invasive surgery	• Still in development • Requires two donors for one receiver • Loss of functionality in the long term • Requests as transplantation immunosuppressive treatment

(Bruttomesso, Costa, & Baritussio, 2009). This approach is based on the subcutaneous delivery of insulin through a catheter connected to a peristaltic pump (Galderisi, Schlissel, & Cengiz, 2017). This allows the control of the insulinemia 24 h maintaining the basal level of glucose in the blood. The control carried out by the insulin pump mimics quite well the pattern of glucose concentration given by a healthy pancreas. However, possible infections and fibrosis at the site of catheter insertion are limiting factors of the use of the insulin pump as therapy. Despite the great advances that have been made in recent years for the development of this device (El-Khatib et al., 2017), the response time is another limiting factor in terms of abrupt changes in glucose concentration (Tauschmann & Hovorka, 2014).

Depending on the patient clinical profile of the T1DM, transplantation of the pancreas is sometimes chosen as a strategy to control glycemia. Since 1966, the success rates of transplantation of the pancreas have been increasing thanks to technical improvements in extraction, preservation and implantation. Up to now, more than 1500 pancreas transplants have been carried out according to the Collaborative Islet Transplant Registry (CITR) (Shapiro, Pokrywczynska, & Ricordi, 2016). However, it remains an invasive intervention that is usually carried out when kidney transplantation is also required. And most importantly, it involves the submission of the patient to immunosuppressants for the rest of his life.

The transplantation of islets of Langerhans is another approach that is applied to the treatment of diabetes (Chang, Lawrence, & Naziruddin, 2017; Ludwig et al., 2012, 2013; Ludwig & Ludwig, 2015). Since the 1960s, the purification of pancreatic islets and their transplantation into different animal models have been the objects of many groups of research. Pancreatic islet transplantation is a promising therapy for patients with T1DM difficult to control (Bertuzzi et al., 2018). It is a technique that provides an efficient and robust control of the homeostasis of glucose against the administration of insulin. However, islet transplantation remains controversial because it requires continuous immunosuppression that is harmful to both the graft and the patient (Nourmohammadzadeh et al., 2013).

2 The concept of bioartificial pancreas

In the above-mentioned therapeutic strategies, the objectives are to replace either the structure (transplantation) or some functions (insulin injection) to compensate organ failure. Another approach is the design of a BAP based on the two major pillars in tissue engineering: cells and scaffolds. The objectives would be to mimic as much as possible the physiology of the native organ, using the cells for the production and release of insulin, but also as "glucose sensor" and the scaffold as biocompatible environment and immunoprotection for the cells (Fig. 3).

Depending on the amount of tissue to be encapsulated, there are two major configurations of pancreatic islet immunoisolation: macroencapsulation and microencapsulation (Pandolfi, Pereira, Dufresne, & Legallais, 2017) (Fig. 4). In addition to the amount of tissue to

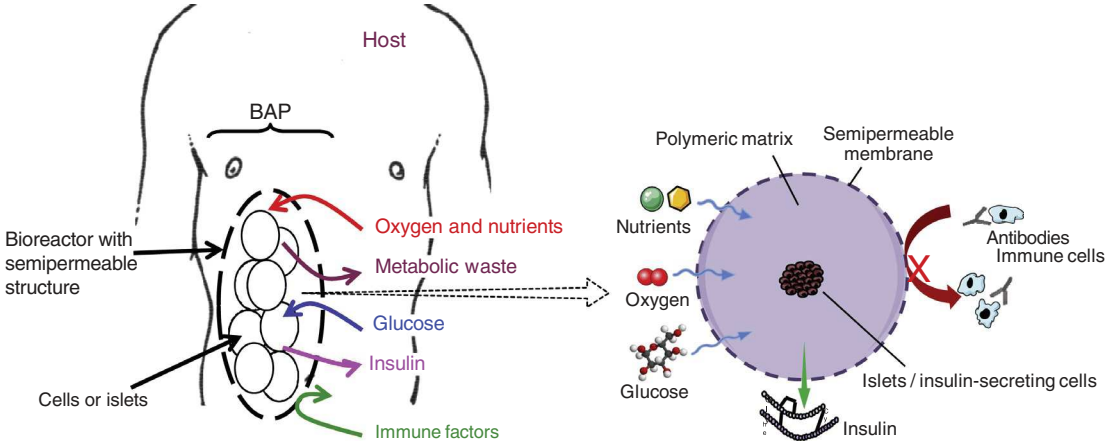

Fig. 3
Concept of implantable bioartificial pancreas.

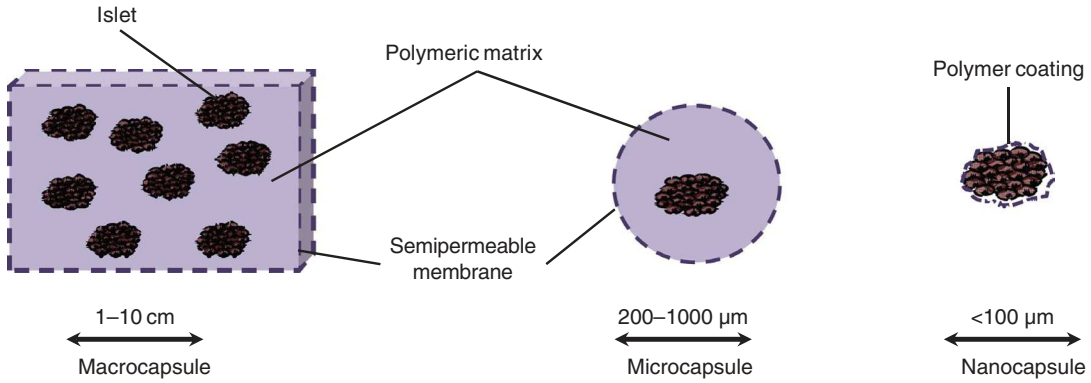

Fig. 4
Different concept of islet encapsulation, from macro to nanoscale.

be encapsulated, the content of the implant also determines the type of encapsulation implemented. It is not the same to encapsulate isolated beta cells than to encapsulate cellular aggregates or islets of Langerhans. In case the islets are directly covered by a polymer, the term of nanoencapsulation is commonly employed.

Macroencapsulation consists in the assembly of a large number of islets or cells within a selectively permeable membrane forming a macrocapsule with a dimension in the centimeter range or even larger. Depending on the site of implantation, macrocapsule-based devices are classified in two categories: intravascular and extravascular ones (Iacovacci, Ricotti, Menciassi, & Dario, 2016; Kepsutlu, Nazli, Bal, & Kizilel, 2014). Intravascular system is directly connected to the vessels of the host via an arteriovenous shunt (Iacovacci et al., 2016).

Microencapsulation is the entrapment of individual or few islets of Langerhans in a polymeric matrix (Skrzypek, Nibbelink, Karperien, van Apeldoorn, & Stamatialis, 2018). Due to optimal volume-to-surface ratio, microcapsules allow fast exchange of insulin, oxygen and nutrients. Generally, microcapsules are produced from hydrogels like alginate, chitosan, agarose, polyethylene glycol (PEG), copolymers of acrylonitrile and polyacrylates (de Vos, Hamel, & Tatarkiewicz, 2002; Skrzypek et al., 2018). The most widely used microcapsules for islet immunoisolation is the ionically cross-linked alginate system (de Vos, Faas, Strand, & Calafiore, 2006). In this process, cells are mixed within alginate solution and extruded dropwise into an aqueous calcium chloride gelation solution. The droplet entrapping islets solidify to become hydrogel beads in contact with Ca^{2+} divalent cations (Pandolfi et al., 2017). Finally, alginate beads are coated with cationic poly-amino acid (usually poly (L-lysine)) solution, which forms a semipermeable membrane around the microcapsule (de Vos et al., 2002, 2006).

To overcome the limitations associated to micro- and macroencapsulation (size, diffusion), the use of nanoscale immune-isolation layer has been developed. This strategy called nanoencapsulation allows the immunoisolation of single islet/β-cells, and the obtained devices are less than 100 μm in diameter (Iacovacci et al., 2016). Different strategies have been developed including photopolymerization of PEG and layer-by-layer deposition of polycation and polyanion (Iacovacci et al., 2016; Kepsutlu et al., 2014; O'Sullivan, Vegas, Anderson, & Weir, 2011). The reduced distance between the implanted islet and the host enhances the diffusion of oxygen, nutrients and insulin.

3 Overview of the specificities of currently developed BAP

The BAP is an implantable device formed by endocrine tissue encapsulated by a semipermeable biomaterial that provides protection against immunological agents and allowing the mass transfer of hormones, nutrients, oxygen and waste. In the process of BAP development, it is essential to know the different variables to be considered (donor, host, material and shape of the BAP, transplantation site, etc.) and how to combine them to get the optimal design.

There are various requirements depending on the components of the BAP.

1. Cell functions and number: the objective is to get the same type of response (amount of insulin/glucagon synthesized, sensitivity to glucose concentration) than from the native pancreas. Therefore, the cells have to be correctly supplied for nutrients and oxygen, and with kinetics of blood glucose concentration.
2. Immuno-isolation ensured by the material: a compromise has to be found between rapid transfer of low- and medium-molecular weight solutes (glucose, insulin) and sieving of immunoglobulins and cells such as macrophages and leukocytes (Fig. 5).
3. Biocompatible material for the cells and for the host.

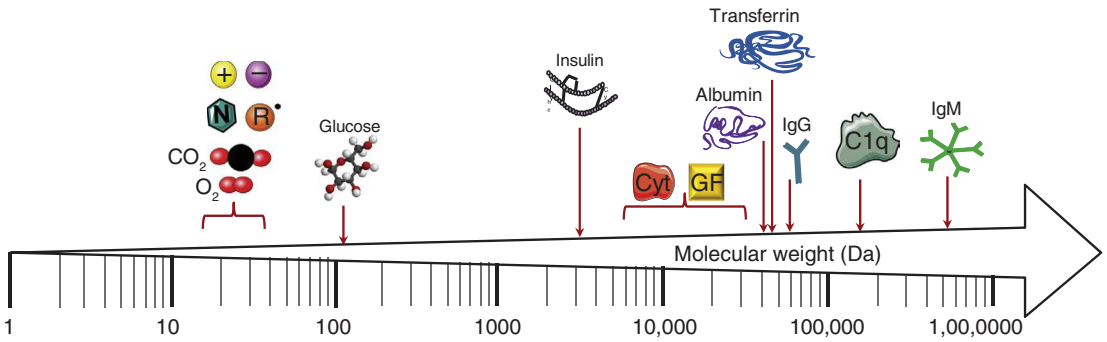

Fig. 5
Classification of the elements implicated in BAP inmuno-isolation by their molecular weight. −, anion; +, cation; *C1q*, complement component 1q; *Cyt*, cytokines; *GF*, growth factors; *N*, nitrogen metabolites; *R*, free radicals. *Adapted from Schweicher, J. (2014). Membranes to achieve immunoprotection of transplanted islets.* Frontiers in Bioscience, 19, *49–76.*

4. Adequacy of the implantation site: to mimic the physiology, blood glucose should reach easily the b-cells to stimulate if necessary insulin synthesis and secretion, insulin should be ideally released in the portal system. Minimally invasive surgery should be preferred, and the device should also be easily removable in case of failure.

3.1 Number and potential sources of pancreatic islets

Before addressing the cell type to use in a BAP, it is fundamental to answer the question of the number of cells/islets to implement. A human adult pancreas contains about a million and a half islets of Langerhans. However, as for other organs such as kidney or liver, they do not all operate simultaneously. To achieve normoglycemia in human, it is now widely considered that 15×10^3 islets equivalent (IEQ) per kilogram are needed in a BAP (Kepsutlu et al., 2014). These figures come from experiments performed either in human or in small animals. In the past, our group was interested in BAP mass transfer modeling. In a full model including glucose, insulin and O_2 transfer, we clearly outlined that O_2 was the limiting factor for BAP efficiency, and that oxygen starvation led to significant decrease in insulin release (Dulong & Legallais, 2005). In some cases, most of the implanted islets were necrosed, because their density in the implant was too high. In contrast, implementing a lower number of well oxygenated islets may lead to a better response in term of insulin release. We concluded that about 500,000 islets (i.e. 5×10^3 IEQ/kg) would be enough for human scale supply, if they maintain their functions.

Concerning primary human cells, it is reported that 2/3 of the endocrine tissue is lost in the purification stage during the pancreatic islet isolation process (Hwang et al., 2016; Ryan et al., 2001; Schweicher, 2014; Shapiro et al., 2016). Therefore, the actual availability of human donor pancreases can never fulfill the requirements for treating more than a

small fraction of patients who need islet transplantation (Kepsutlu et al., 2014). Actually, the insufficient number of human donors is the major motives for scientists to focus on exploration of other cell sources to replace the function of insulin-secreting beta cells. Table 2 summarizes the advantages and limitations of different types of cells employed up to now in BAP.

The immunoisolation provided by encapsulation within semipermeable membrane indeed enabled investigation into the use of other sources of insulin-secreting cells. In the past, the use of xenogeneic porcine islets represented an interesting alternative because the close homology between porcine and human insulin (O'Sullivan et al., 2011; Song et al., 2017; Sykes et al., 2006). Several porcine islets transplantation demonstrated efficacy (Dufrane, D'hoore, et al., 2006; Dufrane, Goebbels, & Gianello, 2010; Dufrane, Goebbels, Saliez, Guiot, & Gianello, 2006; Dufrane & Gianello, 2012). Studies by Dufrane et al. showed survival and function of encapsulated adult pig islets after implantation without immunosuppression into nonhuman primates. Diabetes was corrected up 6 months posttransplant in diabetic primates (Dufrane et al., 2010; Dufrane, van Steenberghe, et al., 2006). However, adult pig islets are expensive, fragile and difficult to maintain in culture after isolation. Alternatively, neonatal porcine islets represent an attractive source of cell for transplantation because of their ability for proliferation

Table 2: Cells' sources, pros, and cons to be used in BAP.

Cells source	Advantages	Limitations
Porcine	• Homology between porcine and human insulin • Low coast • Availability • Hypoxia tolerance	• Retroviral disease transmission • Fragile during encapsulation • Immune rejection caused by porcine proteins no identified by human system
Stem cells hESCs and hiPSCs	• Sensitiveness as good as the original pancreas • Immunological safety • Unlimited source of human insulin-producing cells	• Risk of teratoma formation • Risk of mutagenesis due to vectors used for reprogramming • Ethical preoccupation • Expansive • Reactivity to glucose
Exocrine	• Available as a by-product of islet transplantation (90% of the pancreatic tissue). • Possibility of differentiation in situ without a surgical intervention. • Full biocompatibility and immunological safety	• Limited source of cells • Difficult control of the differentiation in a specific type of endocrine pancreatic cells • Reactivity to glucose
Immortalized human pancreatic cell lines	• Unlimited sources (easily proliferate) • Low cost • Easy to maintain	• Low insulin production • Low reactivity to glucose • Risk of metastasis • Risk of massive proliferation • Need of a effective encapsulation

and differentiation, ease of isolation/purification and low cost (Nagaraju, Bottino, Wijkstrom, Trucco, & Cooper, 2015). Survival and function of encapsulated neonatal porcine islets after transplantation into human and animals were reported by , Elliott et al. (2007), Elliott, Escobar, Calafiore, et al., 2005, Elliott, Escobar, Tan, et al., 2005, Matsumoto et al. (2014), and Valdes-Gonzalez et al. (2005). Despite the encouraging results provided by encapsulated pig islets, new regulations, in Europe, prevent the use of such cells to avoid the risk of zoonosis (Hwang et al., 2016; Lima et al., 2016).

Several autologous alternatives are thus being investigated: differentiation of induced pluripotent stem cells (iPSCs) and embryonic stem cells (ESCs) into beta cells (Espes, Lau, & Carlsson, 2017; Iacovacci et al., 2016), and genetic modification of the exocrine pancreatic tissue in insulin-secreting cells (Iacovacci et al., 2016; Skrzypek et al., 2018). Some of these strategies are in advanced preclinical stages.

The differentiation of stem cells to insulin-secreting cells represents an attractive alternative to human islets. Stem cells are able to self-renew and differentiate into specialized cell types, allowing the generation of all cell types of the human body (Chhabra & Brayman, 2013). Among stem cells, ESCs and iPSCs are the most commonly studied for differentiation in pancreatic islets (Amer et al., 2014; Millman et al., 2016). The ideal source to obtain beta cells would be iPSCs since the tissue generated in vitro would be genetically identical to the pancreatic endocrine tissue of the patient. In the last years, several studies reporting insulin-secreting cells production from ESCs (Cavelti-Weder, Zumsteg, Li, & Zhou, 2017; D'Amour et al., 2006; Kirk, Hao, Lahmy, & Itkin-Ansari, 2014; Li et al., 2014; Pepper et al., 2017; Rezania et al., 2014) and iPSCs (Bruin et al., 2015; Chang, Faleo, et al., 2017; Motté et al., 2014; Robert et al., 2018) have been published. Rezania et al. reported the normalization of blood glucose levels in diabetic mice after 120 days of human embryonic stem cells (hESCs) transplantation in vivo (Rezania et al., 2012). After transplantation, the differentiation of hESCs cells was similar to human fetal pancreas development, with similar gene and protein expression profiles. Normalization of hyperglycemia in diabetic mice by hESCS, human-induced pluripotent stem cells (hiPSCs) and mouse iPSCs-derived β cells was also demonstrated by Pagliuca et al. (2014), Yabe et al. (2017), and Alipio et al. (2010), respectively. However, there are still concerns regarding the ability of β-cells generated from stem cells to regulate insulin physiological levels in response to glucose (Iacovacci et al., 2016).

Exocrine pancreatic tissue is the main part of the pancreas. This tissue, about 95% of total mass of pancreas, is discarded following each islet isolation procedure. Recently, scientists have been interested in a new approach based on reprogramming of exocrine acinar and ductal cells into insulin-secreting β-cells (Shen, Cheng, Han, Mu, & Han, 2013). Exocrine cells are close of β-cells and have similar epigenetic profiles since they arise from the same progenitor common for all pancreatic cells ($Pdx1^+$ cells) (Bonal & Herrera, 2008). Moreover, pancreatic exocrine cells are known by plasticity of their phenotype. Therefore, interconversion of exocrine cells in β-cells is easily possible (Minami et al., 2011). Reprogramming of exocrine

cells can occur through manipulation of pancreatic transcription factors (Pdx1, Ngn3, MafA, and Pax4), in combination with growth factors (betacellulin, exendin-4, and nicotinamide) (Lima et al., 2016). In vitro and in vivo generation of insulin-secreting β-cells from pancreatic exocrine cells has been widely studied and reported in literature (Lemper et al., 2015; Lima et al., 2016; Minami et al., 2011; Zhou, Brown, Kanarek, Rajagopal, & Melton, 2008). Nevertheless, further developments are needed to guarantee high efficacy and safety of β-cells derived from exocrine cells (O'Sullivan et al., 2011).

In addition to stem, exocrine and xenogenic cells, several other strategies of β cells generation were/are studied. Among these strategies, the most studied are the use of immortalized human pancreatic cell lines and the reprogramming of cells from other organs such as liver cells and gastrointestinal cells (Benthuysen, Carrano, & Sander, 2016; Cito, Pellegrini, Piemonti, & Sordi, 2018; Iacovacci et al., 2016).

3.2 Mass transfer issues in BAP and implantation site

As previously described, islets of Langerhans in a native pancreas are highly vascularized, providing the cells with glucose signal (from systemic circulation), oxygen (local PO_2) and releasing insulin directly in the portal system to reach the liver. In addition, in the situation of hyperglycemia, the flow rate can be multiplied by six to improve the response kinetics.

3.2.1 Intravascular systems combining convection and diffusion

Ideally, the BAP should be located at the same position as in the native pancreas, that is, as a shunt between arterial and venous circulation in the portal area. In such situation, both convective and diffusive bidirectional mass transfer would occur between the blood and the isolated islets.

Local mass transfer (Js) combining diffusion and convection can be described by the following equation:

$$\mathrm{Js} = \mathrm{Jf} \times \mathrm{S} \times \mathrm{Cs} + \mathrm{Ds} \times grad\left(\mathrm{Cs}\right)$$

With:

Js in $\mathrm{kg\,m^{-2}\,s^{-1}}$
Jf: local solvent convective flux ($\mathrm{m\,s^{-1}}$): $\mathrm{Jf} = \mathrm{UFR} \times \Delta\mathrm{P}$, with ΔP the local transmembrane pressure and UFR the membrane ultrafiltration rate
S: membrane sieving coefficient for the solute of interest
Cs ($\mathrm{kg\,m^{-3}}$): solute concentration in the compartment from which convection process is issued
Ds ($\mathrm{m\,s^{-1}}$): diffusive coefficient of the solute between both compartments (NB: this coefficient takes into account resistance in the fluids but also across the scaffold/membrane)
Grad (Cs): concentration gradient between compartments.

Design and limits of perfusion chambers

The Fig. 6A illustrates in a simple way the exchanges that can take place between the host and the islets isolated in a perfusion chamber, and the associated governing factors. Such chambers, with various designs, have been investigated since the mid-1970s employing either flat or hollow fiber membrane, inspired from artificial kidney devices (Chick et al., 1975; Reach & Jaffrin, 1990.; Scharp, Mason, & Sparks, 1984; Sun, Parisius, Healy, Vacek, & Macmorine, 1977).

Based on the kinetic modeling of glucose and insulin transfer through the porous structure, the group of Reach designed a system optimizing convective fluxes across the membrane, and yielded excellent kinetics in vitro (Reach, Jaffrin, & Desjeux, 1984) and in vivo in rats (Reach et al., 1986) and in dogs (Lepeintre et al., 1990). The correction of hyperglycaemia in diabetic rats with this system was demonstrated over a few hours (Reach & Jaffrin, 1987). However, the system was unable to avoid blood clotting inside the fiber. Another major effort in this field was made by the group working with Chick, who used a radically opposite approach. They focused on the hemocompatibility of the system, and reported the successful graft of a vascular device in dogs over several months in the absence of any heparinization of the animals, which only received aspirin (Monaco et al., 1991; Sullivan et al., 1991). Hyperglycemia was corrected, but the authors recognize that improvements in the kinetics of insulin release by this device were still required. Last results showed that a device seeded with xenogeneic porcine islets implanted into pancreatectomized dogs allowed to reduce exogenous insulin requirement for up to 9 months (Maki et al., 1996). This work led to an FDA authorization to initiate clinical studies. During one of the last preclinical transplants, the device failed leading to the death of the animals and the program was cancelled.

A similar system was proposed by Calafiore et al. who implanted microencapsulated islets inside the wall of a Dacron-based prosthesis connected to an arterial bypass. Plasma crossed the Dacron meshes and perfused the islets, which were immunoprotected by the membrane of the microcapsules, and which released insulin into the bloodstream. This system was investigated in a small number of dogs (Calafiore et al., 1992) and in two diabetic patients (Calafiore, 1992).

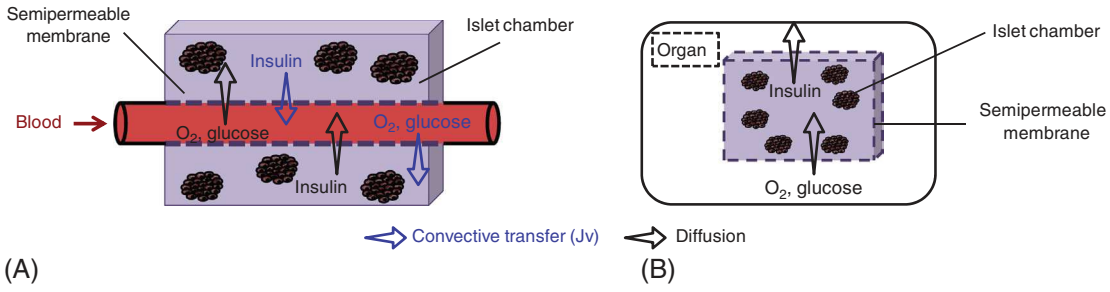

Fig. 6
Schematic representation of intravascular BAP (A) and diffusion chamber (B).

It is obvious that the development of these systems was hindered by the need for vascular access and by its thrombotic risk: indefinite prevention of clotting represents a formidable challenge. This may be one reason why the intravenous route for insulin delivery by implantable pumps has been almost abandoned in the late 1990s. More recently, Prochorov et al. revisited the concept using an intravascular device that contains around 6000 IEQ/kg isolated from fetal rabbit (Prochorov, Tretjak, Goranov, Glinnik, & Goltsev, 2008). Nineteen patients with T1DM received a nylon microporous device into the arteria profunda femoris (APF) using autovenous angioplastics (Prochorov et al., 2008). After 18 months, the patients showed no complications related to the transplantation. Although insulin secreted was not enough to reestablish normoglycemia, it helps to reduce the insulin dose injected per day and protect against episodes of hyperglycemia or hypoglycemia.

Direct perfusion of encapsulated islets implanted in vascularized organs

This approach is inspired from the first transplantation of pancreatic islets into the portal vein of the liver which had been carried out successfully in the 1990s (Scharp et al., 1990). Choosing the liver as a site of implantation of the BAP is driven by physiology, since liver is the first organ through which the hormones secreted by the pancreas pass. In addition, liver is a major site for glucose storage (glycogenesis) and release (gluconeogenesis). Finally, thanks to the last advances in minimally invasive surgery, BAP implantation could be carried out easily by percutaneous transhepatic portal embolization technique (Goss et al., 2002; Ryan et al., 2001; Scharp et al., 1991). This site required to deploy microencapsulation of the islets, due to the size of the vessels. To overcome mass transfer limitations leading to cell necrosis, several groups even attempted to reduce the thickness of the encapsulating material by surface treatment of the islets directly instead of creating a continuous barrier around them (antibodies, heparin, cells, etc.) (Arifin, Valdeig, Anders, Bulte, & Weiss, 2016; Cabric et al., 2007; Giraldo et al., 2017; Lau, Vasylovska, Kozlova, & Carlsson, 2015; Teramura & Iwata, 2010) or by using new improved biomaterials (Mooranian, Negrulj, Arfuso, & Al-Salami, 2016; Teramura & Iwata, 2011, 2009), leading to so-called nano-encapsulation.

The coating or superficial treatment of the islets presents some very promising results after its implantation in rodents. The superficial treatment significantly reduces the size of the implant, allowing its insertion in highly vascularized organs as well as increasing postoperative survival up to 78% (Fotino, Fotino, & Pileggi, 2015; Teramura & Iwata, 2010, 2009; Teramura, Oommen, Olerud, Hilborn, & Nilsson, 2013; Tomei et al., 2014). But despite the good glycemic control obtained in diabetic subjects, the long-term stability of this encapsulation technique is quite questionable (Arifin et al., 2016). The deterioration of the protective layer exposes the islets to the attack of the immune system (Giraldo et al., 2017).

However, the liver as an implantation site presents some drawbacks. First, the space available is rather small for the size of the graft; it is necessary to consider that the microencapsulated islets in spheres of material containing one or two islets have a diameter of 400 μm each one.

Secondly, microspheres hosting pancreatic islets generate problems of embolization and thrombosis of the small blood vessels around the implantation site induced by the instant blood-mediated inflammatory responses (IBMIR). The third drawback of the intraportal implantation is the partial pressure of oxygen to which the pancreatic islets will be exposed (Zhu et al., 2018). The partial pressure of oxygen in the liver portal system is considerably lower than in the pancreas (5–10 against 40 mmHg) (Carlsson, Palm, Andersson, & Liss, 2001; Olsson, Olerud, Pettersson, & Carlsson, 2011; Zhu et al., 2018): the islets are permanently in hypoxia, which affect significantly their viability. Usually, a large amount of IEQ islet per kilogram is needed for the pancreatic islets transplantation, considering that half of them die in a few hours after the intervention (Shapiro et al., 2016).

At first sight, the spleen could be also a good candidate as a BAP implantation site. It is a very vascularized organ with similar characteristics to the portal vein without the risk of hypertension induced after intraportal transplantation. The limited number of publications about intrasplenic transplantation in rodents and dogs shows that it is safe and feasible as a procedure. However, there are not enough studies to corroborate the suitability of the site for the BAP. The lake of studies is due to the small space available to place the majority of the devices, the risk of hemorrhage during surgery, the concentration of the immune system cells that could activate easily the IBMIR and the difficulty to remove the graft in case of failure (Aoki et al., 2005; Gores & Sutherland, 1993; Itoh, Nishinakamura, Kumano, Takahashi, & Kodama, 2017).

3.2.2 Diffusion-based extravascular systems

If perfusion cannot be considered, the alternative option is to enhance/promote diffusion, since the substances to exchange present relatively low molecular weight. In this case, the limiting parameter is the diffusion capacity of the solute, which is mostly governed by the diffusivity within the scaffold (Fig. 6B). Mass transfer can thus be enhanced either by increasing the porosity of the structure, or by reducing the diffusion length. The diffusion length can be defined as the mean distance between islets and surrounding blood: it can thus be decreased either by decreasing the scaffold/device thickness, or by promoting neovascularization of the implant.

We will see in the following subchapter that these different strategies have been investigated in various implantation sites.

Omental pouch and intraperitoneal transplantation

Intraperitoneal transplantation is the most common site for the BAP in the clinical setting (Basta et al., 2011; Calafiore et al., 2006; Jacobs-Tulleneers-Thevissen et al., 2013; Soon-Shiong et al., 1994; Tuch et al., 2009). One major advantage is the ease and safety of implantation through minimally invasive surgery and accessibility to the graft. It is an ideal choice for macroencapsulation systems due to the space available for the placement of the

device. It benefits from appropriate environment considering that the encapsulated cells are in contact with the surrounding fluids allowing the exchange of insulin and nutrients.

Takeuchi and his group succeeded in restoring blood glucose level of diabetic rodents by the transplantation of different hydrogel-based microfibers (Onoe et al., 2013; Ozawa, Okitsu, & Takeuchi, 2017; Ozawa, Sawayama, & Takeuchi, 2017; Sugimoto et al., 2011). Hollow fiber devices have been explored since early in the 1980s. They give a good responsiveness to changes in glucose blood levels (Jun et al., 2013). However, they had some drawbacks such the little amount of tissue that could be encapsulated in a fiber, requesting to consider significant lengths to be implanted (Lacy, Hegre, Gerasimidi-Vazeou, Gentile, & Dionne, 1991). Takeuchi's group proposed an innovative technique based on microtechnology to produce fibers with small diameters without compromising the viability of the tissue (Ozawa, Sawayama, & Takeuchi, 2017).

Alginate beads as a microencapsulated device seems to be more suitable device for intraperitoneal transplantation than macrodevices in terms of long-term viability and performance (Elliott et al., 2007; Elliott, Escobar, Calafiore, et al., 2005; Elliott, Escobar, Tan, et al., 2005; Matsumoto, Abalovich, Wechsler, Wynyard, & Elliott, 2016; Matsumoto et al., 2014; Ryan et al., 2001; Valdes-Gonzalez et al., 2005). However, microbeads injected in the peritoneal cavity move from their original implantation site and end up in the lower part of the pelvis due to the upright position adopted by human and nonhuman primates (Dufrane, Goebbels, et al., 2006; Jacobs-Tulleneers-Thevissen et al., 2013; Lanza, Beyer, Staruk, & Chick, 1993; Omer et al., 2003; Sun, Ma, Zhou, Vacek, & Sun, 1996; U.S. National Library of Medicine, ClinicalTrials.gov: NCT01739829, n.d.; Vegas et al., 2016).

The peritoneal cavity has also certain drawbacks that do not fully meet to the requirements of the BAP. On the one hand, due to the anatomy and physiology, it has small or null revascularization capacity around the implant, which hinders the exchange of oxygen and nutrients and submits the encapsulated islets to hypoxia. On the other hand, not being in direct contact with the bloodstream limits the ability of the implanted device to respond to changes in glucose concentration is slow and delayed, which subjects the body constantly to hypoglycemia or hyperglycemia.

To mitigate the hypoxia, polydimethylsiloxane (PDMS)-based materials with high oxygen permeability have been used for the graft encapsulation (Coronel, Geusz, & Stabler, 2017; McQuilling & Opara, 2017; Pedraza, Coronel, Fraker, Ricordi, & Stabler, 2012). But the most representative device with an effective mechanism to improve the oxygen supply for islets survival is the β-air (Barkai et al., 2013; Ludwig et al., 2012, 2013; Neufeld et al., 2013) or its new version beta-O_2 (Ludwig et al., 2017). β-Air is a disk diffusion chamber where the islets are loaded in an alginate-based core and a polytetrafluoroethylene (PTFE)-based semipermeable membrane. But the most important characteristic is the central oxygen module connected with the outside of the host body that provides more O_2 than the blood transporters.

To improve the neovascularization of the graft, devices in development like Sernova cell pouch (Kriz et al., 2012; U.S. National Library of Medicine, ClinicalTrials.gov: NCT01652911, n.d.) and Viacyte (U.S. National Library of Medicine, ClinicalTrials.gov: NCT02239354, n.d.) have made interesting progresses in recent years. Both devices are currently in phases I or II of the clinical study. Sernova cell pouch has shown that omental transplantation with a subcutaneous access point (for the subsequent replacement of the islets) can induce a good neovascularization of the device thanks to the close position of the portal vein and the microenvironment that provides the great omentum. The omental pouch can be stimulated by neoangiogenic factors to create new blood vessels in a short time. A total of 70% of the rodents involved in Kriz et al. study have shown long-term normoglycemia (Kriz et al., 2012). Several studies corroborated the suitability of the omentum as a site for the transplantation of encapsulated pancreatic islets (Harrington, Williams, Rawal, Ramachandran, & Stehno-Bittel, 2017; Opara, Mirmalek-Sani, Khanna, Moya, & Brey, 2010; Pareta et al., 2014).

Kidney capsule

The renal subcapsular site is the most widely used for islet transplantation in experimental studies, especially in rodents. Islet transplantation into the kidney is easy and has been reported to restore normoglycemia (Zhu et al., 2018). Kidney subcapsular space offers good vascular network and desirable growth conditions for islets (Kepsutlu et al., 2014). Previous studies reported that mice and human islets transplanted in kidney subcapsular present better morphology and function, compared with islets implanted in liver, lung and spleen of mice (Hayek & Beattie, 1997; Mellgren, Schnell Landström, Petersson, & Andersson, 1986). In comparative study between intraportal and kidney subcapsular transplantation in mice, Sakata et al. demonstrated that 200 islets yielded normoglycemia in renal subcapsular grafts, while minimum 800 islets are required for normoglycemia with intraportal transplantation (Sakata et al., 2009).

Transplantations of encapsulated islets with different shapes into kidney subcapsular space were also studied and have shown their ability to correct glycemia. Dufrane et al. investigated transplantation of pig islets microencapsulated with alginates into Kidney subcapsular space of monkey. The results demonstrated the functionality of alginate microcapsules and the absence of capsule fibrosis (Dufrane, Goebbels, et al., 2006). In other study, the same group has shown that alginate microcapsules transplanted under kidney capsule of rat demonstrate better biocompatibility than capsules transplanted in the peritoneum. In addition, due to restricted mobility of the grafts, alginate microcapsules integrity was preserved to a greater extent in the kidney, compared to peritoneal cavity. Rat islet cells encapsulated within alginate microfibers and mice islets protected by PEGylation were also transplanted in kidney subcapsular of mice. Islets into alginate microfibers normalized blood glucose concentrations for 2 weeks in diabetic mice (Onoe et al., 2013). Concerning PEGylated islets, the transplanted diabetic mice exhibited long term normoglycemia (>100 days) (Giraldo et al., 2017).

Despite the promising results observed in animal experiments, clinical transplantation into renal subcapsular would be difficult given the limited space within this site. It is impossible to implant devices with the islets number necessary to correct human glycemia. In addition, renal cortex has an oxygen tension of 15 mmHg, which represents a hypoxic environment for islets (the oxygen partial pressure in pancreas is about 40 mmHg).

Subcutaneous tissues

The first clinical trial of subcutaneous transplantation of a BAP has been carried out by Scharp et al. (1994). The islets has been encapsulated by semipermeable membrane in the form of hollow fiber (Scharp et al., 1994). In an attempt to verify the biocompatibility and survival of human pancreatic islets, the results were quite promising. Although not surprisingly, the response time to the stimulus of insulin secretion was slow.

Subcutaneous transplantation is usually carried out for the macroencapsulated devices in the form of hollow fiber, planar or when an external oxygenation mechanism is integrated, like in the β-air device (Barkai et al., 2013; Ludwig et al., 2012, 2013, 2017; Neufeld et al., 2013). The advantages of the subcutaneous transplantation are the easy access and monitoring of the graft, the good biocompatibility and the high viability of the islets in the postoperative period (Pepper et al., 2015). However, the difficulty of neovascularization of the macrodevices and the low partial pressure of oxygen remain the major drawbacks in the subcutaneous transplantation.

The most representative device of subcutaneous transplantation is the TheraCyte System or its new generations Viacyte and Encaptra (Robert et al., 2018). The first was initiated by Baxter Healthcare in the late 1990s as a planar device of two composite membranes sealed at all sides with a loading port or ports (Cañibano-Hernández, Sáenz del Burgo, Espona-Noguera, Ciriza, & Pedraz, 2018). The outside of the device is designed for strength and to encourage host tissue to incorporate into its outer portions. The other sections are a Teflon-based membrane (PTFE) to encourage capillary ingrowth and a hydrogel semipermeable membrane (alginate based) for allograft immune protection. TheraCyte has evolved in parallel with the safety level of experiments, from rodents to large animals implementing different cell sources including human cells (Bruin et al., 2013; Elliott et al., 2007; Kirk et al., 2014; Kumagai-Braesch et al., 2013; Motté et al., 2014).The latest innovation provided by the manufacturers of Viacyte is the device-less character in its new trials thanks to the implemented prevascularization technique whose objective is the preparation of a suitable microenvironment for grafting before the cells implantation to improve the viability and the sensibility of the graft (Kroon et al., 2008; Pepper et al., 2015, 2017).

Another original approach has been described by Farina et al. They implemented a prevascularized polylactic acid (PLA) scaffold printed in 3D (Farina et al., 2017). The porous biomaterial was tested in nude mice with human pancreatic islets. The islets were injected into the device 4 weeks after its transplantation. The angiogenesis of the islets was

demonstrated, but it was necessary a second injection of islets to get the same amount of insulin secreted in the positive because of the slow neovascularization.

Subcutaneous transplantation remains controversial regardless the problem of angiogenesis and the mechanical requirements of the BAP. The superficial location of a graft so sensitive and so important for the control of metabolism can suffer irreversible damage due to temperature variations or physical trauma (Zhu et al., 2018).

4 Porous scaffolds—Membranes

Different materials have been employed as "membrane" structure. In intravascular devices, islets are encapsulated within hollow semipermeable tubes or fibers made of polymeric materials such as polyacrylonitrile-polyvinylchloride copolymer, polyethylene-vinyl alcohol, polycarbonate and nylon (de Vos et al., 2002; Skrzypek et al., 2018; Song & Roy, 2016). In extravascular devices, two main geometries are used: tubular and planar devices. Various polymeric or inorganic biomaterials have been investigated. However, polymeric materials are the most commonly used. These include alginate, 2-hydroxy-ethyl methacrylate (HEMA), nitro-cellulose acetate, acrylonitrile, sodium-methallylsulfonate, and PTFE (de Vos et al., 2002).

Micro or macroencapsulation using alginate as basic material is probably the best response to biocompatibility since alginate is an inert polysaccharide. However, as material from natural origin, it may contain impurities promoting fibrosis. Alginate, when jellified with calcium or other divalent cations, is also not very stable over time and might lose its polymeric state. Therefore, crosslinking agents or additional layers have been added, changing the overall mass transfer and interactions with the host tissue (Basta et al., 2011; Calafiore et al., 2006; Jacobs-Tulleneers-Thevissen et al., 2013; Soon-Shiong et al., 1994; Tuch et al., 2009; Veiseh et al., 2015). Strand et al. reviewed the progress that have been made in alginate encapsulated pancreatic islets (Strand, Coron, & Skjak-Braek, 2017). The lack of long-term trials and cohort studies plus the fibrosis of the alginate-based capsules are the most important drawbacks to overcome.

According to the BAP requirements, all the scaffolds/membranes entrapping the insulin-secreting cells or the islets are designed with the same objectives in term of sieving: allow the exchange of oxygen, nutrients, insulin and waste products and prevent immune response from the host (Fotino et al., 2015).

If this second point is fulfilled by the membrane-based devices, there is no need for immunosuppressive therapy after the implantation. Describing in detail the rejection process of a graft and the factors involved is far beyond the scope of this review. Briefly, this immune response, in the case of type I diabetic patients, can be of two different types: (i) allogenic or xenogenic response of the host to the transplanted tissue, leading to the activation of the innate immune system due the detection of foreign cells by the host; (ii) auto-immunity

(following the same mechanisms than those inducing the pathology in the native pancreas (Scharp & Marchetti, 2014). The first response is mainly supported by cells (lymphocytes B and T) but can also be mediated by immunoglobulins.

As indicated in Table 3, most of the synthetic polymer-based membranes/scaffolds present pore size average 0.2–0.4 μm (Colton, 1995; Schweicher, 2014), which is a sieve for cells only and not immunoglobulins. So far, immune rejection seems to be effective on relatively short-term basis. In these cases, the membrane demonstrated a very high porosity, and the diffusive transport is not hindered. Only the thickness of the device and the seeding density of the islets/cells influenced the mass transfer. In such case, Dulong and Legallais (2007) demonstrated that a too high density may lead to islet necrosis in case of implantation in poorly oxygenated sites.

Besides the sieving effect, in most of the case, one has to consider that the membrane is in contact with the host tissues. One major problem in biocompatibility for implanted device is the development of a fibrous and inert structure around the device. It represents an additional resistance to mass transfer and increases the risk of islets' necrosis due to oxygen starvation. A way to circumvent this issue would be to use materials that can promote neovascularization.

5 Conclusions and future trends

Pancreatic islet transplantation can successfully control glucose levels and has been validated as a treatment for type 1 diabetes on short periods. The development of BAP that consists of islets encapsulation within semipermeable membrane is considered as a promising strategy to overcome some obstacles of classical islet transplantation. Despite the significant progress in the laboratory, clinical applications of BAP are few. To increase the impact of the BAP translation from the bench to the bed side, it appears necessary to combine the progress made in different disciplines such as nanotechnology, biomaterials, immunology, and tissue engineering.

Hypoxia adversely affects the functionality of encapsulated islets and represents a major limitation in the development of efficient BAP devices. Limited oxygen supply causes apoptosis and reduces the capacity of islets to secrete insulin (Barkai et al., 2013). In the last years, different strategies including prevascularization and in situ oxygen supply have been investigated to improve encapsulated islet oxygenation. The combination of conformal coating and extravascular microencapsulation has shown some promising results. Other studies reported the use of proangiogenic factors (vascular endothelial growth factor (VEGF)) to induce BAP prevascularization (Pileggi et al., 2006; Trivedi, Steil, Colton, Bonner-Weir, & Weir, 2000). Several researchers are working on the co-encapsulation of insulin-secreting cells with another cell type in order to improve viability and stimulate graft neovascularization without compromising immunological safety (Valdes-Gonzalez et al.,

Table 3: In vivo studies of some bioartificial pancreas in development.

Encapsulation	Device (category)	Shape	Materials	Pore size	Cells source (quantity)	Transplantation site	Recipient	Outcomes	Ref
Macroencapsulation	Macrochamber β-Air (extravascular)	Disk diffusion chamber	PTFE, alginate	0.2 µm	Rat (2500 IEQ)	Interperitoneal	Rat	Normoglycemia and hypervascularization around the disk after 3 months	Ludwig et al. (2012)
Macroencapsulation	β-Air (extravascular)	Disk diffusion chamber	PTFE, alginate	0.2 µm	Rat (62,890 IEQ)	Interperitoneal	Pig	Normoglycemia for 3 months	Neufeld et al. (2013)
Macroencapsulation	β-Air (extravascular)	Disk diffusion chamber	PTFE, alginate	0.4 µm	Rat (1092 IEQ)	Interperitoneal	Rat	Normoglycemia for 6 months	Barkai et al. (2013)
Macroencapsulation	β-Air (extravascular)	Disk diffusion chamber	PTFE, alginate	0.4 µm	Human (2100 IEQ/kg)	Interperitoneal	Human	Reduction of insulin requirement for 10 months	Ludwig et al. (2013)
Macroencapsulation	Beta O_2 β-Air (extravascular)	Disk diffusion chamber	PTFE, alginate	0.4 µm	Pig (~20,000 IEQ/kg)	Interperitoneal	Monkey	Reduction of insulin requirement for 6 months	Ludwig et al. (2017)
Macroencapsulation	Islets sheet (extravascular)	Planar	Alginate	50–75 µm	Dog (75,000 IEQ)	Interperitoneal	Dog	Fibrotic reaction and Normoglycemia for 84 days	Storrs, Dorian, King, Lakey, and Rilo (2001)
Macroencapsulation	TheraCyte (extravascular)	Planar	PTFE, alginate	0.4 µm	Human ($1.5–3 \times 10^5$ cells/µL × 20 µL)	Subcutaneous	Mice	Ameliorate diabetes in mice for up to 150 days	Kirk et al. (2014)
Macroencapsulation	TheraCyte (extravascular)	Planar	PTFE, alginate	0.4 µm	Rat (1000 islets)	Subcutaneous	Rat	Slow insulin response to changes in blood glucose level after 6 months	Kumagai-Braesch et al. (2013)
Macroencapsulation	TheraCyte (extravascular)	Planar	PTFE, alginate	0.4 µm	Human (4×10^6 cells)	Subcutaneous	Mice	Macroencapsulation of hESC induce their differentiation into insulin-producing cells after 20–30 weeks	Motté et al. (2014)
Macroencapsulation	Viacyte vs Encaptra (extravascular)	Planar	PTFE, alginate	0.4 µm	Human (4×10^6 cells)	Subcutaneous	Mice	Differentiation of hESC into insulin-producing cells; 50 weeks	Robert et al. (2018)

Macroencapsulation	TheraCyte (extravascular)	Planar	PTFE, alginate	0.4 µm	Human (5×10^6 cells)	Kidney capsule, subcutaneous	Mice	Effective differentiation of hESC into insulin producing cells	Bruin et al. (2013)
Macroencapsulation	Viacyte (extravascular)	Device-less Cells transplantation into a retrievable prevascularized subcutaneous site	Gelfoam/ Matrigel	/	Human ($0.5–1\times10^7$ cells or 3000–5000 islets)	Kidney capsule, subcutaneous	Mice	Evidence of insulin production by hESC for up to but not full normoglycemia 3 months	Kroon et al. (2008)
Macroencapsulation	Viacyte (extravascular)	Device-less Cells transplantation into a retrievable prevascularized subcutaneous site	/	/	Human ($0.5–1.0\times10^7$ cells of PECs or 1000 IEQ)	Subcutaneous	Mice	Mostly normoglycemic mice up to 20 weeks	Pepper et al. (2017)
Macroencapsulation	Diffusion chamber (intravascular)	Flat nucleopore membrane	Polycarbonate	0.22 µm	Rat	Carotid arteries	Dog	Thrombosis and failure	Scharp et al. (1984)
Macroencapsulation	Cylinder-shap (intravascular)	Fiber	Nylon	1–2 µm	Rabbit (>6000 IEQ)	Arteria profunda femoris (APF)	Human	2 years without immune rejection with a considerable decrease of insulin demand 60%–65%	Prochorov et al. (2008)
Macroencapsulation	Biohybrid© (intravascular)	Hollow fiber	PTFE	Permeability of 50 kDa	Dog ($1–2\times10^5$ islets)	External iliac artery and vein	Dog	Control of hyperglycemia for up to 5 months	Sullivan et al. (1991)
Macroencapsulation	Sernova's Cell Pouch System (extravascular)	Tubular	/	/	Rat (10,000 IEQ)	Intraperitoneal	Rat	Normoglycemia in 70% of the cases for 120 days	Kriz et al. (2012)
Microencapsulation	Microfiber (extravascular)	Fiber	CAC	/	Rat (1200 IEQ)	Intraperitoneal	Mice	Normoglycemia for up to 2 months	Jun et al. (2014)
Microencapsulation	Microfiber (extravascular)	Fiber	Alginate-agarose IPN hydrogel	/	Rat/mice (0.6×10^6 cells)	Kidney	Mice	Normoglycemia for up to 13 days	Onoe et al. (2013)
Microencapsulation	/ (extravascular)	Beads	Alginate + TMTD	1–3 µm	Human /	Intraperitoneal	Mice	174 days	Vegas et al. (2016)

Continued

Table 3 In vivo studies of some bioartificial pancreas in development.—cont'd

Encapsulation	Device (category)	Shape	Materials	Pore size	Cells source (quantity)	Transplantation site	Recipient	Outcomes	Ref
Microencapsulation	/ (extravascular)	Beads	Alginate	/	Human (2×10^6 cells)	Intraperitoneal	Mice	Effective correction of blood glucose concentration for 3 months	Jacobs-Tulleneers-Thevissen et al. (2013)
Microencapsulation	Diabecell (extravascular)	Beads	Alginatepoly-L-ornithine-alginate	/	Pig (10,000 and 20,000 IEQ)	Peritoneal	Human	The most recent clinical trial was for 600 days that shows the safety and efficiency of xenotransplantation	Matsumoto et al. (2014, 2016), Elliott et al. (2007)
Microencapsulation	/ (extravascular)	Beads	Alginate	/	Pig /	Kidney, Intraperitoneal	Monkey	180 days	Dufrane, D'hoore, et al. (2006), Dufrane, van Steenberghe, et al. (2006)
Nanoencapsulation	/ (extravascular)	Islets coating	PEG combined with LFA-1	/	Mice (700–800 IEQ)	Kidney	Mice	Degradation of the coating after 100 days	Giraldo et al. (2017)

CAC, collagen-alginate composite; *IEQ*, islets equivalent; *IPN*, interpenetrating networks; *kDa*, kilodalton; *LFA-1*, lymphocyte function-associated antigen-1; *PECs*, pancreatic endoderm cells; *PEG*, polyethylene glycol; *PTFE*, polytetrafluoroethylene; *TMTD*, triazole-thiomorpholine dioxide.

2005; Véritер et al., 2014). Johansson et al. provided evidence that the coculture of MSCs and endothelial cells with human islets in vitro before transplantation initiated the formation of vessel-like structures that may promote further neovascularization (Johansson et al., 2008). In other approach, Barkai et al. developed a device that can be refueled with oxygen via subdermally implanted access ports. The transplantation of this device normalized glucose levels in diabetic rats for 6 months. The authors demonstrated that the functionality of the device was dependent on oxygen supply (Barkai et al., 2013).

In recent years, microfluidic technology has emerged as a valuable tool for a wide range of applications such as biotechnology, tissue engineering and analytical applications. This technology has been used to generate precise micro-scaled encapsulation. Onoe et al. developed microfibers encapsulating ECM proteins and islets cells using microfluidic device (Onoe et al., 2013). The fabricated microfibres reconstitute intrinsic morphologies and functions of living tissues. In other study, Tomei et al. developed an encapsulation method that allows conformal coating of islets through microfluidics and minimizes capsule size, capsule thickness and graft volume. The reduction of capsule thickness improves oxygen and insulin exchange (Tomei et al., 2014). Microfluidic devices can be used in differentiation of stem cells, which can be alternative sources of islets for transplantation to solve the critical problem of the shortage of human islet donors. Indeed, the destiny of stem cells is highly regulated by microenvironment. Such devices provide a new support of cells culture with unique advantages to mimic complex physiological microenvironments in vivo (Zhang, Wei, Zeng, Xu, & Li, 2017): high oxygenation, 3D tissue reorganization, dynamic stimulation, continuous nutrient supply, and waste removal. Microsystems can be also used to assess islets or beta cells functionality before transplantation, in an environment close to in vivo conditions.

In conclusion, the interactions between the graft and its microenvironment still remain a huge challenge for the BAP. It is well known that the structural organization of the pancreatic beta cells and its interaction with the host cells influences the amount of insulin secreted (Desai & Shea, 2017).

List of Symbols

Cs	solute concentration
Ds	diffusion coefficient of the solute
Jf	local convective flux of the solvent
Js	local mass transfer
MafA	MAF bZIP transcription factor A
Ngn3	neurogenin 3
P	pressure
ΔP	local transmembrane pressure
Pax4	paired box 4
Pdx1	pancreatic and duodenal homeobox 1
PO_2	oxygen partial pressure
S	sieving coefficient of the membrane
UFR	membrane ultrafiltration rate

List of Acronyms

APA	alginate-poly-L-ornithine-alginate
APF	arteria profunda femoris
BAP	bioartificial pancreas
CAC	collagen-alginate composite
CITR	collaborative islet transplant registry
ESCs	embryonic stem cells
FDA	food and drug administration
HEMA	2-hydroxy-ethyl methacrylate
hESCs	human embryonic stem cells
hiPSCs	human-induced pluripotent stem cells
IBMIR	instant blood-mediated inflammatory responses
IDF	International Diabetes Federation
IEQ	islets equivalent
IPN	interpenetrating network
iPSCs	induced pluripotent stem cells
LFA-1	function-associated Antigen-1
PDMS	polydimethylsiloxane
PECs	pancreatic endoderm cells
PEG	polyethylene glycol
PLA	polylactic acid
PP	pancreatic polypeptide
PTFE	polytetrafluoroethylene
T1DM	type I diabetes mellitus
TMTD	triazole-thiomorpholine dioxide
VEGF	vascular endothelial growth factor
WHO	World Health Organization

References

Alipio, Z., Liao, W., Roemer, E. J., Waner, M., Fink, L. M., Ward, D. C., et al. (2010). Reversal of hyperglycemia in diabetic mouse models using induced-pluripotent stem (iPS)-derived pancreatic beta-like cells. *Proceedings of the National Academy of Sciences of the United States of America*, *107*, 13426–13431.

Amer, L. D., Mahoney, M. J., & Bryant, S. J. (2014). Tissue engineering approaches to cell-based type 1 diabetes therapy. *Tissue Engineering. Part B, Reviews*, *20*, 455–467.

Aoki, T., Hui, H., Umehara, Y., LiCalzi, S., Demetriou, A. A., Rozga, J., et al. (2005). Intrasplenic transplantation of encapsulated genetically engineered mouse insulinoma cells reverses streptozotocin-induced diabetes in rats. *Cell Transplantation*, *14*, 411–421.

Arifin, D. R., Valdeig, S., Anders, R. A., Bulte, J. W. M., & Weiss, C. R. (2016). Magnetoencapsulated human islets xenotransplanted into swine: a comparison of different transplantation sites. *Xenotransplantation*, *23*, 211–221.

Barkai, U., Weir, G. C., Colton, C. K., Ludwig, B., Bornstein, S. R., Brendel, M. D., et al. (2013). Enhanced oxygen supply improves islet viability in a new bioartificial pancreas. *Cell Transplantation*, *22*, 1463–1476.

Barrett, K. E., Barman, S. M., Boitano, S., & Brooks, H. L. (2015). *Ganong's review of medical physiology* (25th ed.). McGraw Hill Education. ISBN-13: 978-0071825108. ISBN-10: 007182510X.

Basta, G., Montanucci, P., Luca, G., Boselli, C., Noya, G., Barbaro, B., et al. (2011). Long-term metabolic and immunological follow-up of nonimmunosuppressed patients with type 1 diabetes treated with microencapsulated islet allografts: four cases. *Diabetes Care*, *34*, 2406–2409.

Benthuysen, J. R., Carrano, A. C., & Sander, M. (2016). Advances in β cell replacement and regeneration strategies for treating diabetes. *The Journal of Clinical Investigation*, *126*, 3651–3660.

Bertuzzi, F., De Carlis, L., Marazzi, M., Rampoldi, A. G., Bonomo, M., Antonioli, B., et al. (2018). Long-term effect of islet transplantation on glycemic variability. *Cell Transplantation*, *27*, 840–846.

Bonal, C., & Herrera, P. L. (2008). Genes controlling pancreas ontogeny. *The International Journal of Developmental Biology*, *52*, 823–835.

Bruin, J. E., Asadi, A., Fox, J. K., Erener, S., Rezania, A., & Kieffer, T. J. (2015). Accelerated maturation of human stem cell-derived pancreatic progenitor cells into insulin-secreting cells in immunodeficient rats relative to mice. *Stem Cell Reports*, *5*, 1081–1096.

Bruin, J. E., Rezania, A., Xu, J., Narayan, K., Fox, J. K., O'Neil, J. J., et al. (2013). Maturation and function of human embryonic stem cell-derived pancreatic progenitors in macroencapsulation devices following transplant into mice. *Diabetologia*, *56*, 1987–1998.

Bruttomesso, D., Costa, S., & Baritussio, A. (2009). Continuous subcutaneous insulin infusion (CSII) 30 years later: still the best option for insulin therapy. *Diabetes/Metabolism Research and Reviews*, *25*, 99–111.

Cabric, S., Sanchez, J., Lundgren, T., Foss, A., Felldin, M., Källen, R., et al. (2007). Islet surface heparinization prevents the instant blood-mediated inflammatory reaction in islet transplantation. *Diabetes*, *56*, 2008–2015.

Calafiore, R. (1992). Transplantation of microencapsulated pancreatic human islets for therapy of diabetes mellitus. A preliminary report. *ASAIO Journal*, *38*, 34–37.

Calafiore, R., Basta, G., Falorni, A., Ciabattoni, P., Brotzu, G., Cortesini, R., et al. (1992). Intravascular transplantation of microencapsulated islets in diabetic dogs. *Transplantation Proceedings*, *24*, 935–936.

Calafiore, R., Basta, G., Luca, G., Lemmi, A., Montanucci, M. P., Calabrese, G., et al. (2006). Microencapsulated pancreatic islet allografts into nonimmunosuppressed patients with type 1 diabetes: first two cases. *Diabetes Care*, *29*, 137–138.

Cañibano-Hernández, A., Sáenz del Burgo, L., Espona-Noguera, A., Ciriza, J., & Pedraz, J. L. (2018). Current advanced therapy cell-based medicinal products for type-1-diabetes treatment. *International Journal of Pharmaceutics*, *543*, 107–120.

Carlsson, P. O., Palm, F., Andersson, A., & Liss, P. (2001). Markedly decreased oxygen tension in transplanted rat pancreatic islets irrespective of the implantation site. *Diabetes*, *50*, 489–495.

Cavelti-Weder, C., Zumsteg, A., Li, W., & Zhou, Q. (2017). Reprogramming of pancreatic acinar cells to functional beta cells by in vivo transduction of a polycistronic construct containing Pdx1, Ngn3, MafA in mice. *Current Protocols in Stem Cell Biology*, *40*, 4A.10.1–4A.10.12.

Chang, R., Faleo, G., Russ, H. A., Parent, A. V., Elledge, S. K., Bernards, D. A., et al. (2017). Nanoporous immunoprotective device for stem-cell-derived β-cell replacement therapy. *ACS Nano*, *11*, 7747–7757.

Chang, C. A., Lawrence, M. C., & Naziruddin, B. (2017). Current issues in allogeneic islet transplantation. *Current Opinion in Organ Transplantation*, *22*, 437–443.

Chhabra, P., & Brayman, K. L. (2013). Stem cell therapy to cure type 1 diabetes: from hype to hope. *Stem Cells Translational Medicine*, *2*, 328–336.

Chick, W. L., Like, A. A., Lauris, V., Galletti, P. M., Richardson, P. D., Panol, G., et al. (1975). A hybrid artificial pancreas. *Transactions—American Society for Artificial Internal Organs*, *21*, 8–15.

Cito, M., Pellegrini, S., Piemonti, L., & Sordi, V. (2018). The potential and challenges of alternative sources of β cells for the cure of type 1 diabetes. *Endocrine Connections*, *7*, R114–R125.

Colton, C. K. (1995). Implantable biohybrid artificial organs. *Cell Transplantation*, *4*, 415–436.

Coronel, M. M., Geusz, R., & Stabler, C. L. (2017). Mitigating hypoxic stress on pancreatic islets via in situ oxygen generating biomaterial. *Biomaterials*, *129*, 139–151.

D'Amour, K. A., Bang, A. G., Eliazer, S., Kelly, O. G., Agulnick, A. D., Smart, N. G., et al. (2006). Production of pancreatic hormone–expressing endocrine cells from human embryonic stem cells. *Nature Biotechnology*, *24*, 1392–1401.

de Vos, P., Faas, M. M., Strand, B., & Calafiore, R. (2006). Alginate-based microcapsules for immunoisolation of pancreatic islets. *Biomaterials*, *27*, 5603–5617.

de Vos, P., Hamel, A. F., & Tatarkiewicz, K. (2002). Considerations for successful transplantation of encapsulated pancreatic islets. *Diabetologia*, *45*, 159–173.

Desai, T., & Shea, L. D. (2017). Advances in islet encapsulation technologies. *Nature Reviews Drug Discovery*, *16*, 338–350.
Dufrane, D., D'hoore, W., Goebbels, R. M., Saliez, A., Guiot, Y., & Gianello, P. (2006). Parameters favouring successful adult pig islet isolations for xenotransplantation in pig-to-primate models. *Xenotransplantation*, *13*(3), 204–214.
Dufrane, D., & Gianello, P. (2012). Macro- or microencapsulation of pig islets to cure type 1 diabetes. *World Journal of Gastroenterology*, *18*, 6885–6893.
Dufrane, D., Goebbels, R.-M., & Gianello, P. (2010). Alginate macroencapsulation of pig islets allows correction of streptozotocin-induced diabetes in primates up to 6 months without immunosuppression. *Transplantation*, *90*, 1054–1062.
Dufrane, D., Goebbels, R.-M., Saliez, A., Guiot, Y., & Gianello, P. (2006). Six month survival of microencapsulated pig islets and alginate biocompatibility in primates: proof of concept. *Transplantation*, *81*, 1345–1353.
Dufrane, D., van Steenberghe, M., Goebbels, R.-M., Saliez, A., Guiot, Y., & Gianello, P. (2006). The influence of implantation site on the biocompatibility and survival of alginate encapsulated pig islets in rats. *Biomaterials*, *27*, 3201–3208.
Dulong, J.-L., & Legallais, C. (2005). What are the relevant parameters for the geometrical optimization of an implantable bioartificial pancreas? *Journal of Biomechanical Engineering*, *127*, 1054–1061.
Dulong, J.-L., & Legallais, C. (2007). A theoretical study of oxygen transfer including cell necrosis for the design of a bioartificial pancreas. *Biotechnology and Bioengineering*, *96*, 990–998.
El-Khatib, F. H., Balliro, C., Hillard, M. A., Magyar, K. L., Ekhlaspour, L., Sinha, M., et al. (2017). Home use of a bihormonal bionic pancreas versus insulin pump therapy in adults with type 1 diabetes: a multicentre randomised crossover trial. *Lancet*, *389*, 369–380.
Elliott, R. B., Escobar, L., Calafiore, R., Basta, G., Garkavenko, O., Vasconcellos, A., et al. (2005). Transplantation of micro- and macroencapsulated piglet islets into mice and monkeys. *Transplantation Proceedings*, *37*, 466–469.
Elliott, R. B., Escobar, L., Tan, P. L. J., Garkavenko, O., Calafiore, R., Basta, P., et al. (2005). Intraperitoneal alginate encapsulated neonatal porcine islets in a placebo controlled study with 16 diabetic cynomolgus primates. *Transplantation Proceedings*, *37*, 3505–3508.
Elliott, R. B., Escobar, L., Tan, P. L. J., Muzina, M., Zwain, S., & Buchanan, C. (2007). Live encapsulated porcine islets from a type 1 diabetic patient 9.5 yr after xenotransplantation. *Xenotransplantation*, *14*, 157–161.
Espes, D., Lau, J., & Carlsson, P. O. (2017). MECHANISMS IN ENDOCRINOLOGY: towards the clinical translation of stem cell therapy for type 1 diabetes. *European Journal of Endocrinology*, *177*, R159–R168.
Farina, M., Ballerini, A., Fraga, D. W., Nicolov, E., Hogan, M., Demarchi, D., et al. (2017). 3D printed vascularized device for subcutaneous transplantation of human islets. *Biotechnology Journal*, *12*(9), 1700169.
Fotino, N., Fotino, C., & Pileggi, A. (2015). Re-engineering islet cell transplantation. *Pharmacological Research*, *98*, 76–85.
Galderisi, A., Schlissel, E., & Cengiz, E. (2017). Keeping up with the diabetes technology: 2016 endocrine society guidelines of insulin pump therapy and continuous glucose monitor management of diabetes. *Current Diabetes Reports*, *17*, 111.
Giraldo, J. A., Molano, R. D., Rengifo, H. R., Fotino, C., Gattás-Asfura, K. M., Pileggi, A., et al. (2017). The impact of cell surface PEGylation and short-course immunotherapy on islet graft survival in an allogeneic murine model. *Acta Biomaterialia*, *49*, 272–283.
Gores, P. F., & Sutherland, D. E. R. (1993). Pancreatic islet transplantation: is purification necessary? *American Journal of Surgery*, *166*, 538–542.
Goss, J. A., Schock, A. P., Brunicardi, F. C., Goodpastor, S. E., Garber, A. J., Soltes, G., et al. (2002). Achievement of insulin independence in three consecutive type-1 diabetic patients via pancreatic islet transplantation using islets isolated at a remote islet isolation center. *Transplantation*, *74*, 1761–1766.
Harrington, S., Williams, J., Rawal, S., Ramachandran, K., & Stehno-Bittel, L. (2017). Hyaluronic acid/collagen hydrogel as an alternative to alginate for long-term immunoprotected islet transplantation. *Tissue Engineering. Part A*, *23*, 1088–1099.

Hayek, A., & Beattie, G. M. (1997). Experimental transplantation of human fetal and adult pancreatic islets. *The Journal of Clinical Endocrinology and Metabolism*, *82*, 2471–2475.
Hwang, P. T. J., Shah, D. K., Garcia, J. A., Bae, C. Y., Lim, D.-J., Huiszoon, R. C., et al. (2016). Progress and challenges of the bioartificial pancreas. *Nano Convergence*, *3*, 28.
Iacovacci, V., Ricotti, L., Menciassi, A., & Dario, P. (2016). The bioartificial pancreas (BAP): biological, chemical and engineering challenges. *Biochemical Pharmacology*, *100*, 12–27.
International Diabetes Federation official web site. (2019). https://www.idf.org/.
Itoh, T., Nishinakamura, H., Kumano, K., Takahashi, H., & Kodama, S. (2017). The spleen is an ideal site for inducing transplanted islet graft expansion in mice. *PLoS One*, *12*, e0170899.
Jacobs-Tulleneers-Thevissen, D., Chintinne, M., Ling, Z., Gillard, P., Schoonjans, L., Delvaux, G., et al. (2013). Sustained function of alginate-encapsulated human islet cell implants in the peritoneal cavity of mice leading to a pilot study in a type 1 diabetic patient. *Diabetologia*, *56*, 1605–1614.
Jansson, L., Barbu, A., Bodin, B., Drott, C. J., Espes, D., Gao, X., et al. (2016). Pancreatic islet blood flow and its measurement. *Upsala Journal of Medical Sciences*, *121*, 81–95.
Johansson, U., Rasmusson, I., Niclou, S. P., Forslund, N., Gustavsson, L., Nilsson, B., et al. (2008). Formation of composite endothelial cell-mesenchymal stem cell islets: a novel approach to promote islet revascularization. *Diabetes*, *57*, 2393–2401.
Jouvet, N., & Estall, J. L. (2017). The pancreas: bandmaster of glucose homeostasis. *Experimental Cell Research*, *360*, 19–23.
Jun, Y., Kang, A. R., Lee, J. S., Park, S. J., Lee, D. Y., Moon, S. H., et al. (2014). Microchip-based engineering of super-pancreatic islets supported by adipose-derived stem cells. *Biomaterials*, *35*, 4815–4826.
Jun, Y., Kim, M. J., Hwang, Y. H., Jeon, E. A., Kang, A. R., Lee, S.-H., et al. (2013). Microfluidics-generated pancreatic islet microfibers for enhanced immunoprotection. *Biomaterials*, *34*, 8122–8130.
Kepsutlu, B., Nazli, C., Bal, T., & Kizilel, S. (2014). Design of bioartificial pancreas with functional micro/nano-based encapsulation of islets. *Current Pharmaceutical Biotechnology*, *15*, 590–608.
Kirk, K., Hao, E., Lahmy, R., & Itkin-Ansari, P. (2014). Human embryonic stem cell derived islet progenitors mature inside an encapsulation device without evidence of increased biomass or cell escape. *Stem Cell Research*, *12*, 807–814.
Klonoff, D. C., Ahn, D., & Drincic, A. (2017). Continuous glucose monitoring: a review of the technology and clinical use. *Diabetes Research and Clinical Practice*, *133*, 178–192.
Kriz, J., Vilk, G., Mazzuca, D. M., Toleikis, P. M., Foster, P. J., & White, D. J. G. (2012). A novel technique for the transplantation of pancreatic islets within a vascularized device into the greater omentum to achieve insulin independence. *American Journal of Surgery*, *203*, 793–797.
Kroon, E., Martinson, L. A., Kadoya, K., Bang, A. G., Kelly, O. G., Eliazer, S., et al. (2008). Pancreatic endoderm derived from human embryonic stem cells generates glucose-responsive insulin-secreting cells in vivo. *Nature Biotechnology*, *26*, 443–452.
Kumagai-Braesch, M., Jacobson, S., Mori, H., Jia, X., Takahashi, T., Wernerson, A., et al. (2013). The TheraCyte™ device protects against islet allograft rejection in immunized hosts. *Cell Transplantation*, *22*, 1137–1146.
Kumar, M., & Melton, D. (2003). Pancreas specification: a budding question. *Current Opinion in Genetics & Development*, *13*, 401–407.
Lacy, P. E., Hegre, O. D., Gerasimidi-Vazeou, A., Gentile, F. T., & Dionne, K. E. (1991). Maintenance of normoglycemia in diabetic mice by subcutaneous xenografts of encapsulated islets. *Science*, *254*, 1782–1784.
Lanza, R. P., Beyer, A. M., Staruk, J. E., & Chick, W. L. (1993). Biohybrid artificial pancreas. Long-term function of discordant islet xenografts in streptozotocin diabetic rats. *Transplantation*, *56*, 1067–1072.
Lau, J., Vasylovska, S., Kozlova, E. N., & Carlsson, P.-O. (2015). Surface coating of pancreatic islets with neural crest stem cells improves engraftment and function after intraportal transplantation. *Cell Transplantation*, *24*, 2263–2272.
Lemper, M., Leuckx, G., Heremans, Y., German, M. S., Heimberg, H., Bouwens, L., et al. (2015). Reprogramming of human pancreatic exocrine cells to β-like cells. *Cell Death and Differentiation*, *22*, 1117–1130.
Lepeintre, J., Briandet, H., Moussy, F., Chicheportiche, D., Darquy, S., Rouchette, J., et al. (1990). Ex vivo evaluation in normal dogs of insulin released by a bioartificial pancreas containing isolated rat islets of Langerhans. *Artificial Organs*, *14*, 20–27.

Li, W., Nakanishi, M., Zumsteg, A., Shear, M., Wright, C., Melton, D. A., et al. (2014). In vivo reprogramming of pancreatic acinar cells to three islet endocrine subtypes. *eLife*, *3*, e01846.
Lima, M. J., Muir, K. R., Docherty, H. M., McGowan, N. W. A., Forbes, S., Heremans, Y., et al. (2016). Generation of functional beta-like cells from human exocrine pancreas. *PLoS One*, *11*, e0156204.
Ludwig, B., & Ludwig, S. (2015). Transplantable bioartificial pancreas devices: current status and future prospects. *Langenbeck's Archives of Surgery*, *400*, 531–540.
Ludwig, B., Ludwig, S., Steffen, A., Knauf, Y., Zimerman, B., Heinke, S., et al. (2017). Favorable outcome of experimental islet xenotransplantation without immunosuppression in a nonhuman primate model of diabetes. *Proceedings of the National Academy of Sciences*, *114*, 11745–11750.
Ludwig, B., Reichel, A., Steffen, A., Zimerman, B., Schally, A. V., Block, N. L., et al. (2013). Transplantation of human islets without immunosuppression. *Proceedings of the National Academy of Sciences*, *110*, 19054–19058.
Ludwig, B., Rotem, A., Schmid, J., Weir, G. C., Colton, C. K., Brendel, M. D., et al. (2012). Improvement of islet function in a bioartificial pancreas by enhanced oxygen supply and growth hormone releasing hormone agonist. *Proceedings of the National Academy of Sciences of the United States of America*, *109*, 5022–5027.
Mahadevan, V. (2016). Anatomy of the pancreas and spleen. *Surgery*, *34*, 261–265.
Maki, T., Otsu, I., O'Neil, J. J., Dunleavy, K., Mullon, C. J., Solomon, B. A., et al. (1996). Treatment of diabetes by xenogeneic islets without immunosuppression. Use of a vascularized bioartificial pancreas. *Diabetes*, *45*, 342–347.
Malik, F. S., & Taplin, C. E. (2014). Insulin therapy in children and adolescents with type 1 diabetes. *Pediatric Drugs*, *16*, 141–150.
Matsumoto, S., Abalovich, A., Wechsler, C., Wynyard, S., & Elliott, R. B. (2016). Clinical benefit of islet xenotransplantation for the treatment of type 1 diabetes. *eBioMedicine*, *12*, 255–262.
Matsumoto, S., Tan, P., Baker, J., Durbin, K., Tomiya, M., Azuma, K., et al. (2014). Clinical porcine islet xenotransplantation under comprehensive regulation. *Transplantation Proceedings*, *46*, 1992–1995.
McQuilling, J. P., & Opara, E. C. (2017). *Methods for incorporating oxygen-generating biomaterials into cell culture and microcapsule systems*. In E. Opara (Ed.), *Methods in molecular biology*: Vol. 1479. *Cell microencapsulation*. (pp. 135–141).
Mellgren, A., Schnell Landström, A. H., Petersson, B., & Andersson, A. (1986). The renal subcapsular site offers better growth conditions for transplanted mouse pancreatic islet cells than the liver or spleen. *Diabetologia*, *29*, 670–672.
Miller, R. E. (1981). Pancreatic neuroendocrinology: peripheral neural mechanisms in the regulation of the islets of langerhans. *Endocrine Reviews*, *2*, 471–494.
Millman, J. R., Xie, C., Van Dervort, A., Gürtler, M., Pagliuca, F. W., & Melton, D. A. (2016). Generation of stem cell-derived β-cells from patients with type 1 diabetes. *Nature Communications*, *7*, 11463.
Minami, K., Doi, R., Kawaguchi, Y., Nukaya, D., Hagiwara, Y., Noguchi, H., et al. (2011). In vitro generation of insulin-secreting cells from human pancreatic exocrine cells. *Journal of Diabetes Investigation*, *2*, 271–275.
Monaco, A. P., Maki, T., Ozato, H., Carretta, M., Sullivan, S. J., Borland, K. M., et al. (1991). Transplantation of islet allografts and xenografts in totally pancreatectomized diabetic dogs using the hybrid artificial pancreas. *Annals of Surgery*, *214*, 339–3612.
Mooranian, A., Negrulj, R., Arfuso, F., & Al-Salami, H. (2016). Characterization of a novel bile acid-based delivery platform for microencapsulated pancreatic β-cells. *Artificial Cells, Nanomedicine, and Biotechnology*, *44*, 194–200.
Motté, E., Szepessy, E., Suenens, K., Stangé, G., Bomans, M., Jacobs-Tulleneers-Thevissen, D., et al. (2014). Composition and function of macroencapsulated human embryonic stem cell-derived implants: comparison with clinical human islet cell grafts. *American Journal of Physiology Endocrinology and Metabolism*, *307*, E838–E846.
Nagaraju, S., Bottino, R., Wijkstrom, M., Trucco, M., & Cooper, D. K. C. (2015). Islet xenotransplantation: what is the optimal age of the islet-source pig? *Xenotransplantation*, *22*, 7–19.
Neufeld, T., Ludwig, B., Barkai, U., Weir, G. C., Colton, C. K., Evron, Y., et al. (2013). The efficacy of an immunoisolating membrane system for islet xenotransplantation in minipigs. *PLoS One*, *8*, e70150.

Nourmohammadzadeh, M., Lo, J. F., Bochenek, M., Mendoza-Elias, J. E., Wang, Q., Li, Z., et al. (2013). Microfluidic array with integrated oxygenation control for real-time live-cell imaging: effect of hypoxia on physiology of microencapsulated pancreatic islets. *Analytical Chemistry*, *85*, 11240–11249.

O'Sullivan, E. S., Vegas, A., Anderson, D. G., & Weir, G. C. (2011). Islets transplanted in immunoisolation devices: a review of the progress and the challenges that remain. *Endocrine Reviews*, *32*, 827–844.

Olsson, R., Olerud, J., Pettersson, U., & Carlsson, P. O. (2011). Increased numbers of low-oxygenated pancreatic islets after intraportal islet transplantation. *Diabetes*, *60*, 2350–2353.

Omer, A., Keegan, M., Czismadia, E., De Vos, P., Van Rooijen, N., Bonner-Weir, S., et al. (2003). Macrophage depletion improves survival of porcine neonatal pancreatic cell clusters contained in alginate macrocapsules transplanted into rats. *Xenotransplantation*, *10*, 240–251.

Onoe, H., Okitsu, T., Itou, A., Kato-Negishi, M., Gojo, R., Kiriya, D., et al. (2013). Metre-long cell-laden microfibres exhibit tissue morphologies and functions. *Nature Materials*, *12*, 584–590.

Opara, E. C., Mirmalek-Sani, S.-H., Khanna, O., Moya, M. L., & Brey, E. M. (2010). Design of a bioartificial pancreas. *Journal of Investigative Medicine*, *58*, 831–837.

Ozawa, F., Okitsu, T., & Takeuchi, S. (2017). Improvement in the mechanical properties of cell-laden hydrogel microfibers using interpenetrating polymer networks. *ACS Biomaterials Science & Engineering*, *3*, 392–398.

Ozawa, F., Sawayama, J., & Takeuchi, S. (2017). Mechanical enhanced hydrogel fiber encapsulating cells for long-term transplantation. In *Proceedings of the IEEE international conference on micro electro mechanical systems (MEMS)*.

Pagliuca, F. W., Millman, J. R., Gürtler, M., Segel, M., Van Dervort, A., Ryu, J. H., et al. (2014). Generation of functional human pancreatic β cells in vitro. *Cell*, *159*, 428–439.

Pandolfi, V., Pereira, U., Dufresne, M., & Legallais, C. (2017). Alginate-based cell microencapsulation for tissue engineering and regenerative medicine. *Current Pharmaceutical Design*, *23*, 3833–3844.

Pareta, R., McQuilling, J. P., Sittadjody, S., Jenkins, R., Bowden, S., Orlando, G., et al. (2014). Long-term function of islets encapsulated in a redesigned alginate microcapsule construct in omentum pouches of immune-competent diabetic rats. *Pancreas*, *43*, 605–613.

Pedraza, E., Coronel, M. M., Fraker, C. A., Ricordi, C., & Stabler, C. L. (2012). Preventing hypoxia-induced cell death in beta cells and islets via hydrolytically activated, oxygen-generating biomaterials. *Proceedings of the National Academy of Sciences*, *109*, 4245–4250.

Pepper, A. R., Gala-Lopez, B., Pawlick, R., Merani, S., Kin, T., & Shapiro, A. M. J. (2015). A prevascularized subcutaneous device-less site for islet and cellular transplantation. *Nature Biotechnology*, *33*, 518–523.

Pepper, A. R., Pawlick, R., Bruni, A., Wink, J., Rafiei, Y., O'Gorman, D., et al. (2017). Transplantation of human pancreatic endoderm cells reverses diabetes post transplantation in a prevascularized subcutaneous site. *Stem Cell Reports*, *8*, 1689–1700.

Pileggi, A., Molano, R. D., Ricordi, C., Zahr, E., Collins, J., Valdes, R., et al. (2006). Reversal of diabetes by pancreatic islet transplantation into a subcutaneous, neovascularized device. *Transplantation*, *81*, 1318–1324.

Prochorov, A. V., Tretjak, S. I., Goranov, V. A., Glinnik, A. A., & Goltsev, M. V. (2008). Treatment of insulin dependent diabetes mellitus with intravascular transplantation of pancreatic islet cells without immunosuppressive therapy. *Advances in Medical Sciences*, *53*, 240–244.

Reach, G., Chenard, P. S., Darquy, S., Lepeintre, J., Desjeux, J. F., Cannon, R., et al. (1986). Kinetics of insulin delivery by a bioartificial pancreas: in vivo evaluation in conscious normal rats. *Progress in Artif Organs*, *1*, 621–626.

Reach, G., & Jaffrin, M. Y. (1987). Bioartificial pancreas as an approach to closed-loop insulin delivery. In W. D. Emsinger & J. L. Selam (Eds.), *Drug delivery system* (pp. 99–102). Mount Kisco, New York: Futura.

Reach, G., & Jaffrin, M. Y. (1990). Kinetic modelling as a tool for the design of a vascular bioartificial pancreas: feedback between modelling and experimental validation. *Computer Methods and Programs in Biomedicine*, *32*, 277–285.

Reach, G., Jaffrin, M. Y., & Desjeux, J. F. (1984). A U-shaped bioartificial pancreas with rapid glucose-insulin kinetics. In vitro evaluation and kinetic modelling. *Diabetes*, *33*, 752–761.

Rezania, A., Bruin, J. E., Arora, P., Rubin, A., Batushansky, I., Asadi, A., et al. (2014). Reversal of diabetes with insulin-producing cells derived in vitro from human pluripotent stem cells. *Nature Biotechnology*, *32*, 1121–1133.

Rezania, A., Bruin, J. E., Riedel, M. J., Mojibian, M., Asadi, A., Xu, J., et al. (2012). Maturation of human embryonic stem cell-derived pancreatic progenitors into functional islets capable of treating pre-existing diabetes in mice. *Diabetes*, *61*, 2016–2029.

Robert, T., De Mesmaeker, I., Stangé, G. M., Suenens, K. G., Ling, Z., Kroon, E. J., et al. (2018). Functional beta cell mass from device-encapsulated hESC-derived pancreatic endoderm achieving metabolic control. *Stem Cell Reports*, *10*, 739–750.

Ryan, E. A., Lakey, J. R., Rajotte, R. V., Korbutt, G. S., Kin, T., Imes, S., et al. (2001). Clinical outcomes and insulin secretion after islet transplantation with the Edmonton protocol. *Diabetes*, *50*, 710–719.

Sakata, N., Tan, A., Chan, N., Obenaus, A., Mace, J., Peverini, R., et al. (2009). Efficacy comparison between intraportal and subcapsular islet transplants in a murine diabetic model. *Transplantation Proceedings*, *41*, 346–349.

Scharp, D. W., Lacy, P. E., Santiago, J. V., McCullough, C. S., Weide, L. G., Boyle, P. J., et al. (1991). Results of our first nine intraportal islet allografts in type 1, insulin-dependent diabetic patients. *Transplantation*, *51*, 76–85.

Scharp, D. W., Lacy, P. E., Santiago, J. V., McCullough, C. S., Weide, L. G., Falqui, L., et al. (1990). Insulin independence after islet transplantation into type I diabetic patient. *Diabetes*, *39*, 515–518.

Scharp, D. W., & Marchetti, P. (2014). Encapsulated islets for diabetes therapy: history, current progress, and critical issues requiring solution. *Advanced Drug Delivery Reviews*, *67–68*, 35–73.

Scharp, D. W., Mason, N. S., & Sparks, R. E. (1984). Islet immuno-isolation: the use of hybrid artificial organs to prevent islet tissue rejection. *World Journal of Surgery*, *8*, 221–229.

Scharp, D. W., Swanson, C. J., Olack, B. J., Latta, P. P., Hegre, O. D., Doherty, E. J., et al. (1994). Protection of encapsulated human islets implanted without immunosuppression in patients with type I or type II diabetes and in nondiabetic control subjects. *Diabetes*, *43*, 1167–1170.

Schweicher, J. (2014). Membranes to achieve immunoprotection of transplanted islets. *Frontiers in Bioscience*, *19*, 49–76.

Shapiro, A. M. J., Pokrywczynska, M., & Ricordi, C. (2016). Clinical pancreatic islet transplantation. *Nature Reviews Endocrinology*, *13*, 268–277.

Shen, J., Cheng, Y., Han, Q., Mu, Y., & Han, W. (2013). Generating insulin-producing cells for diabetic therapy: existing strategies and new development. *Ageing Research Reviews*, *12*, 469–478.

Skrzypek, K., Nibbelink, M. G., Karperien, M., van Apeldoorn, A., & Stamatialis, D. (2018). *Membranes for bioartificial pancreas: macroencapsulation strategies*. In *Biomedical membranes and (bio)artificial organs*. World Scientific.(pp. 211–244).

Song, S., Blaha, C., Moses, W., Park, J., Wright, N., Groszek, J., et al. (2017). An intravascular bioartificial pancreas device (iBAP) with silicon nanopore membranes (SNM) for islet encapsulation under convective mass transport. *Lab on a Chip*, *17*, 1778–1792.

Song, S., & Roy, S. (2016). Progress and challenges in macroencapsulation approaches for type 1 diabetes (T1D) treatment: cells, biomaterials, and devices. *Biotechnology and Bioengineering*, *113*, 1381–1402.

Soon-Shiong, P., Heintz, R. E., Merideth, N., Yao, Q. X., Yao, Z., Zheng, T., et al. (1994). Insulin independence in a type 1 diabetic patient after encapsulated islet transplantation. *Lancet*, *343*, 950–951.

Stephens, E. (2015). Insulin therapy in type 1 diabetes. *The Medical Clinics of North America*, *99*, 145–156.

Storrs, R., Dorian, R., King, S. R., Lakey, J., & Rilo, H. (2001). Preclinical development of the islet sheet. *Annals of the New York Academy of Sciences*, *944*, 252–266.

Strand, B. L., Coron, A. E., & Skjak-Braek, G. (2017). Current and future perspectives on alginate encapsulated pancreatic islet. *Stem Cells Translational Medicine*, *6*, 1053–1058.

Sugimoto, S., Heo, Y. J., Onoe, H., Okitsu, T., Kotera, H., & Takeuchi, S. (2011). Implantable hydrogel microfiber encapsulating pancreatic beta-cells for diabetes treatment. In *15th international conference on miniaturized systems for chemistry and life sciences 2011, MicroTAS 2011*.

Sullivan, S. J., Maki, T., Borland, K. M., Mahoney, M. D., Solomon, B. A., Muller, T. E., et al. (1991). Biohybrid artificial pancreas: long-term implantation studies in diabetic, pancreatectomized dogs. *Science*, *252*, 718–721.

Sun, Y., Ma, X., Zhou, D., Vacek, I., & Sun, A. M. (1996). Normalization of diabetes in spontaneously diabetic cynomologus monkeys by xenografts of microencapsulated porcine islets without immunosuppression. *The Journal of Clinical Investigation*, *98*, 1417–1422.

Sun, A. M., Parisius, W., Healy, G. M., Vacek, I., & Macmorine, H. G. (1977). The use, in diabetic rats and monkeys, of artificial capillary units containing cultured islets of Langerhans (artificial endocrine pancreas). *Diabetes*, *26*, 1136–1139.

Sykes, M., Cozzi, E., d'Apice, A., Pierson, R., O'Connell, P., Cowan, P., et al. (2006). Clinical trial of islet xenotransplantation in Mexico. *Xenotransplantation*, *13*, 371–372.

Tauschmann, M., & Hovorka, R. (2014). Insulin pump therapy in youth with type 1 diabetes: toward closed-loop systems. *Expert Opinion on Drug Delivery*, *11*, 943–955.

Teramura, Y., & Iwata, H. (2009). Surface modification of islets with PEG-lipid for improvement of graft survival in intraportal transplantation. *Transplantation*, *88*, 624–630.

Teramura, Y., & Iwata, H. (2010). Bioartificial pancreas: microencapsulation and conformal coating of islet of Langerhans. *Advanced Drug Delivery Reviews*, *62*, 827–840.

Teramura, Y., & Iwata, H. (2011). Improvement of graft survival by surface modification with poly(ethylene glycol)-lipid and urokinase in intraportal islet transplantation. *Transplantation*, *91*, 271–278.

Teramura, Y., Oommen, O. P., Olerud, J., Hilborn, J., & Nilsson, B. (2013). Microencapsulation of cells, including islets, within stable ultra-thin membranes of maleimide-conjugated PEG-lipid with multifunctional crosslinkers. *Biomaterials*, *34*, 2683–2693.

Tomei, A. A., Manzoli, V., Fraker, C. A., Giraldo, J., Velluto, D., Najjar, M., et al. (2014). Device design and materials optimization of conformal coating for islets of Langerhans. *Proceedings of the National Academy of Sciences*, *111*, 10514–10519.

Tortora, G. J., & Derrickson, B. (2013). *Principles of anatomy and physiology* (14th ed.). Wiley. ISBN: ES8-1-118-34500-9.

Trivedi, N., Steil, G. M., Colton, C. K., Bonner-Weir, S., & Weir, G. C. (2000). Improved vascularization of planar membrane diffusion devices following continuous infusion of vascular endothelial growth factor. *Cell Transplantation*, *9*, 115–124.

Tuch, B. E., Keogh, G. W., Williams, L. J., Wu, W., Foster, J. L., Vaithilingam, V., et al. (2009). Safety and viability of microencapsulated human islets transplanted into diabetic humans. *Diabetes Care*, *32*, 1887–1889.

U.S. National Library of Medicine, ClinicalTrials.gov: NCT01652911 (n.d.). A phase I/II study of the safety and efficacy of sernova's cell pouch™ for therapeutic islet transplantation.

U.S. National Library of Medicine, ClinicalTrials.gov: NCT01739829 (n.d.). Open-label investigation of the safety and effectiveness of DIABECELL® in patients with type 1 diabetes mellitus.

U.S. National Library of Medicine, ClinicalTrials.gov: NCT02239354 (n.d.). A safety, tolerability, and efficacy study of VC-01™ combination product in subjects with type I diabetes mellitus.

Valdes-Gonzalez, R. A., Dorantes, L. M., Garibay, G. N., Bracho-Blanchet, E., Mendez, A. J., Davila-Perez, R., et al. (2005). Xenotransplantation of porcine neonatal islets of Langerhans and Sertoli cells: a 4-year study. *European Journal of Endocrinology*, *153*, 419–427.

Vegas, A. J., Veiseh, O., Gürtler, M., Millman, J. R., Pagliuca, F. W., Bader, A. R., et al. (2016). Long-term glycemic control using polymer-encapsulated human stem cell-derived beta cells in immune-competent mice. *Nature Medicine*, *22*, 306–311.

Veiseh, O., Doloff, J. C., Ma, M., Vegas, A. J., Tam, H. H., Bader, A. R., et al. (2015). Size- and shape-dependent foreign body immune response to materials implanted in rodents and non-human primates. *Nature Materials*, *14*, 643–651.

Vériter, S., Gianello, P., Igarashi, Y., Beaurin, G., Ghyselinck, A., Aouassar, N., et al. (2014). Improvement of subcutaneous bioartificial pancreas vascularization and function by coencapsulation of pig islets and mesenchymal stem cells in primates. *Cell Transplantation*, *23*, 1349–1364.

World Health Organization, Global report on diabetes. (2016). http://www.who.int/diabetes/global-report/en/.

World Health Organization official web site. (2019). http://www.who.int/diabetes/en/.

Yabe, S. G., Fukuda, S., Takeda, F., Nashiro, K., Shimoda, M., & Okochi, H. (2017). Efficient generation of functional pancreatic β-cells from human induced pluripotent stem cells. *Journal of Diabetes*, *9*, 168–179.

Zhang, J., Wei, X., Zeng, R., Xu, F., & Li, X. (2017). Stem cell culture and differentiation in microfluidic devices toward organ-on-a-chip. *Future Science OA*, *3*, FSO187.

Zhou, Q., Brown, J., Kanarek, A., Rajagopal, J., & Melton, D. A. (2008). In vivo reprogramming of adult pancreatic exocrine cells to β-cells. *Nature*, *455*, 627–632.

Zhu, H., Li, W., Liu, Z., Li, W., Chen, N., Lu, L., et al. (2018). Selection of implantation sites for transplantation of encapsulated pancreatic islets. *Tissue Engineering. Part B, Reviews*, *24*, 191–214.

Molecular and Cellular Endocrinology 514 (2020) 110892

Contents lists available at ScienceDirect

Molecular and Cellular Endocrinology

journal homepage: www.elsevier.com/locate/mce

Microwell-based pancreas-on-chip model enhances genes expression and functionality of rat islets of Langerhans

Amal Essaouiba[a,b], Teru Okitsu[c], Rachid Jellali[a,**], Marie Shinohara[d], Mathieu Danoy[b], Yannick Tauran[e], Cécile Legallais[a], Yasuyuki Sakai[d], Eric Leclerc[a,b,*]

[a] Université de technologie de Compiègne, CNRS, Biomechanics and Bioengineering, Centre de recherche Royallieu, CS 60319, 60203, Compiègne Cedex, France
[b] CNRS UMI 2820, Laboratory for Integrated Micro Mechatronic Systems, Institute of Industrial Science, University of Tokyo, 4-6-1 Komaba, Meguro-ku, Tokyo, 153-8505, Japan
[c] Institute of Industrial Science, University of Tokyo, 4-6-1 Komaba, Meguro-ku, Tokyo, 153-8505, Japan
[d] Department of Chemical Engineering, Faculty of Engineering, University of Tokyo, 7-3-1 Hongo, Bunkyo-ku, Tokyo, 113-8656, Japan
[e] Université Claude Bernard Lyon 1, Laboratoire des Multimatériaux et Interfaces, UMR CNRS 5615, F-69622, Villeurbanne, France

ARTICLE INFO

Keywords:
Pancreas
Islets of langerhans
Microfluidic biochips
Glucose homeostasis
Glucagon
Insulin

ABSTRACT

Organ-on-chip technology is a promising tool for investigating physiological *in vitro* responses in drug screening development, and in advanced disease models. Within this framework, we investigated the behavior of rat islets of Langerhans in an organ-on-chip model. The islets were trapped by sedimentation in a biochip with a microstructure based on microwells, and perfused for 5 days of culture. The live/dead assay confirmed the high viability of the islets in the biochip cultures. The microfluidic culture leads to upregulation of mRNA levels of important pancreatic islet genes: *Ins1*, *App*, *Insr*, *Gcgr*, *Reg3a* and *Neurod*. Furthermore, insulin and glucagon secretion were higher in the biochips compared to the Petri conditions after 5 days of culture. We also confirmed glucose-induced insulin secretion in biochips *via* high and low glucose stimulations leading to high/low insulin secretion. The high responsiveness of the pancreatic islets to glucagon-like peptide 1 (GLP-1) stimulation in the biochips was reflected by the upregulation of mRNA levels of *Gcgr*, *Reg3a*, *Neurog3*, *Ins1*, *Ins2*, *Stt* and *Glp-1r* and by increased insulin secretion. The results obtained highlighted the functionality of the islets in the biochips and illustrated the potential of our pancreas-on-chip model for future pancreatic disease modeling and anti-diabetic drugs screening.

1. Introduction

The pancreas is a gland organ that plays a key role in endocrine regulation. The functional units of the endocrine system are the islets of Langerhans. These islets are clusters of cells whose size varies between 20 and 500 μm, with five different cell types: α, β, δ, ε, and γ cells (Jouvet and Estall, 2017; Kumar and Melton, 2003). The most abundant cells are the glucagon-producing α cells and insulin-producing β cells. Blood glucose levels are obtained through the interaction of two antagonistic hormones secreted by pancreatic α and β cells. During a period of starvation, when glucose levels are low, glucagon is released by alpha cells to promote glycogenolysis and gluconeogenesis in the liver in coordination with cortisol (a hormone secreted by the adrenal gland). In contrast, insulin secretion from β cells is stimulated by elevated glucose levels and activates glycogenesis in the liver and glucose uptake by muscles and adipose tissues, thereby decreasing postprandial blood sugar levels (Baker, 2016; Jellali et al., 2020).

Diabetes mellitus is the most significant endocrine system dysfunction in the pancreas. According to the latest estimates by the International Diabetes Federation (IDF), 1 in 11 adults are living with diabetes in 2019 (463 million people worldwide, IDF official web site, 2019). The incidence of diabetes is increasing dramatically, and is predicted to reach more than 700 million people by 2045 (IDF official web site, 2019). Type 1 diabetes mellitus (T1DM) is an autoimmune disorder which leads to the destruction of insulin-secreting β cells, resuting a lack of insulin production (Jellali et al., 2020; Rogal et al., 2019). This pathology affects about 10% of diabetic patients, mostly the young population (Aghamaleki et al., 2019). The daily insulin

* Corresponding author. Université de technologie de Compiègne, CNRS, Biomechanics and Bioengineering, Centre de recherche Royallieu, CS 60319, 60203, Compiègne Cedex.
** Corresponding author.
E-mail addresses: rachid.jellali@utc.fr (R. Jellali), eleclerc@iis.u-tokyo.ac.jp, eric.leclerc@utc.fr (E. Leclerc).

https://doi.org/10.1016/j.mce.2020.110892
Received 3 January 2020; Received in revised form 18 May 2020; Accepted 3 June 2020
Available online 09 June 2020

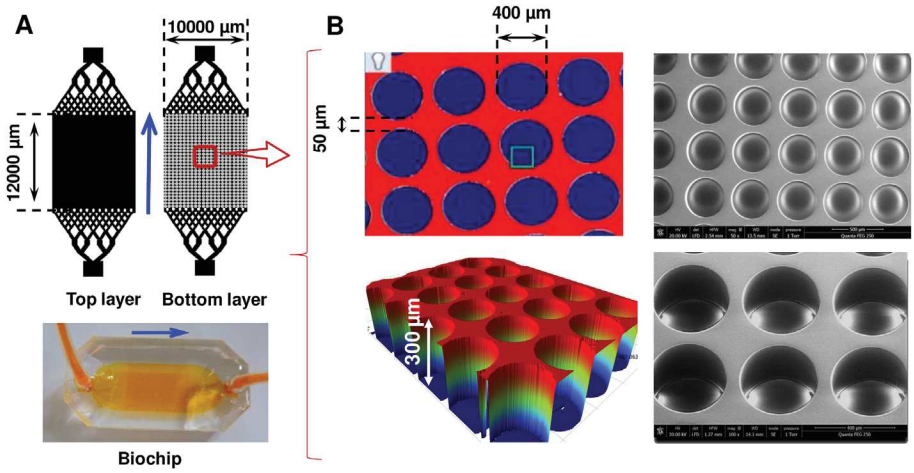

Fig. 1. Biochip design: (A) top and bottom layers used in the biochip manufacturing (the blue arrowa indicate the flow direction) and (B) structures of microwells in culture chamber (bottom layer).

administration is currently the most common treatment of T1DM (King and Bowe, 2016). Type 2 diabetes mellitus (T2DM) is the most prevalent form of diabetes, accounting for 90% of all adult diabetic patients, i.e. 20-79 years old (Sardu et al., 2019). T2DM is a metabolic disorder characterized by insulin resistance coupled to impaired insulin secretion from the pancreatic β cells (Jun et al., 2019; Zbinden et al., 2020). Insulin resistance is the organs incapacity to respond properly to normal insulin levels (mainly the liver, muscles and adipose tissue, Rogal et al., 2019). The treatment of T2DM involves lifestyle adjustments and drug therapy such as metformin, sulphonylureas, glitazones and GLP-1 receptor agonists (Rogal et al., 2019; Zbinden et al., 2020).

Nowadays, Diabetes is one of the most prevalent chronic diseases (Silva et al., 2018). This raises a need for developing pancreatic models to increase knowledge of the underlying mechanisms of diabetes and to screen and identify new anti-diabetic drugs. Pancreatic disease modeling and pertinent models for pancreatic drug screening involve considering the pancreas and its interaction with other organs, such as the liver, muscle, adipose tissues, kidney and gut (Efanov et al., 2004; Artunc et al., 2016; Bauer et al., 2017; Rogal et al., 2019). This is the reason why the disease models involve transgenic and knockout animals (King and Bowe, 2016). However, animal experimentation is ethically controversial, and often, the animal models developed in other species lose relevance when extrapolating the results to humans (Ghaemmaghami et al., 2012;Merlier et al., 2017; Rogal et al., 2019). Concerning *in vitro* models, the cell cultures used for drug screening and biomarker discovery are mainly performed in static 2D cultures using conventional Petri dishes or multi-well plates. Although these models have significantly contributed to medical research and drugs screening, they present certain limitations. Today, it seems clear that 2D cultures are poorly representative of human *in vivo* physiology, metabolism and toxicity, due to the physiological gap between the cells cultivated in static 2D mode and human cells as they exist in their native state (3D, dynamic mode) and the lack of physiological integration between cells and organs (Merlier et al., 2017). As a result, it is essential to improve these basic plate cultures to understand and model metabolic processes and human disorders. This is why many groups are developing tissue-engineering and 3D culture processes in order to provide a more appropriate micro-environment for tissue maintenance and development. This environment must reproduce, as closely as possible, the characteristics found *in vivo*.

The organ-on-chip approach is one way of mimicking organ physiology to help in the development of therapeutic solutions and pharmacological studies (Huh et al., 2012; Bhatia and Ingber, 2014). This approach has many advantages to reproduce the characteristics of physiological microenvironments, including three-dimensional architectures, cell-cell interactions and dynamic flow that ensures the transport and exchange of culture medium, hormones, metabolic waste and other chemicals (Merlier et al., 2017 merlier et al., 2017; Lee et al., 2018; Zbinden et al., 2020Zbinden et al., 2020). Unlike the static cultures in Petri dishes, organ-on-chip approach provides the possibility to perform co-cultures, where the different cell types can be cultivated in separated microbioreactors and the cell-cell interactions are ensured by soluble factors exchange (Merlier et al., 2017). The co-culture of two or more organ is a promising tool to study multi-organs diseases such as T2DM (Rogal et al., 2019). In the last years, organ-on-chip technology has been used to reproduce pancreas *in vitro* models (Schulze et al., 2017; Li et al., 2017; Brooks et al., 2016; Lee et al., 2018; Jun et al., 2020). A literature review highlighted that most of the current microfluidic platforms have been designed mainly for islet quality assessment for subsequent *in vivo* implantation (Rogal et al., 2019). In parallel, some recent works have also demonstrated the potential of organ-on-chip technology for more complex pancreatic physiopathology analysis (Bauer et al., 2017; Zbinden et al., 2020).

In this work, we developed a simple microfluidic biochip for assessment of pancreatic islet function and long-term cultures. We also presented and demonstrated that the islets functionality was maintained in microfluidic biochips when compared to conventional islet cultures inside polystyrene (TCPS) dishes.

2. Material and methods

2.1. Device design and fabrication

The microfluidic biochip consists of a cell culture chamber manufactured with two polydimethylsiloxane (PDMS) layers (Fig. 1A). The micro-structured bottom layer, used for trapping the islets, is composed of 600 micro-wells of 400 µm in diameter (depth of 300 µm), and spaced 50 µm apart (Fig. 1B). The second PDMS layer, with a reservoir (depth of 100 µm), is placed on top of the first layer and includes an inlet and outlet for culture medium perfusion. A micro-channel network placed at the inlet and outlet of each layer ensures homogeneous culture medium distribution within the biochip (Fig. 1A).

The PDMS biochip was manufactured using the replica molding process. First, photolithography was performed to create the mold masters of the bottom and top layer of the biochips using SU-8 photosensitive resin. Then, the PDMS prepolymer (in a mixture of 10:1 base polymer: curing agent; Sylgard 184, Dow Corning) was poured on to the SU-8 master and cured for 2 h at 75 °C. The surfaces of the PDMS layers obtained were activated with reactive air plasma (1 min; Harrick Scientific) and brought together immediately to form an irreversible

seal.

2.2. Pancreatic islets isolation

Islets of Langerhans were isolated from male Wistar rats (8–9 weeks old, 200–300 g) (CLEA Japan, Inc, Tokyo, Japan) following a slight modification to the protocol described by Yonekawa et al. (2006) and Kiba et al. (2013). All animal experimentation procedures were carried out in accordance with the guidelines of the University of Tokyo and the Japanese Ministry of Education.

The rats were anesthetized with isoflurane inhalation solution (Pfizer). After clamping of all irrigation blood vessels, the enzymatic solution (Liberase™ TL by Roche) was injected through the bile duct, previously identified and clamped. After the pancreatectomy, there was selective chemical digestion of the organ at 37 °C for 30 min with Liberase TL/ET-K solution (ET-Kyoto solution, Otsuka Pharmaceutical). The digestion was followed by washing and purification steps using a discontinuous OptiPrep® (Sigma-Aldrich) density gradient. The islets of Langerhans were then identified, individually hand-picked with a Pasteur pipette under a stereomicroscope (Leica S9 D), and transferred to a cold preservation solution made of UW solution (University of Wisconsin, Kneteman et al., 1990) complemented with Miraclid (Mochika pharmacy, Japan) and heparin (Mochika pharmacy, Japan). After assessing and counting the islets, the tissue was stored at 4 °C until starting the culture in order to maintain full functional properties as shown in Kimura et al. (2013).

2.3. Pancreas on chip and petri culture

The biochips and perfusion circuits (silicone/Teflon tubing and bubble trap) were sterilized by autoclaving and dried in an oven. The biochips were then assembled with the perfusion system and filled with culture medium in order to remove air bubbles and moisturize the circuits. The bubble trap was used as a reservoir interconnected to the biochips by the silicone/Teflon tubing of 0.65 mm in diameter. The preconditioning process was carried out for 1 h at 37 °C in the incubator. The entire setup is presented in Fig. S1 (supplementary file).

The pancreatic islets in the preservation solution were washed with cold culture medium and gently diluted in the appropriate amounts in order to ensure fair and even distribution of the tissue in the biochips and Petri culture. The estimated number of islets per biochip or well is ≈ 40. In order to minimize damage to the islets, wide orifice pipette tips with low binding were used throughout the handling process. Once the islets were loaded in the biochips from the inlet port or seeded in the 24-well plate, the counting step took place under the microscope in order to keep a record of the islets per biochip and/or well. The cultures were continuously maintained at 37 °C in a 5% CO_2 supplied incubator.

Two groups of study (biochip and Petri) and 4 conditions were established: Petri control; Petri with GLP-1; biochip control and biochip with GLP-1. The basal culture medium used in our study were the classic RPMI 1640 Medium (Gibco, 10 mM of glucose) supplemented with 10% FBS (Gibco), 100 units/mL of penicillin, 100 mg/mL streptomycin (Gibco) and GlutaMAX™ (Gibco™) at 10 mM. For the hormone-stimulated media, GLP-1 (Peprotech, USA) was added for a final concentration of 100 nM. The biochips were perfused in a circuit loop containing ≈2 ml of culture medium with a peristaltic pump (flow rate of 20 μL/min). The medium was renewed every 2 days. In static conditions, the islets were seeded in 1 mL of medium/well and the culture medium was exchanged every day.

2.4. Islets viability

At the end of the experiment, the islets were incubated in a solution of propidium iodide (PI) at 4.5 μmol/L and calcein-AM at 2 μmol/L (Cellstain kit, Dojingo) in RPMI 1640 medium for 30 min in the dark. Then, the samples were washed with RPMI 1640 medium and observed under an epifluorescence microscope (Olympus, Japan). The size of necrotic core was quantified by ImageJ software (NIH, Bethesda, Maryland) using the collected images. The area of the cells stained with PI was measured and normalized by the islet area.

2.5. RTqPCR assays

Total RNAs were extracted and purified from samples using a hybrid protocol that combines Trizol™ Reagent (Life Technologies) and RNeasy Mini Kit (QIAGEN 74104) following the manufacturer's instructions. The concentrations and qualities of the RNAs extracted were assessed using a BioSpec-nano (Shimadzu Scientific Instruments). Reverse-transcription into cDNA was performed from 0.5 μg of total RNA using the ReverTra Ace qPCR RT Master Mix with gDNA Remover (TOYOBO). Real-time quantitative PCR was then performed with the THUNDERBIRD SYBR qPCR Mix (TOYOBO) according to the manufacturer's protocol and a StepOnePlus Real-Time PCR system (Applied Biosystems). The primer sequences of the genes are shown in Table S1 β-Actin was used as the reference gene and fresh isolated islets (days 0) as the reference sample for the normalization of gene expression data.

2.6. Immunostaining

Immunofluorescent detection was investigated at the end of the experiment (day 5). We selected to stain the GCK because the coding protein glucokinase is a key enzyme using glucose as substrate. We also stained two important markers in the pancreatic islets: insulin and glucagon that are markers of β-cells and α-cells, respectively.

After transfer to an untreated TCPS 24-well plate (not a plate treated for cell cultures, to prevent the islet cells from attaching to the plate), the islets were washed with phosphate buffer saline solution (PBS) and fixed in paraformaldehyde 4% at 4 °C for 24 h. In order to perform the immunostaining in a 3D structure, the islets were permeabilized with 1% Triton X100 in PBS for 3 h at 4 °C and washed 3 times with PBS for 30 min. Then, the islets were blocked with a gelatin buffer for 24 h at 4 °C. Primary antibodies (anti-insulin [ab6995, Abcam], anti-glucagon [ab167078, Abcam] and anti-glucokinase [sc-17819, Santa Cruz]) were incubated for 48 h at 4 °C in a BSA/PBS solution. Secondary antibodies coupled with Alexa Fluor fluorochromes (Glucagon: anti-rabbit Alexa Fluor 680 [A-21109, ThermoFisher], Insulin: anti-mouse Alexa Fluor 594 [ab150116, Abcam] and Glucokinase GCK: anti-mouse Alexa Fluor 647 [ab150107, Abcam]) were further incubated overnight in a BSA/PBS solution at 4 °C in the dark. Finally, the nuclei were stained with DAPI (342-07431, Dojindo) at 1/1000 for 30 min at room temperature (RT) in the dark. All the incubations and washing steps were carried out using a shaker. Observations were made with an Olympus IX-81 confocal laser-scanning microscope.

2.7. Functional assays

2.7.1. Glucose-stimulated insulin secretion (GSIS) assays

After 4 days of culture, we performed a low high glucose stimulation. In biochips, the culture medium was removed from the bubble trap and the circuit (biochip, tubing and bubble trap) was washed with a 0-glucose solution (D-MEM, No Glucose, Wako) for 2 h. This washing 0-glucose solution was removed from the bubble trap, and 1 mL of fresh 0-glucose was added and perfused for 2 h. After this low glucose perfusion, the islets were exposed to a high glucose culture medium for 2 h (D-MEM high Glucose, Wako, 25 mM of glucose). For that purpose, the low glucose solution was removed from the bubble trap and replaced with 1 mL of high glucose. In a Petri dish, this protocol led to 2 h of 0-glucose exposure, followed by another 2 h of 0-glucose exposure and finally 2 h of high glucose stimulation. At the end of the assays, basal media were re-established for all conditions.

2.7.2. Glucagon-like peptide-1 (GLP-1) stimulations

In order to test the response of the islets to hormone stimulation, we exposed the cultures to GLP-1. For that purpose, we followed the same protocols described in section 2.3, to which we added 100 nM of GLP-1 (Peprotech, USA) at each culture medium change step.

2.8. Insulin, glucagon and C-peptide measurements

The hormones released into the culture medium were assessed using ELISA assays, following the manufacturer's protocol. To measure each hormone concentration, we used a rat Insulin ELISA kit (10-1250-01; Mercodia) for insulin, a Glucagon DuoSet ELISA kit (DY1249; R&D Systems) with the DuoSet ELISA Ancillary Reagent Kit 2 (DY008; R&D Systems) for glucagon, and a rat C-Peptide ELISA kit (10-1172-01; Mercodia) for C-peptide.

2.9. Glucose and lactate quantification

Glucose and lactate were measured using an YSI 2950 Biochemistry Analyzer. For that purpose, 150 μL of culture medium were inserted into the analyzer. Measurements were based on a direct reading of L-lactate (L-lactic acid) and glucose in the culture medium by the YSI enzyme sensors, as the enzymes L-lactate oxidase, and glucose oxidase are respectively immobilized in the lactate and glucose sensors.

2.10. Statistics

All experiments were repeated at least three times, and the data are presented as the mean ± SD. For the overall experimental campaign, we have used 6 rats corresponding to 6 independent experiments. The rat islets were used in 6–12 biochips according to the experiments. The RTqPCR were performed on three samples for each condition in three independent experiments ($n = 3 \times 3$). The Kruskal Wallis test was performed for the statistical analysis. Data with P-values < 0.05 were identified as statistically significant.

3. Results

3.1. Characterization of islet biochip cultures when compared to petri dish cultures

3.1.1. Viability assay showed highly viable islets in the biochip

After extraction (Fig. 2A), the islets were cultivated in Petri dishes (Fig. 2B) and in biochip dynamic culture for 5 days (Fig. 2C). In the device, the islets sedimented into the microwells located at the bottom of the culture chamber. Then, we confirmed that the islets had not been washed away by the flow rate after 5 days of perfusion. Indeed, the number of islets seeded at the beginning of the experiments and collected at the end of the perfusion remained similar, as shown in Fig. 2D. In addition, the islets presented a round shape at the end of the perfusion (Fig. 2B and C and Fig. S2, supplementary file). The typical size of the islets was about 150 ± 50 μm.

The fluorescent images of islets stained with calcein AM/PI are presented in Fig. 2E. We found a different size to the necrotic core of the islets between static and dynamic conditions after 5 days of culture. Nevertheless, the viability was higher in the islets cultivated in the biochips inasmuch as the IP staining was weaker when compared to Petri situations. The quantification of the necrotic core showed that the proportion of dead cells in dynamic biochip was significantly lower when compared to the Petri culture. The normalized size of necrotic core was of 0.34 ± 0.15 and 0.12 ± 0.03 for islets cultivated in Petri and biochip, respectively (Fig. S3, supplementary file).

3.1.2. RTqPCR analysis revealed higher mRNA levels of pancreatic islets markers in biochip cultures

At the end of the experiments, we compared the mRNA levels of the cells in the islets cultivated in biochips and Petri dishes (Fig. 3). The markers related to maintaining islet differentiation, such as *Reg3a* and *Neurod*, were upregulated in the biochips when compared to the Petri cultures (fold change, FC, of 190 and 13, respectively). In addition, the markers related to islet functions such as *App* (4.3 FC), *Ins1* (1.7 FC), *Sst* (2.8 FC) and *Gcg* (2.1 FC) were also upregulated in the biochips. Finally, the levels of several receptors and transporters such as *Gcgr*, *Insr*, and *Glut2* were 3.2–5.5 times higher in the biochip compared to the Petri dishes (Fig. 3).

3.1.3. Immunostaining confirmed the expression of pancreatic islets markers and glucose regulators in both biochips and petri dishes

The immunostaining of the islets, prior to inoculation in the biochips, demonstrated that the islets were positive for insulin and glucagon (day 0, Fig. 4A and Fig. S4 in supplementary file). At the end of the experiments, the islets from the Petri dishes and biochips were positive for insulin and glucagon as shown in Fig. 4A and Fig. S4 (supplementary file). We observed three types of cell populations, insulin positive cells, glucagon positive cells and a third subpopulation expressing both insulin and glucagon (those bihormonal cells may reflect a partial switch from β−cells to α-cells, supplementary file). We confirmed also that the islets in both culture modes were positive for GCK (Fig. 4B and Fig. S5 in supplementary file), consistently with the composition of the culture medium containing 10 mM of basal glucose (nb: GCK, in the pancreas, plays a role in glucose-stimulated insulin secretion).

3.1.4. Functional assays revealed higher insulin secretion in the islets in the biochips

The basal functionality of the islets was demonstrated by measuring insulin, C-peptide and glucagon secretion. At the end of each experiment, the islets were counted to normalize the data. We found that the insulin concentration in the culture medium decreased in both biochips and Petri dishes. However, the biochip cultures contributed to maintaining relatively high levels for all experiments until day 4, whereas a drop occur between day 3 and day 4 in Petri (Fig. 5A). Biochip cultures contributed to maintaining insulin secretion close to 130 ng/islet/day until day 4, and decreasing to 44 ng/islet/day at day 5. In the Petri dishes, we found a significant reduction in days 3 and 4, leading to measured secretion close to 30 ng/islet/day before dropping to 17 ng/islet/day at day 5. We also observed higher secretion of C-peptide in the biochips when compared to the Petri dish cultures, as shown in Fig. 5B. Secretion was about 5 times higher in the biochips from days 3–5. C-peptide secretion in Petri dishes decreased significantly since day 2, whereas it decreased only at day 5 in the biochips.

The glucagon levels were higher in the biochips than in the Petri dishes, as shown in Fig. 5C. Furthermore, the levels remained constant in the biochip cultures for 4 days of culture, close to 1000 pg/islet/day, before decreasing to 500 pg/islet/day on day 5. In the Petri dishes, glucagon secretion decreased from day 3 to day 4 and leading to a drop from 560 to 180 pg/islet/day between day 2 to day 5. The ratio between insulin and glucagon secretion is shown in Fig. 5D. In the biochips, the ratio increased from 130 to 250 between days 2 and 4, before dropping to 85 on day 5. In the Petri dishes, the ratio decreased continuously from 380 to 80, but with high intra and extra experiment variability.

Finally, glucose and lactate levels were measured during culture. As the culture medium was frequently changed during the experiments, we observed that glucose levels remained relatively stable and very high in our experiments. Both in the Petri dishes and biochips, we were unable to detect any significant glucose depletion (Fig. 5E). Furthermore, lactate production was higher in the biochips than in the Petri dishes (Fig. 5E).

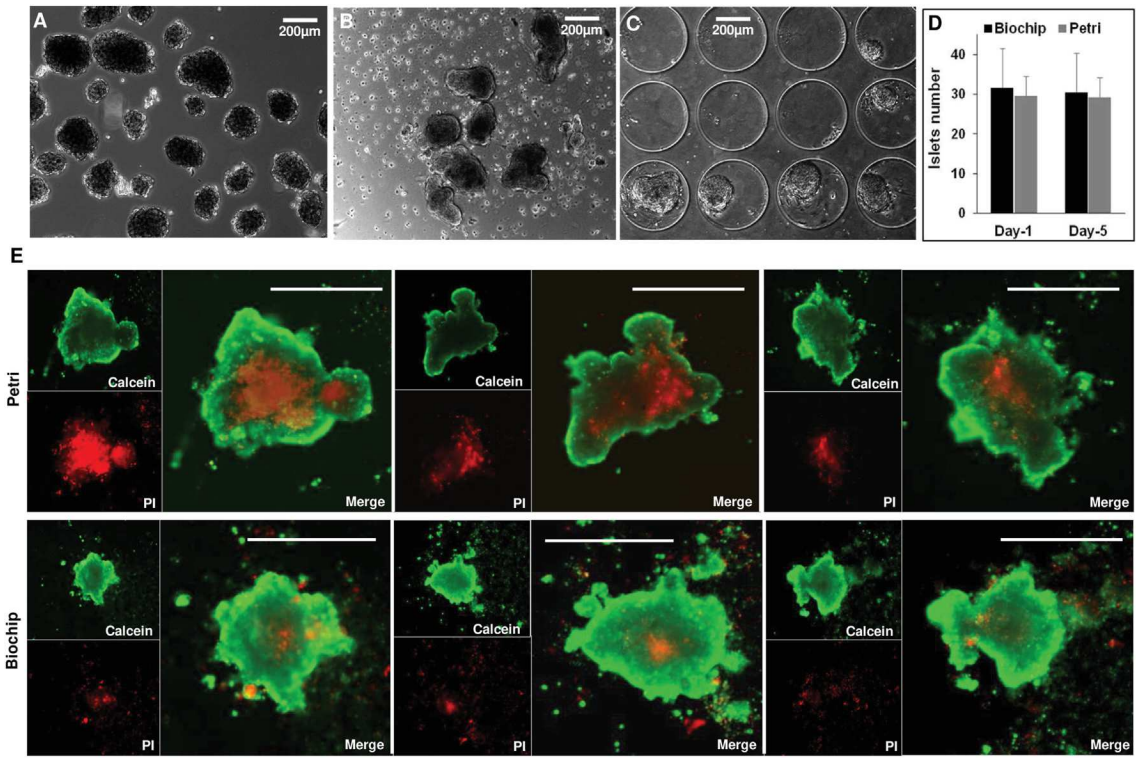

Fig. 2. Morphology of islets after extraction (A), after 5 days of culture in Petri (B) and after 5 days of culture in biochip (C); number of islets at days 1 and 5 in biochip and Petri (D); and calcein AM/propidium iodide staining of islets after 5 days of culture in Petri and biochip (E, PI: propidium iodide, scale bar: 100 µm).

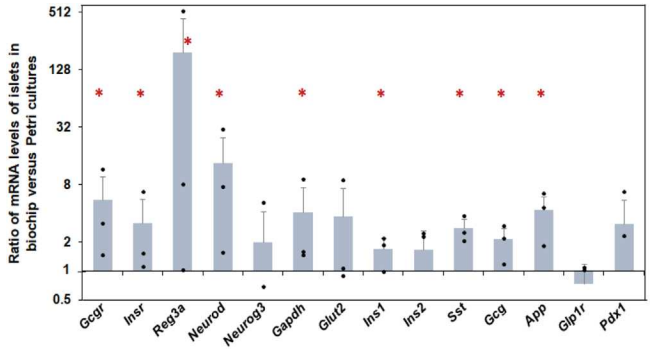

Fig. 3. Ratio (biochip/Petri) of mRNA levels of selected important pancreatic islets genes after 5 days of culture. *$P < 0.05$, mRNA level significantly different between biochip and Petri cultures (each dot correspond to one experiment (mean of 3 biochips/Petri); $n = 3 \times 3 = 9$).

3.2. Pancreatic islet response to stimulations demonstrated functional and active biochip culture conditions

3.2.1. Low-high glucose stimulations

After 4 days of culture, we performed a low-high glucose stimulation. The islets demonstrated lower insulin secretion in low glucose stimulation when compared to high glucose stimulation. To evaluate islets responsiveness to low/high glucose stimulation, we calculated the GSIS (glucose-stimulated insulin secretion) index by dividing insulin measured in high-glucose and low-glucose media (Fig. 5F). The GSIS index values were of 5 and 2.1 in the Petri dishes and biochip, respectively. These results indicate that glucose response of islets was maintained in both culture modes. However, we should mention that we observed wide variability in this assay inasmuch as some Petri dishes or biochips were not induced, thus leading to a significant error bar and dispersion.

3.2.2. Effect of glucagon-like peptide-1 (GLP-1)

The GLP-1 stimulation contributed to the modification of mRNA levels, both in Petri dishes and biochips (Fig. 6A). GLP-1 increased the mRNA levels of the receptors *Glp-1r*, *Gcgr*, and of the *Reg3a*, *Ins1*, *Ins2* and *Stt* genes in the biochips (when compared to non-treated biochip controls) and downregulated *Neurod*. In Petri dishes, we also found upregulation of *Gcgr*, *Insr, Ins2*, and downregulation of *Neurod* (Fig. S6, supplementary file). Furthermore, the mRNA levels in the GLP-1-treated biochips were upregulated when compared to GLP-1-treated Petri dishes (data not shown).

Fig. 6B shows the insulin immunostaining of islets treated by GLP-1. The data demonstrated high fluorescence intensity in GLP-1-treated Petri and biochip. We also found that the levels of the GCK protein in the islets were not over-expressed by the GLP-1 treatment (Fig. 6B). At the functional levels, insulin secretion was increased in both Petri dishes and biochips by the GLP-1 treatments (Fig. 7A). On days 2, 3 and 4, the levels of insulin in the biochips were up to 3 times higher than those attained in control. However, after 5 days, this induction was weaker (2 times). We then performed the low-high glucose stimulation tests after pre-treatment with GLP-1. As expected, GLP-1 did not inhibit the effect of the high/low glucose stimulations and maintained a high level of insulin production in the biochips under high glucose stimulation (Fig. 7B). In this assay, the low/high glucose stimulation led to an insulin over production of 2.2 and 4 in biochips and Petri, respectively (GSIS index of 2.24 and 4, respectively). Furthermore, we did not observe variability in the assay when compared to the untreated conditions (cf. Fig. 5F).

4. Discussion

In this study, we investigated the performance of islets of Langerhans in a closed loop microfluidic system. Several investigations have reported microfluidic techniques for keeping islet or spheroid cultures on chip, including the pancreas (Tan and Takeuchi, 2007; Zbinden et al., 2020; Lee et al., 2018; Mohammed et al., 2009). Those

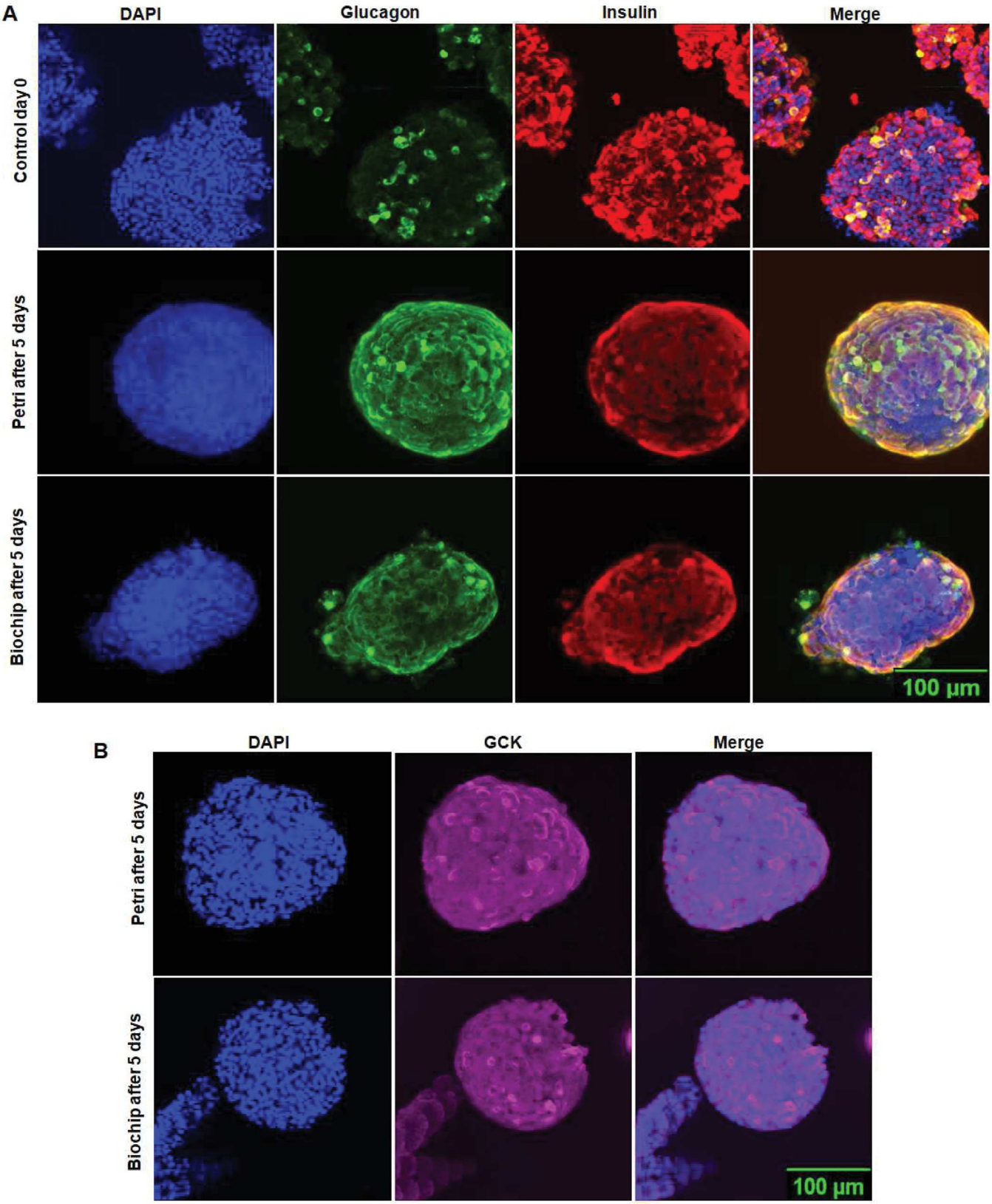

Fig. 4. Islets immunostainings: (A) DAPI, glucagon, insulin and merge at day 0 and after 5 days of culture in biochip and petri; (B) DAPI, GCK and merge after 5 days of culture in biochip and Petri.

devices are based on a flow trapping process (Tan and Takeuchi, 2007; Zbinden et al., 2020). We built a simple culture biochip where the pancreatic islets can be trapped by sedimentation in the bottom microstructure. This type of trapping was also reported by Lee et al. (2018). In our biochip, the microstructure contributed to create an array of 600 microwells allowing to trap an important quantity of islets.

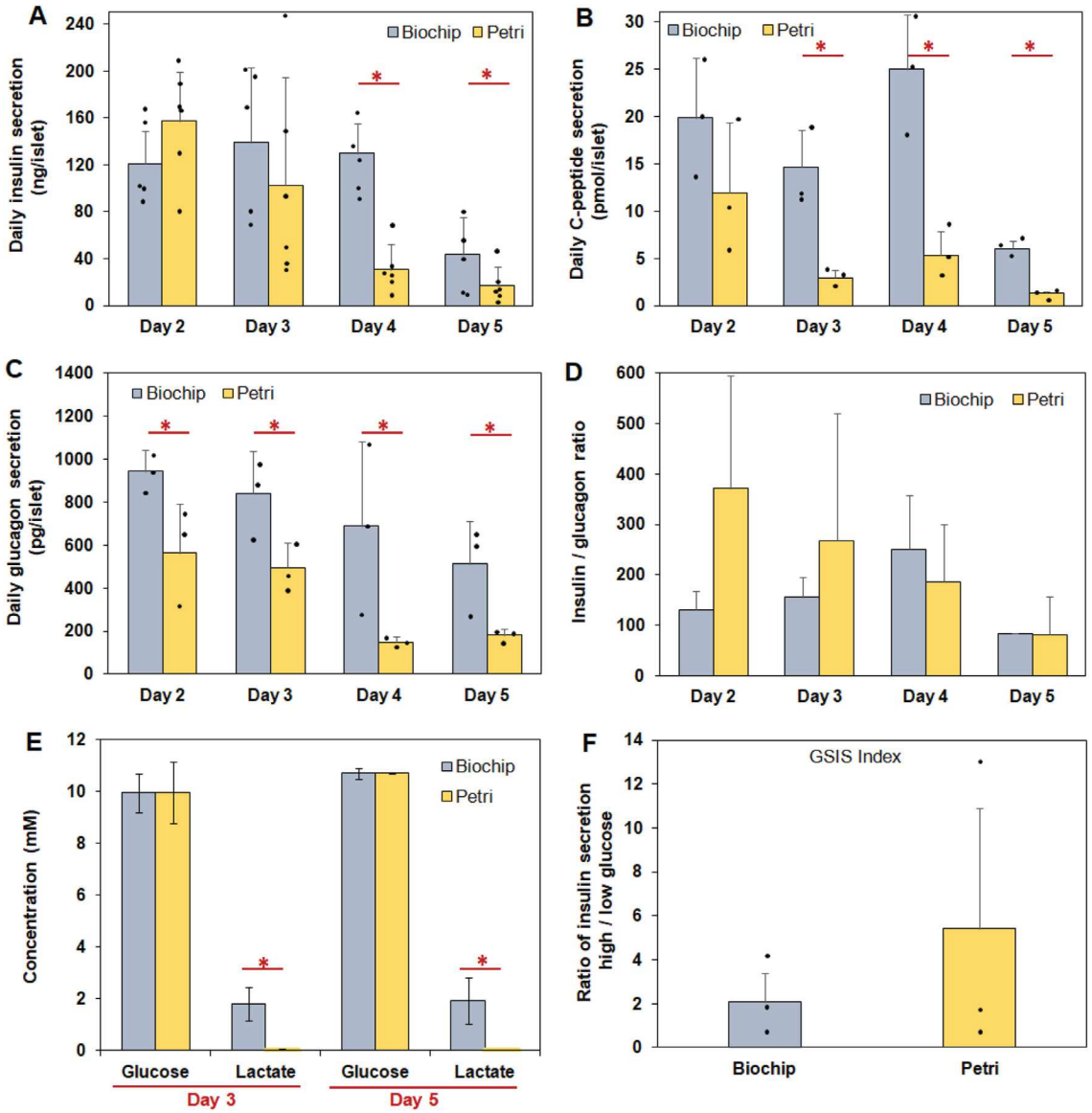

Fig. 5. (A) Insulin, (B) C-peptide and (C) glucagon secretion during 5 days of culture in biochip and Petri (n = 6 for insulin and n = 3 for C-peptide and glucagon, $^*P < 0.05$); (D) insulin/glucagon ratio; (E) glucose and lactate production in Petri and biochip after 3 and 5 days of culture (n = 3, $^*P < 0.05$) and (F) ratio of insulin production (high/low, GSIS index) in biochip and Petri after high/low glucose stimulations (n = 3, $^*P < 0.05$). GSIS: glucose-stimulated insulin secretion.

The depth of microwells made it possible to protect the islets from flow circulation and thus prevent them from being washed away and from mechanical damage. As a result, we maintained a constant number of islets between the beginning and the end of the perfusion. Furthermore, due to sedimentation in the microwells, the islets were protected from the fluid shear stresses created by the laminar flow.

In biochip, we observed higher viability for the cells located in the center of the pancreatic islets when compared to the Petri dish cultures. This was illustrated by the viability assay in which a larger number of dead cells was observed in the center of the islets when they were cultivated in Petri dishes. Central necrosis and apoptosis in pancreas islets are due mainly to the high density of the tissue and the lake irrigation as has been widely reported in literature (Giuliani et al., 2005; Moritz et al., 2002). Several hypotheses are proposed to explain central necrosis and apoptosis in pancreatic islets (and also in cell spheroids), including deprivation of oxygen, nutrients and serum as a result of limited diffusion (Giuliani et al., 2005). In the case of the pancreatic islets, the blood micro-vessels usually reach the center of the structure *in vivo* but the microvasculature gets closed in *ex vivo* tissue (Jansson et al., 2016). In parallel, microfluidic cultures have been shown to improve the viability of spheroid tissue by reducing the central necrotic core thanks to control of local glucose concentrations and local oxygenation through the dissolved oxygen provided by the medium flows (Barisam et al., 2018; Baye et al., 2017). As a result, those literature reports appeared consistent with our findings.

In our investigation, we found that the microfluidic culture maintained and improved pancreatic regeneration and maturation markers of the rat islet cells. This was illustrated by higher levels of mRNA in important pancreatic islet markers, including receptor genes (*Gcr* and *Insr*), hormone secretion-related genes (*App*, *Sst* and *Ins1*) and differentiation genes (*Neurod* and *Reg3a*). More particularly, we found a 190-fold upregulation of *Reg3a*, which is an islet regeneration marker (Coffey et al., 2014) involved in the pro-islet gene cascade and their protection against induced diabetes mellitus (Xiong et al., 2011). In addition, *Neurod* was 13 times higher in the biochips compared to Petri dish levels. *Neurod* is an important gene (an insulin trans activator) required to maintain functional maturity in pancreatic beta cells, including insulin production through *Ins1* (Gu et al., 2010). We also

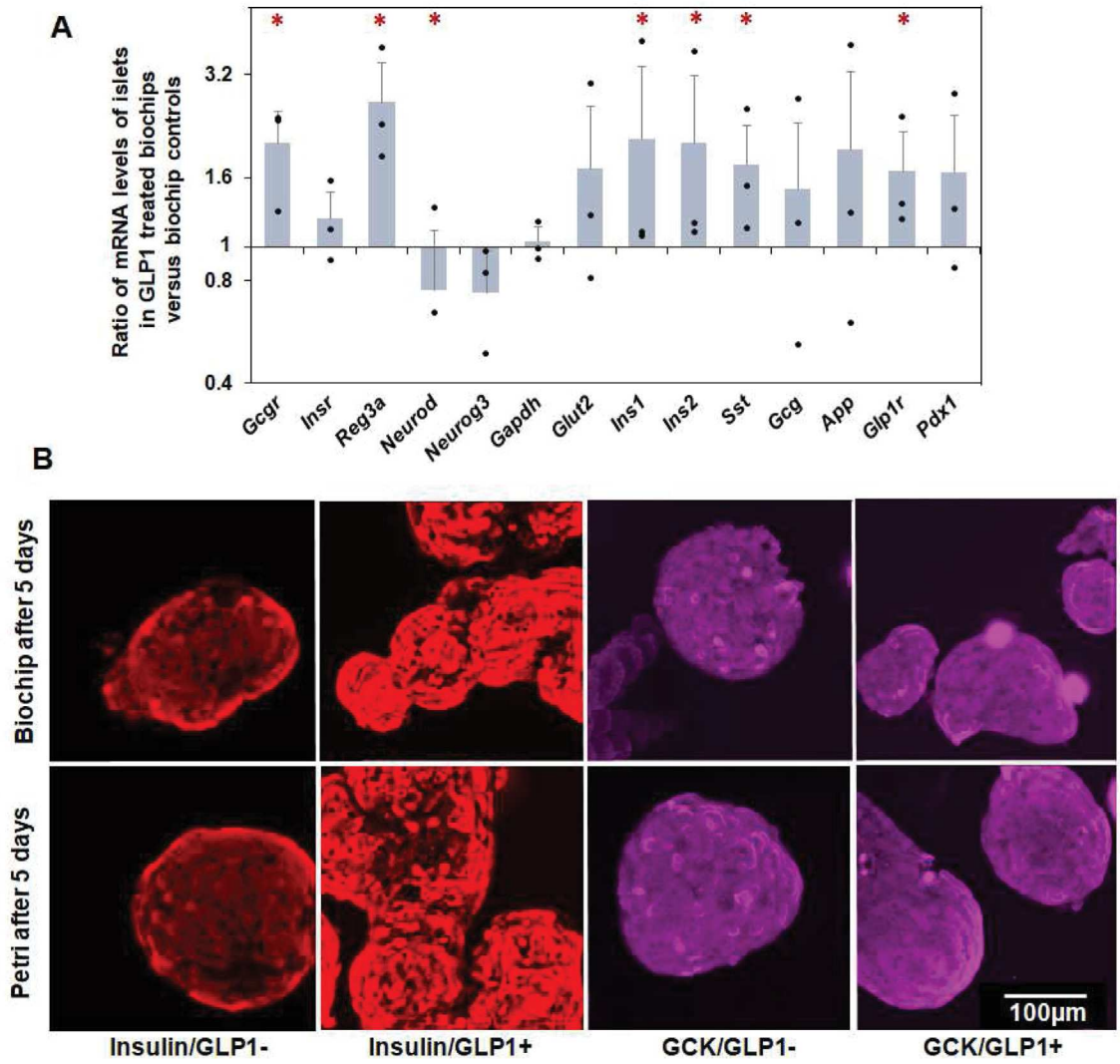

Fig. 6. (A) Ratio of mRNA levels (GLP1 treated biochip/control biochip) of selected pancreatic islets genes after GLP1 stimulation; and (B) insulin and GCK immunostainings in controls and GLP1 treated biochip/Petri. *$P < 0.05$, mRNA level significantly different between GLP1 treated biochip and control biochip (each dot correspond to one experiment (mean of 3 biochips/Petri); $n = 3 \times 3 = 9$).

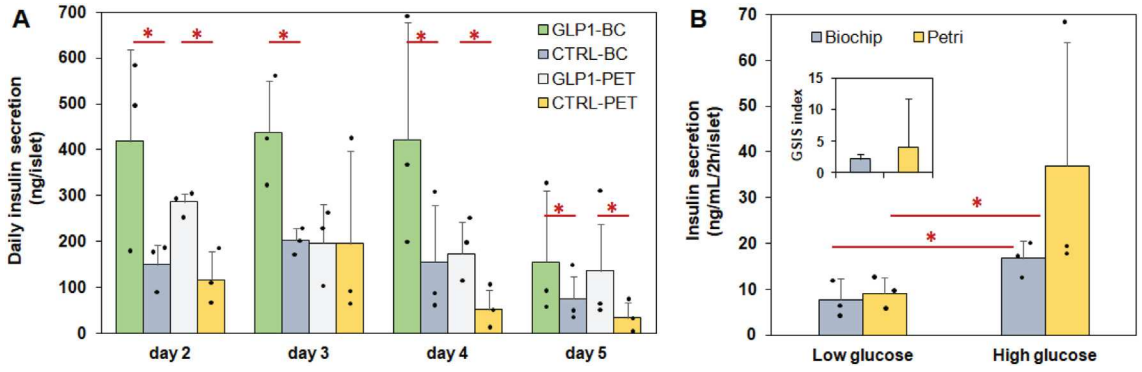

Fig. 7. (A) Insulin secretion in controls and GLP1 treated biochip and Petri during 5 days of culture ($n = 3$, *$P < 0.05$); and (B) insulin secretion and GSIS index in GLP1 treated biochip and Petri during high/low glucose stimulations ($n = 3$, *$P < 0.05$). GSIS: glucose-stimulated insulin secretion.

consistently found upregulation of the *Ins1* gene in the biochips, which is consistent with *Ins1* silencing in *Neurod* KO mice (Gu et al., 2010). *Neurod* KO-mice expressed the *Ins2* gene and were thus able to produce insulin in a glucose stimulation test, which also appeared consistent with our findings in which *Ins2* was commonly expressed in both the Petri dishes and the biochips (Gu et al., 2010).

In parallel, an over-expression of the insulin receptor *Insr* was observed. *Insr* is involved in controlling glucose-stimulated insulin secretion *via* its relationship with insulin gene expression, *Glut2* and *Pdx1* (Wang et al., 2018). We consistently observed a tendency for higher mRNA levels in the *Glut2* and *Pdx1* genes in the biochips. The upregulation of *Gcgr*, the glucagon receptor, in the biochips also indicated a

probable beneficial effect of the microfluidic cultures on the alpha cells inasmuch as the lack of glucagon receptors is correlated with several pancreas disorders and alteration to glucose homeostasis, such as hyperplasia and hyperglucagonemia (Charron and Vuguin, 2015).

At the functional level, we analyzed the performances of the pancreas islets when they were cultivated in the biochips. At first, this was illustrated by the kinetics of the secretion of insulin in the culture medium. Although the overall secretion decreased between the first day and fifth day of culture in both culture conditions, the biochip levels remained higher when compared to those of the Petri dishes. Secondly, the high/low glucose stimulation assay demonstrated that islets response to stimuli was preserved in our biochip culture. However, in the biochips, the protocol required an extended washing process to remove the insulin and remaining glucose from the basal culture medium in the perfusion circuit (mainly due to the dilution of high glucose solution in washing solution that would lead to bias stimulation). This need of washing process synchronization in the biochips, when compared to conventional Petri dishes, has already been reported in pancreas-on-chip investigations (Zbinden et al., 2020). Nevertheless, enhancements of basal islets functions such as insulin secretion and glucose-induced insulin secretion in microfluidic devices have been observed consistently in the literature (Sankar et al., 2011). In our dataset, this over-secretion of insulin was not correlated with over-expression of *Gck*, as demonstrated by the immunostaining. The glucose-stimulated insulin secretion was regulated by the rate of glucose metabolism within β cells, and a key event in this process is the phosphorylation of glucose by glucokinase (the coding gene is *Gck*, Wu et al., 2004). Although we worked in a closed loop perfusion circuit, the flow rate led to continuously renewing the culture medium locally in the biochips. Furthermore, the level of glucose remained high in the medium, probably due to the number of islets. The microfluidic culture completely modulated the chemical cellular microenvironment (*via* a complex gradient of molecules, a balance between diffusion and convection, cellular consumption) leading to complex signals (Young and Beebe, 2010; Halldorsson et al., 2015). In parallel, the microwells almost certainly influenced the local nutrient islets' microenvironment (a balance between glucose consumption, glucose renewal, secreted insulin concentration, etc …). As a result, additional local measurements (*via* integrated sensors) and numerical simulations are needed to understand the complex kinetics of insulin secretion in relation to local glucose concentrations in our biochips.

Finally, we tested the effect of the glucagon-like peptide-1 (GLP-1) in both culture conditions. GLP-1 physiologically induces glucose-dependent insulin secretion from β-cells and GLP-1 analogues improve hyperglycemia in T2DM patients (Drucker and Nauck, 2006; DeFronzo et al., 2005, Vilsbøll et al., 2007). Furthermore, GLP-1 treatment increases *Gck* activity (Ding et al., 2011). However, long term GLP-1 exposure (about 18 h) also resulted in the promotion of the metabolic reprogramming of β-cells through mTOR-dependent HIF signaling, and independently of *Gck* post-translational activation (Carlessi et al., 2017). In the present study, GLP-1 stimulation clearly upregulated several pancreatic islet genes such as *Glp-1r* and *Gcgr,* in both Petri dishes and biochips. In addition, those mRNA levels were upregulated in the biochips compared to the Petri dishes when the GLP-1 was loaded. At the functional level, GLP-1 induced an increase in insulin secretion in both culture modes (as confirmed by the immunostaining of insulin and the insulin extracellular concentrations in the medium). The secretion levels in the culture medium were found to be higher in the biochips. However, we did not find any of the inhibitory effect we expected in the alpha cells of the islets of Langerhans (glucagon secretion) (Tan and Takeuchi, 2007). In our biochips, we found mRNA *Glut2* over-expression compared to the Petri dishes, leading to the suspicion of higher glucose transport, and thus metabolism, in the islets. We did not find an effect of GLP-1 on the *Gck* at the immunostaining fluorescent level. Although these findings seems consistent with the observations made by Carlessi et al. (2017), more extensive investigations are needed to confirm the underlying mechanism in biochips.

5. Conclusion

In this work, we studied the behavior of rat islets of Langherans when cultivated in microfluidic biochips or in Petri dishes. The microfluidic biochips cultures maintained high islet viability throughout the 5 days of culture. More particularly, several important pancreatic islet genes, including *Reg2a*, *Neurod*, *Insr*, *Gcgr*, *Glut2*, *Ins1*, *App* and *Stt* were overexpressed in biochips cultures (compared to islets cultivated in Petri). The islets were able to secrete insulin and glucagon, as well as to respond to GLP-1 stimulation and high-low glucose test. Furthermore, the levels of insulin secretion appeared higher in biochips when compared to the Petri dishes. Our dataset illustrated the fact that the microfluidic culture is beneficial for maintaining *in vitro* maturation and functionality of islets of Langerhans. We believe that our results are encouraging for the development of functional pancreas *in vitro* models using the advantages of organ-on-chip technology.

CRediT authorship contribution statement

Amal Essaouiba: Methodology, Investigation, Validation, Formal analysis, Conceptualization, Data curation, Writing - original draft. **Teru Okitsu:** Resources, Validation. **Rachid Jellali:** Methodology, Visualization, Writing - review & editing. **Marie Shinohara:** Resources. **Mathieu Danoy:** Resources. **Yannick Tauran:** Resources. **Cécile Legallais:** Supervision. **Yasuyuki Sakai:** Supervision. **Eric Leclerc:** Funding acquisition, Project administration, Supervision, Conceptualization, Visualization, Writing - review & editing.

Declaration of competing interest

The authors declare no conflict of interests.

Acknowledgments

A part of the project was funded by the French National Research Agency (ANR-16-RHUS-0005). Amal Essaouiba's PhD grant was supported by the French Ministry of Research and Higher Education. We thank the CNRS/IIS UMI 2820, the UMR 7338 and the universite de technologie de Compiegne for their mobility supports to A. Essaouiba to Tokyo.

Appendix A. Supplementary data

Supplementary data to this article can be found online at https://doi.org/10.1016/j.mce.2020.110892.

References

Aghamaleki, M.A., Hajiahmadi, M., Pornasrollah, M., Oruji, Z., Aghajanpour, F., 2019. Effect of vitamin D supplementation on pancreatic B -cell function in patients with Type 1 Diabetes Mellitus and vitamin D deficiency: a clinical trial study. Int. J. Pediatr. 7, 8977–8984.

Artunc, F., Schleicher, E., Weigert, C., Fritsche, A., Stefan, N., Häring, H.U., 2016. The impact of insulin resistance on the kidney and vasculature. Nat. Rev. Nephrol. 12, 721–737.

Baker, K., 2016. Comparison of bioartificial and artificial pancreatic transplantation as promising therapies for Type I Diabetes Mellitus. Biosci. Horiz. 9, hzw002.

Barisam, M., Saidi, M.S., Kashaninejad, N., Nguyen, N.T., 2018. Prediction of necrotic core and hypoxic zone of multicellular spheroids in a microbioreactor with a U-shaped barrier. Micromachines 9, 94.

Bauer, S., Wennberg Huldt, C., Kanebratt, K., Durieux, I., Gunne, D., Andersson, S., Ewart, L., Haynes, W., Maschmeyer, I., Winter, A., Ämmälä, C., Marx, U., Andersson, T., 2017. Functional coupling of human pancreatic islets and liver spheroids on-a-chip: towards a novel human ex vivo type 2 diabetes model. Sci. Rep. 7, 14620.

Baye, J., Galvin, C., Shen, A.Q., 2017. Microfluidic device flow field characterization around tumor spheroids with tunable necrosis produced in an optimized off-chip process. Biomed. Microdevices 19, 59.

Bhatia, S.N., Ingber, D.E., 2014. Microfluidic organs-on-chips. Nat. Biotechnol. 32, 760–772.
Brooks, J.C., Ford, K.I., Holder, D.H., Holtan, M.D., Easley, C.J., 2016. Macro-to-micro interfacing to microfluidic channels using 3D-printed templates: application to time-resolved secretion sampling of endocrine tissue. Analyst 141, 5714–5721.
Carlessi, R., Chen, Y., Rowlands, J., Cruzat, V.F., Keane, K., Egan, L., Mamotte, C., Stokes, R., Gunton, J., Homem de Bittencourt, P.I., Newsholme, P., 2017. GLP-1 receptor signalling promotes β-cell glucose metabolism via mTOR-dependent HIF-1α activation. Sci. Rep. 7, 2661.
Charron, M.J., Vuguin, P.M., 2015. Lack of glucagon receptor signaling and its implications beyond glucose homeostasis. J. Endocrinol. 224, R123–R130.
Coffey, R., Nam, H., Knutson, M., 2014. Microarray analysis of rat pancreas reveals altered expression of Alox15 and regenerating islet-derived genes in response to iron deficiency and overload. PLoS One 9, e86019.
DeFronzo, R.A., Ratner, R.E., Han, J., Kim, D.D., Fineman, M.S., Baron, A.D., 2005. Effects of exenatide (exendin-4) on glycemic control and weight over 30 weeks in metformin-treated patients with type 2 diabetes. Diabetes Care 28, 1092–1100.
Ding, S.Y., Nkobena, A., Kraft, C., Markwardt, M., Rizzo, M.A., 2011. Glucagon-like peptide 1 stimulates post-translational activation of glucokinase in pancreatic cells. J. Biol. Chem. 286, 16768–16774.
Drucker, D.J., Nauck, M.A., 2006. The incretin system: glucagon-like peptide-1 receptor agonists and dipeptidyl peptidase-4 inhibitors in type 2 diabetes. Lancet 368, 1696–1705.
Efanov, A.M., Sewing, S., Bokvist, K., Gromada, J., 2004. Liver X receptor activation stimulates insulin secretion via modulation of glucose and lipid metabolism in pancreatic beta-cells. Diabetes 53, S75–S78.
Ghaemmaghami, A.M., Hancock, M.J., Harrington, H., Kaji, H., Khademhosseini, A., 2012. Biomimetic tissues on a chip for drug discovery. Drug Discov. Today 17, 173–181.
Giuliani, M., Moritz, W., Bodmer, E., Dindo, D., Kugelmeier, P., Lehmann, R., Gassmann, M., Groscurth, P., Weber, M., 2005. Central necrosis in isolated hypoxic human pancreatic islets: evidence for postisolation ischemia. Cell Transplant. 14, 67–76.
Gu, C., Stein, G., Pan, N., Goebbels, S., Hörnberg, H., Nave, K.A., Herrera, P., White, P., Kaestner, K., Sussel, L., Lee, J., 2010. Pancreatic β cells require NeuroD to achieve and maintain functional maturity. Cell Metabol. 11, 298–310.
Halldorsson, S., Lucumi, E., Gómez-Sjöberg, R., Fleming, R.M.T., 2015. Advantages and challenges of microfluidic cell culture in polydimethylsiloxane devices. Biosens. Bioelectron. 63, 218–231.
Huh, D., Torisawa, Y.S., Hamilton, G.A., Kim, H.J., Ingber, D.E., 2012. Microengineered physiological biomimicry: organs-on-chips. Lab Chip 12, 2156–2164.
International diabetes federation official. web site. https://www.idf.org/.
Jansson, Leif, Barbu, Andreea, Bodin, Birgitta, Drott, Carl Johan, Espes, Daniel, Gao, Xiang, Grapensparr, Liza, Källskog, Örjan, Lau, Joey, Liljebäck, Hanna, Palm, Fredrik, Quach, My, Sandberg, Monica, Strömberg, Victoria, Ullsten, Sara, Carlsson, Per-Ola, 2016. Pancreatic islet blood flow and its measurement. Ups J Med Sci 121 (2). https://doi.org/10.3109/03009734.2016.1164769.
Jellali, R., Essaouiba, A., Leclerc, E., Legallais, C., 2020. Chapter 4 - membrane bioreactors for bio-artificial pancreas. In: Basile, A., Annesini, M.C., Piemonte, V., Charcosset, C. (Eds.), Current Trends and Future Developments on (Bio-) Membranes. Elsevier, pp. 77–108.
Jouvet, N., Estall, J.L., 2017. The pancreas: bandmaster of glucose homeostasis. Exp. Cell Res. 360, 19–23.
Jun, Y., Lee, J., Choi, S., Yang, J.H., Sander, M., Chung, S., Lee, S.H., 2019. In vivo-mimicking microfluidic perfusion culture of pancreatic islet spheroids. Sci. Adv. 5, eaax4520.
Kiba, T., Tanemura, M., Yagyu, K., 2013. High-quality RNA extraction from rat pancreatic islet. Cell Biol. Int. Rep. 20, 1–4.
Kimura, Y., Okitsu, T., Xibao, L., Teramae, H., Okonogi, A., Toyoda, K., Uemoto, S., Fukushima, M., 2013. Improved hypothermic short-term storage of isolated mouse islets by adding serum to preservation solutions. Islets 5, 45–52.
King, A., Bowe, J., 2016. Animal models for diabetes: understanding the pathogenesis and finding new treatments. Biochem. Pharmacol. 99, 1–10.
Kneteman, N.M., Warnock, G.L., Evans, M.G., Dawidson, I., Rajotte, R.V., 1990. Islet isolation from human pancreas stored in UW solution for 6 to 26 hours. Transplant. Proc. 22, 763–764.
Kumar, M., Melton, D., 2003. Pancreas specification: a budding question. Curr. Opin. Genet. Dev. 13, 401–407.
Lee, S.H., Hong, S., Song, J., Cho, B., Han, E.J., Kondapavulur, S., Kim, D., Lee, L.P., 2018. Microphysiological analysis platform of pancreatic islet β-cell spheroids. Adv. Healthc. Mater. 7, 1701111.
Li, X., Brooks, J.C., Hu, J., Ford, K.I., Easley, C.J., 2017. 3D-templated, fully automated microfluidic input/output multiplexer for endocrine tissue culture and secretion sampling. Lab Chip 17, 341–349.
Merlier, Franck, Jellali, Rachid, Leclerc, Eric, 2017. Online hepatic rat metabolism by coupling liver biochip and mass spectrometry. Analyst 142. https://doi.org/10.1039/C7AN00973A.
Mohammed, J.S., Wang, Y., Harvat, T.A., Oberholzer, J., Eddington, D.T., 2009. Microfluidic device for multimodal characterization of pancreatic islets. Lab Chip 9, 97–106.
Moritz, W., Meier, F., Stroka, D.M., Giuliani, M., Kugelmeier, P., Nett, P.C., Lehmann, R., Candinas, D., Gassmann, M., Weber, M., 2002. Apoptosis in hypoxic human pancreatic islets correlates with HIF-1alpha expression. Faseb. J. 16, 745–747.
Rogal, J., Zbinden, A., Schenke-Layland, K., Loskill, P., 2019. Stem-cell based organ-on-a-chip models for diabetes research. Adv. Drug Deliv. Rev. 140, 101–128.
Sankar, K.S., Green, B.J., Crocker, A.R., Verity, J.E., Altamentova, S.M., Rocheleau, J.V., 2011. Culturing pancreatic islets in microfluidic flow enhances morphology of the associated endothelial cells. PloS One 6, e24904.
Sardu, C., De Lucia, C., Wallner, M., Santulli, G.4., 2019. Diabetes mellitus and its cardiovascular complications: new insights into an old disease. J. Diabetes Res. 2019, 1905194.
Schulze, T., Mattern, K., Früh, E., Hecht, L., Rustenbeck, I., Dietzel, A., 2017. A 3D microfluidic perfusion system made from glass for multiparametric analysis of stimulus-secretion coupling in pancreatic islets. Biomed. Microdevices 19, 47.
Silva, J.A.D., Souza, E.C.F., Echazú Böschemeier, A.G., Costa, C.C.M.D., Bezerra, H.S., Feitosa, E.E.L.C., 2018. Diagnosis of diabetes mellitus and living with a chronic condition: participatory study. BMC Publ. Health 18, 699.
Tan, W.H., Takeuchi, S., 2007. A trap-and-release integrated microfluidic system for dynamic microarray applications. Proc. Natl. Acad. Sci. U.S.A. 104, 1146–1151.
Vilsbøll, T., Zdravkovic, M., Le-Thi, T., Krarup, T., Schmitz, O., Courrèges, J.P., Verhoeven, R., Bugánová, I., Madsbad, S., 2007. Liraglutide, a long-acting human glucagon-like peptide-1 analog, given as monotherapy significantly improves glycemic control and lowers body weight without risk of hypoglycemia in patients with type 2 diabetes. Diabetes Care 30, 1608–1610.
Wang, J., Gu, W., Chen, C., 2018. Knocking down insulin receptor in pancreatic Beta cell lines with lentiviral-small hairpin RNA reduces glucose-stimulated insulin secretion via decreasing the gene expression of insulin, GLUT2 and Pdx1. Int. J. Mol. Sci. 19, 985.
Wu, L., Nicholson, W., Knobel, S.M., Steffner, R.J., May, J.M., Piston, D.W., Powers, A.C., 2004. Oxidative stress is a mediator of glucose toxicity in insulin-secreting pancreatic islet cell lines. J. Biol. Chem. 279, 12126–12134.
Xiong, X., Wang, X., Li, B., Chowdhury, S., Lu, Y., Srikant, C.B., Ning, G., Liu, J.L., 2011. Pancreatic islet- specific overexpression of Reg3beta protein induced the expression of pro-islet genes and protected the mice against streptozotocin-induced diabetes mellitus. Am. J. Physiol. Endocrinol. Metab. 300, E669–E680.
Yonekawa, Y., Okitsu, T., Wake, K., Iwanaga, Y., Noguchi, H., Nagata, H., Liu, X., Kobayashi, N., Matsumoto, S., 2006. A new mouse model for intraportal islet transplantation with limited hepatic lobe as a graft site. Transplantation 82, 712–715.
Young, E.W.K., Beebe, D.J., 2010. Fundamentals of microfluidic cell culture in controlled microenvironments. Chem. Soc. Rev. 39, 1036–1048.
Zbinden, A., Marzi, J., Schlünder, K., Probst, C., Urbanczyk, M., Black, S., Brauchle, E.M., Layland, S.L., Kraushaar, U., Duffy, G., Schenke-Layland, K., Loskill, P., 2020. Non-invasive marker-independent high content analysis of a microphysiological human pancreas-on-a-chip model. Matrix Biol. 85–86, 205–220.

Biochemical Engineering Journal 164 (2020) 107783

Contents lists available at ScienceDirect

Biochemical Engineering Journal

journal homepage: www.elsevier.com/locate/bej

Regular article

Development of a pancreas-liver organ-on-chip coculture model for organ-to-organ interaction studies

Amal Essaouiba [a,b], Teru Okitsu [c], Rie Kinoshita [c], Rachid Jellali [a], Marie Shinohara [c], Mathieu Danoy [b], Cécile Legallais [a], Yasuyuki Sakai [d], Eric Leclerc [a,b,*]

[a] Université de technologie de Compiègne, CNRS, Biomechanics and Bioengineering, Centre de recherche Royallieu CS 60319, 60203, Compiègne Cedex, France
[b] CNRS UMI 2820, Laboratory for Integrated Micro Mechatronic Systems, Institute of Industrial Science, University of Tokyo, 4-6-1 Komaba, Meguro-ku, Tokyo, Japan
[c] Institute of Industrial Science, University of Tokyo, 4-6-1 Komaba, Meguro-ku, Tokyo, Japan
[d] Department of Chemical Engineering, Faculty of Engineering, University of Tokyo, 7-3-1 Hongo, Bunkyo-ku, Tokyo, Japan

ARTICLE INFO

Keywords:
Organ-on-chip
Islets of Langerhans
Hepatocytes
Coculture
Glucose homeostasis
Diabetes

ABSTRACT

Type 2 diabetes mellitus (T2DM) is a widespread chronic disease with a high prevalence of comorbidity and mortality. The exponential increase of TD2M represents an important public health challenge and leads a strong demand for the development of relevant *in vitro* models to improve mechanistic understanding of diabetes and identify new anti-diabetic drugs and therapies. These models involve considering the multi-organ characteristic of T2DM. The organ-on-chip technology has made it possible to connect several organs thanks to dedicated microbioreactors interconnected by microfluidic network. Here, we developed pancreas-liver coculture model in a microfluidic biochip, using rat islets of Langerhans and hepatocytes. The behavior and functionality of the model were compared to islets and hepatocytes (with/without insulin) monocultures. Compared to monoculture, the islets coculture presented high C-peptide and insulin secretions, and downregulation of *Pdx1*, *Glut2*, *App*, *Ins1*, *Neurod*, *Neurog3* and *Gcgr* genes. In the hepatic compartment, the monocultures without insulin were negative to CK18 staining and displayed a weaker albumin production, compared to monoculture with insulin. The hepatocytes cocultures were highly positive to INSR, GLUT2, CK18 and CYP3A2 immunostaining and allowed to recover mRNA levels similar to monocultures with insulin. The result showed that islets could produce insulin to supplement the culture medium and recover hepatic functionality. This model illustrated the potential of organ-on-chip technology for reproducing crosstalk between liver and pancreas.

1. Introduction

Diabetes mellitus (DM) is a chronic metabolic disorder characterized by deregulation of glucose homeostasis that results from insulin deficiency or systemic insulin resistance [1]. DM is one of the most prevalent and costly diseases in the world, affecting approximately 463 million people worldwide (1 in 11 adults), according to the latest International Diabetes Federation (IDF) estimation [2]. In 2016, the World Health Organization (WHO) estimated that 1.6 million deaths were directly caused by diabetes [3]. The complications of diabetes are also associated with multiple medical problems such as blindness, kidney failure, cardiovascular diseases, sexual dysfunction, neuropathy, and peripheral vascular disease [4,5]. Type 2 diabetes mellitus (T2DM, known as insulin-independent diabetes) is the most common form of diabetes, representing 90% of diabetic patients (415 million people worldwide) [2,6]. T2DM is caused by the insensitivity of target-tissues to insulin, and impaired insulin secretion [4]. Currently, there is no curative treatment for T2DM. Most treatments help patients control the disease and include lifestyle adjustments and drug therapy such as metformin, sulphonylureas, glitazones and GLP-1 receptor agonists [4,7].

T2DM is a complex disease involving interactions between several organs, including the pancreas, liver, muscle, adipose tissues, kidneys, and gut [4]. One of the key features of T2DM is the insulin resistance state characterized by a drop-down of glucose uptake by the skeletal muscle, fatty tissue, and liver [5]. In the pancreas, the state of hyperglycemia triggers the increase in insulin secretion, which can lead to hyperinsulinemia and beta cell proliferation as a compensatory effect for the insulin resistance state. T2DM occurs when the pancreas fails to adapt to increased blood glucose levels [4,8]. The liver is one of the first organs to be severely affected by insulin resistance. The liver responds to

* Corresponding author.
E-mail addresses: eleclerc@iis.u-tokyo.ac.jp, eric.leclerc@utc.fr (E. Leclerc).

https://doi.org/10.1016/j.bej.2020.107783
Received 4 June 2020; Received in revised form 25 August 2020; Accepted 30 August 2020
Available online 1 September 2020

chronic systemic hyperglycemia by increasing gluconeogenesis. In the diabetic state, gluconeogenesis is increased because of the decreased insulin released by the beta cells and/or the suppressed insulin action on the liver [4]. TD2M is associated with high prevalence of hepatic comorbidities, such as non-alcoholic fatty liver disease (NAFLD) [9]. NAFLD is a rapidly-growing disease affecting 30% of the general population and around 90% of T2DM patients [10]. Furthermore, it is still controversial whether NAFLD is a consequence or a cause of pancreas disorders. The relevant pathophysiological models involving organ-to-organ interactions are critical for extracting the relevant biomarkers and therapeutic solutions. As a result, it is of crucial importance to reproduce the physiology of both the liver and the pancreas to control and properly identify the interaction with the development of diabetes and its systemic relationship with the liver.

New, advanced *in vitro* technologies can create ample opportunities for a more modern approach to toxicology and pharmacology, replacing the traditional "black box" of animal-based and conventional 2D *in vitro*-based paradigms. Animal models fail to faithfully reproduce the human condition and lose relevance when extrapolating the results to humans [11,12]. *In vitro* cell cultures are mainly performed in static 2D cultures using conventional multi-well plates, which do not accurately reflect the physiological *in vivo* micro-environment [12,13]. Consequently, it is essential that those basic plate cultures be improved in order to reproduce the characteristics found *in vivo* as closely as possible. This is why many groups are developing tissue-engineering 3D culture (spheroids, culture in 3D hydrogel and organoid), dynamic organ-on-chip culture and coculture models in order to provide a more appropriate micro-environment for tissue maintenance and development [14].

Of those *in vitro* complex models, organ-on-chip technology seems to be one of the suited methods for reproducing the behavior of an organ or a group of organs, as well as the controlled physiological micro-environment [12,15]. Microfluidic organ-on-chip culture improve the exchange and transport of nutrients, oxygen, metabolic waste, hormones and other chemical, and creates "physiological-like" situations such as the liver zonation, shear stress and chemical gradients [12,14]. In particular, organ-on-chip technology allows the cocultures of two or more organs in separated microbireactors and connected by soluble factors exchange through the microfluidic network [12]. In recent years, several teams have proposed organ-on-chip devices that reproduce diverse behaviors of various organs and tissues including the liver, kidneys, gut, lung, heart, and intestines [15,16]. While many organ-on-chip technologies have been developed and advanced for the liver, only a few studies have focused on the pancreas, and even less, to our knowledge, on liver-pancreas interactions. Of these studies, organ-on-chip technology has been used to reproduce an *in vitro* pancreas-on-chip model [17–22]. However, most of the current microfluidic platforms have mainly been designed for the quality assessment of islets for subsequent *in vivo* implantation [14]. In parallel, a few recent works have also demonstrated the potential of organ-on-chip technology for complex pancreatic analysis and pancreatic islet-liver crosstalk studies [18,23]. Therefore, it was demonstrated the potential of technology for liver and pancreas interaction *via* the insulin – glucose regulation [23].

In this paper we propose an alternative design of coculture organ-on-chip microfluidic technology making long-term culture of hepatocytes and pancreatic islets possible. We represented the hepatic disturbance by removing the insulin from the culture medium. Then, we investigated the restoration of hepatic function thanks to the interaction between the liver and endocrine pancreas through the circulating hormones and cofactors in the coculture configuration. We also included new features by investigating mRNA response of important liver and pancreas gene marker (differentiation and functional pattern) during the glucose-insulin regulation.

2. Material and methods

2.1. Device design and fabrication

The microfluidic coculture consists of two different biochips (one for the liver, one for the pancreas) that were connected serially. Each biochip was manufactured with two polydimethylsiloxane (PDMS) layers.

In the pancreas-on-chip model, the micro-structured bottom layer, used to trap islets, was composed of 600 microwells measuring 400 μm in diameter (depth of 300 μm), and spaced by 50 μm (Fig. 1A,) [24]. The second PDMS layer, with a reservoir (depth of 100 μm, Fig. 1A), was placed on top of the first layer and included an inlet and outlet for culture medium perfusion. A microchannels network placed at the inlet and outlet of each layer made it possible to distribute the culture medium homogenously in the biochip (Fig. 1A).

Concerning the liver-on-chip model, we used a micro-structured bottom layer composed of microchannels and microchambers network in a cell culture chamber measuring 1.2 cm in length, 1 cm in width and 100 μm in height (Fig. 1A). The second PDMS layer, with a reservoir (depth of 100 μm, Fig. 1A), was sealed on top of the first layer. As described above, a microchannels network was also present in the inlet and outlet to ensure homogenous culture medium distribution. The design and dimensions of the biochip were described in our previous work [25,26].

The PDMS biochips were manufactured using a replica molding process. First, photolithography was performed to create the mold masters of the bottom and top layer of the biochips using SU-8 photosensitive resin. Then, PDMS prepolymer (mixture of 10:1 base polymer/curing agent; Sylgard 184, Dow Corning) was poured onto the SU-8 master and cured for 2 h at 75 °C. The surfaces of the PDMS layers obtained were activated with reactive air plasma (1 min; Harrick Scientific) and brought together immediately to form an irreversible seal.

2.2. Isolation of rat islets and hepatocytes

Pancreatic islets and hepatocytes were isolated from male Wistar rats aged 8–9 and 6 weeks old, respectively (CLEA Japan, Inc, Tokyo, Japan). The rats were housed at the University of Tokyo with a 12-h light/dark cycle at 22 °C with food and water *ad libitum*. All animal experimentation procedures were carried out according to the guidelines of the University of Tokyo and the Japanese Ministry of Education.

2.2.1. Isolation of islets

Pancreatic islets were isolated following the protocol described by Yonekawa et al., and Kiba et al., [27,28]. The rats were anesthetized by isoflurane inhalation solution (Pfizer). After clamping all the irrigation blood vessels, the enzymatic solution (Liberase™ TL, Roche) was injected through the bile duct, previously identified and clamped. After the pancreatectomy, the selective chemical digestion of the organ was carried out at 37 °C for 30 min with the Liberase TL/ ET-K solution (ET-Kyoto solution, Otsuka Pharmaceutical). The digestion was followed by washing and purification steps using a discontinuous Opti-Prep® density gradient (Merck/Sigma-Aldrich). Then, the islets of Langerhans were identified and hand-picked with a Pasteur pipette under a stereomicroscope (Leica S9 D) and transferred to a cold solution made of UW solution (University of Wisconsin [29]) complemented with Miraclid (Mochika pharmacy, Japan) and Heparin (Mochika pharmacy, Japan). After assessment and counting of the islets (Dithizone staining), the tissue was stored at 4 °C until the start of culture.

2.2.2. Isolation of hepatocytes

Primary hepatocytes were isolated using the two-step collagenase protocol based on the protocol of Seglen [30–32]. Briefly, after animal anesthesia by isoflurane inhalation solution (Pfizer), the liver was perfused with buffer solution in order to washout the blood. Then, the

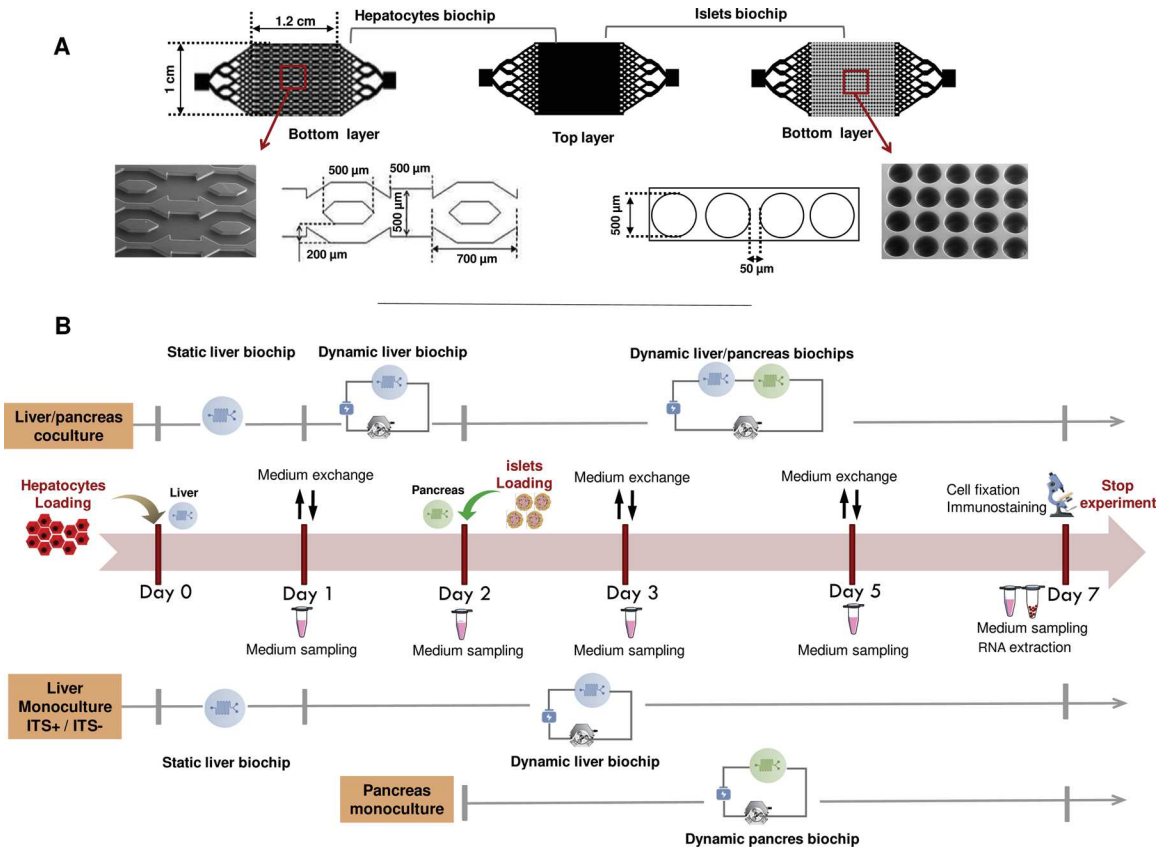

Fig. 1. (A) design of biochips used for hepatocytes and islets cultures; (B) experimental procedures.

buffer was switched with the collagenase IV solution (Wako Pure Chemical Industries) to start the tissue's chemical digestion. Subsequently, the liver was extracted, deposited in Dulbecco's Modified Eagle Medium (DMEM, Gibco™ – Life Technologies) and the tissue was gently disrupted. The digested tissues were filtered through 100 µm filters (cell strainer 100 µm nylon; Falcon®) and the liver cell suspensions were centrifuged three times. The resulting pellets were mixed and suspended in Percoll (Sigma-Aldrich) and HBSS (Sigma-Aldrich) separating solution. Percoll isogradient centrifugation was performed to isolate both dead cells and a significant portion of the nonparenchymal cells in a floating top layer that was discarded. Finally, the cells obtained were suspended in seeding medium (William's E medium (Gibco™) supplemented with 10% fetal bovine serum (FBS, Gibco™), 100 units/mL of penicillin and 100 mg/mL of streptomycin (Gibco™). Cell viability was assessed by Trypan blue dye exclusion and hepatocytes cultures with a viability of more than 85% were used. The purity obtained was over 98%.

2.3. Biochip culture

The experimental setup used for culture in the biochip was composed of a perfusion loop, including the culture medium tank (bubble trap), the peristaltic pump, and one or two biochips. They were interconnected using 0.65 mm interior diameter silicone/Teflon tubing (Fig.S1, supplementary file). The bubble trap contained 2 mL of culture medium and the flow rate was set at 20 µL/min. Before each experiment, the circuit (biochip, tubing and bubble trap) was sterilized by autoclaving and dried in an oven.

Four groups of biochips were investigated and compared: (i) hepatocytes biochip monoculture with insulin (hepatocytes monoculture ITS +); (ii) hepatocytes biochip monoculture without insulin (hepatocytes monoculture ITS -); (iii) pancreatic islets biochip monoculture (islets monoculture) and (iv) hepatocytes/islets biochips coculture without insulin (hepatocytes/islets coculture). The detailed experimental procedure is shown in Fig. 1B.

2.3.1. Pancreatic islets culture in the biochip (pancreas-on-chip)

The biochips were previously filled with culture media in order to remove the air bubbles and moisturize the circuits. The preconditioning process was carried out for one hour at 37 °C in the incubator. The pancreatic islets in the preservation solution were washed with cold culture media and gently diluted in the appropriate amount. In order to minimize islets damage, wide orifice pipette tips with low binding were used throughout the handling process. After loading in the biochips, the islets were counted under microscope in order to keep a record of the islets number per biochip (≈40 islets/biochip). The circuit was then connected to the peristaltic pump and the perfusion started. The entire setup was continuously incubated at 37 °C in a 5% CO_2 supplied incubator. The basal culture medium used for the pancreatic islets culture was a classic RPMI 1640 medium (Gibco™) supplemented with 10% FBS (Gibco™), 100 units/mL of penicillin, 100 mg/mL of streptomycin (Gibco™) and GlutaMAX™ (Gibco™) at 10 mM.

2.3.2. Hepatocytes biochip culture (liver-on-chip)

After sterilization, the biochips were coated with rat tail type 1 collagen (Corning®, 300 µg/mL in phosphate-buffered saline: PBS Gibco™) and incubated at 37 °C in an atmosphere supplied with 5% CO_2. After 1 h, the collagen solution was washed using the seeding medium and the freshly isolated hepatocytes (5×10^5 cells/biochip) loaded into the microfluidic device *via* biochip inlet ports using a micropipette tip. To keep the seeding medium inside the culture chamber, the biochip inlet ports were closed using two syringes (containing 500 µL of seeding medium), and the biochips were placed in an incubator at 37 °C and 5% CO_2. After 24 h of static conditions to

promote cell adhesion, the seeding medium was replaced by the culture medium, and the biochip integrated into the perfusion experimental setup to launch the dynamic culture.

The primary hepatocytes culture medium was composed of William's E medium (Gibco™) supplemented with 100 units/mL of penicillin / 100 mg/mL of streptomycin (Gibco™), GlutaMAX™ (Gibco™) at 10 mM, 1% non-essential amino acids (Invitrogen), 3% Bovine Serum Albumin (BSA, Sigma), 1% Insulin-Transferrin-Selenium ITS-100X (PanBiotech), 0.1 µM Dexamethasone (Wako Pure Chemical Industries), 10 ng/mL mouse Epidermal Growth Factor (Takara Bio), 0.5 mM ascorbic acid 2-phosphate (from magnesium salt n-hydrate; Wako Pure Chemical Industries) and 20 mM HEPES (Gibco™). For the hepatocytes monoculture without insulin (monoculture ITS -), we used the same medium composition excluding ITS.

2.3.3. Hepatocytes/islets coculture (pancreas/liver-on-chip)

The liver and pancreas biochips were prepared separately. First, the hepatocytes were inoculated into the liver biochip (as in section 2.3.2). After 24 h of adhesion, the hepatocytes were cultivated inside the liver biochips for 24 h in perfusion (this resulted in 48 h of culture in the liver biochip including 24 h for adhesion in static conditions and 24 h of perfusion). The pancreatic islets biochips were prepared after those 48 h. The islets were inoculated into the biochips as described in section 2.3.1. After 1 h at rest and islets sedimentation, the liver perfusions were stopped and one pancreas biochip and one liver biochip were serially connected to each other to create a pancreas-liver coculture model (Fig. 1A and Fig.S1, supplementary file). The culture medium for the coculture condition was a 1:1 mixture of pancreatic islets (RPMI 1640) and hepatocytes (William's E) media, excluding ITS from the last one.

2.4. RTqPCR assays

Total RNAs were extracted and purified from samples using a hybrid protocol that combines Trizol™ Reagent (Life Technologies) and RNeasy Mini Kit (QIAGEN 74104) following the manufacturer's instructions. Concentrations and qualities of extracted RNAs were assessed using a BioSpec-nano (Shimadzu Scientific Instruments). Reverse-transcription into cDNA was performed from 0.5 (hepatocytes) and 0.1 µg (islets) of total RNA using the ReverTra Ace qPCR RT Master Mix with gDNA Remover (TOYOBO). Real-time quantitative reverse transcription polymerase chain reaction (RTqPCR) was then performed with the THUNDERBIRD SYBR qPCR Mix (TOYOBO) according to the manufacturer's protocol and a StepOnePlus Real-Time PCR system (Applied Biosystems). The primer sequences of the genes are shown in Tables S1 and S2. β-Actin was used as the reference gene.

2.5. Immunostaining

The islets were transferred to an untreated TCPS 24-wells plate. The hepatocytes immunostaining was performed in the biochip. The islets and hepatocytes were washed with phosphate buffer saline solution (PBS, Gibco) and fixed in paraformaldehyde 4% at 4 °C for 24 h. In order to perform the immunostaining in a 3D structure, the islets were permeabilized with 1% Triton X100 in PBS for 3 h at 4 °C and washed 3 times with PBS for 30 min, while the hepatocytes were permeabilized with 0.1% Triton X100 in PBS for 15 min. Then, both islets and hepatocytes were blocked with a gelatin buffer for 24 h at 4 °C. Primary antibodies were incubated at 4 °C in a BSA/PBS solution for 48 h and overnight for the pancreatic islets and hepatocytes, respectively. After several washing steps, secondary antibodies were incubated in a BSA/PBS solution at 4 °C in the dark (24 h for islets and overnight for hepatocytes). Actin filaments were stained with Phalloidin-iFluor488 Reagent (abcam). Finally, the nuclei were stained with Hoechst 33342 (H342, Dojindo) at 1/800 for 30 min at room temperature in the dark.

All the incubations and washing steps were carried out using a shaker for the islets of Langerhans immunostaining process. For the hepatocytes, the biochips were cut with a scalpel to remove the PDMS top layer in order to increase the resolution of the image. Observations were made with an Olympus IX-81 confocal laser-scanning microscope. The primary and secondary antibodies used are presented in Table S3 (supplementary file). The quantitative assessment of fluorescence intensity was performed by grey value intensity analysis (ImageJ software; NIH, Bethesda, Maryland) using the collected images.

2.6. Insulin, glucagon, C-peptide and albumin measurements

The hormones and albumin released into the culture medium samples from the different culture conditions were assessed using ELISA assays, following the manufacturer's protocol. The following kits were used: insulin (rat Insulin ELISA kit, 10-1250-01, Mercodia), glucagon (Glucagon DuoSet ELISA kit, DY1249 and DuoSet ELISA Ancillary Reagent Kit 2, DY008, R&D Systems), C-peptide (rat C-Peptide ELISA kit, 10-1172-01, Mercodia) and albumin (Rat Albumin ELISA quantification set E110-125 from Bethyl, combined with the Enzyme Substrate, TMB, E102). The results were obtained with an iMark microplate reader (Bio-Rad, Osaka, Japan) set to a wavelength of 450 nm.

2.7. Glucose and lactate measurements

Glucose and lactate were measured using a YSI 2950 Biochemistry Analyzer. To do so, 160 µL of culture medium were inserted into the analyzer. Measurements were based on a direct reading of L-lactate (L-lactic acid) and glucose in the culture medium by the YSI enzyme sensors, as the enzymes L-lactate oxidase, and glucose oxidase are respectively immobilized in the lactate and glucose sensors.

2.8. Statistics

All experiments were repeated at least three times. The data are presented as the mean ± standard deviations (SD) of 9 biochips (3 biochips from 3 different experiments, $n = 3 \times 3$). The Kruskal Wallis test was performed for the statistical analysis using GraphPad software (Prism 8). Data with P-values < 0.05 were identified as statistically significant and highlighted in the figures.

3. Results

3.1. Cell morphology analysis

The hepatocytes were successfully attached in the collagen-coated biochip after a few hours of culture. They were kept under static conditions in an incubator. After 24 h, the hepatocytes created a confluent tissue and displayed typical cuboidal hepatocyte phenotypes (Fig. S2, supplementary file).

The hepatocytes morphology at the end of the experiments (24 h in static conditions and 6 days of perfusion) is presented in Fig. 2. The hepatocytes monoculture with insulin (hepatocytes monoculture ITS +) displayed typical hepatic monolayer cultures (cells with the typical cuboid shape). The cell monolayer was maintained over 7 days of culture, including 24 h at rest and 6 days in perfusion (Fig. 2A). Without insulin (hepatocytes monoculture ITS -), the hepatocytes cultures were heterogeneous from one biochip to another. A few hepatic cultures in the biochips without insulin presented similar morphologies when compared to the hepatic culture with insulin (Fig. 2B). In most of the biochips, the hepatocytes formed some aggregated structures or degraded tissue (Fig. 2C). Finally, in the hepatocytes/islets biochips coculture, the typical hepatic phenotypes (similar to hepatocytes monoculture ITS +) were recovered, as shown in Fig. 2D.

Concerning islets cultures, we did not detect any modification in the morphologies of the pancreatic islets when we compared the islets monoculture and the islets/hepatocytes coculture. The islets were trapped in the microwells of the pancreas biochips and displayed the

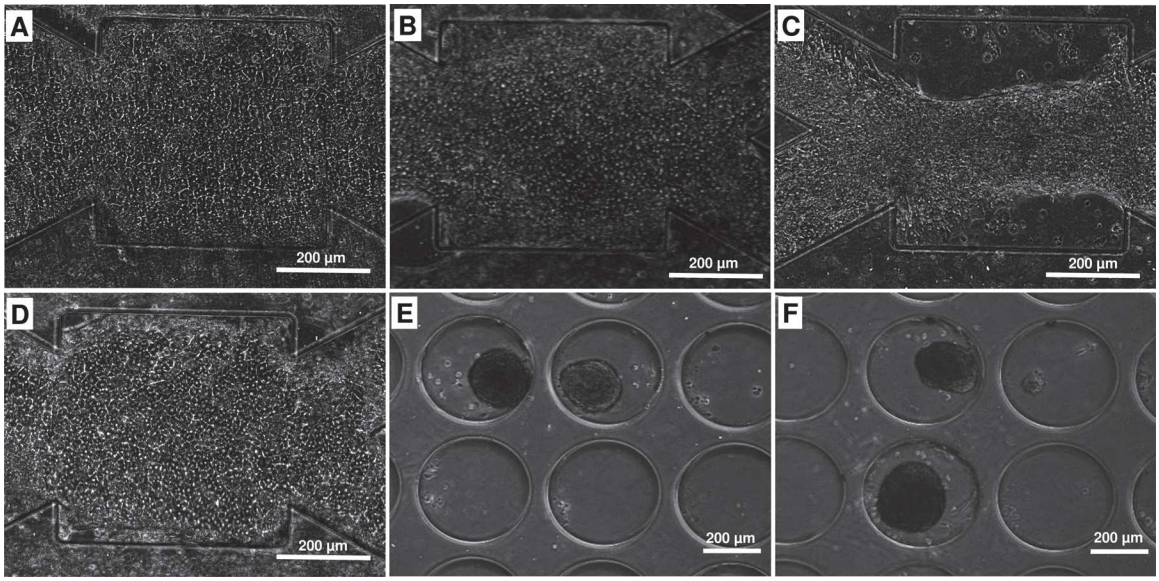

Fig. 2. Hepatocytes and islets morphologies at the end of the experiments: (A) hepatocytes monoculture with insulin (ITS +), (B) and (C) hepatocytes monoculture without insulin (ITS -), (D) hepatcytes in coculture with islets, (E) islets monocultures and (F) islets in cocultre with hepatocytes.

typical spheroid shapes of islets of Langerhans (Fig. 2E and F). Furthermore, we counted the number of islets at the end of the experiments (5 days of perfusion). The result showed that the number of islets collected at the end of the perfusion remained similar to the number of islets seeded.

3.2. Immunostaining analysis

Immunofluorescence staining was performed at the end of the experiment (days 5 and 7 for islets and hepatocytes, respectively). For hepatocytes, we chose to stain several hepatic markers: CYP3A2 (one of the most abundant cytochrome P450 in the liver), CK18 (differentiation marker), INSR (insulin receptor) and GLUT2 (glucose transporter). We also stained two important markers in the pancreatic islets: insulin and glucagon, which are markers of β-cells and α-cells, respectively.

The immunostaining of the hepatic cells on day 7 is presented in Fig. 3. The immunostaining demonstrated that the hepatocytes monoculture with insulin and the hepatocytes/islets coculture led to positive cell populations expressing CYP3A2 and CK18. These results illustrate that the differentiation of hepatocytes in both types of culture was maintained. On the contrary, the CK18 was not expressed and the CYP3A2 was moderately expressed in hepatocytes monoculture without insulin (Fig. 3A). The quantification of staining intensity revealed that CK18 level was around 13 in coculture and monoculture with insulin, and close to zero for monoculture without insulin. The intensities of CYP3A2 staining were of 30, 32 and 26 for coculture, monoculture with insulin and monoculture without insulin, respectively (Fig.S4, supplementary file). In parallel, the hepatocytes monoculture with insulin and the hepatocytes/islets coculture showed an intense positive cell population for INSR (intensity level at 14.5 and 14, respectively) and GLUT2 (staining intensity around 35 for both cultures). Whereas the expressions of those markers were weaker in hepatocytes without insulin (Fig. 3B). The fluorescence intensities were of 6 and 27 for INSR and GLUT2, respectively (Fig.S4, supplementary file).

In the case of pancreatic islets, the level of insulin and glucagon expression inside the islets after extraction (day 0) appeared variable from one rat to another, probably due to the rat fed state at the moment of the extractions (Fig.S3, supplementary file). Then, in the pancreatic islets monoculture and islets of pancreas/liver coculture, we found an expression of both glucagon and insulin hormones at the end of the experiments (Fig. 4). Furthermore, the levels of insulin appeared over-expressed in coculture when compared to the islets monoculture levels (2 times higher in coculture; Fig.S4, supplementary file). The glucagon was similarly expressed, in both monoculture and coculture of islets, and we did not detect any difference between the immunostaining images.

3.3. RTqPCR analysis

At the end of the experiments, we analyzed the expression levels of selected hepatic genes in the different culture conditions (monoculture ITS +, monoculture ITS - and coculture). The comparison of the mRNA levels between the hepatocytes cultivated in monoculture with and without insulin is presented in Fig. 5 (ratio of mRNA levels in monoculture ITS- *versus* monoculture ITS+). We found that the mRNA level of *Alb* was downregulated in monoculture without insulin (fold change, FC of 0.55). On the contrary, the expression levels of *Hnf4a* (FC 40), *Insr* (FC 4.5), *Igfbp1* (FC 2.5) and *Pck1* (FC 10) were significantly increased. Considerable variability in the levels of *Gcgr*, *Glut2* and *Cyp3a2* in the monoculture without insulin was measured, which led to no statistical difference between the two culture conditions for those genes.

The comparison was then performed for gene expression in the hepatocytes cultivated in coculture with pancreatic islets and the hepatocytes monoculture with insulin. As shown in Fig. 5, the coculture contributed to recovering similar mRNA levels regarding *Gcgr*, *Insr*, *Hnf4a*, *Igfbp1* and *Alb* when compared to the monoculture of hepatocytes with insulin. However, the mRNA level of *Cyp3a2*, *Cyp1a2* appeared lower when compared to monoculture with insulin (FC of 0.1 and 0.35 respectively). Conversely, the mRNA level of *Pck1* remained high in coculture when compared to the hepatocytes with insulin monoculture, and at similar levels when compared to hepatocytes monoculture without insulin.

Finally, we investigated the effect of coculture with hepatocytes on expression levels of pancreatic islet-specific genes. The comparison of the mRNA levels is shown in Fig. 6 (ratio of mRNA levels in coculture *versus* islets monoculture). We found that the coculture with the hepatocytes contributed to downregulate the levels of *Gcgr*, *Neurod*, *Neurog3*, *Glut2*, *Ins1*, *Gcg*, *App* and *Pdx1* (FC between 0.1 and 0.36). In contrast, expression of *Reg3a*, *Ins1* and *Glp1r* was 5–15.5 times higher in the coculture compared to the islets monoculture. However, wide variability was found for *Ins1* and *Glp1r* in both culture conditions.

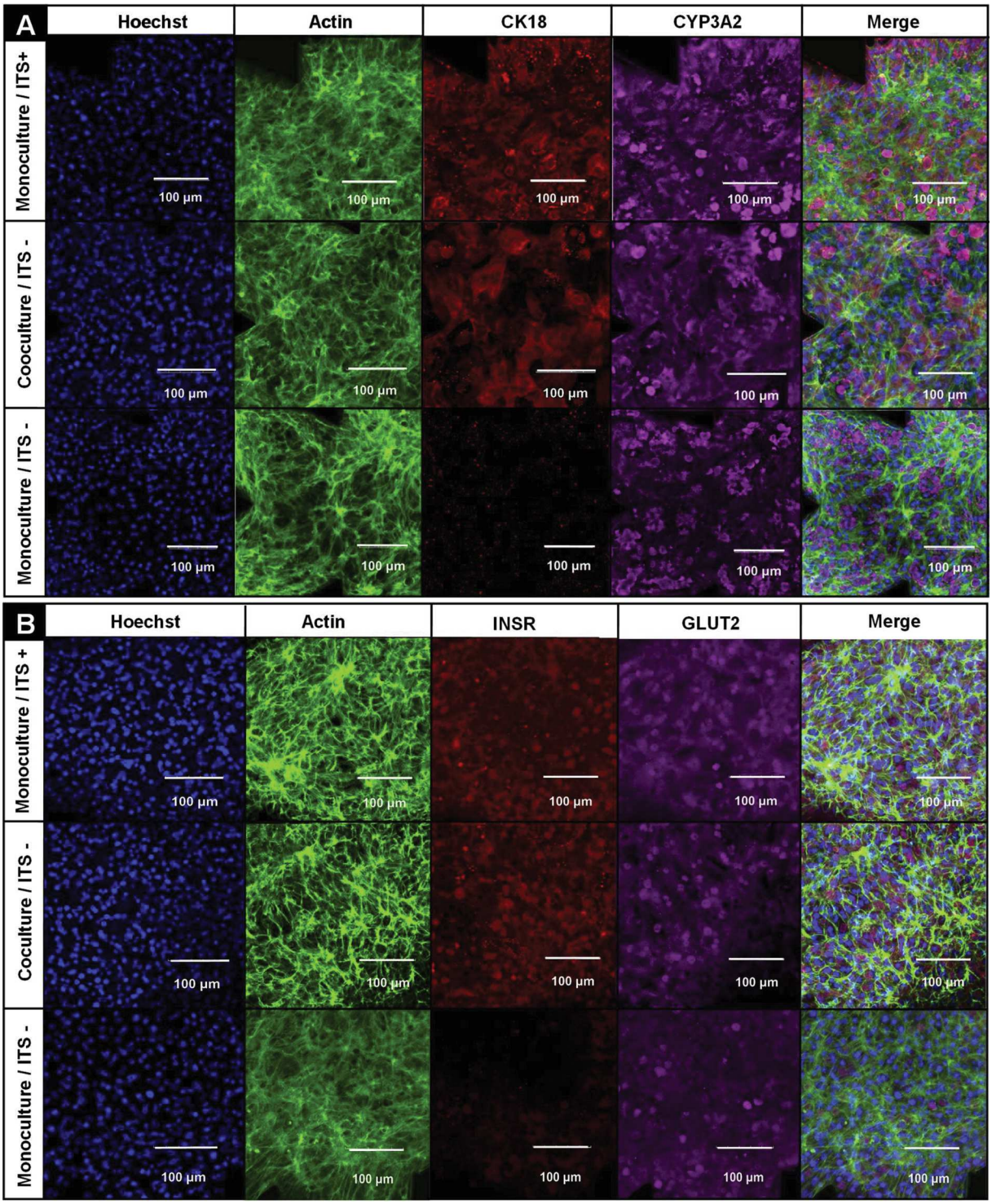

Fig. 3. Immunostainings of hepatocytes in monoculture with insulin, without insulin and coculture with islets at the end of the experiments: (A) DAPI, actin, CK18, CYP3A2 and merge; (B) INSR, GLUT2 and merge with DAPI and actin.

3.4. Functional assays revealed higher insulin and C-peptide secretions in the islets in coculture with hepatocytes when compared to islets monoculture

The basal functionality of the pancreatic islets in both culture modes (islets monoculture and coculture with hepatocytes) was investigated by measuring the levels of insulin, C-peptide and glucagon secretions. The daily secretions of the three hormones on days 3 and 5 (end of the experiment) are presented in Fig. 7.

We found that the insulin concentration in the culture medium decreased between days 3 and 5, in both culture conditions (monoculture and coculture). However, the coculture with hepatocytes contributed to maintaining relatively high levels of secretion when compared to monoculture (Fig. 7A). Especially on day 5, we found a secretion of 0.4 µg/mL/day and 2 µg/mL/day in monoculture and coculture, respectively. Similarly, we measured higher production of C-peptide in coculture when compared to monoculture. The secretion was about 1.5 (245 pmol/mL/day) and 5 (340 pmol/mL/day) times higher

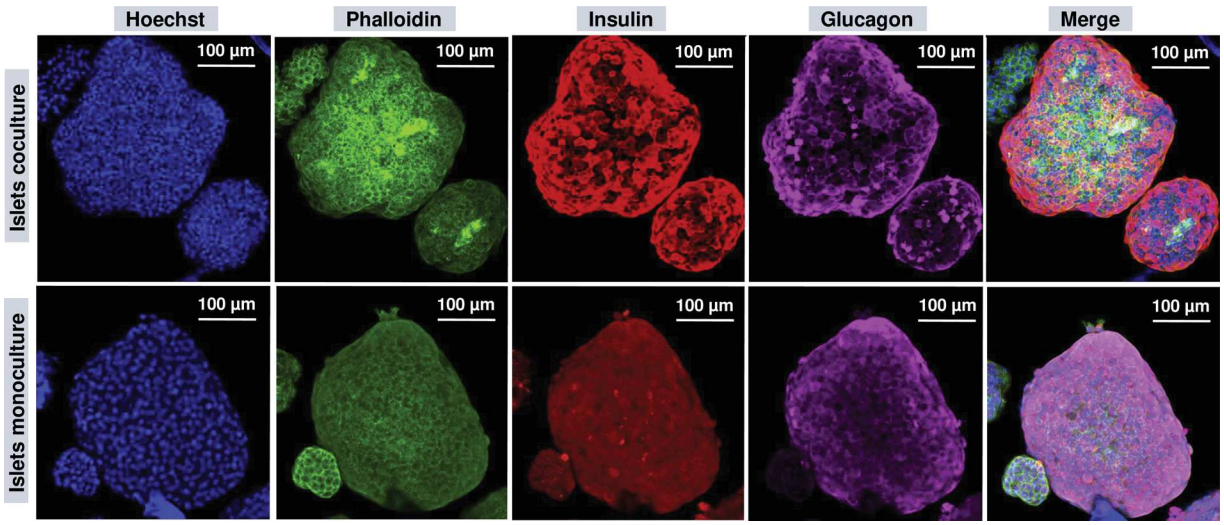

Fig. 4. DAPI, phalloidin, insulin, glucagon and merge immunostainings of islets cultivated in monoculture and coculture with hepatocytes (at end of the experiments).

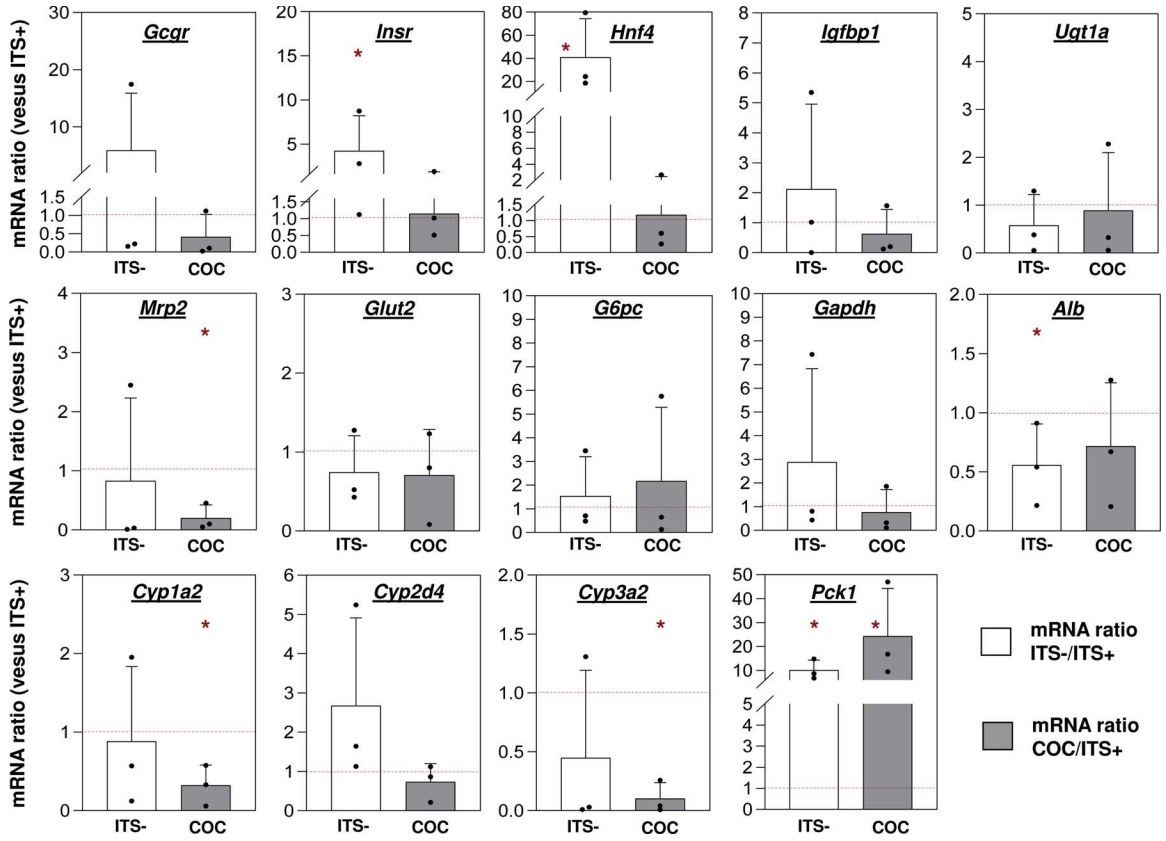

Fig. 5. Ratio of mRNA levels of selected hepatic genes after 7 days of culture. White bars: hepatocytes monoculture without insulin (ITS -) *versus* hepatocytes monoculture with insulin (ITS +), and gray bars: hepatocytes in coculture with islets (COC) *versus* hepatocytes monoculture with insulin (ITS +). *$P < 0.05$, mRNA level significantly different when compared to monoculture (ITS +); each dot corresponds to one independent experiment (one independent rat; mean of 3 biochips).

in the islets coculture with hepatocytes on days 3 and 5, respectively (Fig. 7B and D). The levels of glucagon remained constant in the coculture during the 5 days of the experiment, close to 10 ng/mL/day, but with wide dispersion on day 3 (Fig. 7C). Conversely, the level of glucagon in islets monoculture dropped from 9 to 5 ng/mL/day between days 3 and 5 of culture. Finally, the pancreatic compartment (islets monoculture) was responsive to the high/low glucose stimulations (GSIS stimulation). Indeed, the high glucose stimulation lead to a 2–3 fold higher insulin production when compared to the low glucose condition (GSIS index, results not shown).

Hepatocytes functionality was assessed by measuring the levels of albumin in the three culture modes (monoculture ITS+, monoculture ITS- and coculture). The hepatocytes in monoculture with insulin and in coculture with pancreatic islets produced similar quantities of albumin (constant over time, from days 3–7, till the end of the experiment). Conversely, without insulin in the culture medium, the hepatocytes

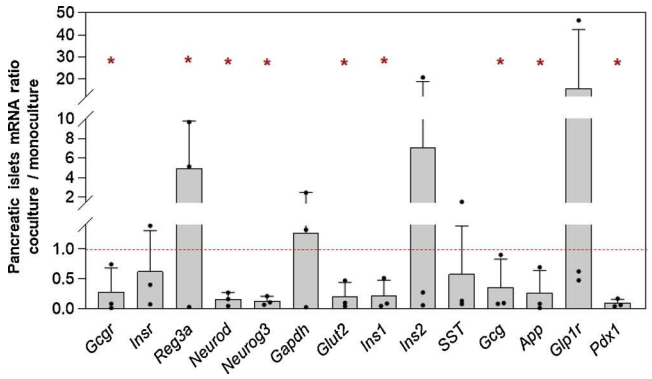

Fig. 6. Ratio of mRNA levels of selected pancreatic islets genes after 5 days of culture (islets coculture *versus* islets monoculture). *$P < 0.05$, mRNA level significantly different between islets monoculture and coculture; each dot corresponds to one independent experiment (one independent rat; mean of 3 biochips).

monoculture presented a drop in albumin production between days 3 and 7, as shown in Fig. 8A. This led to attaining albumin production of close to 750 ± 100 µg/10^6 cells in hepatocytes/islets biochip coculture and the liver biochip monoculture with insulin, whereas the values dropped to close to 440 ± 230 µg/10^6 cells in the liver biochip monoculture without insulin (Fig. 8A).

Finally, we measured glucose and lactate levels during the cultures in the different conditions (Fig. 8B, C and Table S4, supplementary file). The data showed wide dispersion, but the tendency illustrated higher glucose consumption in coculture compared to liver monoculture conditions with and without insulin. Furthermore, this consumption (in hepatocytes/islets coculture) seemed to be constant between days 3 and 7 (Fig. 8B). Concerning lactate production, we could not distinguish any significant difference between the different culture conditions, with lactate production of around 0.6−0.8 mmol/L (Fig. 8C).

4. Discussion

We developed a coculture model for rat hepatocytes with rat islets of Langerhans, using organ-on-chip technology. The liver biochip was the result of our previously developed liver-on-chip technology that had already been successfully applied to rat and human primary hepatocytes [33–36]. We coupled this liver-on-chip model, with a recent update to our technology, to a pancreas-on-chip model [24]. The interconnection of both organ-on-chip technologies produced a new model of interaction between the organs: the liver and the pancreas. The coculture of two cell/tissue types required an adapted coculture medium capable of maintaining their characteristics. Preliminary tests (data not shown) were carried out to define the culture medium adapted to islets/hepatocytes coculture: i) hepatocytes monoculture in William's E medium (the standard medium for rat hepatocytes culture) and in a 1:1 mixture of William's E/RPMI 1640; ii) islets monoculture in RPMI 1640 medium (the standard medium for islets culture) and in a 1:1 mixture of William's E/RPMI 1640. The analyses performed (viability, morphology, gene expression of selected markers, albumin and insulin secretion) showed that islets and hepatocytes monoculture in a mixture of William's E and RPMI 1640 maintained their characteristics (when compared to islets and hepatocytes cultivated in their standard medium). Consequently, a 1:1 mixture of William's E/RPMI 1640 medium was chosen for the islets/hepatocytes coculture experiments.

In this study, the suppression of insulin in hepatocytes monoculture led to a downregulation of the *Alb* mRNA (Fig. 5) and to weaker albumin

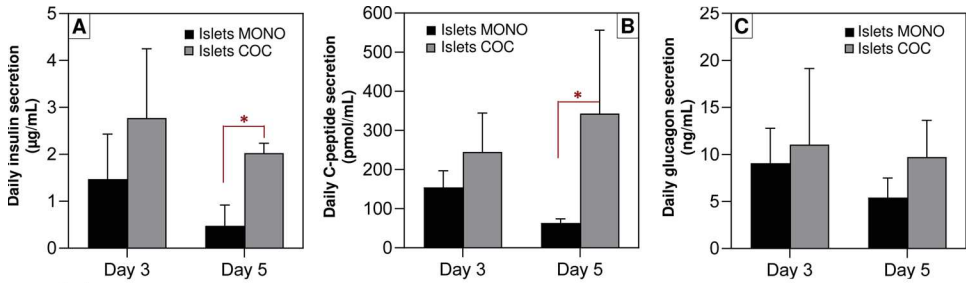

D

	Ratio of hormone secretion (islets coculture / islets monoculture)		
	Insulin	C-peptide	Glucagon
Day 3	1.88±1.53	1.58±1.08	1.21±1.3
Day 5	4.24±1.47	5.48±4.24	1.8±1.39

Fig. 7. (A) Insulin, (B) C-peptide, (C) glucagon daily secretions after 3 and 5 days of islets culture in monoculture and coculture with hepatocytes (*$P < 0.05$) and (D) ratio of hormones (insulin, C-peptide and glucagon) secretion between islets coculture and islets monoculture.

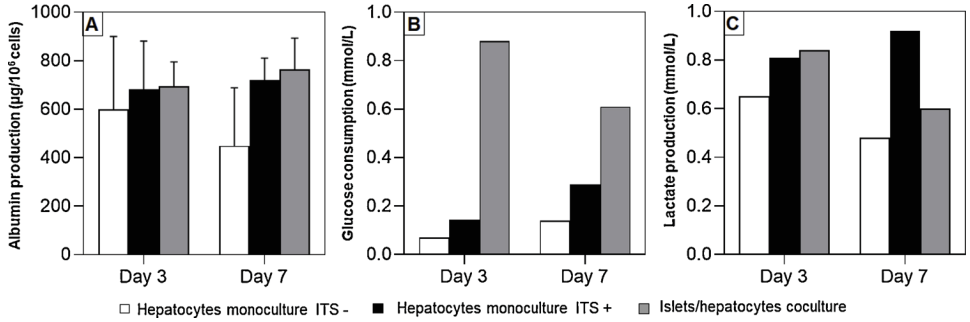

Fig. 8. (A) Albumin production; (B) glucose consumption and (C) lactate production in hepatocytes monoculture without insulin (ITS -), monoculture with insulin (ITS +) and coculture with islets after 3 and 7 days.

production (Fig. 8) in culture medium, compared to monoculture with insulin. The decrease in albumin production and *Alb* gene expression with the lack of insulin has already been reported in the literature on *in vitro* data in rats and *in vivo* in mice [37–39]. The lack of insulin also led to weaker CYP3A2 expression and to the lack of CK18 expression at the protein level (Fig. 3, the *Cyp3a2* was also downregulated at the mRNA level, Fig. 5). Both markers are hepatic differentiation markers. It is reported that rat hepatocytes presented a reduction of about 30 % in the mRNA level of *Cyp3a* in the absence of insulin [40]. Although there is no literature showing the results of the effect of insulin on CK18 immunostaining, various reports have mentioned the crosstalk between CK18 and insulin resistance as in diabetic patients or patients with non-alcoholic steatohepatitis, in which CK18 fragments are elevated in plasma [41,42]. The HNF4 transcription factor is involved in the mechanism of liver differentiation *via* the HNF1, HNF4, PXR and CYP450 axis, but it is also involved in glucose homeostasis, liver-pancreas interactions and diabetes [43–45]. HNF4 is targeted and repressed by insulin in hepatocytes, which was consistent with our result in as much as *Hnf4a* was upregulated without insulin [46,47].

The hepatocytes monoculture without insulin also presented modulation of *Igfpb1* (Insulin-like growth factor binding proteins, upregulation of mRNA levels), *Insr* (lower expression of the protein in the immunostaining and gene upregulation), and *Pck1* (gene upregulation, Figs. 3,5). Interestingly, our results are consistent with the literature reporting that insulin inhibits *Igfpb1* in the liver [48]. *Pck1* catalyzes the first step in gluconeogenesis. By silencing *Pck1* in mice, insulin signaling improved in the liver [49]. Conversely, insulin is also reported as reducing the expression of *Pck1* [50]. Once more, these data appeared consistent with our biochip findings. Finally, the overall hepatic biochip culture without insulin illustrated a consistent behavior when compared to the literature.

The pancreatic islets in coculture were able to produce insulin to counterbalance the suppression of ITS. However, the level of insulin detected (about 3000 µg/L) was lower than the insulin level used in "conventional" hepatocytes culture models (in the present experiment, the hepatocytes monoculture with insulin were performed at 10 mg/L of insulin *via* ITS supplementation in the medium). This could explain why, at the mRNA level, the hepatic markers (Alb and Cyp3a2) remained lower in the hepatocytes coculture (when compared to hepatocytes monoculture with insulin, Fig. 5). Furthemore, *Pck1* remained higher than the level in the hepatocytes monoculture with insulin [37–40,50]. Nevertheless, at the protein level, the expression of CYP3A2, CK18 and the production of albumin were restored in coculture (Fig. 3). The expression of insulin-related genes such as *Igfbp1* and *Insr* were also restored, including *Hnf4a* (Fig. 5). In addition, the protein expression of Insr and Glut2 appeared similar in the immunostaining in both hepatocytes monoculture with insulin and in islets/hepatocytes coculture (Fig. 3). These data illustrate the functional crosstalk between the pancreas and the liver. They also demonstrate the partial restoration of the expected effect of insulin on hepatocytes. Nevertheless, additional experiments, involving tuning the number of islets to increase the production of insulin, are needed to confirm the full recovery of *Pck1* and *Cyp3a2* mRNA levels.

High glucose levels normally lead to high production of insulin. In the present culture conditions, the glucose level in the medium was 9.1–9.8 mM and did not decrease significantly between the two time points of culture medium change (*nb* a similar glucose concentration was used in all culture modes). This led to continuous stimulation for insulin secretion in the pancreatic islets monoculture and during the islets/hepatocytes coculture (and thus contributes to restore the hepatic functions in the coculture by insulin secretion stimulated by glucose). Regarding the effect of hepatocytes coculture on the pancreatic islets, we found that the coculture downregulated *Gcgr*, *Glut2*, *Ins1*, *Neurod*, *Neurog3*, *App*, *Gcg*, *Pdx1* and upregulated *Glp1r* at the mRNA level (Fig. 6). *Pdx1*, *Neurod* and *Neurog3* are important markers in the differentiation of islets [51,52]. *Neurod* is an important gene (an insulin trans activator) required to maintain functional maturity in pancreatic beta cells, including insulin production through *Ins1* [51]. We consistently found both downregulation of *Ins1* and *Neurod* in coculture biochips (which is consistent with *Ins1* silencing in *Neurod* KO mice [51]). *Neurod* KO-mice express the *Ins2* gene and are thus able to produce insulin in glucose tolerance tests, which also appeared consistent with our findings in which *Ins2* was over-expressed in pancreas biochip cocultures [51]. *Pdx1* is a pivotal important gene in β cells. *Pdx1* is a homeobox-containing transcription factor that plays a key role in pancreatic development and adult β cell function [53]. Depletion of *Pdx1* leads to hyperglycemia in mice, cell reprogramming in mice islets and glucagon over-expression in Min6 β cells [53]. Furthermore, *Pdx1*-deficient β cells led to a reduction in the transcript levels of *Pdx1*, *Ins1* and *Glut2*, and the maintenance of glucagon levels [53]. This result was partially consistent with our dataset, in which we found a concomitant downregulation of *Pdx1*, *Ins1* and *Glut2* genes in coculture. However, as *Neurod* and *Pdx1* are also marker of islets health, additional investigation would be required to fully understand the crosstalk between the liver and pancreas.

Glucagon is produced during hypoglycemia to stimulate hepatic glucose output. In our study, the glucose concentration remained high in the culture medium, leading to a high insulin/glucagon ratio being detected, which is consistent with the downregulation of the levels of *Gcg* (glucagon) and *Gcgr* (glucagon receptor) mRNA. However, we also measured high levels of *Glp1r* mRNA. It is reported that paracrine glucagon stimulates insulin secretion through both *Gcgr* and *Glp1r*. More particularly, the activity of glucagon and GLP-1 receptors was reported as being essential for β cell secretory responses *via* paracrine intra-islet glucagon actions for maintaining appropriate insulin secretion [54], which is consistent with our findings in coculture. Although we described those behaviors in the pancreatic tissue as a result of the hepatic coculture, we did not clearly identify the underlying mechanisms or the endocrine liver signaling that drives such crosstalk. As a result, additional analysis is needed to complete our investigation, including metabolome and proteome analysis.

5. Conclusion

In this study, we proposed a new liver/pancreas interaction model in biochips to investigate the crosstalk between the two organs. The characteristic functions of the hepatocytes/islets coculture model were evaluated, comparing them with those of islets or hepatocytes (with and without insulin) monoculture. The hepatocytes monoculture without insulin led to modulation of both glucose homeostasis targets and hepatic differentiation markers. Conversely, the coculture with pancreatic cells producing insulin helped recover the hepatic function, illustrating the benefits of the two-organ model. For pancreatic functions, the presence of the hepatocytes in the coculture model helped modify the islets response *via* the increase in insulin secretion and the modification of the expression of the gene involved in insulin/glucagon homeostasis. The pancreas-liver organ-on-chip model presented here was capable of reproducing several physiological responses and demonstrated the potential of our approach to reproduce and investigate complex *in vivo* patterns using alternative *in vitro* methods.

CRediT authorship contribution statement

Amal Essaouiba: Methodology, Investigation, Validation, Formal analysis, Conceptualization, Data curation, Writing - original draft. **Teru Okitsu:** Resources, Validation. **Rie Kinoshita:** Resources, Validation. **Rachid Jellali:** Methodology, Visualization, Writing - review & editing. **Marie Shinohara:** Resources. **Mathieu Danoy:** Resources. **Cécile Legallais:** Supervision. **Yasuyuki Sakai:** Supervision. **Eric Leclerc:** Funding acquisition, Project administration, Supervision, Conceptualization, Visualization, Writing - review & editing.

Declaration of Competing Interest

The authors reported no declarations of interest.

Acknowledgments

The project was funded by the French National Research Agency (ANR-16-RHUS-0005). Amal Essaouiba Ph.D.'s grant was supported by the French Ministry of Higher Education and Research. We thank Yannick Tauran for his help in the technical aspects of this project.

Appendix A. Supplementary data

Supplementary material related to this article can be found, in the online version, at doi:https://doi.org/10.1016/j.bej.2020.107783.

References

[1] W. Fan, Epidemiology in diabetes mellitus and cardiovascular disease, Cardiovasc. Endocrinol. 6 (2017) 8–16.
[2] International Diabetes Federation, IDF Diabetes Atlas, 9th edn., 2019 (Accessed May 2020), https://www.diabetesatlas.org/en/.
[3] World Health Organization official web site: http://www.who.int/diabetes/en/. (Accessed May 2020).
[4] R.A. DeFronzo, E. Ferrannini, L. Groop, R.R. Henry, W.H. Herman, J.J. Holst, F. B. Hu, C.R. Kahn, I. Raz, G.I. Shulman, D.C. Simonson, M.A. Testa, R. Weiss, Type 2 diabetes mellitus, Nat. Rev. Dis. Primers. 1 (2015) 15019.
[5] J.M. Forbes, M.E. Cooper, Mechanismes of diabetic complications, Physiol. Rev. 93 (2013) 137–188.
[6] C. Sardu, C. De Lucia, M. Wallner, G. Santulli, Diabetes mellitus and its cardiovascular complications: New insights into an old disease, J. Diabetes Res. (2019), 1905194.
[7] A. King, J. Bowe, Animal models for diabetes: understanding the pathogenesis and finding new treatments, Biochem. Pharmacol. 99 (2016) 1–10.
[8] D. Tripathy, A.O. Chavez, Defects in insulin secretion and action in the pathogenesis of type 2 diabetes mellitus, Curr. Diab. Rep. 10 (2010) 184–191.
[9] R.J. Perry, V.T. Samuel, K.F. Petersen, G.I. Shulman, The role of hepatic lipids in hepatic insulin resistance and type 2 diabetes, Nature 510 (2014) 84–91.
[10] C. Saponaro, M. Gaggini, A. Gastaldelli, Nonalcoholic fatty liver disease and type 2 diabetes: common pathophysiologic mechanisms, Curr. Diab. Rep. 15 (2015) 607.
[11] A.M. Ghaemmaghami, M.J. Hancock, H. Harrington, H. Kaji, A. Khademhosseini, Biomimetic tissues on a chip for drug discovery, Drug. Discov. Today 17 (2012) 173–181.
[12] F. Merlier, R. Jellali, E. Leclerc, Online hepatic rat metabolism by coupling liver biochip and mass spectrometry, Analyst 142 (2017) 3747–3757.
[13] A.K. Capulli, K. Tian, N. Mehandru, A. Bukhta, S.F. Choudhury, M. Suchyta, K. K. Parker, Approaching the in vitro clinical trial: engineering organs on chips, Lab Chip 14 (2014) 3181–3186.
[14] J. Rogal, A. Zbinden, K. Schenke-Layland, P. Loskill, Stem-cell based organ-on-a chip models for diabetes research, Adv. Drug Deliv. Rev. 140 (2019) 101–128.
[15] H. Kimura, Y. Sakai, T. Fujii, Organ/body-on-a-chip based on microfluidic technology for drug discovery, Drug Metab. Pharmacokinet. 33 (2018) 43–48.
[16] A. Polini, L. Prodanov, N.S. Bhise, V. Manoharan, M.R. Dokmeci, A. Khademhosseini, Organs-on-a-chip: a new tool for drug discovery, Expert Opin. Drug Discov. 9 (2014) 335–352.
[17] Y. Jun, J. Lee, S. Choi, J.H. Yang, M. Sander, S. Chung, S.H. Lee, In vivo-mimicking microfluidic perfusion culture of pancreatic islet spheroids, Sci. Adv. 5 (2019) eaax4520.
[18] A. Zbinden, J. Marzi, K. Schlünder, C. Probst, M. Urbanczyk, S. Black, E. M. Brauchle, S.L. Layland, U. Kraushaar, G. Duffy, K. Schenke-Layland, P. Loskill, Non-invasive marker-independent high content analysis of a microphysiological human pancreas-on-a-chip model, Matrix Biol. 85-86 (2020) 205–220.
[19] T. Schulze, K. Mattern, E. Früh, L. Hecht, I. Rustenbeck, A. Dietzel, A 3D microfluidic perfusion system made from glass for multiparametric analysis of stimulus-secretion coupling in pancreatic islets, Biomed. Microdevices 19 (2017) 47.
[20] S.H. Lee, S. Hong, J. Song, B. Cho, E.J. Han, S. Kondapavulur, D. Kim, L.P. Lee, Microphysiological analysis platform of pancreatic islet β-cell spheroids, Adv. Healthc. Mater. 7 (2018), 1701111.
[21] X. Li, J.C. Brooks, J. Hu, K.I. Ford, C.J. Easley, 3D-templated, fully automated microfluidic input/output multiplexer for endocrine tissue culture and secretion sampling, Lab Chip 17 (2017) 341–349.
[22] J.C. Brooks, K.I. Ford, D.H. Holder, M.D. Holtan, C.J. Easley, Macro-to-micro interfacing to microfluidic channels using 3D-printed templates: application to time-resolved secretion sampling of endocrine tissue, Analyst 141 (2016) 5714–5721.
[23] S. Bauer, C. WennbergHuldt, K.P. Kanebratt, I. Durieux, D. Gunne, S. Andersson, L. Ewart, W.G. Haynes, I. Maschmeyer, A. Winter, C. Ämmälä, U. Marx, T. B. Andersson, Functional coupling of human pancreatic islets and liver spheroids on-a-chip: towards a novel human ex vivo type 2 diabetes model, Sci. Rep. 7 (2017) 14620.
[24] A. Essaouiba, T. Okitsu, R. Jellali, M. Shinohara, M. Danoy, Y. Tauran, C. Legallais, Y. Sakai, E. Leclerc, Microwell-based pancreas-on-chip model enhances genes expression and functionality of rat islets of Langerhans, Mol. Cell Endocrinol. 514 (2020), 110892.
[25] R. Jellali, M.J. Fleury, P. Paullier, E. Leclerc, Liver and kidney cells cultures in a new perfluoropolyether biochip, Sens. Actuator B-Chem. 229 (2016) 396–407.
[26] R. Baudoin, L. Griscom, J.M. Prot, C. Legallais, E. Leclerc, Behaviour of HepG2/C3a cell culture in a microfluidic bioreactor, Biochem. Eng. J. 53 (2011) 172–181.
[27] Y. Yonekawa, T. Okitsu, K. Wake, Y. Iwanaga, H. Noguchi, H. Nagata, X. Liu, N. Kobayashi, S. Matsumoto, A new mouse model for intraportal islet transplantation with limited hepatic lobe as a graft site, Transplantation 82 (2006) 712–715.
[28] T. Kiba, M. Tanemura, K. Yagyu, High-quality RNA extraction from rat pancreatic islet, Cell. Biol. Int. Rep. 20 (2013) 1–4.
[29] N.M. Kneteman, G.L. Warnock, M.G. Evans, I. Dawidson, R.V. Rajotte, Islet isolation from human pancreas stored in UW solution for 6 to 26 hours, Transplant. Proc. 22 (1990) 763–764.
[30] P.O. Seglen, Preparation of isolated rat liver cells, Methods Cell Biol. 13 (1976) 29–83.
[31] A. Rizki-Safitri, M. Shinohara, M. Tanaka, Y. Sakai, Tubular bile duct structure mimicking bile duct morphogenesis for prospective in vitro liver metabolite recovery, J. Biol. Eng. 14 (2020) 11.
[32] W. Xiao, G. Perry, K. Komori, Y. Sakai, New physiologically-relevant liver tissue model based on hierarchically cocultured primary rat hepatocytes with liver endothelial cells, Integr. Biol. 7 (2015) 1412–1422.
[33] R. Baudoin, G. Alberto, A. Legendre, P. Paullier, M. Naudot, M.J. Fleury, S. Jacques, L. Griscom, E. Leclerc, Investigation of the levels of expression and activity of detoxication genes of primary rat hepatocytes under various flow rates and cell densities in microfluidic biochips, Biotechnol. Prog. 30 (2014) 401–410.
[34] R. Jellali, T. Bricks, S. Jacques, M.J. Fleury, P. Paullier, F. Merlier, E. Leclerc, Long term human primary hepatocyte cultures in a microfluidic liver biochip show maintenance of mRNA levels and higher drugs metabolisms when compared to Petri cultures, Biopharm. Drug. Dispo. 37 (2016) 264–275.
[35] T. Bricks, J. Hamon, M.J. Fleury, R. Jellali, F. Merlier, Y.E. Herpe, A. Seyer, J. M. Regimbeau, F. Bois, E. Leclerc, Investigation of omeprazole and phenacetin first-pass metabolism in humans using a microscale bioreactor and pharmacokinetic models, Biopharm. Drug. Dispo. 36 (2015) 264–275.
[36] A. Legendre, R. Baudoin, G. Alberto, P. Paullier, M. Naudot, T. Bricks, J. Brocheton, S. Jacques, J. Cotton, E. Leclerc, Metabolic characterization of primary rat hepatocytes cultivated in parallel microfluidic biochips, J. Pharm. Sci. 102 (2013) 3264–3276.
[37] S.R. Kimball, R.L. Horetsky, L.S. Jefferson, Hormonal regulation of albumin gene expression in primary cultures of rat hepatocytes, Am. J. Physiol. 268 (1995) E6–14.
[38] K.E. Flaim, S.M. Hutson, C.E. Lloyd, J.M. Taylor, R. Shiman, L.S. Jefferson, Direct effect of insulin on albumin gene expression in primary cultures of rat hepatocytes, Am. J. Physiol. 249 (1985) E447–453.
[39] Q. Chen, M. Lu, B. Monks, M. Birnbaum, Insulin is required to maintain albumin expression by inhibiting forkhead box O1 protein, J. Biol. Chem. 291 (2016) 2371–2378.
[40] K.J. Woodcroft, R.F. Novak, Insulin differentially affects xenobiotic-enhanced, cytochrome P-450 (CYP)2E1, CYP2B, CYP3A, and CYP4A expression in primary cultured rat hepatocytes, J. Pharmacol. Exp. Ther. 289 (1999) 1121–1127.
[41] M. Civera, A. Urios, M.L. Garcia-Torres, J. Ortega, J. Martinez-Valls, N. Cassinello, J. del Olmo, A. Ferrandez, J. Rodrigo, C. Montoliu, Relationship between insulin resistance, inflammation and liver cell apoptosis in patients with severe obesity, Diabetes Metab. Res. Rev. 26 (2010) 187–192.
[42] M. Kitade, H. Yoshiji, R. Noguchi, Y. Ikenaka, K. Kaji, Y. Shirai, M. Yamazaki, M. Uemura, J. Yamao, M. Fujimoto, A. Mitoro, M. Toyohara, M. Sawai, Y. Yoshida, C. Morioka, T. Tsujimoto, H. Kawaratani, H. Fukui, Crosstalk between angiogenesis, cytokeratin-18, and insulin resistance in the progression of non-alcoholic steatohepatitis, World J. Gastroenterol. 15 (2009) 5193–5199.
[43] J. Chiang, Hepatocyte nuclear factor 4α regulation of bile acid and drug metabolism, Expert Opin. Drug Metab. Toxicol. 5 (2009) 137–147.
[44] M. Stoffel, S.A. Duncan, The maturity-onset diabetes of the young (MODY1) transcription factor HNF4 alpha regulates expression of genes required for glucose transport and metabolism, Proc. Natl. Acad. Sci. U. S. A. 94 (1997) 13209–13214.
[45] H.H. Lau, N.H.J. Ng, L.S.W. Loo, J.B. Jasmen, A.K.K. Teo, The molecular functions of hepatocyte nuclear factors – in and beyond the liver, J. Hepatol. 68 (2018) 1033–1048.
[46] K. Hirota, H. Daitoku, H. Matsuzaki, N. Araya, K. Yamagata, S. Asada, T. Sugaya, A. Fukamizu, Hepatocyte nuclear factor-4 is a novel downstream target of insulin via FKHR as a signal-regulated transcriptional inhibitor, J. Biol. Chem. 278 (2003) 13056–13060.
[47] X. Xie, H. Liao, H. Dang, W. Pang, Y. Guan, X. Wang, J. Shyy, Y. Zhu, F. Sladek, Down-regulation of hepatic HNF4α gene expression during hyperinsulinemia via SREBPs, Mol. Endocrinol. 23 (2009) 434–443.
[48] D.R. Powell, A. Suwanichkul, M.L. Cubbage, L.A. DePaolis, M.B. Snuggs, P.D. Lee, Insulin inhibits transcription of the human gene for insulin-like growth factor-binding protein-1, J. Biol. Chem. 266 (1991) 18868–18876.
[49] A.G. Gómez-Valadés, A. Méndez-Lucas, A. Vidal-Alabró, F.X. Blasco, M. Chillon, R. Bartrons, J. Bermúdez, J.C. Perales, Pck1 gene silencing in the liver improves glycemia control, insulin sensitivity, and dyslipidemia in db/db mice, Diabetes 57 (2008) 2199–2210.

[50] Y. Zhang, W. Chen, R. Li, Y. Li, Y. Ge, G. Chen, Insulin-regulated Srebp-1c and Pck1 mRNA expression in primary hepatocytes from zucker fatty but not lean rats is affected by feeding conditions, PLoS One 6 (2011), e21342.
[51] C. Gu, G. Stein, N. Pan, S. Goebbels, H. Hörnberg, K.A. Nave, P. Herrera, P. White, K. Kaestner, L. Sussel, J. Lee, Pancreatic β cells require NeuroD to achieve and maintain functional maturity, Cell Metab. 11 (2010) 298–310.
[52] P. McGrath, C. Watson, C. Ingram, M. Helmrath, J. Wells, The basic Helix-Loop-Helix transcription factor NEUROG3 is required for development of the human endocrine pancreas, Diabetes 64 (2015) 2497–2505.
[53] T. Gao, B. McKenna, C. Li, M. Reichert, J. Nguyen, T. Singh, C. Yang, A. Pannikar, N. Doliba, T. Zhang, D. Stoffers, H. Edlund, F. Matschinsky, R. Stein, B. Stanger, Pdx1 maintains β-cell identity and function by repressing an α-cell program, Cell Metab. 19 (2014) 259–271.
[54] B. Svendsen, O. Larsen, M.B.N. Gabe, C.B. Christiansen, M.M. Rosenkilde, D. J. Drucker, J.J. Holst, Insulin secretion depends on intra-islet glucagon signaling, Cell Rep. 25 (2018) 1127–1134.